A THEORETICAL AND EXPERIMENTAL INVESTIGATION OF THE ULTIMATE LOAD BEHAVIOUR OF GLUED AND NAILED PLYWOOD-WEB I-BEAMS

A thesis submitted for the degree of
Doctor of Philosophy
of London University

by

Omer Mohamed El Hassan Fageiri, B.Sc., D.I.C., M.Sc.

Department of Civil Engineering,
Imperial College of Science and Technology,
London.

August 1974

To

the memory of my parents

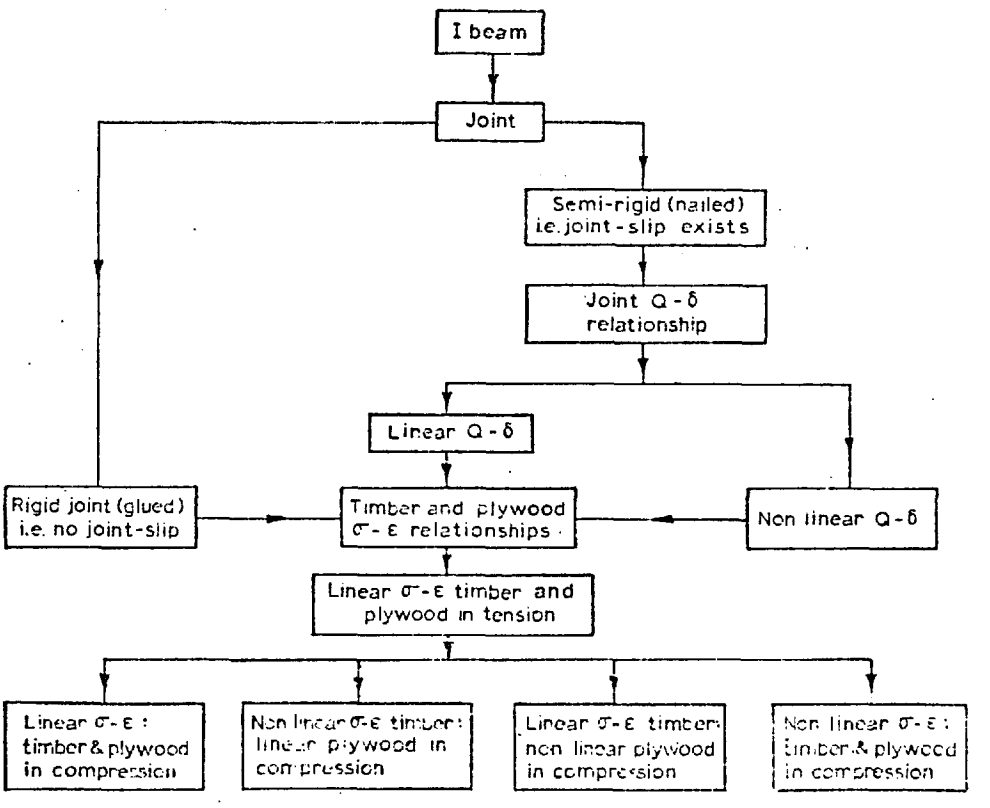
Abstract

The ultimate load behaviour of glued and nailed plywood web I-beams has been investigated theoretically and experimentally.

In the theoretical investigation the following joint and material characteristics have been considered.

The timber to plywood flange-web joints may be rigid (glued) or semi-rigid (nailed). In the rigid joint no joint slip is assumed (i.e. no strain difference between the timber and plywood) whereas joint slip is assumed in the semi-rigid joint. Hence in the case of the semi rigid joint a joint load-slip ($Q - \delta$) relationship is required and both a linear and a generalised non linear $Q - \delta$ relationships have been considered. The flange and web material may be elastic or elastoplastic. Linear and idealised elastoplastic stress-strain ($\sigma - \varepsilon$) relationships are used to describe the behaviour of timber and plywood in compression whereas a linear $\sigma - \varepsilon$ relationship is used in tension.

The relationship of the various combinations of joint and material characteristics is shown in the following diagram:



Generalised governing differential equations for the I-beam have been derived in terms of the top and bottom flanges direct forces (N) and the flange-web joint slip . Governing differential equations based on any of the above cases may be obtained from the generalised ones. Solutions to the governing differential equations have been found by applying numerical procedures based on the predictor corrector and the Newton Raphson methods. Solutions to the bending stress and strain distributions, deflections, shear stresses and flange-web joint-slip have been found at different points along the span. Although the analysis of rigid and semi-rigid beams with linear $Q - \delta$ and $\sigma - \varepsilon$ characteristics may be considered as particular cases of the generalised procedure given above, they have been considered separately as they may be solved by simpler procedures.

The effect of slip on shear deflection has been investigated theoretically and analytical solutions to shear deflections at mid span of symmetrical plywood web I-beams under uniformly distributed load and four point loading are given.

Two computer programs have been written to find solutions for the flange direct forces, joint flange-web slip, distributions of bending stresses and strains across the depth of the beams, deflections and shear stresses at different points along the span of rigid and semi-rigid beams. Solutions are based on the different cases given in the above diagram.

The experimental work included the testing of two glued and two nailed simply supported plywood web I-beams under four point loading. Results for strains, deflections and slips were recorded.

The predicted theoretical behaviour of the beam and the experimental results are compared and it is shown that there is a good agreement.

ACKNOWLEDGEMENTS

I gratefully acknowledge the guidance and encouragement I have received from my supervisor, Dr. L.G. Booth. I should like to thank Professor B.G. Neal for permission to conduct the research in the Engineering Structures Section and Laboratories of the Civil Engineering Department at Imperial College. Thanks are also due to Mr. F.H. Potter, with whom valuable discussions were made on some of the experimental techniques.

Thanks are due to Mr. J. Neale and other members of the Engineering Structures Laboratories and workshop staff who gave valuable assistance in the experimental work.

Thanks are also due to Mr. W.T. Curry and the staff of the mechanical testing department and laboratory of the Princes Risborough Laboratory of the Building Research Establishment, for providing the material for the timber flanges and also for the assistance they gave to conduct some of the tests on small clear specimens of timber and plywood.

Thanks are also due to Miss J. Gurr for providing the photographing facilities and also to Miss D. Lombard for typing the thesis.

My presence in England was made possible by both a British Council and a University of Khartoum, Sudan, Scholarship. I am grateful to both of these organisations for the opportunity they have given me.

CONTENTS

		Page
Notation		12
Part I		13
Introduction		13
Chapter 1	General Comments	14
Chapter 2	Review of relevant literature	19
2.1	Analysis of solid timber beams in bending	19
2.2	Timber to plywood nailed joints	23
2.3	Analysis of plywood web I-beams in bending	23
2.3.1	Rigid plywood web I-beams	23
2.3.2	Semi-rigid plywood web I-beams	24
2.4	Electrical resistance strain gauges on timber and plywood	25
Part II		26
Theory		26
Chapter 3	Introduction	27
3.1	Scope	27
3.2	General assumptions	28
Chapter 4	Rigid plywood web I-beams	28
4.1	Stress strain relationships for flanges and web	28
4.2	Determination of bending strains distribution and curvature	29
4.2.1	Linear $\sigma - \varepsilon$ timber and plywood	29
4.2.2	Non-linear $\sigma - \varepsilon$ timber, linear plywood	33
4.2.3	Linear $\sigma - \varepsilon$ timber, non-linear plywood	39
4.2.4	Non-linear $\sigma - \varepsilon$ timber and plywood.	41
4.3	Bending deflection	43
4.3.1	Governing differential equation	43
4.3.2	Analytical solution	44
4.3.3	Finite difference formulation of the problem.	44

		page
4.4	Web shear stress distribution	48
4.5	Flange web shear stress distribution	48
4.6	Computer program	49
Chapter 5	Semi-rigid plywood web I-beams	50
5.1	Additional assumptions	50
5.2	Stress-strain relationship and implied stress distribution	51
5.3	Flange-web force-displacement relationship	51
5.3.1	Linear displacement function	51
5.3.2	Non-linear displacement function	53
5.4	Generalised governing simultaneous differential equations	54
5.4.1	Derivation of governing equations	54
5.4.2	Features of governing equations	57
	(a) Linear $Q - \delta$ relationship	57
	(b) Non-linear $Q - \delta$ relationship	58
5.5	Governing simultaneous differential equations for a linear flange-web force-displacement equation.	58
5.5.1	Linear $\sigma - \varepsilon$ timber and plywood in compression	59
5.5.2	Non-linear $\sigma - \varepsilon$ timber and plywood in compression	61
5.6	Governing simultaneous differential equations for a non-linear flange-web force displacement equation	67
5.6.1	Linear $\sigma - \varepsilon$ timber and plywood in compression	68
5.6.2	Non-linear $\sigma - \varepsilon$ timber and plywood in compression	68
5.7	Analytical solutions of governing differential equations	68
5.7.1	Limitations to linear stress-strain and force-displacement equations.	68
5.7.2	Solution of governing differential equation in terms of flange force.	70
5.7.3	Deflection due to bending	73

		page
	5.7.4 Bending stresses in the flanges	75
	5.7.5 Bending stresses in the web	76
	5.7.6 Shear force at flange web interface	76
	5.7.7 Shear stress at neutral axis of web	77
Chapter 6	Numerical solutions of generalised governing differential equations	78
	6.1 Outline of procedure	78
	6.2 Numerical integration algorithms: predictor corrector method	79
	6.2.1 Choice of predictor corrector type	79
	6.2.2 Milne type predictor corrector method due to Hamming.	80
	6.3 Convergence criteria	84
	6.3.1 Direct search routine	85
	6.3.2 Directional search routine	88
	6.4 Bending deflection	93
	6.5 Bending stresses in the flanges and web	93
	6.6 Shear force at flange web interface	93
	6.7 Web shear stress at neutral axis of web	94
	6.8 Computer program	95
Chapter 7	Shear deflection in plywood web I-beams	98
	7.1 Assumptions	98
	7.2 Shear stress distributions	98
	7.2.1 Timber flanges	100
	7.2.2 Plywood web	100
	7.3 Shear strain energy	101
	7.3.1 Timber flanges	101
	7.3.2 Plywood web	102
	7.3.3 Total shear energy	104
	7.4 Shear deflection at mid span.	104
	7.5 Shear stiffness factor using non-dimensional parameters α and β.	106
	7.6 Other loading conditions.	109

		Page
Part III		110
Experimental Investigation		110
Chapter 8	Scope and objectives	111
Chapter 9	Sampling and specimen cutting	111
	9.1 Timber for flanges	111
	9.2 Plywood for web	115
Chapter 10	Small clear specimens and joints tests	117
	10.1 Timber for flanges	117
	10.2 Plywood for web	125
	10.3 Timber to plywood nailed joints	132
Chapter 11	Tests on timber flanges prior to fabrication	138
	11.1 Scope and objectives	138
	11.2 Preparation of flanges	139
	11.3 Description of test equipment	143
	11.3.1 End fixings	143
	11.3.2 Lateral restraints during compression tests	145
	11.3.3 Loading equipment	145
	11.3.4 Measuring equipment	145
	11.4 Loading procedure	146
	11.5 Test results	147
Chapter 12	Tests on plywood web I-beams	149
	12.1 Scope and objectives	149
	12.2 Fabrication of beams	150
	12.2.1 Glued beams: Series I and II	150
	12.2.2 Nailed beams: Series III	154
	12.3 Description of test equipment	155
	12.3.1 End supports	155
	12.3.2 Lateral restraints	155
	12.3.3 Loading equipment	159
	12.3.4 Strain measuring equipment	159
	12.3.5 Deflection measuring equipment for beam and flange web joint	160

Page

12.4 Loading procedure 161

12.4.1 General 161

12.4.2 Glued beams: Series II 162

12.4.3 Nailed beams: Series III 163

12.5 Analysis of test data. 163

Part IV 165

Theoretical and Experimental Results 165

Chapter 13 Scope and objectives 166

Chapter 14 Theoretical results for shear stiffness factor at mid span of a symmetrical s.s. semi-rigid plywood web I-beam under u.d.l. 167

14.1 General 167

14.2 Effect of varying α, β, C and m on shear stiffness factors 167

14.3 Effect of slip on shear deflection 175

14.4 Shear stiffness factors for beam models 1, 2, 3 and 4 180

Chapter 15 Theoretical results for beam models 1, 2, 3 & 4. 182

15.1 General 182

15.2 Theoretical results based on solutions of the generalised governing differential equations 183

15.2.1 Direct stresses and strains along the spans of beam models, 1,2,3 & 4 under four point loading at ultimate load 183

15.2.2 Results for beam models (1) and (3) under uniformly distributed load 190

15.2.3 Other theoretical results 195

15.3 Comparison between results for beam model (3) obtained from solutions based on linear, semi-linear and totally non-linear governing differential equations 195

15.3.1 General 195

15.3.2 Low load level 196

15.3.3 Medium load level 196

15.3.4 High load level 198

		Page
Chapter 16	Comparison of theoretical and experimental results	199
16.1	General	199
16.2	Results for tests Series II: Beam models (1)&(2)	199
16.2.1	Beam model (1)	199
16.2.2	Beam model (2)	208
16.3	Results for tests Series III: Beam models (3) & (4)	212
16.3.1	General	212
16.3.2	Distribution of stresses at mid span	214
16.3.3	Mid span deflection	218
16.3.4	Neutral axis web shear stress	218
16.3.5	Top flange-web slip	222
16.3.6	Corollary	222
Part V		228
Summary, conclusions and future work		228
Chapter 17	Summary	229
17.1	Scope	229
17.2	Theoretical	229
17.2.1	Rigid plywood web I-beams	229
17.2.2	Semi-rigid plywood web I-beams	230
17.3	Experimental	232
Chapter 18	Conclusions and application to design	234
18.1	Conclusions	234
18.2	Applications to the analysis and design of semi-rigid plywood web I-beams	237
Chapter 19	Suggestions for future work.	239
Bibliography		240
Appendix		243

NOTATION

P	Total applied load
p	Applied load per unit length
N	Direct force
V	Shear force
M	Moment
Q	Interface shear force
q	Interface shear force per unit length
σ	Direct stress
τ	Shear stress
E	Modulus of elasticity
G	Modulus of rigidity
ε	Strain due to direct force
γ	Shear strain
d	Depth
b	Breadth
L	Span
n	Depth of neutral axis
I	Second moment of area
A	Area
H	Interval of integration
h	Depth of penetration of compression yield from top edge
w	Deflection
δ	Slip
θ	Curvature
Ø	Nail diameter
s	Nail spacing

Subscripts:

s	Shear
b	Bending
u	Ultimate
y	Yield
c	Compression
t	Tension
ex	External
in	Internal

PART I

INTRODUCTION

PART I
INTRODUCTION

Chapter 1 General Comments

A plywood web I-beam of the type considered in this thesis essentially consists of solid timber flanges which are glued, nailed and glued or simply nailed to a vertical plywood web, refer to fig. 1.1. Also in a plywood web I-beam vertical solid timber stiffeners are provided at the ends of the beam and at intermediate points along the span so as to separate the top and bottom flanges and also to stabilise the plywood web against buckling.

In this thesis the terminology rigid plywood web I-beam will apply to a plywood web I-beam with a glued joint between the flanges and web where complete transfer of strain between flanges and web will be assumed, i.e. no joint slip. Also the terminology semi-rigid plywood web I-beam will apply to a plywood web I-beam with a nailed joint between flanges and web where incomplete transfer of strain at the interfaces between the flanges and web will occur i.e. difference of strain between flanges and web and hence joint slip will occur.

Plywood I-beams provide an efficient way to utilise the beam materials economically. The solid timber flanges are provided mainly to resist bending stresses and hence they are placed as far from the neutral axis as possible. The thin plywood web is mainly provided to carry the web shear stresses, but it also carries bending stresses.

In the past rigid plywood web I-beams were used in aircraft construction. Recently, rigid and semi-rigid plywood web I-beams have been used extensively as structural members to support roofs and flooring systems of various types of buildings. They may also be used in other aspects, e.g. bridges.

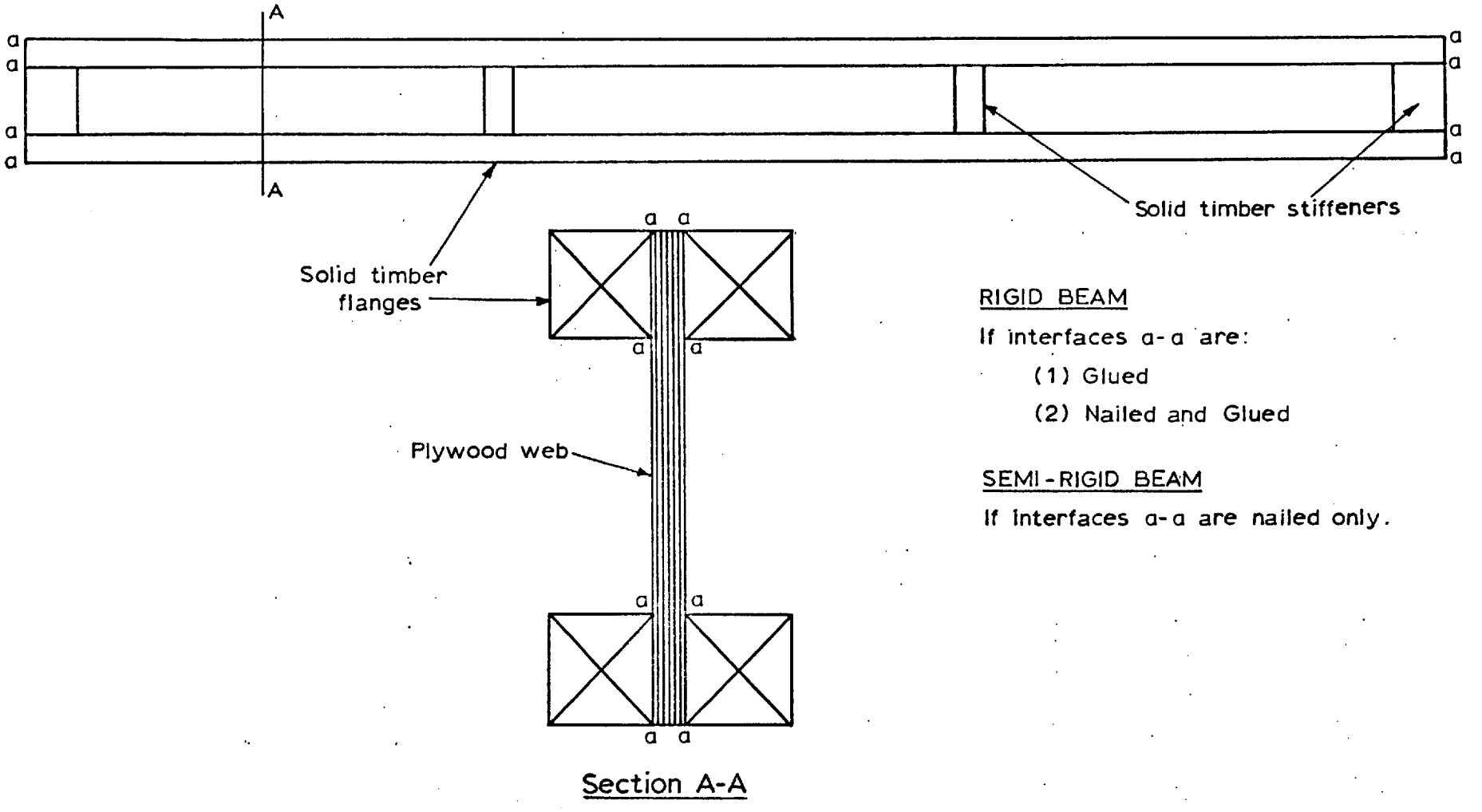


Fig. 1·1. Details of a glued and a nailed plywood web I-beam

The method of the structural analysis of rigid plywood web I-beams which has been followed by many designers, e.g. Plywood Manufacturers Association of British Columbia (1958), is based on linear stress-strain relationship ($\sigma - \varepsilon$). Their method of design is to limit their load bearing capacity to the most critical load obtained from the governing permissible design factor, e.g. permissible bending stresses, permissible deflection, permissible web shear stress, etc. Permissible design factors for various species of timber and plywood are given by many codes of practice, e.g. cp 112 (1967). Permissible design factors are well within the proportional limit and hence linear structural analysis is justified. On the other hand the methods of the analysis and design of semi-rigid plywood web I-beams, have not been established as a standard format as in the case of the glued beams. Booth (1969, 1974) has suggested a method of their analysis and design based on a linear $\sigma - \varepsilon$ relationship for timber and plywood in tension and compression and also on a linear $Q - \delta$ relationship for a timber to plywood joint.

The work dealt with in this thesis is of a theoretical and an experimental nature on the ultimate load behaviour of rigid and semi-rigid plywood web I-beams. Ultimate load behaviour is considered in this thesis in order to have a better understanding about the behaviour of rigid and semi-rigid plywood I-beams at failure so as to promote their methods of structural analysis and designs with the objective to design economical sections.

In the theoretical work described in this thesis, the rigid and semi-rigid cases are treated separately. In the semi-rigid case the behaviour

of the plywood web I-beam is affected by the $Q - \delta$ relationship of the timber to plywood joint. Linear and non-linear $Q - \delta$ relationships are considered separately. For each of the above cases, rigid, semi-rigid with linear $Q - \delta$ relationship and semi-rigid with non-linear $Q - \delta$ relationship, the following two $\sigma - \varepsilon$ relationships for timber and plywood in compression are considered to find the bending stresses distributions across the depth of the beam:

(1) A linear $\sigma - \varepsilon$ relationship

(2) An idealized $\sigma - \varepsilon$ relationship to represent the non-linear case, refer to fig.1.2.

It should also be noted that all the theoretical solutions described in this thesis are based on linear $\sigma - \varepsilon$ relationship for timber and plywood in tension. Also the theoretical solutions described in this thesis include solutions for deflections, direct forces, slip and flange web forces per unit length, in case of the semi-rigid beam, at different points along the span based on the previous $\sigma - \varepsilon$ and $Q - \delta$ relationships. Webs are assumed to be thick enough to prevent web buckling at ultimate load and analytical solutions are given for web shear stresses and shear deflections based on linear $\sigma - \varepsilon$ relationships for timber and plywood in compression. Numerical procedures are employed to find solutions describing the behaviour of the rigid and semi-rigid beams when the analysis is based on idealized non-linear $\sigma - \varepsilon$ relationship for timber and plywood in compression and/or non-linear $Q - \delta$ relationship for a timber to plywood joint.

The object of the experimental work described in this thesis is to verify the results obtained from the theoretical solutions described above. In these experiments strain measurements across the depths of beams using

electrical resistance gauges, deflection measurements and slip measurements in case of the semi-rigid beams are made at certain points along the span. Web shear strains are also measured using rosettes at certain points along the span.

Chapter 2 Review of relevant literature

2.1 Analysis of solid timber beams in bending:

The concepts that have been adopted by many investigators when analysing beams in bending may be summarised in the following points:

(i) To assume that plane sections before bending remain plane after bending, i.e. Linear strain distribution across depth of beam.

(ii) To assume that the material being analysed will follow certain stress-strain relationships in tension and compression ($\sigma - \varepsilon$).

(iii) To consider the equilibrium of direct forces and equilibrium of moments at any section of a beam to find the stress distribution across the depth of that beam relevant to the assumed $\sigma - \varepsilon$ relationships.

(iv) To consider the equilibrium of direct and shear forces to find the shear stress distribution across depth of the beam.

(v) To assume that the theory of small deflections may be applied at any section of the beam.

The concepts mentioned above have been adopted by many investigators for the analysis of solid timber beams and the validity of some of the assumptions have been considered by several research workers.

Dietz (1942), Comben (1957), Ramos (1961) have all considered the validity of the assumption that plane sections before bending remain plane after bending.

Dietz (1942) carried out bending tests on Douglas-fir beams subjected to four point loading at $\frac{1}{3}$ span. He measured strains at both sides across central cross section of the beams. He concluded that sections plane before bending apparently do not remain plane after bending. He noted marked non-linear distribution of strain near the top compression fibre of the beam.

Comben (1957) concluded after testing Douglas-fir beams in bending that the strain distribution across depth of timber beams is basically linear at all load levels except at high loads when the compressive strains near the top edge are slightly increased and hence the strain distribution tend to be slightly non linear.

Ramos (1959) also concluded that the strain distribution across depth of timber beams is basically linear.

Different investigators have adopted different $\sigma - \varepsilon$ relationships for timber in tension and compression to find the distribution of stress across the depth of timber beams at all load levels, especially at load levels when the timber in compression is behaving non-linearly. Almost all investigators cited in literature have adopted linear $\sigma - \varepsilon$ relationship for timber in tension. While many investigators have adopted linear $\sigma - \varepsilon$ relationship for timber in compression, some have adopted non-linear ones to find the distribution of stress across the depth of timber beams. According to Kollman and Cote (1968) and Dietz (1942), Baumann (1922) has solved graphically the distribution of stress across depths of timber beams by applying the exact tension and compression $\sigma - \varepsilon$ relationships, equilibrium of direct forces and equilibrium of moments at any section of the beam. Also Kollman and Cote (1968) have cited Suenson (1941) who adopted a parabolic $\sigma - \varepsilon$ relationship for compression, Ros (1936) and Thunel (1939, 1940) who adopted a $\sigma - \varepsilon$ relationship similar to that

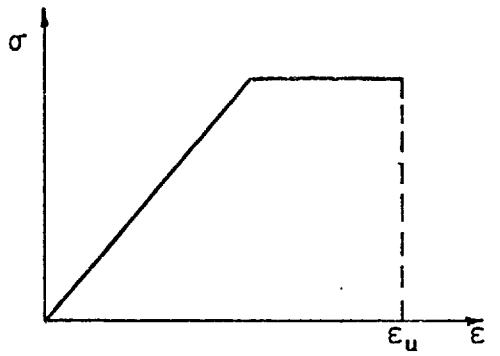


Fig. 1·2. Idealized $\sigma - \varepsilon$ relationship for timber in compression

given in Fig.1.2 for compression and they have all solved the distribution of stress across the depth of a timber beam by considering equilibrium of direct forces and equilibrium of moments.

Beghtel and Norris (1959) applied the concept to analyse beams in bending, as outlined before, to rectangular solid timber beams. They adopted a linear $\sigma - \varepsilon$ relationship for timber in tension, a non-linear one similar to that adopted by Ros (1936), fig.1.2, for timber in compression. They also assumed that the moduli of elasticity of timber in tension and compression are the same. They gave theoretical solutions for distributions of direct stresses and shear stresses across timber beams depths and also they gave an approximate solution for mid-span deflections. They also tested rectangular solid timber beams of various span-depth ratios subjected to four point loading at $\frac{1}{4}$ points of the span. Their predicted results from theoretical solutions compared reasonably well with their experimental findings. They did not measure strains at any section of the beams.

Ramos (1961) followed a similar theoretical approach as that given by Beghtel and Norris (1959). In his experimental work he included strain measurements across critical cross-sections of Douglas-fir beams subjected to four-point loading up to failure. He used electrical resistance strain gauges to measure strains. He computed the corresponding stresses from the relationship:

$$\sigma = E(\varepsilon - \varepsilon_r) \qquad - \ 1.1$$

where ε_r : computed residual strain

To compute residual strains he adopted Nadai's (1950) assumption that "a compression specimen subjected to a gradually applied load follows a typical $\sigma - \varepsilon$ curve. If at any time the sustained load is gradually released, at the same rate as it was applied, the $\sigma - \varepsilon$ curve descends along the straight line substantially parallel to the straight line portion of the curve within the proportional limit". i.e.

$$\Delta\varepsilon = \frac{P\ \varepsilon_e}{P_e} \qquad - \ 1.2$$

$$\varepsilon_r = \varepsilon - \Delta\varepsilon \qquad - \ 1.3$$

where P_e : load at proportional limit

ε_e : corresponding strain at proportional limit

Needless to say that $\varepsilon_r = 0$ when the compressive stresses are below the proportional limit stress and thebeam is in elastic tension.

His experimental findings agreed reasonably well with his theoretical work and hence validated Nadai's assumption for timber beams.

2.2 Timber to plywood nailed joints

Many investigators have done experimental work on glued and mechanically fastened timber to timber, and timber to plywood joints tested in direct tension and compression. Mechanically fastened joints relevant to this thesis are timber to plywood nailed joints. Many research workers have tested timber to plywood nailed joints in direct compression. Mack (1966) tested and analysed similar joints with the objective of expressing the joint displacement in terms of the corresponding applied load. The parameters he considered that might affect the joint behaviour were many. Those which he found to be more actively interacting are species, nail diameter and displacement parameters. The curve obtained experimentally was found to be curvilinear with a marked yield point at about 0.14 inch displacement for a joint with a standard gap of 0.028 inch between members before test. He reported that the yield point is due to apparent increase in joint stiffness when the gap closes. Mack's equation applies to joints with displacements up to 0.1 inch, i.e. to displacements less than the yield point displacement. Morris (1968) arrived at a similar equation as that obtained by Mack (1966).

According to Mack (1966), Jansson (1955), Niskanen (1961), and Noren (1962) have also giventheoretical load displacement curves for timber to timber nailed joints.

2.3 Analysis of plywood web I-beams in bending

2.3.1 Rigid plywood web I-beams

Most of the theoretical work on rigid plywood web I-beams is based on linear $\sigma - \varepsilon$ relationships for timber and plywood in tension and compression, e.g. Council of Forest Industries of British Columbia (1958).

A lot of experimental work has been done at Forest Products Laboratory at Madison with the objective of designing plywood webs in plywood box and I-beams, e.g. Withey (1943), Lewis and Dawley (1943), Lewis, Heebink, Cottingham and Dawley (1960, 1960), Lewis, Heebink and Cottingham (1959, 1959).

2.3.2. Semi-rigid plywood web I-beams

Most of the theoretical work on semi-rigid plywood web I-beams cited in literature and described hereafter in this section is based on linear $\sigma - \varepsilon$ and $Q - \delta$ relationships.

Booth (1969) applied the concept of bending as outlined in section 2.1 to derive analytical solutions to describe the behaviour of semi-rigid plywood web I-beams subjected to bending. His solutions were based on linear $\sigma - \varepsilon$ and linear $Q - \delta$ relationships. Similar solutions for highway composite concrete slab and rolled steel joist (RSJ) were given by Siess, Newmark and Viest (1951).

Booth (1969) suggested the use of linear $\sigma - \varepsilon$ relationship while adopting a non-linear connector $Q - \delta$ relationship when analysing semi-rigid plywood web box and I-beams. He suggested the use of mononomials and exponential functions to describe connector $Q - \delta$ relationship similar to those given by eqns. 1.4 and 1.5.

$$Q = a\,\delta^{b} \qquad - 1.4$$

$$Q = c(1 - \bar{e}^{d\delta}) \qquad - 1.5$$

where: a, b, c and d are constants depending on joint characteristics, i.e. nail diameter, species etc.

He also suggested that the non-linear differential equation can be solved numerically. He reported that similar equations for composite highway concrete slab and RSJ were solved by Yam and Chapman (1968) .

Vermeyden (1968) has conducted experimental work on semi-rigid plywood box beams with the objective of designing them.

2.4 Electrical resistance strain gauges on timber and plywood

Some investigators have considered the performance of electrical resistance strain gauges compared with mechanical ones, with special attention to the effects of type of bonding material, bonding technique and grain orientation.

Youngquist (1957) reported that strains measured by electrical resistance gauges were less than those measured by mechanical strain gauges by up to 10%. Solvey and Blecher (1952) also found similar results when they tested plywood panels.

Amana (1967) considered different bonding materials with different types of electrical resistance strain gauges on plywood tested in direct tension parallel and perpendicular to the face grain. He arrived at similar conclusions as those reported by Youngquist, and Solvey and Blecher; but in some special cases when certain glue types are used with certain strain gauge types he found that strains measured by electrical resistance gauges can be higher than those measured by extensometers by up to 33%. While most high strain variations were reported for specimens tested and strains measured perpendicular to the face grain, some high variations were reported for specimens tested and strains measured parallel to the face grain.

PART II

THEORY

PART II

THEORY

Chapter 3 Introduction

3.1 Scope

The theoretical work given hereafter in part II of this thesis is to describe the behaviour of rigid and semi-rigid plywood web I-beams in bending taking into consideration linear and non-linear $\sigma - \varepsilon$ relationships for timber and plywood in compression, linear $\sigma - \varepsilon$ relationship for timber and plywood in tension and also linear and non-linear $Q - \delta$ relationships to describe the joint behaviour for the semi-rigid case.

Generalised differential equations are derived to solve for the direct forces in the top and bottom flanges (refer to eqns. 2.21 - 2.24) at different load levels and different sections along the beam, and hence deflection, direct stress and shear stresses may be found. These generalised differential equations are solved by applying an iterative procedure using a computer program, refer to chapter 6.

Although the rigid case may be solved as a particular case of the generalised, it is found that it is an advantage to consider the rigid and semi-rigid cases separately as the first case will require a simpler procedure than the rather slow general procedure required to solve the second case and hence some computer time is saved, refer to chapters 4 and 5.

Also it is found in the case of a semi-rigid beam that a linear $Q - \delta$ relationship to describe the timber to plywood joint behaviour of the beam may lead to simple problem formulations and solutions. Accordingly

the two cases of linear and non-linear $Q - \delta$ relationships are treated separately, refer to sections 5.5 and 5.6.

3.2 General assumptions

(1) Plane sections before bending remain plane after bending, i.e. linear strain distribution across depths of flanges and web.

(2) Deflections are small.

(3) The moduli of elasticity in tension and compression are the same for timber: similarly for plywood.

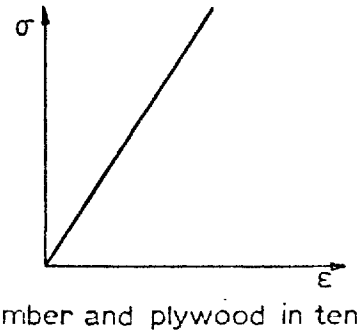
(4) Webs are thick enough and stiffeners are provided at appropriate distances such that the webs do not buckle.

Chapter 4 Rigid plywood web I-beams

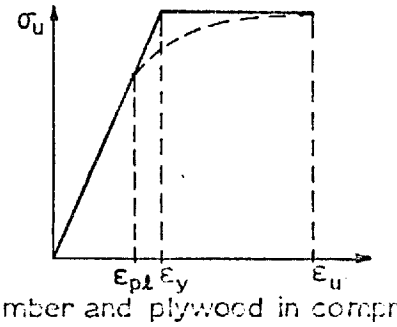
4.1 Stress-strain relationships for flanges and web

For the analysis of rigid plywood web I-beams, the general assumptions mentioned in section 3.2 apply and also complete transfer of strains between timber flanges and plywood web at joints interface is assumed.

The analysis is based on idealised $\sigma - \epsilon$ relationships for timber and plywood in tension and compression. While for timber and plywood in tension linear $\sigma - \epsilon$ relationships are assumed, fig.2.1(a), non-linear $\sigma - \epsilon$ relationships similar to that given in fig.2.1(b) are assumed for timber and plywood in compression.



(a) Timber and plywood in tension



(b) Timber and plywood in compression

Fig. 2·1. Idealized $\sigma - \varepsilon$ relationships for timber and plywood in tension and compression

Obviously the values for ultimate and yield stresses and strains (σ_u and σ_y, ε_u and ε_y) depend on the characteristics of the material under consideration.

Stress distributions across depths of beam relevant to the previous $\sigma - \varepsilon$ relationships, refer to figs.2.1 and 2.2, will depend on the applied load level and position of section along the span, i.e. on the external applied moment. To cover the whole range of stress distributions across the beam depths that might occur at any section and load level, the cases described in fig.2.2 will be considered as shown in section 4.2. Needless to say that the stress distributions across the depths of timber and plywood in tension, at all levels and sections, relevant to the linear $\sigma - \varepsilon$ relationship of fig.2.1(a), are linear, fig.2.2.

4.2 Determination of bending stress distribution and curvature

4.2.1 Linear $\sigma - \varepsilon$ timber and plywood

In the following derivation reference is made to fig.2.2(a)

To find position of neutral axis (n) and curvature θ:

we have from bending theory:

$$\theta = \frac{M_{ex}}{\overline{EI}} \qquad - 2.1$$

$$\text{where } \overline{EI} = \Sigma EI + E_1A_1\left(n - \frac{d_1}{2}\right)^2 + E_2A_2\left(n - \frac{d_2}{2}\right)^2 + E_3A_3\left(D - n - \frac{d_3}{2}\right)^2 \qquad - 2.2$$

$$\Sigma EI = E_1I_1 + E_2I_2 + E_3I_3$$

$$n = \Sigma EF\big|_1/\Sigma EA$$

$$\Sigma EF\big|_1 = \tfrac{1}{2}\left[E_1A_1d_1 + E_2A_2d_2 + E_3A_3(2d_2 - d_3)\right]$$

$$\Sigma EA = E_1A_1 + E_2A_2 + E_3A_3$$

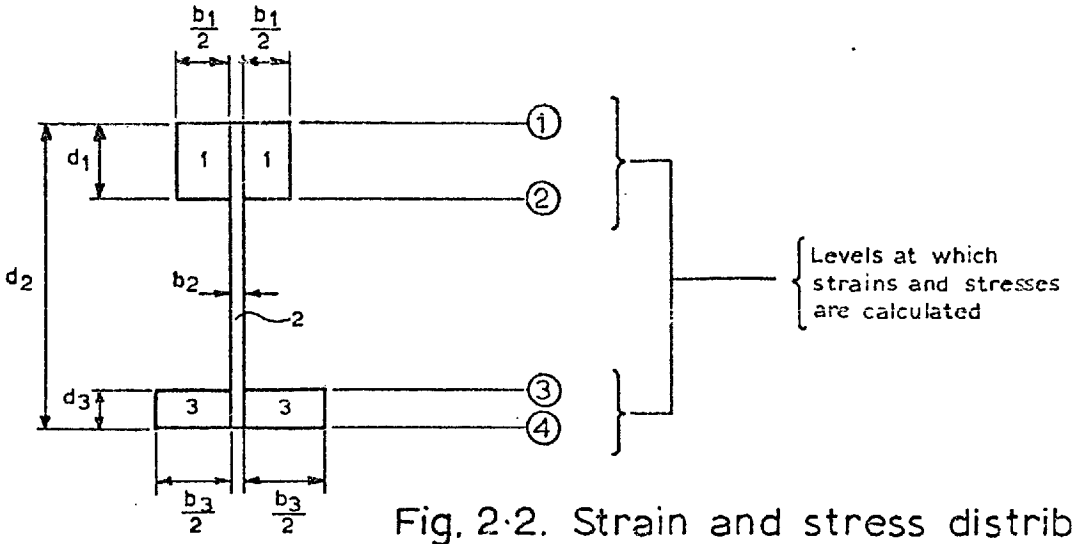
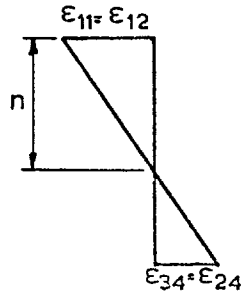
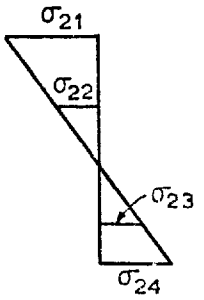
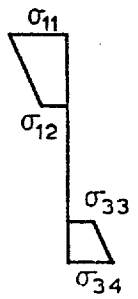
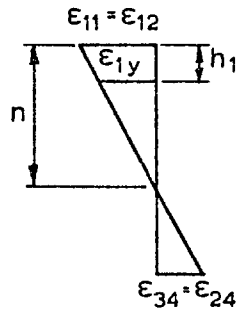
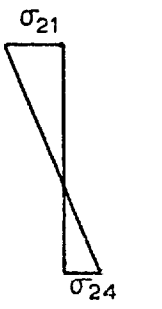
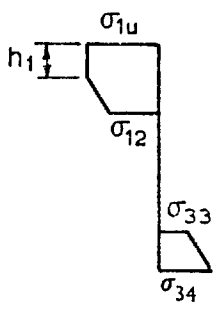
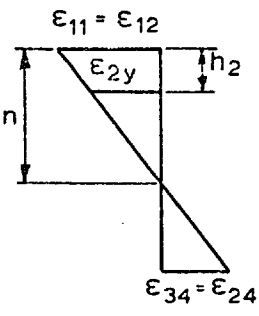
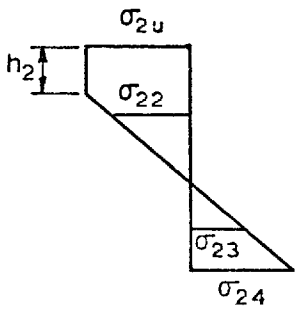
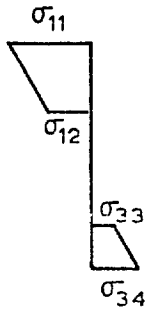
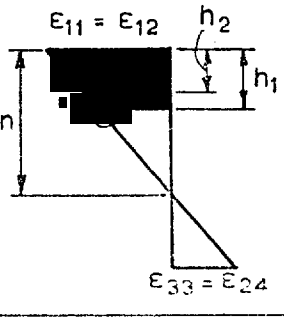
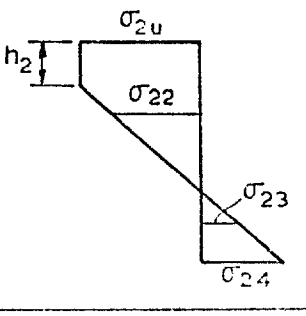
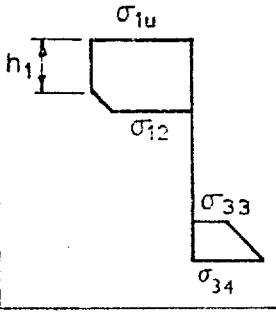
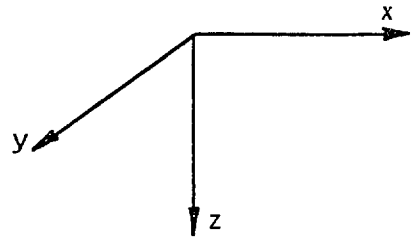


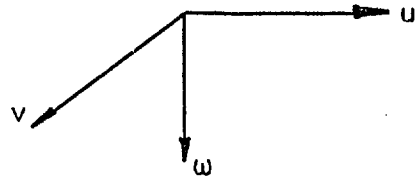
Fig. 2·2. Strain and stress distributions at any section across the depth of a rigid beam

Description	Strain distribution	Web stress distribution	Top and bottom flanges stress distribution	fig. N°.
Linear σ - ε plywood and timber				2·2 (a)
Linear σ - ε plywood, non linear timber				2·2 (b)
Non linear σ - ε plywood linear timber				2·2(c)
Non linear σ-ε plywood and timber				2·2 (d)

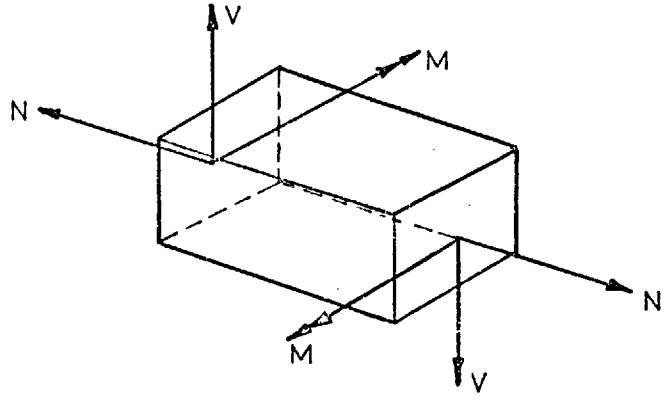
Co-ordinate System

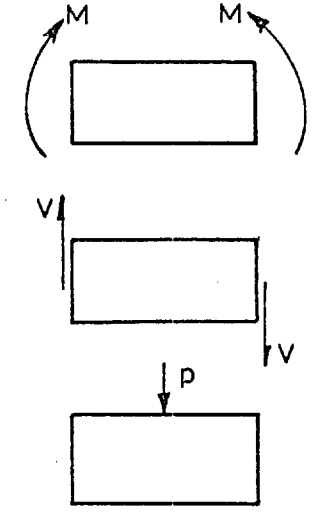


Displacements



Forces





$$\frac{dV}{dx} = -p, \quad \frac{dM}{dx} = V, \quad \frac{d^2\omega}{dx^2} = -\frac{M}{EI}$$

Fig. 2·3. Sign convention

Bending strains and stresses:

Absolute values of stresses and strains may be found as follows:

$$\varepsilon_{11} = \varepsilon_{21} = n\theta$$

$$\varepsilon_{34} = \varepsilon_{24} = (d_2 - n)\,\theta$$

$$\varepsilon_{12} = (n - d_1)\,\theta$$

$$\varepsilon_{33} = (d_2 - n - d_3)\,\theta$$

$$\sigma_{11} = E_1\,\varepsilon_{11}$$

$$\sigma_{12} = E_1\,\varepsilon_{12}$$

$$\sigma_{21} = E_2\,\varepsilon_{11}$$

$$\sigma_{24} = E_2\,\varepsilon_{34}$$

$$\sigma_{33} = E_3\,\varepsilon_{33}$$

$$\sigma_{34} = E_3\,\varepsilon_{34}$$

— 2.3

If $\varepsilon_{11} \leq \varepsilon_{1y}$ and $\varepsilon_{21} \leq \varepsilon_{2y}$, then stress distributions according to fig. 2.2(a) are adopted and deflections, web shear stresses and flange web shear stresses are found as shown in sections 4.3, 4.4 and 4.5.

On the other hand if the compressive extreme fibre strains of timber (ε_{11}) and/or plywood (ε_{21}) are greater than their respective yield strains in compression, then the strain and stress distributions according to fig.2.2(a) are abandoned and distributions according to fig.2.2(b) are adopted.

4.2.2 Non-linear $\sigma - \varepsilon$ timber, linear plywood

Reference in the following derivation is made to fig.2.2(b) and fig.2.4(a).

The following procedure is adopted to find position of neutral axis and hence the distribution of direct stresses across the depths of timber and plywood:

(i) Assume a curvature θ be given by eqn.2.1

(ii) Let position of neutral axis from top fibre be n, then absolute values of stresses across depth of beams are given by:

$$\sigma_{11} = \sigma_{1u} = E_1 \varepsilon_{1y} \quad ; \quad \sigma_{12} = E_1(n - d_1)\theta$$

$$\sigma_{21} = E_2 n\theta \quad ; \quad \sigma_{24} = E_2(d_2 - n)\theta \qquad - 2.4$$

$$\sigma_{33} = E_3(d_2 - n - d_3)\theta \quad ; \quad \sigma_{34} = E_3(d_2 - n)\theta$$

and also depths of yield penetration in flange and web are given by:

$$h_1 = n - \varepsilon_{1y}/\theta \qquad - 2.5$$

$$h_2 = 0$$

(iii) Total compressive force above neutral axis is given by:

$$C = \tfrac{1}{2}\sigma_{21} n b_2 + \sigma_{1u} h_1 b_1 + \tfrac{1}{2}(\sigma_{1u} + \sigma_{12})(d_1 - h_1)b_1$$

substitute values of σ_{21}, σ_{12}, h_1 from eqns. 2.4 and 2.5 and rearrange:

$$C = \tfrac{1}{2} b_1 E_1 \theta \left[(E_{21}\beta_{21} - 1)n^2 + 2\left(\frac{\varepsilon_{1y}}{\theta} + d_1\right)n - \left(\frac{\varepsilon_{1y}}{\theta}\right)^2 - d_1^2 \right] \qquad - 2.6$$

where $\beta_{21} = b_2/b_1$, $E_{21} = E_2/E_1$

(iv) Similarly

$$T = \tfrac{1}{2} b_3 E_3 \theta \left[E_{23}\beta_{23} n^2 - 2(E_{23}\beta_{23} d_2 + d_3) n + E_{23}\beta_{23} d_2^2 + 2d_2 d_3 - d_3^2 \right] \quad 2.7$$

where $\beta_{23} = b_2 / b_3 \qquad E_{23} = E_2 / E_3$

(v) $T - C = o$

Substitute values of C and T from eqn. 2.6 and 2.7 and rearrange

$$\beta_{13}E_{13}n^2 - 2(\beta_{13}E_{13}d_1 + \beta_{23}E_{23}d_2 + d_3 + \beta_{13}E_{13}\frac{\varepsilon_{1y}}{\theta})\, n$$

$$+ \beta_{13}E_{13}d_1^2 + \beta_{23}E_{23}d_2^2 - d_3^2 + 2d_2d_3 + \beta_{13}E_{13}(\frac{\varepsilon_{1y}}{\theta})^2 = 0 \qquad - 2.8$$

$$\text{or} \quad n = \frac{b - \sqrt{[b^2 - ac]}}{a}$$

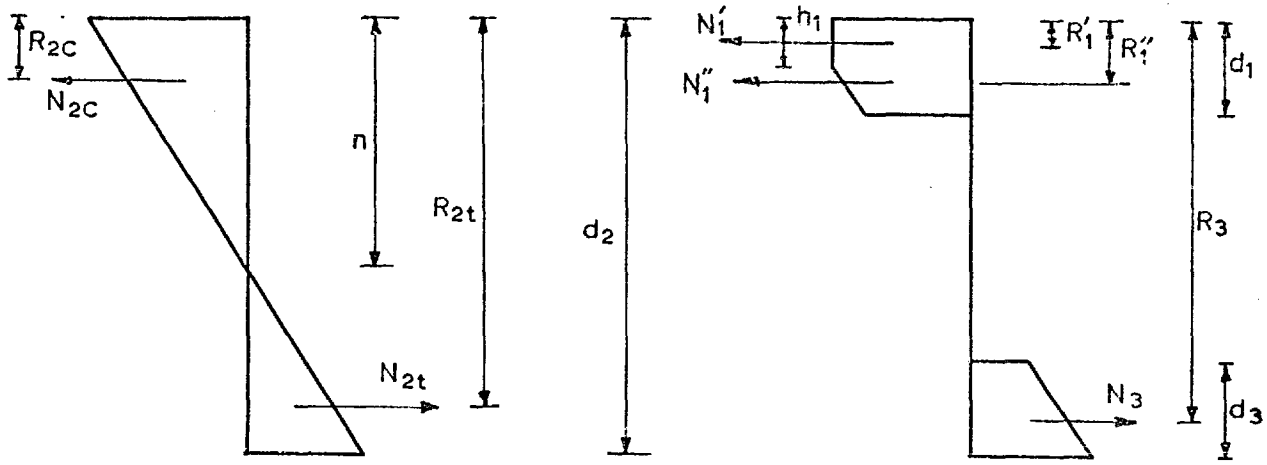
where $a = \beta_{13}E_{13}$

$$b = \beta_{13}E_{13}d_1 + \beta_{23}E_{23}d_2 + d_3 + \beta_{13}E_{13}(\frac{\varepsilon_{1y}}{\theta})$$

$$c \quad \beta_{13}E_{13}d_1^2 + \beta_{23}E_{23}d_2^2 - d_3^2 + 2d_2d_3 + \beta_{13}E_{13}(\frac{\varepsilon_{1y}}{\theta})^2 \qquad - 2.9$$

and h_1 is then calculated from 2.5

(vi) Total internal moment on any section along the beam is calculated by taking moments of all direct forces acting on that section about the top compressive fibre.



Direct forces on web Direct forces on flanges

Fig. 2·4 (a). Stress distribution; non linear $\sigma-\varepsilon$ timber, linear plywood

$$N_{2c} = \tfrac{1}{2}\sigma_{21}b_2 n \quad ; \quad R_{2c} = \tfrac{1}{3}n$$

$$N_1' = \sigma_{1u}b_1h_1 \quad ; \quad R_1' = \tfrac{1}{2}h_1$$

$$N_1'' = \tfrac{1}{2}(\sigma_{1u}+\sigma_{12})(d_1-h_1)b_1 \quad ; \quad R_1'' = \frac{(d_1-h_1)}{3}\,\frac{(2\sigma_{12}+\sigma_{1u})}{(\sigma_{12}+\sigma_{1u})} + h_1$$

$$N_{2t} = \tfrac{1}{2}\sigma_{24}b_2\,(d_2-n) \quad ; \quad R_{2t} = \tfrac{1}{3}(2d_2+n)$$

$$N_3 = \tfrac{1}{2}(\sigma_{34}+\sigma_{33})d_3b_3 \quad ; \quad R_3 = d_2 - \frac{d_3}{3}\,\frac{(2\sigma_{33}+\sigma_{34})}{(\sigma_{33}+\sigma_{34})}$$

- 2.10

$$M_{in} = N_{2c}R_{2c} + N_1'R_1' + N_1''R_1'' - N_{2t}R_{2t} - N_3R_3 \qquad \text{- 2.11.1}$$

Substitute values from eqns. 2.10, 2.4 and 2.5 in eqn. 2.11.1 and rearrange

$$M_{in} = \frac{E_1b_1\theta}{6}\Bigg[n^3 - 3\,\frac{\varepsilon_{1y}}{\theta}\,n^2 - \Big[3E_{21}\beta_{21}d_2^{\,2}+E_{31}\beta_{31}(3d_2d_3-2d_3^{\,2})^2 + 3d_1^{\,2} - 3\Big(\frac{\varepsilon_{1y}}{\theta}\Big)^2\Big]n$$

$$- \Big(\frac{\varepsilon_{1y}}{\theta}\Big)^3 + 2E_{21}\beta_{21}d_2^{\,3} + E_{31}\beta_{31}(3d_2^{\,2}d_3-5d_2d_3^{\,2}+2d_3^{\,3})+2d_1^{\,3}\Bigg] \qquad \text{-2.11.2}$$

We have: $M_{ex} - M_{in} = 0$

Substituting values of M_{ex} and M_{in}, we get:

$$n^3 - 3\frac{\varepsilon_{1y}}{\theta} n^2 - \left[3E_{21}\beta_{21}d_2^{\,2} + E_{31}\beta_{31}(3d_2d_3-2d_3^{\,2}) + 3d_1^{\,2} - 3(\frac{\varepsilon_{1y}}{\theta})^2\right] n$$

$$- \frac{6M_{ex}}{E_1 b_1 \theta} - (\frac{\varepsilon_{1y}}{\theta})^3 + 2E_{21}\beta_{21}d_2^{\,3} + E_{31}\beta_{31}(3d_2^{\,2}d_3-5d_2d_3^{\,2}+2d_3^{\,3})+2d_1^{\,3} = 0$$

- 2.11.3

(vii) Non-linear simultaneous equations 2.8 and 2.11.3 may be solved numerically to find n and θ.

In this thesis equations 2.8 and 2.11.3 are not solved directly, but the following systematic numerical procedure is followed to find n and θ, which is an indirect solution to equations 2.8 and 2.11.3.

(a) Internal moments are found from eqn.2.11.1 using a guessed value for θ as indicated in step (i) and solving for neutral axis position from eqns. 2.9.

Having found internal moments acting on the section, then check for the following:

$$\left| M_{ex} - M_{in} \right| \leq \xi M_{ex}$$

where ξ is desired accuracy.

Two cases arise:

I/ If $\left| M_{ex} - M_{in} \right| \leq \xi M_{ex}$, then a solution is obtained and hence the guessed value of θ and the calculated values of n are correct and hence the direct strains and the corresponding stresses across the depths of timber and plywood are calculated from equations 2.4.

II/ If $\left| M_{ex} - M_{in} \right| > \xi M_{ex}$, then a new curvature closer to the true curvature is found as shown in the following step (b). Having found new curvature θ, then procedure given in step (a) is repeated until desired accuracy is achieved.

(b) To find a new curvature closer to the true curvature, the Newton Raphson method is employed as follows and reference is made to fig. 2.5.

(1) To find θ_1 assume initial guess is A(Mo, θo). Let slope at A be calculated from $(M_\eta - Mo)/\eta\theta o$

where η is a parameter found by trial and error to take the values $10^{-4} \leq \eta \leq 10^{-10}$, so that a good approximation of slope at A is possible.

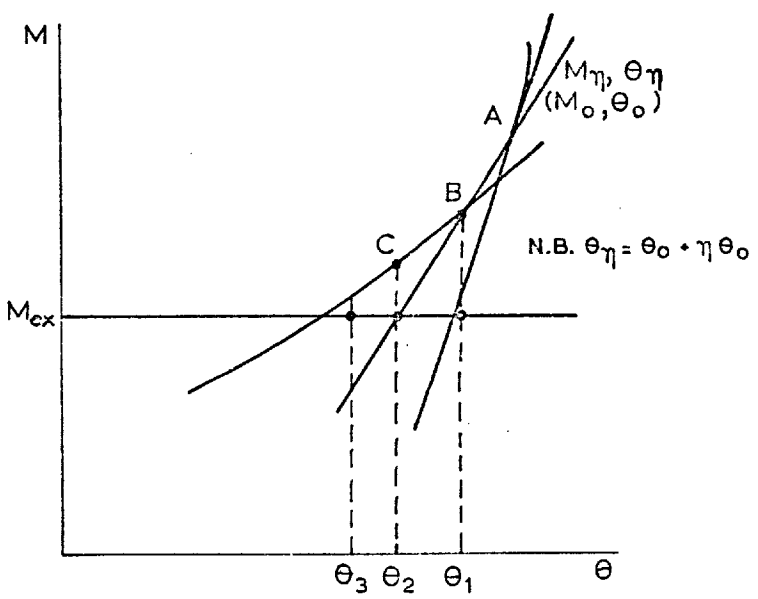


Fig. 2·5. Linear Newton Raphson Method

Also slope at A = $\frac{M_o - M_{ex}}{\theta_o - \theta_1}$

Then $\theta_1 = \theta_o + \frac{\eta\,\theta_o}{M_\eta - M_o}\,(M_{ex} - M_o)$

Corresponding Moment M_1 is calculated as indicated in steps (i - vi) for the new curvature θ_1; this new moment corresponds to Moment M_1 at point B in Fig.2.5.

(2) To find θ_2 or generally θ_n, closer to the true curvature, the slope at B is assumed to pass through point A, and hence,

$$\theta_2 = \theta_1 + \frac{\theta_o - \theta_1}{M_o - M_1}\,(M_{ex} - M_1)$$

or generally,

$$\theta_{i+1} = \theta_i + \frac{\theta_i - \theta_{i-1}}{M_i - M_{i-1}}\,(M_{ex} - M_i)$$

where $i = 1, \ldots i_n$ $\quad$ i_n = number of iterations

Number of iterations to achieve convergence to desired accuracy is found to be less than six iterations in all cases considered in this thesis. It depends on choice of η. Less iterations are achieved at the extreme high limit of η, ie 10^{-10}.

(3) If $\varepsilon_{21} \leq \varepsilon_{2y}$ and $\varepsilon_{11} > \varepsilon_{1y}$, then assumed stress distribution is correct, and is then adopted.

(4) But if $\varepsilon_{21} > \varepsilon_{2y}$ and $\varepsilon_{11} \leq \varepsilon_{1y}$, distributions according to fig. 2.2(b) are incorrect, and are abandoned and those corresponding to fig 2.2(c) are adopted, refer to section 4.2.3.

If $\varepsilon_{21} > \varepsilon_{2y}$ and $\varepsilon_{11} > \varepsilon_{1y}$, distributions according to figs.2.2(b) and 2.2(c) are incorrect, and are abandoned and those corresponding to fig.2.2(d) are adopted, refer to section 4.2.4.

4.2.3. Linear $\sigma - \varepsilon$ timber, non-linear plywood

Reference in the following derivation is made to fig 2.2(c) and fig 2.4(b).

A procedure similar to that used in section 4.2.2 is adopted. The following changes in equations 2.4, 2.5, 2.6, 2.8, 2.9 and 2.10 will make the procedure compatible with the assumed stress distributions.

(1) Equations 2.4 will read the same as given in section 4.2.2 with the exception of the following

$$\sigma_{11} = E_1 n\theta$$

$$\sigma_{21} = \sigma_{2u} \qquad 2.4(a)$$

(2) Equation 2.5 will read as follows

$$h_1 = o$$

$$h_2 = n - \frac{\varepsilon_{2y}}{\theta} \qquad 2.5(a)$$

(3) Equation 2.6 will read as follows:

$$C = \sigma_{2u} b_2 h_2 + \tfrac{1}{2}\sigma_{2u} b_2 (n-h_2) + \tfrac{1}{2}(\sigma_{11}+\sigma_{12}) b_1 d_1$$

$$= \tfrac{1}{2} b_1 E_1 \theta \left[2(E_{21}\beta_{21} \frac{\varepsilon_{2y}}{\theta} + d_1)n - E_{21}\beta_{21}(\frac{\varepsilon_{2y}}{\theta})^2 - d_1^2 \right] \qquad 2.6(a)$$

(4) Equation 2.8 will read as follows:

$$E_{23}\beta_{23}n^2 - 2(E_{13}\beta_{13}d_1+E_{23}\beta_{23}d_2+d_3+E_{23}\beta_{23}\frac{\varepsilon_{2y}}{\theta})n + E_{13}\beta_{13}d_1^2+E_{23}\beta_{23}d_2^2$$

$$-d_3^2 - 2d_2d_3+E_{23}\beta_{23}(\frac{\varepsilon_{2y}}{\theta}) = 0 \qquad 2.8(a)$$

(5) Equations 2.9 will read as given in section 4.2.2 except for ,

$$a = E_{23}\beta_{23}$$

$$b = E_{13}\beta_{13}d_1 + E_{23}\beta_{23}d_2 + d_3 + E_{23}\beta_{23}\frac{\varepsilon_{2y}}{\theta}$$

$$c = E_{13}\beta_{13}d_1^2 + E_{23}\beta_{23}d_2^2 - d_3^2+2d_2d_3+E_{23}\beta_{23}(\frac{\varepsilon_{2y}}{\theta})^2 = 0 \qquad - 2.9(a)$$

(6) Equations 2.10 will read as mentioned in section 4.2.2 with the exception of the following :

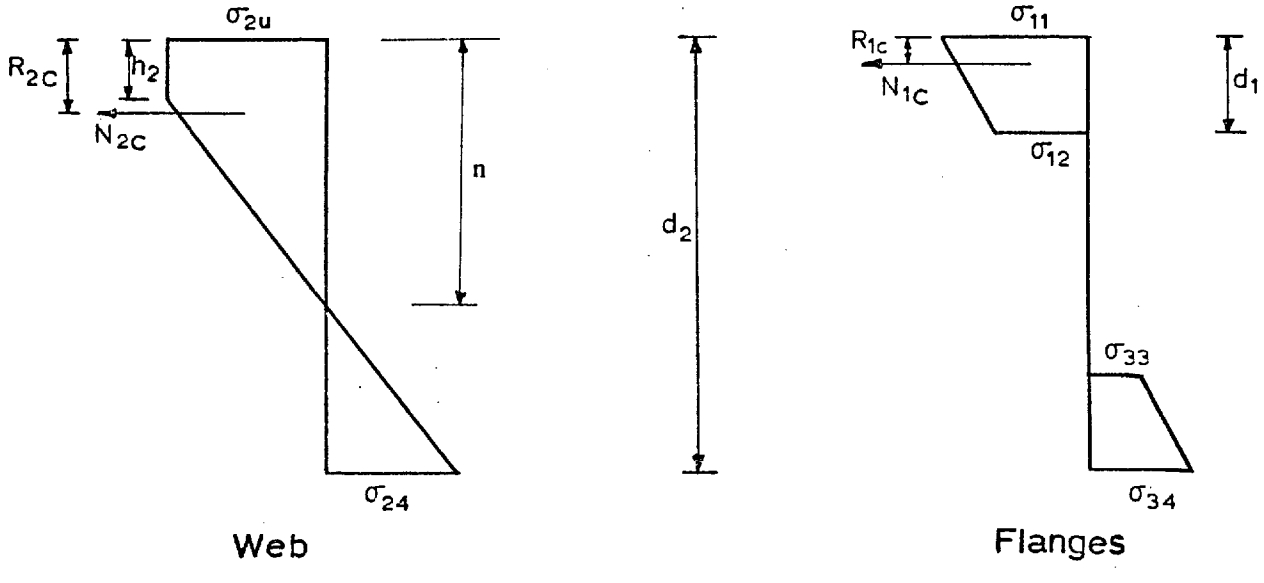


Fig. 2·4 (b). Stress distribution; Linear σ-ε timber, non linear plywood

$$N_{2c} = \tfrac{1}{2}b_2\sigma_{2u}(n+h_2) \quad ; \quad R_{2c} = \frac{(h_2^2+n^2+nh_2)}{3(h_2+n)}$$

replace equations for N_1', N_1'', R_1' & R_1'' by the following equations for N_{1c} and R_{1c} in equations 2.10 and 2.11.1 - 2.10(a)

$$N_{1c} = \tfrac{1}{2}(\sigma_{11}+\sigma_{12})b_1d_1 \quad ; \quad R_{1c} = \frac{d_1}{3}\,\frac{(2\sigma_{12}+\sigma_{11})}{(\sigma_{12}+\sigma_{11})}$$

If $\varepsilon_{11} \leq \varepsilon_{1y}$, then the assumed stress distribution is correct, and is then adopted.

But if $\varepsilon_{11} > \varepsilon_{2y}$, distributions according to fig.2.2(c) are incorrect and abandoned and those corresponding to fig.2.2(d) are adopted, refer to section 4.2.4.

4.2.4 Non-linear $\sigma - \varepsilon$ timber and plywood

Reference in the following derivation is made to fig.2.2(d) and fig.2.4(c).

A procedure similar to that used in section 4.2.2 is adopted. The following changes in equations 2.4, 2.5, 2.6, 2.8, 2.9 and 2.10 will make the procedure compatible with the assumed stress distributions.

(1) Equations 2.4 will read the same as given in section 4.2.2 with the exception of the following

$$\sigma_{21} = \sigma_{2u} \qquad 2.4(b)$$

(2) Equations 2.5 will read the same as given in section 4.2.2 with the exception of the following

$$h_2 = n - \frac{\varepsilon_{2y}}{\theta} \qquad 2.5(b)$$

(3) Equations 2.6 will read as follows

$$C = \sigma_{2u} b_2 h_2 + \tfrac{1}{2}\sigma_{2u} b_2 (n-h_2) + \tfrac{1}{2}(\sigma_{1u}+\sigma_{12})(d_1-h_1)b_1 + \sigma_{1u} h_1 b_1$$

$$= \tfrac{1}{2} b_1 E_1 \theta \left[-n^2 + n\left(2E_{21}\beta_{21}\frac{\varepsilon_{2y}}{\theta} + 2\frac{\varepsilon_{1y}}{\theta} + 2d_1\right) - \left(E_{21}\beta_{21}\left(\frac{\varepsilon_{2y}}{\theta}\right)^2 + \left(\frac{\varepsilon_{1y}}{\theta}\right)^2 + d_1^2\right)\right] \qquad 2.6(b)$$

(4) Equation 2.8 will read as follows:

$$(E_{13}\beta_{13}+E_{23}\beta_{23})n^2 - 2\left(E_{13}\beta_{13}d_1 + E_{23}\beta_{23}d_2 + d_3 + E_{13}\beta_{13}\frac{\varepsilon_{1y}}{\theta} + E_{23}\beta_{23}\frac{\varepsilon_{2y}}{\theta}\right)n$$

$$+ E_{13}\beta_{13}d_1^2 + E_{23}\beta_{23}d_2^2 - d_3^2 + 2d_2d_3 + E_{13}\beta_{13}\left(\frac{\varepsilon_{1y}}{\theta}\right)^2 + E_{23}\beta_{23}\left(\frac{\varepsilon_{2y}}{\theta}\right)^2 = 0 \qquad 2.8(b)$$

(5) Equation 2.9 will read the same as given in section 4.2.2 with the exception of the following:

$$a = (E_{13}\beta_{13}+E_{23}\beta_{23})$$

$$b = E_{13}\beta_{13}d_1 + E_{23}\beta_{23}d_2 + d_3 + E_{13}\beta_{13}\frac{\varepsilon_{1y}}{\theta} + E_{23}\beta_{23}\frac{\varepsilon_{2y}}{\theta}$$

$$c = E_{13}\beta_{13}d_1^2 + E_{23}\beta_{23}d_2^2 - d_3^2 + 2d_2d_3 + E_{13}\beta_{13}\left(\frac{\varepsilon_{1y}}{\theta}\right)^2 + E_{23}\beta_{23}\left(\frac{\varepsilon_{2y}}{\theta}\right)^2 \qquad 2.9(b)$$

(6) Equations 2.10 will read the same as given in section 4.2.2 with the exception of the following:

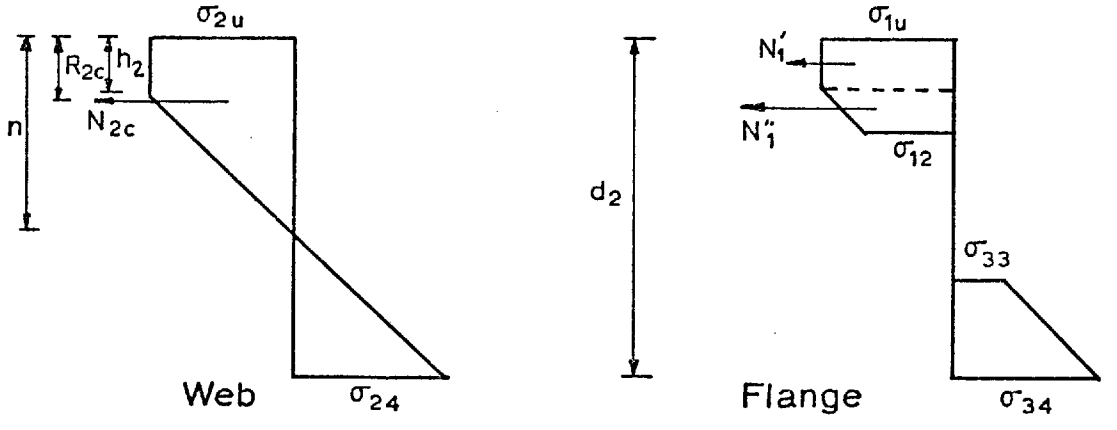


Fig. 2·4(c). Stress distribution; Non linear σ - ε plywood and timber

$$N_{2c} = \tfrac{1}{2} b_2 \sigma_{2u} (n+h_1) \quad ; \quad R_{2c} = \frac{(h_2^2+n^2+nh_2)}{3(h_2+n)} \qquad 2.10(b)$$

4.3 Bending deflection

4.3.1. Governing differential equation

Having found the correct stress distributions across the depths of the beams at different sections along the beam and hence curvatures, then the bending deflection may be calculated.

Assuming small deflection, then bending deflection may be calculated by integrating equation 2.12 along the whole span and applying the relevant boundary conditions.

$$\frac{d^2w}{dx^2} = -\theta \qquad - 2.12$$

4.3.2 Analytical solution

Analytical solutions for deflections may be found if a linear $\sigma - \epsilon$ relationship is assumed over the whole span of the beam, then θ is given by equation 2.1.

e.g. (i) for a simply supported beam loaded with uniformly distributed load (p per unit length) over the whole span, we get

$$w = \frac{pL^4}{24\,EI}\left[\frac{x}{L} - 2\left(\frac{x}{L}\right)^3 + \left(\frac{x}{L}\right)^4\right] \qquad - 2.13$$

(ii) for a simply supported beam under four point loading at $\frac{1}{3}$ span loaded with a total load of magnitude P, we get

$$w = \frac{PL^3}{12EI}\left(-\left(\frac{x}{L}\right)^3 + \left[\frac{x}{L} - \frac{2}{3}\right]^3 + \left[\frac{x}{L} - \frac{1}{3}\right]^3 + \frac{2}{3}\frac{x}{L}\right) \qquad - 2.14$$

where, in eqn. 2.14:

negative values of square brackets are omitted when substituting values of x

i.e. at mid span x = L/2, first square bracket is omitted and

$$w = \frac{23}{1296}\quad\frac{PL^3}{EI} \qquad - 2.14(a)$$

4.3.3 Finite difference formulation of the problem

A more general approach which is valid for any kind of loading, boundary conditions, support conditions and $\sigma - \epsilon$ relationships is by applying a finite difference approach.

The generalised formulation of the problem over the whole span may be given by equation 2.12 and satisfying the following boundary conditions, refer to fig.2.6.

$$w\ (0) = k_1$$

$$w\ (L) = k_{m+1}$$

where: k_1 and k_{m+1} are parameters depending on support conditions, ie for rigid supports $k_1 = k_{m+1} = 0$

Also θ in equation 2.12 may be found at any section along the span corresponding to the appropriate stress and strain distributions as shown in sections (4.2.1 - 4.2.4).

The finite difference formulation of the problem may be obtained by dividing the span into intervals of equal lengths H and obtaining the

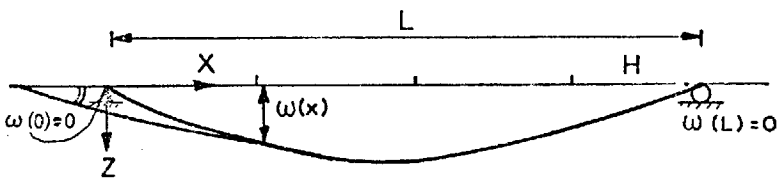


Fig. 2·6. Deflected shape of a simply supported beam

central difference approximation of the second derivative at any point along the span excluding the boundary points. The central difference approximation of the second derivative is given by many authors as:

$$f''(x_i) = \frac{1}{H^2}\left[f(x_i+H) - 2f(x_i) + f(x_i-H)\right] + O(H^2) \qquad - 2.15$$

where: $O(H^2)$ is the truncation error function

$i = 2, \ldots m$

$m = \frac{L}{H}$

The problem formulation over the whole span at intervals of H and including the boundary points is given by:

$$\begin{aligned} w_1 &= k_1 \\ w_1 - 2w_2 + w_3 &= -H^2\theta_2 \\ w_{i-1} - 2w_i + w_{i+1} &= -H^2\theta_i \\ w_{m+1} &= k_{m+1} \end{aligned} \qquad - 2.16$$

OR

$$\begin{bmatrix} 1 & 0 & 0 & 0 & \cdots & & 0 \\ 1 & -2 & 1 & 0 & \cdots & & 0 \\ 0 & 1 & -2 & 1 & \cdots & & \\ & & \vdots & & \cdots & & 0 \\ 0 & 0 & 0 & 0 & 1 & -2 & 1 \\ 0 & 0 & 0 & 0 & 0 & 0 & 1 \end{bmatrix} \begin{bmatrix} w_1 \\ w_2 \\ w_3 \\ \vdots \\ w_m \\ w_{m+1} \end{bmatrix} = \begin{bmatrix} k_1 \\ k_2 \\ k_3 \\ \vdots \\ k_m \\ k_{m+1} \end{bmatrix}$$

where: $k_i = -H^2\theta_i$

$i = 2, \ldots m$

For a simply supported beam on rigid supports $k_1 = k_{m+1} = 0$

and hence above matrix reduces to

$$\begin{bmatrix} -2 & 1 & 0 & \cdots & & 0 \\ 1 & -2 & 1 & \cdots & & 0 \\ & \vdots & & \cdots & & 0 \\ & \cdot & & 1 & -2 & 1 \\ 0 & 0 & 0 & \cdots & 1 & -2 \end{bmatrix} \begin{bmatrix} w_2 \\ w_3 \\ \cdot \\ \cdot \\ \cdot \\ w_m \end{bmatrix} = \begin{bmatrix} k_2 \\ k_3 \\ \cdot \\ \cdot \\ \cdot \\ k_m \end{bmatrix}$$

OR $[A]\ [w] = [k]$

which is a banded matrix with the following chracteristics:

(1) all $|i - j| > 1$ elements $= 0$

(2) all diagonal elements $= -2$

(3) all other elements $= 1$

Since it is a feature of the above matrix that each row or column at most involve three active elements, then the method of substitution and elimination is chosen and also it provides higher accuracy and less problems than when inverting matrix $[A]$.

The truncation error in the difference formula for the derivatives is $O(H^2)$ and solution of equation (2.16) is an approximation to the true solution. The truncation error approximately varies with the square of the interval H, i.e. if $H' = \frac{1}{2}H$, then truncation error when H' is chosen, is approximately reduced by $\frac{1}{4}$.

A computer sub-program, based on the above finite difference approach, has been written to solve the problem. In the solution of the set of equations, it is found that a Harwell sub-program MA07A supplied by Imperial College computer centre library is more efficient than that

written by the author and hence MA07A is adopted. MA07A uses a similar method of solution to that used by the author.

4.4 Web shear stress distribution

Webs have been assumed to be thick enough to prevent web shear failures. To check the magnitude of web shear stresses at different load levels their calculation will be assumed to follow a linear $\sigma - \varepsilon$ relationship which results in linear direct stress distribution across the depths of timber and plywood. The maximum web shear stress corresponding to this linear direct stress distribution occurs at the neutral axis and may be given by equation 2.17.

$$\tau_{xz} = \frac{V}{b_2} \frac{\bar{EF}}{\bar{EI}} \qquad - 2.17$$

where $\bar{EF}$ = First moment of area of all components above or below the neutral axis about the neutral axis of the beam.

4.5 Flange-web shear stress distribution

Similar to the calculation of web shear stress, calculation of flange-web shear stress at the interface of timber and plywood is based on linear $\sigma - \varepsilon$ relationship and is given by the following formula.

$$\tau_{yx\,1} = \frac{V}{2d_1} \frac{E_1 F_1}{\bar{EI}}$$

$$\tau_{yx\,3} = \frac{V}{2d_3} \frac{E_3 F_3}{\bar{EI}} \qquad - 2.18$$

where $\tau_{yx\ 1}$ = Flange web shear stress at the interface between the solid timber and plywood of the top flange

$\tau_{yx\ 3}$ = Flange web shear stress at the interface between the solid timber and plywood of the bottom flange

F_1 = First moment of area of the top timber flange about the neutral axis

F_3 = First moment of area of the bottom timber flange about the neutral axis

4.6 Computer program

A computer program is written to solve for strain and stress distributions at different sections along the beam for any loading condition, also curvatures, deflections, web shear and flange web shear stresses are found as indicated in sections 4.3, 4.4 and 4.5. A flow chart of this program is given in the appendix. A general description of this program may be summarised in the following :

(1) To read and check data, i.e. material properties and geometry of the section, loading conditions, interval length (H), accuracy (ξ), etc.

(2) To find section properties, i.e. A_1, A_3 , etc.

(3) To find moments and shear forces at desired nodes along span.

(4) Starting at the left hand support, stress distributions at the desired nodes are found and stored following an iterative procedure similar to that mentioned in sections 4.2.2 - 4.2.4. Also curvatures at the desired nodes are found and stored.

(5) Having found curvatures at the desired nodes along the beam, deflections are found at these nodes by applying the finite difference routine as indicated in section 4.3.3. These deflections are stored.

(6) Web shear and flange web shear stresses are calculated as indicated in sections 4.4 and 4.5.

(7) To write stress and strain distributions across the depths of beam, deflections,web shear and flange web shear stresses at the desired nodes.

Chapter 5 Semi-rigid plywood web I-beams

5.1 Additional assumptions

The assumptions mentioned in section 3.2 will apply together with the following ones for the analysis of semi-rigid plywood web I-beams.

(1) Nail connection between flange and web is assumed to be continuous along the length of the beam.

(2) Shear transfer between flange and web takes place at centre of gravity of joint.

(3) The flange and web deflect equal amounts at all points along their length and to the same curvature.

(4) Friction between flange and web is neglected.

5.2 Stress-strain relationship and implied stress distribution

The idealized $\sigma - \varepsilon$ relationships for timber and plywood in tension and compression given by figs.2.1 may produce any of the stress distributions across the depths of the top and bottom timber flanges and plywood web, at different load levels and sections along the beam, given in fig.2.7.

It is noted in fig.2.7 that non-linear $\sigma - \varepsilon$ relationship is not considered for timber in compression in the bottom flange as it will be assumed that the compressive strains in the bottom flange will not exceed the compressive yield strain of bottom flange timber.

5.3 Flange web force - displacement relationship

The joint load-slip ($Q - \delta$) relationship is given by the following equation, refer to fig.2.8:

$$Q = k_{sf} k_{\emptyset} f(\delta)$$

where: k_{sf} = species factor depending on the timber and plywood

$k_{\emptyset}$ = nail diameter factor

$f(\delta)$ = displacement function

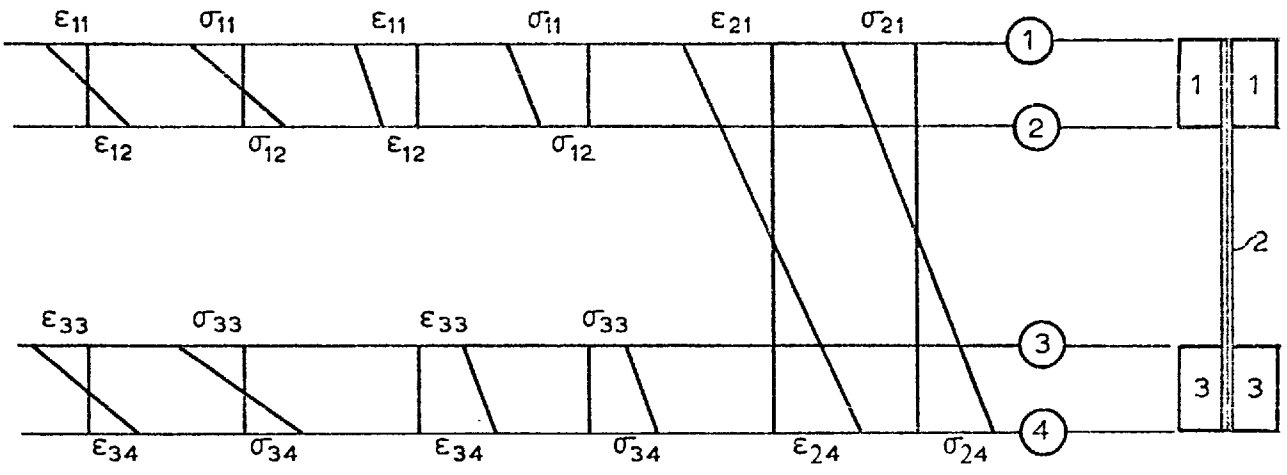
Two displacement functions are considered in this thesis.

5.3.1 Linear displacement function

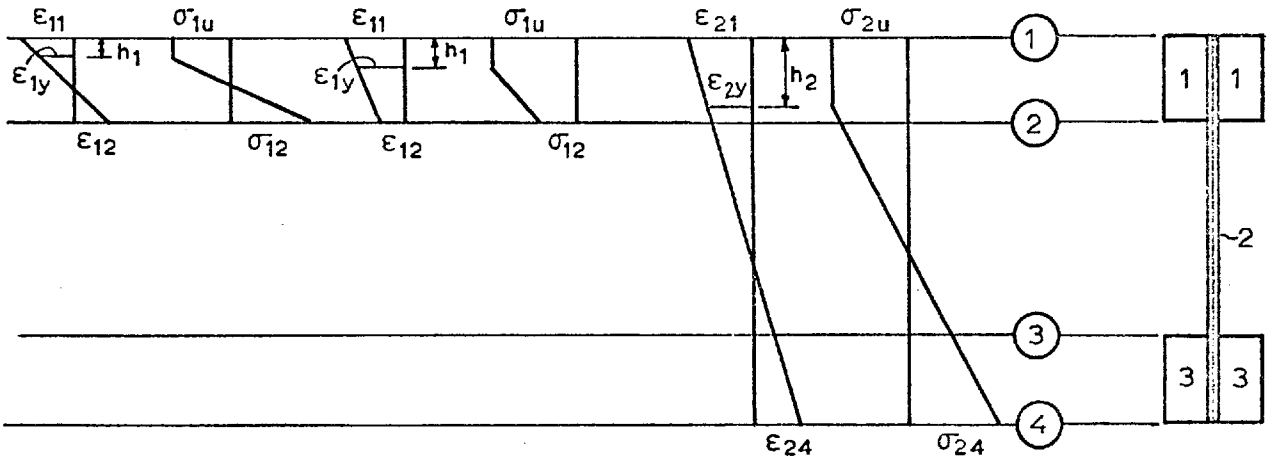
In this case the $Q - \delta$ relationship is given by:

$$Q = k\delta \qquad - 2.19$$

where: $k = k_{sf} k_{\emptyset}$



(a) Linear σ - ε timber and plywood



(b) Non linear σ - ε timber and plywood in compression

Fig. 2·7 Strain and stress distributions for the semi rigid beam

k may be found by considering experimental results for timber to plywood joints tested and finding the slopes of straight lines OA, OB, OC (fig. 2.8) such that an approximation of the joint slip (δ) at certain load levels may be found, i.e. say straight lines OA, OB, OC may be assumed

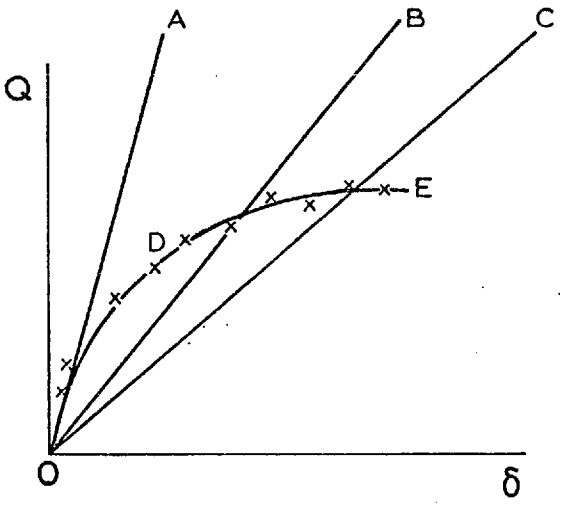


Fig. 2·8. Q - δ relationship for a timber to plywood nailed joint

to describe the behaviour of the joint Q - δ relationships at low, moderate and high load levels respectively.

5.3.2 Non linear displacement function

Mack (1966) obtained equation 2.20 by fitting experimental results of load per nail and the corresponding slip for timber to plywood nailed joints.

$$Q = k_{sf} k_{\phi} (4.1\delta + 0.59)(1 - e^{-75\delta}) \qquad - 2.20$$

where $k_{\phi} = 520\phi^{1.75}$ - 2.20(a)

Equation 2.20 is adopted in this thesis to describe the $Q - \delta$ relationship, curve ODE fig.2.8, of a timber to plywood joint. k_{sf} is found in this thesis by testing timber to plywood joints and fitting the results obtained to equation 2.20.

5.4 Generalized governing simultaneous differential equations

5.4.1 Derivation of governing equations

In the following derivation reference is made to fig.2.9.

Strain distribution across depth of any member subjected to known values of direct force and moment and corresponding to a known $\sigma - \varepsilon$ relationship can be found, refer to section 5.5.1.

$$\varepsilon = f(M, N)$$

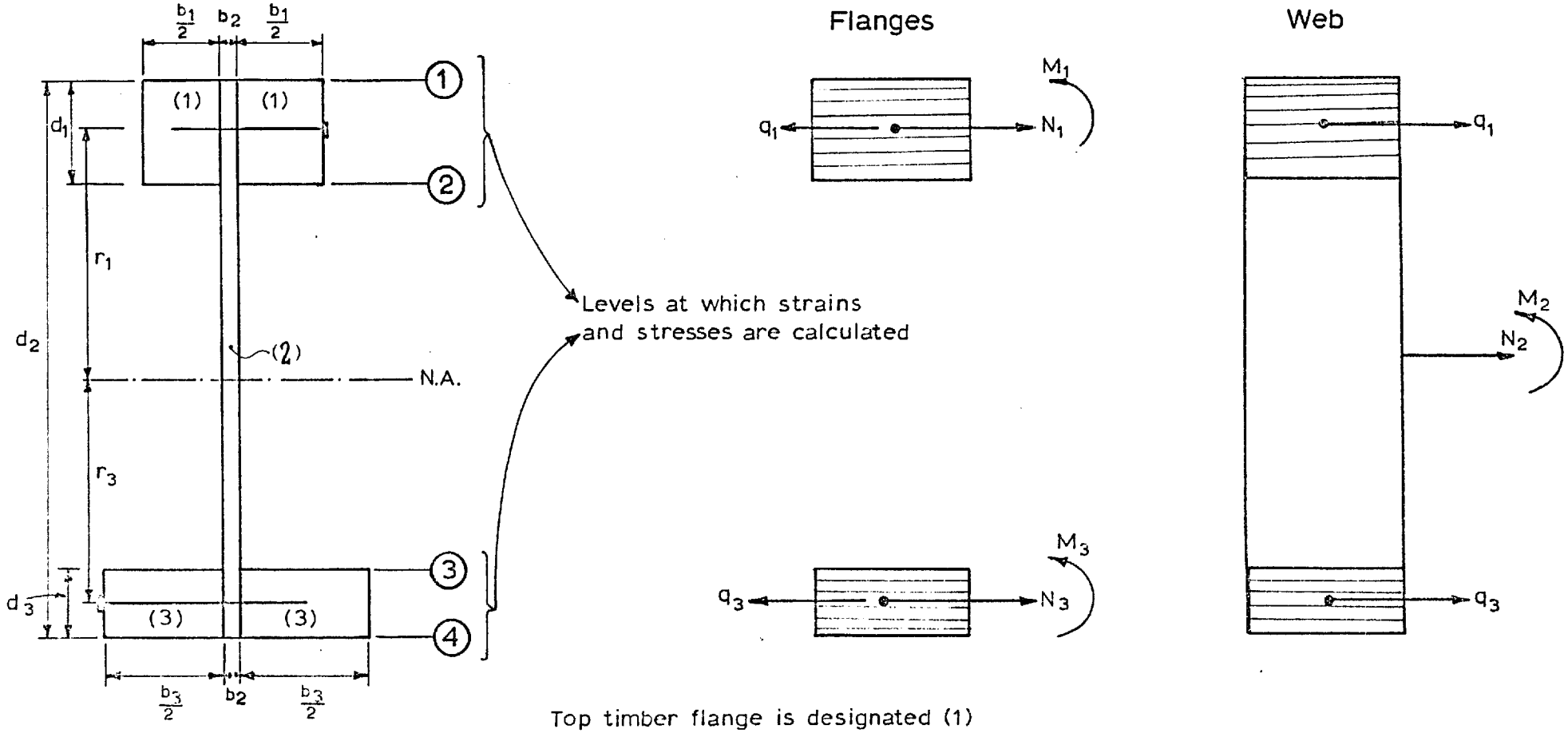
Hence strain in top timber flange may be expressed as:

$$\varepsilon_1 = f(M_1, N_1)$$

and that in plywood web may be expressed as :

$$\varepsilon_2 = f(M_2, N_2)$$

Hence strain difference between top flange and plywood web at point of shear transfer may be expressed as :



Top timber flange is designated (1)
Bottom timber flange is designated (3)
Plywood web is designated (2)
Strain or stress is designated $\varepsilon_{i,j}$ or $\sigma_{i,j}$
where i = number designated to beam part under consideration e.g. top flange (1)
j = number designated to level at which calculation is made

Fig. 2·9. Forces at any section across the depth of a semi-rigid plywood-web I-beam

strain difference $= \varepsilon_1 - \varepsilon_2 = f(M_1, M_2, N_1, N_2)$

Noting

$$N_2 = f(N_1, N_3)$$

$$M_1 = f(M_{ex}, N_1, N_3)$$

$$M_2 = f(M_{ex}, N_1, N_3)$$

Then

$$\varepsilon_1 - \varepsilon_2 = f(M_{ex}, N_1, N_3)$$

and since $\frac{d\delta}{dx}$ = strain difference

Then $$\frac{d\delta_1}{dx} = f(M_{ex}, N_1, N_3) \quad - \quad 2.21$$

similarly $$\frac{d\delta_3}{dx} = g(M_{ex}, N_1, N_3) \quad - \quad 2.22$$

where δ_1 : slip between top timber flange and plywood web

δ_3 : slip between bottom timber flange and plywood web

Also $$Q = qs = k_{sf} k_{\emptyset} f(\delta)$$

$$\frac{dN}{dx} = q = \frac{k_{sf} k_{\emptyset}}{s} f(\delta)$$

Then $$\frac{dN_1}{dx} = \frac{k_{sf1} k_{\emptyset 1}}{s_1} f(\delta_1) \quad - \quad 2.23$$

$$\frac{dN_3}{dx} = \frac{k_{sf3} k_{\emptyset 3}}{s_3} f(\delta_3) \quad - \quad 2.24$$

5.4.2 Features of governing equations

The problem is described by the generalized differential equations (2.21 - 2.24) in terms of the variables N_1, N_3, δ_1 & δ_3. The solution of the problem is found if the previous differential equations are solved for N_1, N_3, δ_1 & δ_3 at different points along the beam and the boundary conditions are satisfied. The following features of the governing differential equations may facilitate the evaluation of the model at different points along the span and also, in some cases, its solution.

(1) The governing differential equations (d.e.) 2.21 - 2.24 may be linear, partially non-linear or totally non-linear depending on whether $Q - \delta$ relationship for joint is linear or non-linear and also whether $\sigma - \varepsilon$ relationship for timber and plywood in compression is linear or non-linear.

(a) Linear $Q - \delta$ relationship:

In this case equations 2.23 and 2.24 are linear and depending on whether $\sigma - \varepsilon$ relationship for timber and/or plywood in compression is assumed to be linear or non-linear, the governing d.e. may be classified as linear or partially non-linear respectively; since for the first case equations 2.21 and 2.22 are linear and analytical solutions are possible while for the latter case equations 2.21 and 2.22 are non-linear and some numerical procedure is required to evaluate them at any point along the beam.

(b) Non-linear $Q - \delta$ relationship

In this case equations 2.23 and 2.24 are non-linear and depending on whether $\sigma - \varepsilon$ relationship for timber and/or plywood in compression is assumed to be linear or non-linear, the governing d.e. may be classified as partially non-linear or totally non-linear respectively; since for the first case equations 2.21 and 2.22 are linear while for the latter case all equations 2.21 - 2.24 are non-linear and a numerical procedure is required to evaluate equations 2.21 and 2.22 and to solve the model over the whole span.

(2) Solution for the rigid case is obtained by setting nail spacing to a small value or $s_1 = s_3 \neq 0$, say 0.01, as this will make $\frac{dN_1}{dx} = \frac{dN_3}{dx}$ very large and hence forcing strain differences between flanges and web to be very small.

5.5 Governing simultaneous differential equations for a linear flange-web force-displacement equation

A linear $Q - \delta$ relationship of the form described by equation 2.19 is assumed to describe the load-slip curves of the joints and hence equations 2.23 and 2.24 will read as follows:

$$\frac{dN_1}{dx} = \frac{k_1}{s_1} \delta_1 \qquad - 2.23(a)$$

$$\frac{dN_3}{dx} = \frac{k_3}{s_3} \delta_3 \qquad - 2.24(a)$$

Evaluation of equation 2.23(a) and 2.24(a) for any point along the beam is possible for given values of δ_1 and δ_3. To evaluate equations 2.21 and 2.22 both linear and non-linear $\sigma - \varepsilon$ material behaviour should be considered.

5.5.1 Linear $\sigma - \varepsilon$ timber and plywood in compression

The stress distributions across the depths of top timber flange, plywood web and bottom timber flange relevant to the assumed $\sigma - \varepsilon$ relationships are given by fig.2.7(a).

Referring to figs.2.9 and 2.7(a) we get the following equations. It should be noted here that N_1 and N_3 are treated as positive values and that they take their respective correct signs in the final equations.

$$N_1 = \tfrac{1}{2}E_1A_1(\varepsilon_{12} + \varepsilon_{11})$$

$$M_1 = \frac{E_1I_1}{d_1}(\varepsilon_{12} - \varepsilon_{11}) \qquad \Big| \; - 2.25$$

OR $$\varepsilon_{11} = \frac{N_1}{E_1A_1} - \frac{M_1d_1}{2E_1I_1} \qquad - 2.26(a)$$

$$\varepsilon_{12} = \frac{N_1}{E_1A_1} + \frac{M_1d_1}{2E_1I_1} \qquad - 2.27(a)$$

Similarly:

$$\varepsilon_{21} = \frac{N_2}{E_2A_2} - \frac{M_2d_2}{2E_2I_2} \qquad - 2.26(b)$$

$$\varepsilon_{24} = \frac{N_2}{E_2A_2} + \frac{M_2d_2}{2E_2I_2} \qquad - 2.27(b)$$

$$\varepsilon_{33} = \frac{N_3}{E_3A_3} - \frac{M_3d_3}{2E_3I_3} \qquad - 2.26(c)$$

$$\varepsilon_{34} = \frac{N_3}{E_3A_3} + \frac{M_3d_3}{2E_3I_3} \qquad - 2.27(c)$$

It is worth mentioning that all these strains may be evaluated if values of N_1, N_2, N_3, M_1, M_2 & M_3 are given and that the strain distribution relevant to the assumed stress distributions are dependent on the magnitude and sign of these variables.

In the case considered in this thesis, the joints centre of gravity lies at mid-depth of the top and bottom flanges, hence the strain difference between web and flange is assumed to occur at these points, i.e.

$$\frac{d\delta_1}{dx} = \frac{\varepsilon_{12} + \varepsilon_{11}}{2} - \left[\varepsilon_{24} - \frac{2d_2 - d_1}{2d_2}(\varepsilon_{24} - \varepsilon_{21})\right] \qquad - 2.28$$

Noting:

$$M_{ex} = M_1 + M_2 + M_3 + N_3(r_1 + r_3) + N_2 r_1 \qquad - 2.29$$

and for simply supported beam

$$\Sigma N = 0 \text{ , or } N_2 = -(N_1 + N_3)$$

$$\theta = -\frac{d^2w}{dx^2} = \frac{M_1}{E_1 I_1} = \frac{M_2}{E_2 I_2} = \frac{M_3}{E_3 I_3} = \frac{M_{ex} - N_3(r_1 + r_3) + N_2 r_1}{\Sigma EI} \qquad - 2.30$$

and substituting values of ε_{11}, ε_{12}, ε_{21} & ε_{24} from equations 2.26 (a and b) and 2.27 (a and b), we get:

$$\frac{d\delta_1}{dx} = N_1\left(\frac{1}{E_1 A_1} + \frac{1}{E_2 A_2} + \frac{r_1^2}{\Sigma EI}\right) + N_3\left(\frac{1}{E_2 A_2} - \frac{r_1 r_3}{\Sigma EI}\right) + \frac{M_{ex}}{\Sigma EI} r_1$$

Similarly it may be found that:

$$\frac{d\delta_3}{dx} = N_1\left(\frac{1}{E_2A_2} - \frac{r_1r_3}{\Sigma EI}\right) + N_3\left(\frac{1}{E_3A_3} + \frac{1}{E_2A_2} + \frac{r_3^2}{\Sigma EI}\right) - \frac{M_{ex}}{\Sigma EI} r_3$$

OR
$$\frac{d\delta_1}{dx} = K_a N_1 + K_b N_3 + K_c M_{ex}(x) \qquad - 2.21(a)$$

$$\frac{d\delta_3}{dx} = K_b N_1 + K_d N_3 - K_e M_{ex}(x) \qquad - 2.22(a)$$

where $K_a = \frac{1}{E_1A_1} + \frac{1}{E_2A_2} + \frac{r_1^2}{\Sigma EI}$

$$K_b = \frac{1}{E_2A_2} - \frac{r_1r_3}{\Sigma EI}$$

$$K_c = \frac{r_1^2}{\Sigma EI} \quad ; \quad K_e = \frac{r_3^2}{\Sigma EI}$$

$$K_d = \frac{1}{E_3A_3} + \frac{1}{E_2A_2} + \frac{r_3^2}{\Sigma EI}$$

Equations 2.21(a), 2.22(a), 2.23(a) and 2.24(a) describe the linear model and may be evaluated at any point along the beam if values of N_1, N_3, δ_1 & δ_3 are given. The procedure to solve the model along the whole span is given in section 5.7 and an analytical solution is possible and is described in the same section.

5.5.2 Non-linear $\sigma - \varepsilon$ timber and plywood in compression

The stress distributions across the depths of top timber flange and plywood web for timber and plywood in compression relevant to the assumed $\sigma - \varepsilon$ relationships are given by fig.2.7(b).

Equations 2.21 and 2.22 cannot be evaluated at any point along the beam using analytical equations as in the case of linear $\sigma - \varepsilon$ relationships, and hence the following iterative procedure is adopted to evaluate equations 2.21 and 2.22 for known values of N_1 and N_3.

Step (i)

(1) Assume linear $\sigma - \varepsilon$ relationships for timber and plywood in compression, fig.2.7(a), and also noting that a linear $\sigma - \varepsilon$ relationship is always assumed for timber in tension.

(2) Assume an initial curvature θ_o and then find M_1, M_2 and M_3 from equation 2.30.

(3) For known values of N_1, N_3 (and hence N_2) and also the calculated values of M_1, M_2 and M_3 from (1) above, find the strains ε_{11}, ε_{12}, ε_{21}, ε_{22}, ε_{33} & ε_{34} from equations 2.26(a, b & c), 2.27(a, b & c), 2.27(a, b & c). Also the corresponding stresses are found.

Step (ii)

If $\varepsilon_{11} > \varepsilon_{1y}$ and $\varepsilon_{21} \leq \varepsilon_{2y}$ then linear stress distribution assumed for the flange is incorrect and is abandoned and a non-linear stress distribution is adopted, refer to fig.2.7(b).

The procedure is as follows:

(1) Assume the same value of the initial curvature θ_o as used in step (i)

(2) M_2 and M_3 are calculated from eqn.2.30.

(3) M_1 is calculated as indicated by one of the following two cases, refer to fig.2.7(b).

Case (1) Reference is made here to fig.2.10.

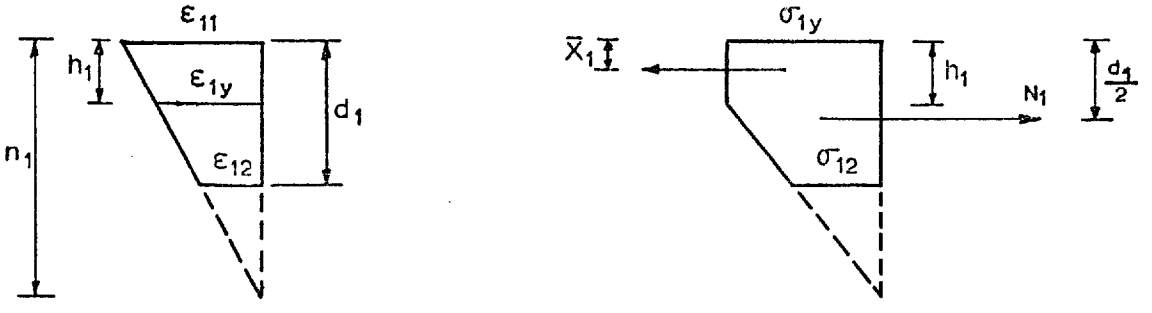


Fig. 2·10. Case(1); Non linear stress distribution for timber in compression flange

A similar procedure to that of section 4.2.2, steps i-v, to find the position of the neutral axis is adopted. n_1 is found to be given by:

$$n_1 = b - \sqrt{[b^2 - c]} \qquad - 2.31$$

where $$b = d_1 + \frac{\varepsilon_{1y}}{\theta_o}$$

$$c = d_1^2 + \left(\frac{\varepsilon_{1y}}{\theta_o}\right)^2 - \frac{2N_1}{E_1 b_1 \theta_o}$$

$$h_1 = n_1 - \frac{\varepsilon_{1y}}{\theta_o} \qquad - 2.32$$

$$\varepsilon_{11} = n_1\theta_o \quad , \quad \varepsilon_{12} = (n_1 - d_1)\theta_o$$

$$\sigma_{12} = E_1\theta_o(n_1 - d_1) \qquad - 2.33$$

$$\bar{X}_1 = \frac{[3\sigma_{1u}h_1^2 + d_1(d_1-h_1)(2\sigma_{12}+\sigma_{1u})]}{3[2\sigma_{1u}h_1+(d_1-h_1)(\sigma_{12}+\sigma_{1u})]} \qquad - 2.34$$

$$M_1 = \frac{N_1}{2}(2\bar{X} - d_1) \qquad - 2.35$$

If $n_1 < d_1$, then distribution according to Case (1) is abandoned and that according to Case (2) is adopted.

Case (2) Reference is made here to fig.2.11.

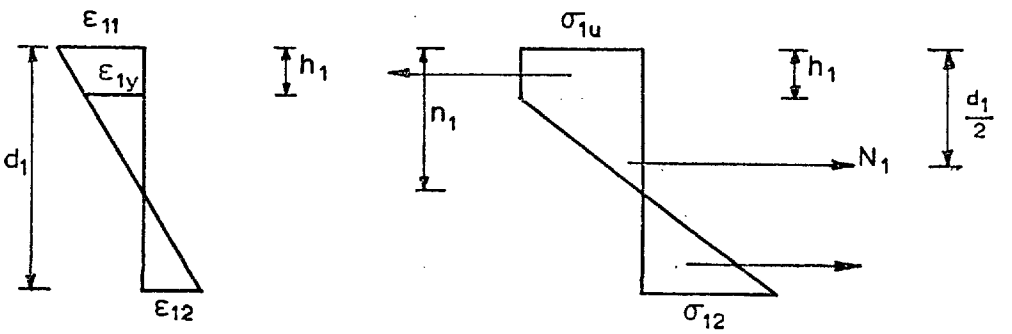


Fig. 2·11. Case (2); Non linear stress distribution for timber in compression flange

n_1 and h_1 are calculated from equations 2.31 and 2.32 where,

$$\varepsilon_{11} = n\theta_o \quad , \quad \varepsilon_{12} = (d_1-n_1)\theta_o \quad , \quad \sigma_{12} = E_1\theta_o(d-n_1) \qquad - 2.36$$

$$M_1 = \tfrac{1}{2}\sigma_{1u}h_1^2 b_1 + \tfrac{1}{6}\sigma_{1u}(n_1-h_1)(n_1+2h_1)b_1 - \tfrac{1}{2}N_1 d_1$$

$$- \tfrac{1}{6}E_1\theta_o(d_1-n_1)^2(2d_1+n_1)b_1 \qquad - 2.37$$

(4) Find internal moment for the whole cross section at any point along the beam from equation 2.29. Check that total moment in section as follows:

$$| M_{ex} - M_{in} | \leq \xi M_{ex} \qquad - 2.38$$

where ξ is thedesired accuracy

If equation 2.38 is not satisfied then a new curvature θ_1 closer to the correct curvature is found in a way similar to that given in section 4.2.2 (step vii-b) for the rigid case. Having found θ_1, the procedure given in step (2) is repeated to find θ_2 closer than θ_1 to the correct curvature and this procedure is repeated several times to find θ_n (where n is number of iterations) such that equation 2.38 is satisfied and hence θ_n is approximately the correct curvature.

(5) ε_{11}, ε_{12} & σ_{12} corresponding to the correct stress distribution have been automatically calculated. They are stored separately.

Step (iii)

If $\varepsilon_{21} > \varepsilon_{2y}$, linear stress distribution assumed for the web in compression is incorrect and is abandoned and a non-linear one is adopted, fig.2.7(b).

(1) From the assumption that flange and web have same curvatures, then initial curvature θ_o is either obtained from step (i) if $\varepsilon_{11} \leq \varepsilon_{1y}$ or from step (ii) if $\varepsilon_{11} > \varepsilon_{2y}$.

(2) M_3 is calculated from equation 2.30. ε_{33}, ε_{34} and corresponding stresses are also calculated.

(3) M_1 may either be calculated as in step (i) if $\varepsilon_{11} \leq \varepsilon_{1y}$ or as in step (ii) if $\varepsilon_{11} > \varepsilon_{1y}$. Also corresponding strains ε_{11} and ε_{12}, and stresses σ_{11} and σ_{12} are calculated.

(4) M_2 is calculated as given by eqn.2.43.

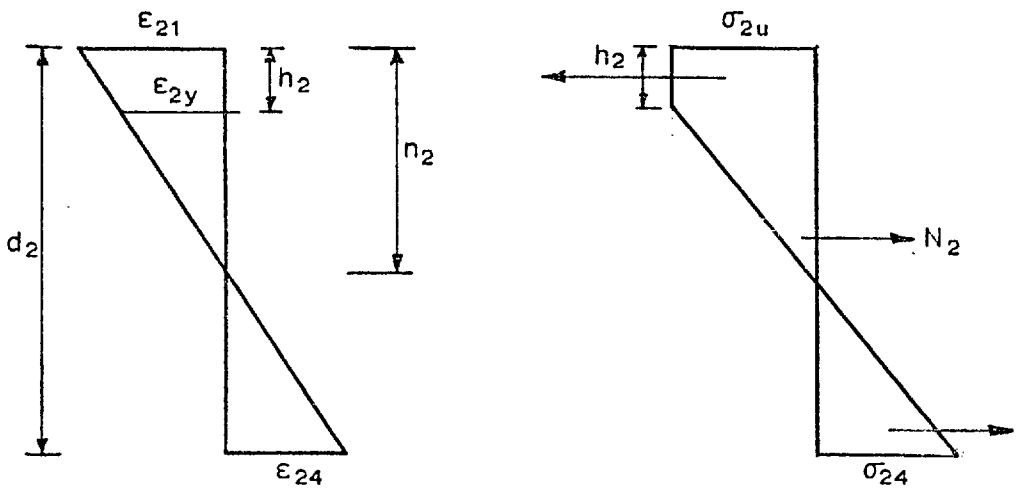


Fig. 2·12. Non linear stress distribution for plywood in compression

Similar to case (1)

$$n_2 = b - \sqrt{[b^2 - c]} \qquad - 2.39$$

where $$b = d_2^2 + \left(\frac{\varepsilon_{2y}}{\theta_o}\right)^2 - \frac{2N_2}{E_2 b_2 \theta_o}$$

$$N_2 = -(N_1+N_3) \quad \text{for no end direct forces i.e. s.s.beam}$$

$$h_2 = n_2 - \frac{\varepsilon_{2y}}{\theta_o} \qquad - 2.40$$

$$\varepsilon_{21} = n_2\theta_o \ , \quad \varepsilon_{24} = (d_2-n_2)\theta_o \ , \quad \sigma_{24} = E_2\theta(d-n_2)\theta_o \qquad - 2.41$$

$$r_1 = n_2 - \frac{d_1}{2} \quad , \quad r_3 = d_2 - n_2 - \frac{d_3}{2} \qquad - 2.42$$

$$M_2 = \tfrac{1}{2}\sigma_{2u} h_2^2 b_2 + \tfrac{1}{6}\sigma_{2u}(n_2-h_2)(n_2+2h_2)b_2 - \tfrac{1}{2}N_2 d_2$$

$$-\tfrac{1}{6}E_2\theta_\phi(d_2-n_2)^2(2d_2+n_2)b_2 \qquad - 2.43$$

(5) Find internal moment for the whole cross section at any point along the span from eqn.2.29 and check equation 2.38, if it is not satisfied a procedure similar to that given in step [(ii) - 4] is implemented until equation 2.38 is satisfied. Also ε_{21}, ε_{24}, and σ_{24} corresponding to the correct stress distribution have been automatically calculated.

Step (iv)

Having determined the correct stress distributions and corresponding stresses and strains in top timber flange, plywood web and bottom timber flange, then the strain difference between the top timber flange and the plywood web and also between the bottom timber flange and the plywood web at the points of shear transfer (in this case at mid depths of both flanges) may be calculated. Hence equations 2.21 and 2.22 are evaluated for given values of N_1 and N_3 at any desired point along the beam.

5.6 Governing simultaneous differential equations for a non-linear flange-web force displacement equation

A non-linear $Q - \delta$ relationship of the form described by eqn.2.20 is assumed to describe the load-slip curves of timber to plywood joints and hence equations 2.23 and 2.24 will read as follows:

$$\frac{dN_1}{dx} = \frac{k_{s1}k_{\phi 1}}{s_1}(4.1\delta_1 + .59)(1 - \bar{e}^{75\delta_1})^{0.6} \qquad - 2.23(b)$$

$$\frac{dN_3}{dx} = \frac{k_{s3}k_{\phi 3}}{s_3}(4.1\delta_3 + .59)(1 - \bar{e}^{75\delta_3})^{0.6} \qquad - 2.24(b)$$

Evaluation of equations 2.23(b) and 2.24(b) at any point along the beam is possible for given values of δ_1 and δ_3.

The two cases of linear and non-linear $\sigma - \varepsilon$ distributions for timber and plywood in compression considered in sections 5.5.1 and 5.5.2 will be considered.

5.6.1 Linear $\sigma - \varepsilon$ timber and plywood in compression

In this case equations 2.21(a) and 2.22(a) will apply and their evaluation at any point along the beam is possible for given values of N_1, N_3 and M_{ex}, refer to section 5.5.1.

5.6.2 Non-linear $\sigma - \varepsilon$ timber and plywood in compression

In this case equations 2.21 and 2.22 will apply and both equations can be evaluated at any point along the beam for known values of N_1, N_3 and M_{ex} following the procedure described in section 5.5.2.

5.7 Analytical solutions of governing differential equations

5.7.1. Limitations to linear stress-strain and force-displacement equations

A linear model is described by equations 2.21(a), 2.22(a), 2.23(a), and 2.24(a). It is described as a linear model because both the $\sigma - \varepsilon$ relationships for timber and plywood in tension and compression and also the $Q - \delta$ relationships for the joint are assumed to be linear at all points along the span and load levels.

Equations 2.21(a) and 2.23(a) may be combined together to give eqn.2.44

$$\frac{s_1}{k_1}\frac{d^2N_1}{dx^2} = K_a N_1 + K_b N_3 + K_c M_{ex}(x) \qquad - 2.44$$

and also eqns. 2.22(a) and 2.24(a) may be combined to give eqn.2.45

$$\frac{s_3}{k_3}\frac{d^2N_3}{dx^2} = K_b N_1 + K_d N_3 - K_c M_{ex}(x) \qquad - 2.45$$

Equations 2.44 and 2.45 may be reduced to one fourth order ordinary linear differential equation with constant coefficients in terms of N_1 or N_3 as follows:

$$\frac{s_1}{k_1}\frac{s_3}{k_3}\frac{d^4N_1}{dx^4} = \left[\frac{s_1}{k_1}K_d + \frac{s_3}{k_3}K_a\right]\frac{d^2N_1}{dx^2} - \left[K_b^2 - K_aK_d\right]N_1$$

$$- \frac{s_3}{k_3}K_c\frac{d^2M_{ex}(x)}{dx^2} + \left[K_cK_d + K_bK_e\right]M_{ex}(x) = 0 \qquad - 2.46(a)$$

$$\frac{s_1}{k_1}\frac{s_3}{k_3}\frac{d^4N_3}{dx^4} - \left[\frac{s_1}{k_1}K_d + \frac{s_3}{k_3}K_a\right]\frac{d^2N_3}{dx^2} - \left[K_b^2 - K_aK_d\right]N_3$$

$$+ \frac{s_1}{k_1}K_e\frac{d^2M_{ex}(x)}{dx^2} - \left[K_aK_e + K_bK_c\right]M_{ex}(x) = 0 \qquad - 2.46(b)$$

equations 2.46(a) and 2.46(b) may be solved for any loading condition and boundary conditions.

Booth (1969) derived equation 2.47 for a symmetrical semi-rigid simply supported beam. His equation,

$$\frac{d^2N_f}{dx^2} - \frac{k}{s}\frac{\overline{EI}}{E_f A_f \Sigma EI} N_f = -\frac{k}{s}\frac{M_{ex}(x)}{\Sigma EI} r \qquad - 2.47$$

may be derived from any of equations 2.44 and 2.45 by substituting for K_a, K_b, K_c, K_d and K_e and also noting the following :

$$s = s_1 = s_3$$

$$k = k_1 = k_3$$

$$r = r_1 = r_3$$

$$E_f = E_1 = E_3$$

$$A_f = A_1 = A_3$$

$$N_f = -N_1 = N_3$$

5.7.2 Solution of governing differential equations in terms of flange force

In this thesis equation 2.47 is solved for a symmetrical semi-rigid simply supported plywood web I-beam under four point loading - refer to fig.2.13.

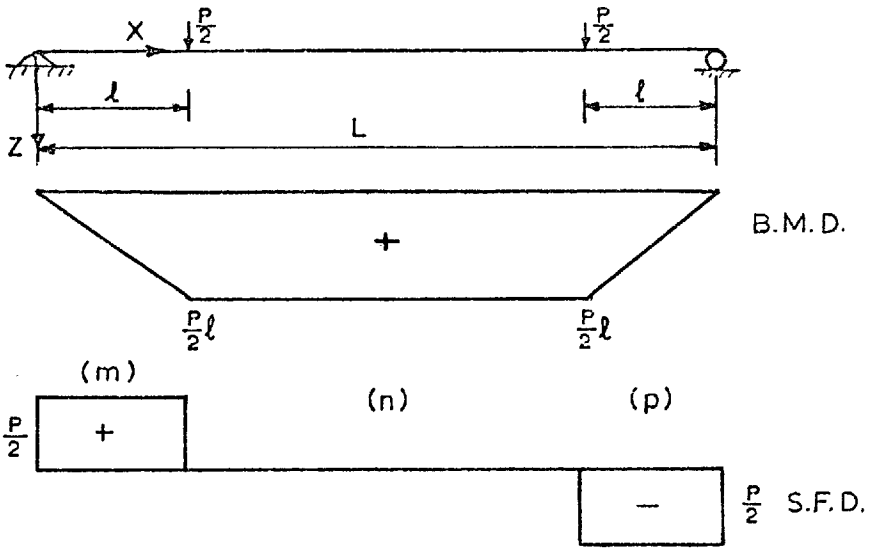


Fig. 2·13. Bending moment and shear force diagrams for a s.s. beam under four point loading

The beam is divided into 3-regions m, n & p as shown in fig.2.13. Equation 2.47 may be rewritten as follows

$$\frac{d^2N_f}{dx^2} - \lambda^2 N_f = -\lambda^2 \frac{E_f A_f}{\Sigma EI} M_{ex}(x) \qquad - 2.47(a)$$

where $\lambda^2 = \frac{1}{C} \frac{\pi^2}{L^2}$

and $C = s \pi^2 E_f A_f \Sigma EI / (kL^2 \overline{EI})$ $\qquad - 2.47(b)$

Solution for equation 2.47(a) along the whole span is given for regions m, n and p separately as follows:

Region (m) - $0 \leq x \leq l$

$$N_{fm} = K_{m1} \text{ Sinh } \lambda x + K_{m2} \text{ Cosh } \lambda x + \frac{E_f A_f}{EI} r \frac{P}{2} x \qquad - 2.48$$

Region (n) - $l \leq x \leq (L - l)$

$$N_{fn} = K_{n1} \text{ Sinh } \lambda x + K_{n2} \text{ Cosh } \lambda x + \frac{E_f A_f}{EI} r \frac{P}{2} l \qquad - 2.49$$

Region (p) - $(L - l) \leq x \leq L$

$$N_{fp} = K_{p1} \text{ Sinh } \lambda x + K_{p2} \text{ Cosh } \lambda x + \frac{E_f A_f}{EI} r \frac{P}{2} (L - x) \qquad - 2.50$$

where K_{m1}, K_{m2}, K_{n1}, K_{n2}, K_{p1}, K_{p2} are constants and may be determined by applying the following boundary conditions

At $x = 0$ $\quad N_{fm} = 0$

At $x = l$ $\quad N_{fm} = N_{fn}$

$$\frac{dN_{fm}}{dx} = \frac{dN_{fn}}{dx}$$

At $x = (L-l)$ $\quad N_{fn} = N_{fp}$

$$\frac{dN_{fn}}{dx} = \frac{dN_{fp}}{dx}$$

At $x = L$ $\quad N_{fp} = 0$

Substituting these boundary conditions in equation 2.48, 2.49 and 2.50, solving and rearranging we get:

$$N_{fm} = \frac{P}{2} \frac{E_f A_f r}{\lambda EI} \left\{ \left[\text{Coth } \lambda L \left(\text{Sinh} \lambda l + \text{Sinh } \lambda (L-l) \right) - \text{Cosh} \lambda (L-l) - \text{Cosh} \lambda l \right] \text{ Sinh} \lambda x + \lambda x \right\} \qquad - 2.48(a)$$

$$N_{fn} = \frac{P}{2} \frac{E_f A_f r}{\lambda EI} \left\{ \left[\text{Coth}\,\lambda L \left(\text{Sinh}\lambda l + \text{Sinh}\lambda(L-l) - \text{Cosh}\lambda(L-l) \right) \right] \text{Sinh}\lambda x - \text{Sinh}\lambda l\, \text{Cosh}\lambda x + \lambda l \right\} \quad - 2.49(a)$$

$$N_{fp} = \frac{P}{2} \frac{E_f A_f r}{\lambda EI} \left\{ \left[\text{Coth}\lambda L \left(\text{Sinh}\,\lambda l + \text{Sinh}\lambda(L-l) \right) \right] \text{Sinh}\lambda x - \left[\text{Sinh}\,\lambda(L-l) + \text{Sinh}\,\lambda l \right] \text{Cosh}\lambda x + \lambda(L-x) \right\} \quad - 2.50(a)$$

Equations 2.48(a) and 2.50(a) are found to be similar and this is evident from symmetry of loading. Accordingly equations for interface shear (q), bending deflection (w_b) etc. are given for regions m and n only.

5.7.3 Deflections due to bending

From eqn.2.30, for $r = r_1 = r_3$ and $N_2 = 0$

$$-\frac{d^2w}{dx^2} = \frac{M_{ex}(x) - 2N_f r}{\Sigma EI} = \frac{M_2}{E_2 I_2} = \frac{M_f}{E_f I_f} \quad - 2.51$$

From 2.47(a) we get

$$N_f = \frac{1}{\lambda^2} \frac{d^2 N_f}{dx^2} + \frac{E_f A_f}{EI} r\, M_{ex}(x) \quad - 2.52$$

substituting N_f from eqn.2.52 in eqn.2.51 and rearranging, we get

$$\frac{d^2w}{dx^2} = -\frac{M_{ex}(x)}{EI} + 2r \frac{s}{k} \frac{E_f A_f}{\Sigma EI} \frac{d^2 N_f}{dx^2} \quad - 2.51(a)$$

substituting values of $M_{ex}(x)$ for regions m, n and p and integrating eqn. 2.51(a), we get

$$\frac{dw_m}{dx} = -\frac{P}{4}\frac{x^2}{EI} + 2r\frac{s}{k}\frac{E_f A_f}{EI}\frac{dN_{fm}}{dx} + G_m$$

$$w_m = -\frac{P}{12}\frac{x^3}{EI} + 2r\frac{s}{k}\frac{E_f A_f}{EI}N_{fm} + G_m x + H_m \qquad - 2.53$$

$$\frac{dw_n}{dx} = -\frac{P}{2}\frac{lx}{EI} + 2r\frac{s}{k}\frac{E_f A_f}{EI}\frac{dN_{fn}}{dx} + G_n$$

$$w_n = -\frac{P}{4}\frac{lx^2}{EI} + 2r\frac{s}{k}\frac{E_f A_f}{EI}N_{fn} + G_{nx} + H_n \qquad - 2.54$$

$$\frac{dw_p}{dx} = \frac{P}{4}\frac{x^2}{EI} - \frac{P}{2}\frac{Lx}{EI} + 2r\frac{s}{k}\frac{E_f A_f}{EI}\frac{dN_{fp}}{dx} + G_p$$

$$w_p = \frac{P}{12}\frac{x^3}{EI} - \frac{P}{4}\frac{Lx^2}{EI} + 2r\frac{s}{k}\frac{E_f A_f}{EI}N_{fp} + G_p x + H_p \qquad - 2.55$$

where G_m, H_m, G_n, H_n, G_p and H_p are constants of integration and may be found by substituting the following boundary conditions

At $x = 0$ $\quad w_m = 0$

$N_{fm} = 0$

At $x = l$ $\quad w_m = w_n$; $\frac{dw_m}{dx} = \frac{dw_n}{dx}$

$N_{fm} = N_{fn}$; $\frac{dN_{fm}}{dx} = \frac{dN_{fn}}{dx}$

At $x = (L-l)$ $\quad w_n = w_p$; $\frac{dw_n}{dx} = \frac{dw_p}{dx}$

$N_{fn} = N_{fp}$; $\frac{dN_{fn}}{dx} = \frac{dN_{fp}}{dx}$

At $x = L$ $\quad w_p = 0$

$N_{fp} = 0$

Substituting values of G_m, H_m, G_n & H_n in 2.54 and 2.55, we get

$$w_m = -\frac{Px^3}{12EI} + \frac{PLl}{4EI}(1 - \frac{l}{L})x + 2r\frac{s}{k}\frac{E_f A_f}{EI}N_{fm} \qquad - 2.54(a)$$

$$w_n = \frac{Pl}{4EI}x^2 + \frac{PLl}{4EI}x - \frac{Pl^3}{12EI} + 2r\frac{s}{k}\frac{E_f A_f}{EI}N_{fn} \qquad - 2.55(a)$$

3.7.4 Bending stresses in the flanges

$$\sigma_f = -\sigma_{11} = \sigma_{34}$$

$$\sigma_f = \frac{M_f}{I_f}\frac{d_f}{2} + \frac{N_f}{A_f}$$

using equation 2.51, we get

$$\sigma_f = \frac{E_f}{2\Sigma EI}(M_{ex}(x) - 2N_f r)\, d_f + \frac{N_f}{A_f} \qquad - 2.56$$

substituting values of $M_{ex}(x)$ and N_f for regions m & n and rearranging we get:

$$\sigma_{fm} = \frac{P}{2}\frac{E_f A_f r}{\lambda EI}(K'_{m1}\mathrm{Sinh}\lambda x + \lambda x)(\frac{1}{A_f} - \frac{E_f d_f r}{\Sigma EI}) + \frac{E_f d_f}{4\Sigma EI}Px \qquad - 2.57$$

$$\sigma_{fn} = \frac{P}{2}\frac{E_f A_f r}{\lambda EI}(K'_{n1}\mathrm{Sinh}\lambda x + K'_{n2}\mathrm{Cosh}\lambda x + \lambda l)(\frac{1}{A_f} - \frac{E_f d_f r}{\Sigma EI}) + \frac{E_f d_f}{4\Sigma EI}Pl \qquad - 2.58$$

where:

$$K'_{m1} = \frac{\lambda}{K_k} K_{m1} = \text{Coth}\,\lambda L \left(\text{Sinh}\lambda l + \text{Sinh}\,\lambda (L-l)\right) - \text{Cosh}\,\lambda(L-l) - \text{Cosh}\lambda l \qquad -2.59$$

$$K'_{m} = \frac{\lambda}{K_k} K_{m} = \text{Coth}\,\lambda L\left(\text{Sinh}\,\lambda l + \text{Sinh}\,\lambda (L-l)\right) - \text{Cosh}\,\lambda(L-l) \qquad -2.60$$

$$K'_{n2} = \frac{\lambda}{K_k} K_{n2} = - \text{Sinh}\,\lambda l \qquad -2.61$$

and $$K_k = \frac{P}{2} \frac{E_f A_f}{EI} r \qquad -2.62$$

5.7.5 Bending stresses in the web

$$\sigma_w = - \sigma_{21} = \sigma_{24}$$

similar to derivation of equations 2.57 and 2.58, we get.

$$\sigma_{wm} = \frac{P}{4} \frac{E_2 d_2}{\Sigma EI} \left[x - 2\frac{E_f A_f}{\lambda EI} r^2 \left(K'_{m1} \text{Sinh}\lambda x + \lambda x\right)\right] \qquad -2.63$$

$$\sigma_{wn} = \frac{P}{4} \frac{E_2 d_2}{\Sigma EI} \left[1 - \frac{2E_f A_f}{\lambda EI} r^2 \left(K'_{n1} \text{Sinh}\lambda x + K'_{n2} \text{Cosh}\lambda x + \lambda l\right)\right] \qquad -2.64$$

where K'_{m1}, K'_{n1} and K'_{n2} are as given by eqns. 2.59, 2.60 & 2.61.

5.7.6 Shear force at flange web interface

$$q = \frac{dN}{dx}$$

differentiating equation 2.48(a) and 2.49(a), we get:

$$q_m = \frac{P}{2} \frac{E_f A_f r}{\Sigma EI} \left\{ \left[\text{Coth}\lambda L \left(\text{Sinh}\lambda l + \text{Sinh}\lambda(L-l) \right) - \text{Cosh}\lambda(L-l) - \text{Cosh}\lambda l \right] * \right.$$
$$\left. * \text{Cosh}\lambda x + 1 \right\} \qquad - 2.65$$

$$q_n = \frac{P}{2} \frac{E_f A_f r}{\Sigma EI} \left\{ \left[\text{Coth}\lambda L \left(\text{Sinh}\lambda l + \text{Sinh}\lambda(L-l) - \text{Cosh}\lambda(L-l) \right) \right] \text{Cosh}\lambda x \right.$$
$$\left. - \text{Sinh}\lambda l \;\; \text{Sinh}\lambda x \right\} \qquad - 2.66$$

5.7.7 Shear stress at neutral axis of web

$$b_2 \tau_{xz} = \frac{dM_2}{dx} \left(\frac{A_2 d_2}{8} \right) \frac{1}{I_2} + q = E_2 \left(\frac{b_2 d_2^2}{8} \right) \frac{d}{dx} \left(\frac{M_2}{E_2 I_2} \right) + q$$

using equation 2.51 and noting $q = \frac{dN_f}{dx}$, we get

$$b_2 \tau_{xz} = \frac{E_2 b_2 d_2^2}{8 \Sigma EI} \left[\frac{dM_{ex}(x)}{dx} - 2rq \right] + q \qquad - 2.67$$

substituting values of q and $d\frac{(M_{ex}(x))}{dx}$ for regions m and n in equation 2.67 and rearranging, we get

$$\tau_{xz}\Big|_m = \frac{P}{16} \frac{E_2 d_2^2}{\Sigma EI} + \frac{P}{2} \frac{E_f A_f r}{b_2 \Sigma EI} K'_{m1} \text{Cosh}\lambda x \left(1 - \frac{r b_2 d_2^2 E_2}{4 \Sigma EI} \right) + \frac{P}{2} \frac{E_f A_f r}{b_2 \Sigma EI} \qquad - 2.68$$

$$\tau_{xz}\Big|_n = \frac{P}{2} \frac{E_f A_f r}{b_2 \Sigma EI} \left[K'_{n1} \text{Cosh}\lambda x + K'_{n2} \text{Sinh}\lambda x \right] \left[1 - \frac{E_2 b_2 d_2^2 r}{4 \Sigma EI} \right] \qquad - 2.69$$

where K'_{m1}, K'_{n1}, and K'_{n2} are as given by equations 2.59, 2.60 and 2.61.

Chapter 6 Numerical solutions of generalised differential equations

6.1 Outline of procedure

The generalised simultaneous differential equations are given by equations 2.21, 2.22, 2.23 and 2.24. They are described as generalised because any of the governing differential equations described in sections 5.5 and 5.6 may be derived from them and evaluated at any point along the beam for given values of N_1, N_3, δ_1 and δ_3. Evaluation of the model at any point along the beam means evaluation of the first derivatives of δ_1, δ_3, N_1 and N_3. The procedure followed to find a solution to the model over the whole span such that the problem boundary conditions are satisfied may be summarised in the following:

(1) Set co-ordinate system at left-hand boundary point of the beam and divide the beam into equal intervals of length (H) as shown in fig.2.6.

(2) Calculate moments and shear forces at all nodes along the beam.

(3) Set boundary conditions of the problem, i.e. in case of simply supported beam boundary conditions are $N_1 = N_3 = 0$ at both boundary points.

(4) Find first derivatives of N_1, N_3, δ_1 and δ_3 at left boundary point. This is done by evaluating the governing differential equations for assumed values of N_1, N_3, δ_1 and δ_3 at that point. In the case of a simply supported beam $N_1 = N_3 = 0$, δ_1 and δ_3 are guessed as shown in section 6.3.1.

(5) Having found first derivatives of N_1, N_3, δ_1 and δ_3 at left hand boundary point integration is advanced to the next node using the predictor corrector method as described in section 6.2.2.

(6) Using a similar procedure to that given in step (5), integration is advanced from one node to the next until the second boundary point where calculated values of N_1 and N_3 are checked against the known boundary conditions. If boundary conditions are not satisfied, then the guessed values for δ_1 and δ_3 are not correct and new guesses are made at the first boundary point (at left-hand support) such that these new guesses give closer values of N_1 and N_3 to the desired ones at the second boundary point (at right-hand support) than those obtained from the initial guesses. The method used to obtain convergence towards desired values of N_1 and N_3 at the second boundary point is described in section 6.3.

6.2 Numerical integration algorithm.: Predictor corrector method

The method which has been adopted in this thesis to integrate the governing simultaneous differential equations is the predictor corrector method.

It is one of the methods by which first order differential equations may be integrated numerically. Other methods include Runge Kutta method whose disadvantages in relation to the type of predictor corrector method adopted in this thesis are discussed later in this chapter.

6.2.1 Choice of predictor corrector type

When choosing a predictor corrector type, three objectives should be aimed at :

(i) Low truncation error

(ii) Large margin of stability

(iii) Protection against round-off troubles

It is difficult to meet all three objectives as they are somewhat incompatible. Truncation errors arise from finite approximations for the derivatives. Propagation of instability errors arise from solving approximate difference equations which do not correspond to the solution of differential equations. Roundoff errors arise due to certain combinations of coefficients in the finite difference formulae. According to Hamming (1959, 1962) the corrector formula plays a more significant part than the predictor, hence its choice is relatively more important. He also suggests that the Milne method modified according to Hamming provides a relatively stable corrector formula that compromises between truncation and stability problems. He also reported that his modified formulae were tried on a range of problems and were found to work for average problems, i.e. problems with average stability and truncation errors.

6.2.2 Milne type predictor corrector method due to Hamming:

The model may be solved along the beam from one node to the next by applying the following formulae to predict the next value of one of the variables, modify it to compute a modified derivative, compute a corrected value using that modified derivative and then applying the predicted and corrected values to find the value of that variable at the next point.

$$\Psi_i^{(m+1)} = \Psi_i \Big|_{c_r}^{(m+1)} + \frac{9 - 5K_b}{121-5K_b} \left[\Psi_i \Big|_{p}^{(m+1)} - \Psi_i \Big|_{c_r}^{(m+1)} \right] \qquad 2.70$$

where

$$\psi_i\Big|_p^{(m+1)} = \psi_i^{(m-3)} + \frac{4H}{3}\left[2\dot{\psi}_i\Big|^{m} - \dot{\psi}_i\Big|^{(m-1)} + 2\dot{\psi}_i\Big|^{(m-2)}\right] \qquad - 2.71$$

$$\psi_i\Big|_{c_r}^{(m+1)} = K_a\,\psi_i^{m} + K_b\,\psi_i^{(m-1)} + K_c\,\psi_i^{(m-2)} + H\left[K_d\,\dot{\psi}_i\Big|_{*}^{(m+1)} + K_e\dot{\psi}_i\Big|^{m} + K_f\dot{\psi}_i\Big|^{m-1}\right] \qquad - 2.72$$

and

$$\dot{\psi}_i\Big|_{*}^{(m+1)} = f(x_{m+1},\ \psi_i\Big|_{m_o}^{(m+1)} \ \ldots\ \psi_n\Big|_{m_o}^{(m+1)}) \qquad - 2.73$$

$$\psi_i\Big|_{m_o}^{(m+1)} = \psi_i\Big|_{p}^{(m+1)} - \frac{112}{121-5b}\left[\psi_i\Big|_{p}^{m} - \psi_i\Big|_{c_r}^{m}\right] \qquad - 2.74$$

$$K_a = \frac{9(1-K_b)}{8}\ ,\quad K_c = \frac{(K_b-1)}{8}\ ,\quad K_d = \frac{9-K_b}{24}$$

$$K_e = \frac{7K_b+9}{12}\ ,\quad K_f = \frac{17K_b-9}{24} \qquad - 2.75$$

where subscripts

- p = predicted value
- c_r = corrected value
- m_o = modified value
- i = variable index - $i = 1, \ldots i_n$ and i_n = number of variables and equations. In the case considered in this thesis $i_n = 4$ corresponding to the four variables (N_1, N_2, δ_1 & δ_3) and four model equations.

m = point considered along span, $m = 5, \ldots m_n$ $(m \geq 5)$

$m_n = L/H + 1$

It should be noted that

$$\left[\psi_i \Big|_p^{(m+1)} - \psi_i \Big|_{c_r}^{m+1} \right]$$

will be assumed to be zero for the first point as it cannot be evaluated for that point.

Obviously to use a predictor corrector method of the type suggested here, one needs four starting points. The procedure adopted here is to use the Runge Kutta method of the fourth order to integrate up to the fourth point when it is abandoned and the predictor corrector method of the type suggested in this thesis is adopted. The formula used to integrate is given as follows:

$$\psi_i^{m+1} = \psi_i^m + \frac{1}{6}\left[\rho_i \Big|_1^m + \rho_i \Big|_2^m + \rho_i \Big|_3^m + \rho_i \Big|_4^m \right]$$

Let;

$$\psi_i' \Big|^m = f(x^m, \psi_i^m \ldots \psi_{i_n}^m) \quad ; \quad \psi_i(\overset{m}{x}) = \psi_i^m$$

Then:

$$\rho_i \Big|_1^m = Hf(x^m, \psi_i^m \ldots \psi_{i_n}^m)$$

$$\rho_i \Big|_2^m = Hf\left(x^m + \frac{H}{2}, \psi_i^m + \frac{\rho_i|_1^m}{2}, \ldots, \psi_{i_n}^m + \frac{\rho_{i_n}|_1^m}{2}\right) \qquad - 2.76$$

$$\rho_i\Big|_3^m = Hf\left(x^m + \frac{H}{2},\ \psi_i^m + \frac{\rho_i}{2}\Big|_2^m,\ \ldots,\ \psi_{in}^m + \frac{\rho_{in}}{2}\Big|_2^m\right)$$

$$\rho_i\Big|_4^m = Hf\left(x^m + \frac{H}{2},\ \psi_i^m + \frac{\rho_i}{2}\Big|_3^m,\ \ldots,\ \psi_n + \frac{\rho_{in}}{2}\Big|_3^m\right)$$

The advantages of this type of predictor corrector method are that:

(a) the numerical value $\left[\psi_i\Big|_p^m - \psi_i\Big|_{c_r}^m\right]$ is an indication of the optimum step size. If the value is too small, then the step is too short and computer time is wasted, whereas if it gradually grows large, then the step size needs to be shortened. If it suddenly becomes large, then that is an indication of a local computational error. Thus the method supplies a means of finding optimum step size and offers a way to check local computations.

(b) Also it requires two evaluations for the derivatives for each step forward, compared with four evaluations in the case of Runge Kutta and hence about half the computer time is saved for each step (Hamming 1959).

According to Hamming (1962), the main disadvantage of the type of predictor corrector method adopted in this thesis is that the high degree of accuaracy, i.e. low truncation errors, obtained from the original Milne method is lowered. This is because Hamming has compromised between high accuaracy obtained from Milne's method and instability as Milne's method may be unstable.

In equations 2.70 and 2.72 the parameter K_b due to Hamming is a parameter to control stability and truncation errors. He reported that for absolute stability the parameter K_b must satisfy $(-\frac{6}{10} < K_b < 1)$. He also found that the truncation error increases linearly as K_b goes from 1 to $-\frac{6}{10}$. He suggested that the parameter K_b takes the value zero to compromise between stability and high accuaracy. This value for K_b is adopted in this thesis. It is worth mentioning that by setting $K_b = 1$, Hamming's modified equations (2.70 - 2.75) are reduced to the original Milne equations.

Also a disadvantage of this type of predictor corrector method is that it requires a starting procedure.

6.3 Convergence criteria

A solution of the model over the whole span is achieved if the following criterion is satisfied at the second boundary point.

$$\left| N_1 - \acute{N}_1 \right| \leq \xi \left| N_1 \right|$$

and

$$\left| N_3 - \acute{N}_3 \right| \leq \xi \left| N_3 \right| \qquad \text{- 2.77}$$

where: $\acute{N}_1$ and $\acute{N}_3$, are computed direct forces at the second boundary point

N_1 and N_3, known values of direct forces at the second boundary point, i.e. boundary conditions

ξ Desired accu racy

This criterion may not be satisfied from the first guess of δ_1 and δ_2 at the first boundary and hence the need to find improved guesses for δ_1 and δ_3 such that the numerical values $\left[\left| N_1 - \acute{N}_1 \right|\right]$ and $\left[\left| N_3 - \acute{N}_3 \right|\right]$ converge towards $\left[\xi \left| N_1 \right|\right]$ and $\left[\xi \left| N_3 \right|\right]$ respectively. To find improved guesses the following systematic procedure is adopted. This systematic procedure may be summarised in the following routines.

6.3.1 Direct search routine

To apply a direct search routine the following definitions are made:

(i) Upper bound slips:

Are those guessed slips (δ_1 and δ_3) at first boundary point that may yield a solution to the model such that the obtained values of N_1 and N_3 at all points along the beam are higher than the correct ones.

(ii) Lower bound slips

Are those guessed slips δ_1 and δ_3 at first boundary point that may yield a solution to the model such that the obtained values of N_1 and N_3 at all points along the beam are lower than the correct ones.

(iii) Good guesses for δ_1 and δ_3

Are those gueses for slips δ_1 and δ_3 at first boundary point that may yield a solution to the model such that the shapes of the solution curves for N_1 and N_3 along the span are evident. In the cases considered in this thesis the criterion that is adopted to determine the shape of the solution curve over the whole span is that a change of sign for the derivatives of N_1 and N_3 is encountered over at least one third of the span, fig.2.14.

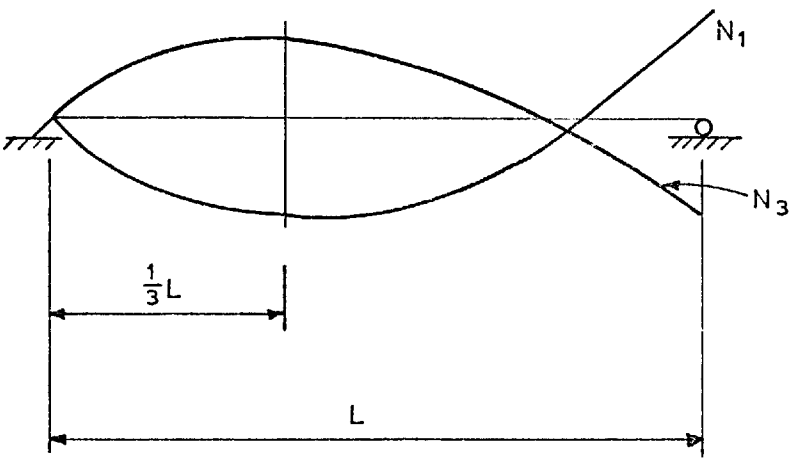


Fig. 2·14. Variation of N_1 and N_3 along the span for any two guessed values of δ_1 and δ_3 at left hand boundary point

This criterion is found by trial and error and applies for the cases considered in this thesis. The object of finding a good guess is that the direct search routine may be abandoned to a faster directional search routine which is based on linear Newton Raphson method to find solutions of simultaneous equations. This method needs good guesses to obtain convergence.

Having defined the previous expressions, the procedure to apply the direct search routine may be outlined as follows;

(1) Guess upper and lower bound slips δ_1 and δ_3 at first boundary point. Certainly, in some cases good guesses may be made, e.g. when solving the general non-linear model described by eqns. 2.21 - 2.24 for a simply supported beam where a linear model may be correctly assumed at low loads and solved analytically to find good guesses for δ_1 and δ_3 at the first boundary, whereas at high loads parabolic extrapolations from low load results may provide a way to find good guesses at these load levels; or at least if good guesses are not achieved, upper or lower bound guesses near enough to the correct guesses may be achieved.

(2) δ_1 and δ_3 are found as follows :

$$\Delta\delta_1 = \left[\delta_1\Big|_{up} - \delta_1\Big|_{Lo}\right] \Big/ m$$

$$\Delta\delta_3 = \left[\delta_3\Big|_{up} - \delta_3\Big|_{Lo}\right] \Big/ m \qquad \text{- 2.78}$$

where: $\delta_1\Big|_{up}$, $\delta_3\Big|_{up}$ are upper bound slips at first boundary point,

$\delta_1\Big|_{Lo}$, $\delta_3\Big|_{Lo}$ are lower bound slips at first boundary point

m number of increments chosen .

$\Delta\delta_1$ and $\Delta\delta_3$ increments are added to $\delta_1\Big|_{Lo}$ and $\delta_3\Big|_{Lo}$ respectively, 1, ..., m times such that all combinations between upper and lower bound slips for δ_1 and δ_3 are iterated until a good guess or a solution is obtained.

(3) If a good guess is obtained, then the direct search routine is abandoned and the directional search routine is adopted to find a solution.

(4) If after incrementing up to both upper bounds of δ_1 and δ_3, neither a good guess nor a solution is obtained, then that means increments chosen are large and hence smaller increments are chosen, i.e. higher number of m. Following this procedure it is found that a good guess may be obtained; but in some cases when coarse guesses of the upper and lower bound slip are inevitable, a considerable amount of computer time may be used to find a good guess such that the direct search routine is abandoned to a faster directional search routine.

6.3.2 Directional search routine

Having obtained a good guess, then the directional search routine is applied to obtain a solution to the model over the whole span, and satisfying the criterion given by eqn. 2.77, faster than if the direct search routine is used.

This routine is based on Newton Raphson method to obtain solutions to simultaneous equations and on the principle that since we have four coupled equations in four variables and since any change in any one of the variables at any point along the beam will produce changes on the other variables at all points on the beam, then incremental changes on the slips δ_1 and δ_3 at first boundary point will produce changes on the variables N_1 and N_3 at the second boundary point. Based on these principles the Newton Raphson method may be applied as follows:

Assume N_1 and N_3 at second boundary point are given by:

$$F(\delta_1, \delta_3) = N_1^* \qquad - 2.79$$
$$G(\delta_1, \delta_3) = N_3^*$$

Also $\delta_1|_o$, $\delta_3|_o$: initial guesses

$\delta_1|_1$, $\delta_3|_1$: first approximation for δ_1 and δ_3 at first boundary and assume these guesses are good close approximations to the correct δ_1 and δ_3, so that they produce values for N_1 and N_3 near enough to the correct ones at the second boundary point (N_1^*, N_3^*).

OR;

$$F(\delta_1|_1, \delta_3|_1) = N_1^* \qquad - 2.80$$
$$G(\delta_1|_1, \delta_3|_1) = N_3^*$$

Expand eqns. 2.79 i.e. $F(\delta_1, \delta_3)$ and $G(\delta_1, \delta_3)$ as Taylor series about $(\delta_1|_o, \delta_3|_o)$ truncating each after first derivative terms, i.e. linear approximation, we get:

$$F(\delta_1|, \delta_3|) = F(\delta_1|_o, \delta_3|_o) + \frac{\partial F}{\partial \delta_1}\Big|_o (\delta_1| - \delta_1|_o) + \frac{\partial F}{\partial \delta_3}\Big|_o (\delta_3| - \delta_3|_o) \qquad - 2.81$$
$$G(\delta_1|, \delta_3|) = G(\delta_1|_o, \delta_3|_o) + \frac{\partial G}{\partial \delta_1}\Big|_o (\delta_1| - \delta_1|_o) + \frac{\partial G}{\partial \delta_3}\Big|_o (\delta_3| - \delta_3|_o)$$

substitute 2.80 in eqn. 2.81, and putting

$$\Delta\delta_1 = \delta_1 - \delta_1\Big|_o$$

$$\Delta\delta_3 = \delta_3 - \delta_3\Big|_o \qquad \text{- 2.82}$$

we get

$$\frac{\partial F}{\partial \delta_1}\Big|_o \Delta\delta_1 + \frac{\partial F}{\partial \delta_3}\Big|_o \Delta\delta_3 = N_1^* - F(\delta_1|_o, \delta_3|_o)$$

$$\frac{\partial G}{\partial \delta_1}\Big|_o \Delta\delta_1 + \frac{\partial G}{\partial \delta_3}\Big|_o \Delta\delta_3 = N_3^* - G(\delta_1|_o, \delta_3|_o) \qquad \text{- 2.83}$$

Noting for a simply supported beam $N_1^* = N_3^* = 0$, at second boundary point, then :

$$\begin{bmatrix}\Delta\delta_1\\ \Delta\delta_3\end{bmatrix} = \begin{bmatrix}a_{11} & a_{12}\\ a_{21} & a_{22}\end{bmatrix}^{-1} \begin{bmatrix}a_{10}\\ a_{20}\end{bmatrix}$$

OR

$$\begin{bmatrix}\Delta\delta_1\\ \Delta\delta_3\end{bmatrix} = \frac{1}{D}\begin{bmatrix}a_{10}\,a_{22} - a_{12}\,a_{20}\\ -a_{10}\,a_{21} + a_{11}\,a_{20}\end{bmatrix} \qquad \text{- 2.84}$$

where

$$a_{11} = \frac{\partial F}{\partial \delta_1}\Big|_o, \quad a_{12} = \frac{\partial F}{\partial \delta_3}\Big|_o$$

$$a_{21} = \frac{\partial G}{\partial \delta_1}\Big|_o, \quad a_{22} = \frac{\partial G}{\partial \delta_3}\Big|_o$$

$$a_{10} = -F(\delta_1|_o, \delta_3|_o), \quad a_{20} = -G(\delta_1|_o, \delta_3|_o)$$

and $D = a_{11}\,a_{22} - a_{12}\,a_{21}$ - 2.85

From 2.82, we find new guesses to be as follows:

$$\delta_1\big|_1 = \delta_1\big|_0 + \Delta\delta_1$$
$$\delta_3\big|_1 = \delta_3\big|_0 + \Delta\delta_3 \qquad \text{- 2.86}$$

The evaluation of eqn. 2.84 and 2.86 to find new guesses $\delta_1\big|_1$ and $\delta_3\big|_1$ necessitates the evaluation of a_{11}, a_{12}, a_{21}, a_{22}, a_{10} and a_{20}.

Since analytical functions are not available for $F(\delta_1, \delta_3)$ and $G(\delta_1, \delta_3)$ the following numerical procedure will be used to find a_{11}, a_{12}, a_{21}, a_{22}, a_{10} and a_{20}.

(1) For initial guesses $\delta_1\big|_0$, $\delta_3\big|_0$ at first boundary point, the model is solved along the beam using corrector predictor method as mentioned before - values of $N_1\big|_0$ and $N_3\big|_0$ are found at second boundary point.

then:
$$a_{10} = -F(\delta_1\big|_0, \delta_3\big|_0) = -N_1\big|_0$$
$$a_{20} = -G(\delta_1\big|_0, \delta_3\big|_0) = -N_3\big|_0 \qquad \text{- 2.87}$$

(2) For initial guess $\delta_1\big|_0$ add a small increment of $\eta\,\delta_1\big|_0$, such that

$$\delta_1\big|_0' = \delta_1\big|_0 + \eta\,\delta_1\big|_0$$

and solve the model along the span for guesses $\delta_1\big|_0'$ and $\delta_3\big|_0$ at first boundary point and find values of $N_1\big|_0^{\delta_1'}$ and $N_3\big|_0^{\delta_1'}$ at second boundary point; then,

$$a_{11} = \frac{N_1\Big|_o^{\delta_1'} - N_1\Big|_o}{\delta_1\Big|_o' - \delta_1\Big|_o} = \frac{N_1\Big|_o^{\delta_1'} - N_1\Big|_o}{\eta\ \delta_1\Big|_o}$$

$$a_{21} = \frac{N_3\Big|_o^{\delta_1'} - N_3\Big|_o}{\delta_1\Big|_o' - \delta_1\Big|_o} = \frac{N_3\Big|_o^{\delta_1'} - N_3\Big|_o}{\eta\ \delta_1\Big|_o} \qquad - 2.88$$

(3) For initial guess $\delta_3\Big|_o$ add a small increment of $\eta\ \delta_3\Big|_o$, such that

$$\delta_3\Big|_o' = \delta_3\Big|_o + \eta\ \delta_3\Big|_o$$

and solve the model along the span for guesses $\delta_1\Big|_o$ and $\delta_3\Big|_o'$ at first boundary point and find values of $N_1\Big|_o^{\delta_3'}$ and $N_3\Big|_o^{\delta_3'}$ at second boundary point, then

$$a_{12} = \frac{N_1\Big|_o^{\delta_3'} - N_1\Big|_o}{\eta\ \delta_3\Big|_o}$$

$$a_{22} = \frac{N_3\Big|_o^{\delta_3'} - N_3\Big|_o}{\eta\ \delta_3\Big|_o} \qquad - 2.89$$

It should be noted that in equations 2.88 and 2.89 the parameter η is found by trial and error to lie between $10^{-3} \leq \eta \leq 10^{-8}$. It is found that faster convergence may be achieved towards the higher limit of η, i.e. 10^{-8}, while slower convergence may be achieved towards the lower limit, 10^{-3}, i.e. higher number of iterations.

Having evaluated equation 2.84, now new guesses $\delta_1|_1$ and $\delta_3|_1$ may be obtained from eqn. 2.86 and these new guesses may be used in the same way as the initial guesses $\delta_1|_0$ and $\delta_3|_0$ to obtain new guesses $\delta_1|_2$ and $\delta_3|_2$ closer to the correct values of δ_1 and δ_3. This procedure is repeated several times to obtain convergence to the desired accu racy of N_1 and N_3 at the second boundary point.

6.4 Bending deflection

Curvatures θ relevant to the solution of the governing simultaneous differential equations have been evaluated automatically at all nodes as integration has advanced from one node to the next along the whole beam span, as shown in sections 5.5, 5.6 and 5.8.1. These values of θ are used to find the bending deflection at these nodes as described in section 5.3.3 using a finite difference approach.

6.5 Bending stresses in the flanges and web

Bending stresses in the flanges and web relevant to the solution of the governing simultaneous differential equations have been evaluated automatically at all nodes along the beam as integration has advanced from one node to the next as shown in sections 5.5, 5.6 and 5.8.1.

6.6 Shear force at flange web interface

Shear force per unit length at flange web interface relevant to the solution of the governing simultaneous differential equations has been evaluated automatically at all nodes along the beam as integration has advanced from one node to the next as shown in sections 5.5, 5.6 and 5.8.1.

It should be noted that shear force at the flange web interface is the value of the first derivative of the direct force acting on the flange under consideration.

6.7 Web shear stress at neutral axis of web

Derivation of web shear stress at the neutral axis is based on a linear distribution of direct stresses across the depths of the timber and plywood. Based on this assumption we get from equation 2.30:

$$\frac{M_2}{E_2 I_2} = \frac{M_{ex}(x) + N_1 r_1 - N_3 r_3}{\Sigma E I}$$

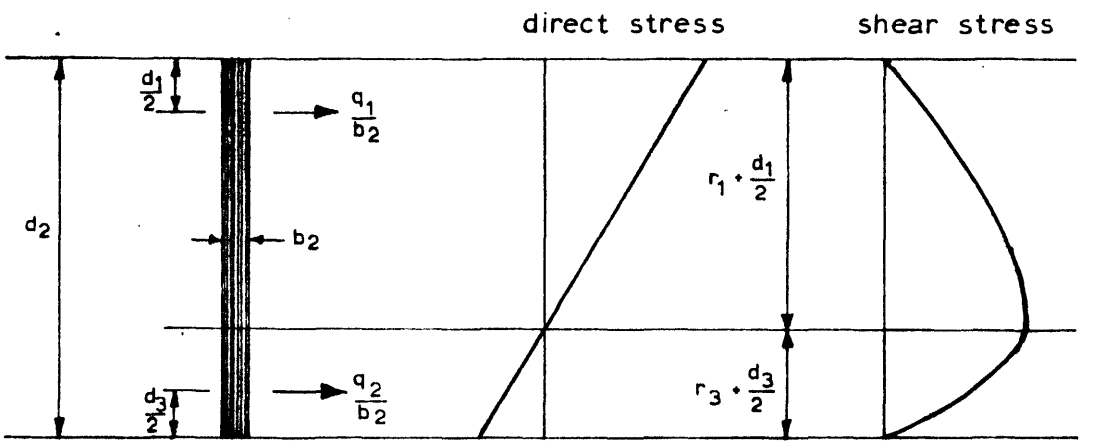


Fig. 2.15. Shear stress distribution across depth of plywood web

Referring to fig. 2.15 we get

$$b_2 \tau_{xz} = \frac{dM_2}{dx}\left[\frac{(2r_1+d_1)^2}{8}\right] \frac{b_2}{I_2} + q_1$$

$$= E_2 b_2 \frac{(2r_1+d_1)^2}{8} \frac{d}{dx}\left[\frac{M_{ex}(x) + N_1 r_1 - N_3 r_3}{\Sigma E I}\right] + q_1$$

$$\tau_{xz} = \frac{E_2}{8\Sigma EI}(2r_1 + d_1)^2 (V - r_1 q_1 - r_3 q_3) + \frac{q_1}{b_2} \qquad - 2.90$$

6.3 Computer programs

A computer program has been written to solve any of the sets of the governing simultaneous differential equations given in sections 5.5 and 5.6 at different points along the span for a desired loading condition such that the problem boundary conditions are met. A flow chart for that program is given in the appendix. A general description of this program may be summarised in the following:

(1) Read and check data, i.e. materials properties, beam geometry, loading conditions, interval length (H), instruction to choose desired model, etc.

(2) Find section properties and nodes along the span corresponding to the chosen interval (H) and calculate moments at these nodes.

(3) Guess upper and lower bounds of slips at first boundary point at left support.

(4) Evaluate derivatives that correspond to the chosen model at first boundary point for upper and lower bounds slips noting that $N_1 = N_3 = 0$. Integration along the beam is done by applying the predictor corrector method. Upper and lower bound solutions are checked to find whether a solution or a good guess is obtained. It should be noted that at each node the external moment is balanced against the internal moment corresponding to the stress distribution relevant to the chosen model. This is done in a separate sub-program which is called at every node.

(5) If neither a solution nor a good guess is obtained, then direct search routine is applied until a good guess or a solution is obtained.

(6) If a good guess is obtained then directional search routine is applied until desired accu racy at the second boundary point is achieved.

(7) If a solution is achieved from either step (5) or (6), then deflections are calculated at different nodes using the finite differences sub-program which is described in section 4.3.3, and also the web shear stresses and interface shear on connector are calculated.

(8) Write slip, direct forces for web and flanges, web shear stresses, interface shear on connector and deflections at desired nodes. Also strain distributions across the depths of timber and plywood and depth of compression yield from top flange edge are written at these nodes.

It is worth mentioning that the program is designed so that if the direct search routine is abandoned for the directional search routine and that a solution is not obtained using the directional search routine, i.e. failure of criterion for a good guess, then the routine is designed to go back to the direct search routine at the point where it was abandoned and find a solution by direct search routine. This trouble is not encountered in the cases solved in this thesis.

Chapter 7 Shear deflection in plywood web I-beams

7.1 Assumptions

The assumptions that are made to derive shear deflection of plywood web I-beams are summarised as follows:

(1) Linear $\sigma - \varepsilon$ relationships will be assumed for timber and plywood in tension and compression, i.e. linear stress distribution across the beam depth.

(2) Linear flange-web force - displacement equation will be assumed.

(3) Uniformly distributed load over the whole span of a symmetrical plywood web I-beam will also be assumed.

(4) The general and additional assumptions mentioned in sections 4.2 and 6.1 will also be adopted.

7.2 Shear stress distributions

The beam layout and the assumed shear stress distributions across the depths of the timber flanges and plywood web that are considered in this thesis are given in fig.2.16.

Booth (1969) gave the following formula for flange web shear force per unit length at interface of flange and web of a simply supported semi-rigid plywood web I-beam symmetrical about y and z axes and carrying uniformly distributed load over the whole span.

$$q_f = p \frac{E_f A_f r}{EI} \left[\frac{L\sqrt{C}}{\pi} \frac{\text{Sinh}\left(\frac{\pi}{\sqrt{C}} \frac{x}{L}\right)}{\text{Cosh}\left(\frac{\pi}{\sqrt{C}} \frac{x}{L}\right)} - x \right] \qquad - 2.91$$

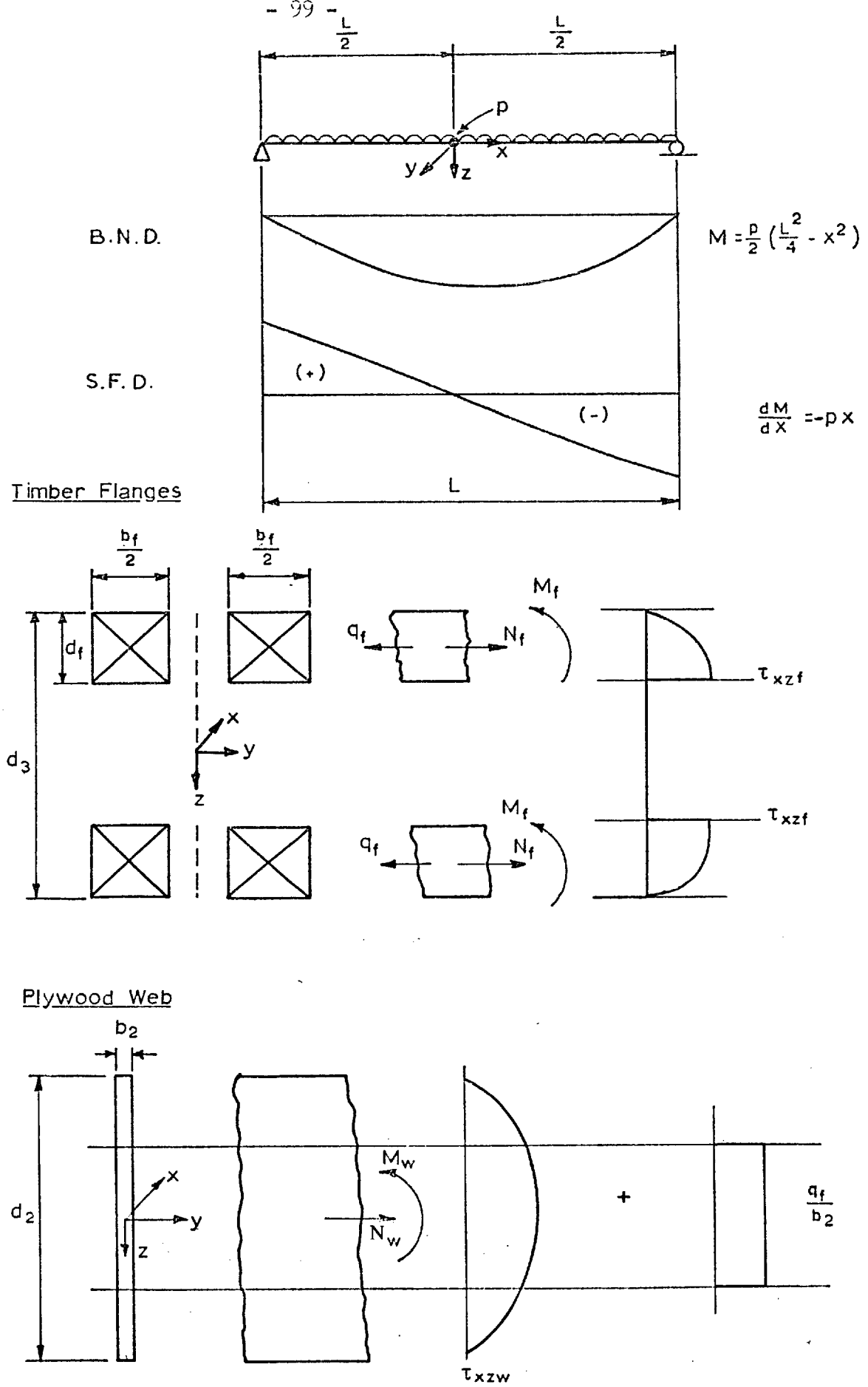


Fig. 2·16. Shear stress distributions at any section across the depths of timber flanges and plywood web

where $C = \frac{\pi^2}{L^2} \frac{s}{k} \frac{E_f A_f \Sigma EI}{EI}$

$E_f = E_1 = E_3$ and $A_f = A_1 = A_3$

7.2.1 Timber Flanges $(\frac{d_2}{2} - d_f) \leq z \leq \frac{d_2}{2}$

Following similar derivation to that for web shear stress given in section 5.8.5 and from shear stress distributions shown in fig 2.16 and also from equation 2.91, we find:

$$\tau_{xzf} = - \frac{E_f}{2}\left[(\frac{d_2}{2})^2 - z^2\right] \frac{V}{\Sigma EI}\left[1 + 2rK_{f1} + K_{qx}\right] \quad - 2.92$$

where $K_{f1} = \frac{E_f A_f r}{EI}$ - 2.93

$$K_{qx} = \frac{L\sqrt{C}}{\pi} \frac{\text{Sinh}(\frac{\pi}{\sqrt{C}} \frac{x}{L})}{x \text{ Cosh}(\frac{\pi}{\sqrt{C}} \frac{x}{L})} - 1 \quad - 2.94$$

7.2.2 Plywood web

(i) $(\frac{d_2}{2} - d_f) \leq z \leq \frac{d_2}{2}$

τ_{xzw1} and τ_{xzw2} will be found in a similar way to that used to find τ_{xzf} in eqn. 2.92.

$$\tau_{xzw1} = - \frac{E_2}{2}\left[(\frac{d_2}{2})^2 - z^2\right] \frac{V}{\Sigma EI}\left[1 + 2rK_{f1}\ K_{qx}\right] \quad - 2.95$$

(ii) $0 \leq z \leq (\frac{d_2}{2} - d_f)$

$$\tau_{xyw2} = V \left\{ -\left[\frac{E_2}{2\Sigma EI}\left(\left(\frac{d_2}{2}\right)^2 - z^2\right) + \frac{K_{f1}}{b_2}\right] + \frac{K_{f1}}{b_2}(K_{qx} + 1)\left[\frac{E_2}{2\Sigma EI}\ 2rb_2\left(\left(\frac{d_2}{2}\right)^2 - z^2\right) + 1\right]\right\} \qquad - 2.96$$

7.3 Shear strain energy

Shear energy may be calculated from the following eqn.

$$U = \iiint_{\text{volume}} \frac{\tau_{xz}^2}{2G}\, dx\, dz\, dy \qquad - 2.97$$

where U = shear strain energy.

7.3.1 Timber flanges

$$(\frac{d_2}{2} - d_f) \leq z \leq \frac{d_2}{2}$$

$$U_f = \iint_{\text{area}} \frac{\tau_{xzf}^2}{2G_f}\, b_f\, dx\, dz \qquad \text{where} \quad \int_{-\frac{b_f}{2}}^{+\frac{b_f}{2}} dy = b_f$$

Substituting τ_{xzf} from 2.92, we get

$$U_f = \frac{2K_f^2 b_f}{2G_f} \int_{-L/2}^{L/2} V^2 Q_x^2\, dx \int_{\frac{1}{2}(d_2 - 2d_f)}^{d_2/2} \left[\frac{d_2^4}{16} - \frac{d_2^2 z^2}{2} + z^4\right] dz$$

$$= \frac{b_2}{G_f} K_f^2 K_{f2} \int_{-L/2}^{L/2} V^2 Q_x^2 \, dx \qquad - 2.98$$

where $K_f = \frac{E_f}{2\Sigma EI}$

$$Q_x = \left[1 + 2rK_{f1} K_{qx}\right]$$

$$K_{f2} = \int_{\frac{1}{2}(d_2-2d_f)}^{d_2/2} \left[\frac{d_2^4}{16} - \frac{d_2^2 z^2}{2} + z^4\right] dz = \frac{1}{30}\left[10d_2^2 d_f^2 - 15d_2 d_f^4 + 6d_f^5\right]$$

7.3.2 Plywood web

U_{w1} and U_{w2} will be found in a similar way to that used to derive U_f in eqn. 2.98

(i) $\underline{\left(\frac{d_2}{2} - d_f\right) \leq z \leq \frac{d_2}{2}}$

$$U_{w1} = \iint_{\text{area}} \frac{\tau_{xzw1}^2}{2G_2} b_2 dx dz \qquad \text{where} \quad \int_{-\frac{b}{2}}^{\frac{b_2}{2}} dy = b_2$$

substituing τ_{xzw1} from eqn. 2.95, we get

$$U_{w1} = \frac{b_2}{G_2} K_w^2 K_{w1} \int_{-L/2}^{L/2} V^2 Q_x^2 \, dx \qquad - 2.99$$

where $K_w = \frac{E_2}{2\Sigma EI}$

$K_{w1} = K_{f2}$

(ii) $\underline{0 \leq z \leq (\frac{d_2}{2} - d_f)}$

$$U_{w2} = \frac{\tau_{xzw2}^2}{2G_2} b_2 \, dx \, dz$$

substituting τ_{xzw2} from eqn. 2.96, we get

$$U_{w2} = \frac{b_2}{G_2} K_w^2 K_{w21} \int_{-L/2}^{L/2} V^2 Q_x^2 \, dx + \frac{K_{f1}^2}{b_2 G_2} K_{w22} \int_{-L/2}^{L/2} V^2 K_{qx}^2 \, dx$$

$$- \frac{2K_w K_{f1}}{G_2} K_{w23} \int_{-L/2}^{L/2} V^2 K_{qx} Q_x \, dx \qquad - 2.100$$

where

$$K_{w21} = \int_0^{\frac{1}{2}(d_2 - 2d_f)} (\frac{d_2^4}{16} - \frac{d_2^2 z^2}{2} + z^4) dz = \frac{1}{60}\left[d_2^5 - 20 d_2^2 d_f^5 + 30 d_2 d_f^4 - 12 d_f^5\right]$$

$$K_{w22} = \int_0^{\frac{1}{2}(d_2 - 2d_f)} dz = \frac{1}{2}(d_2 - 2d_f)$$

$$K_{w23} = \int_0^{\frac{1}{2}(d_2 - 2d_f)} \left(\frac{d_2}{4}^2 - z^2\right) dz = \frac{1}{12}\left(d_2^3 - 6d_2 d_f^2 + 4d_f^3\right)$$

7.33 Total shear energy

$$U_T = U_f + U_{w1} + U_{w2}$$

$$= K_{u1} \int_{-L/2}^{L/2} V^2 Q_x^2 dx + K_{u2} \int_{-L/2}^{L/2} V^2 K_{qx}^2 dx - K_{u3} \int_{-L/2}^{L/2} V^2 Q_x K_{qx} dx \qquad - 2.101$$

where

$$K_{u1} = \frac{b_f}{G_f} K_f^2 K_{f2} + \frac{b_2}{G_2} K_w^2 K_{w1} + \frac{b_2}{G_2} K_w^2 K_{w21}$$

$$K_{u2} = \frac{K_{f1}^2}{G_2 b_2} K_{w22}$$

$$K_{u3} = \frac{2K_w K_{f1}}{G_2} K_{23}$$

7.4 Shear deflection at mid span

Shear deflection may be calculated using Castigliano's theorem which may be formulated as:

$$\text{Deflection due to force P} = w_s = \frac{\partial U_T}{\partial P}$$

In the case of uniformly distributed load a virtual load P may be applied where deflection is desired to be calculated and Castigliano's formula may be rewritten to find shear deflection as follows:

$$w_s = \frac{\partial U_T}{\partial P} = \frac{\partial U_T}{\partial V} \frac{\partial V}{\partial P} \qquad - 2.102$$

Hence shear deflection at mid span may be given by equation 2.103.

$$w_s = 2K_{u1}p\int_0^{L/2}(x\,Q_x^2)dx + 2K_{u2}\,p\int_0^{L/2}(x\,K_{qx}^2)dx - 2K_{u3}p\int_0^{L/2}x\,Q_xK_{qx}\,dx \quad \text{— 2.103}$$

substituting $Q_x^2 = \left[1 + 2rK_{f1}\,K_{qx}\right]^2 = 1 + 4r^2K_{f1}^2K_{qx}^2 + 4rK_{f1}K_{qx}$

then

$$w_s = 2p\left[C_{s1}\int_0^{L/2}x\,dx + C_{s2}\int_0^{L/2}K_{qx}^2\,dx + C_{s3}\int_0^{L/2}x\,K_{qx}dx\right]$$

$$w_s = 2p\left[C_{s1}\,\Omega_1 + C_{s2}\,\Omega_2 + C_{s3}\,\Omega_3\right] \quad \text{- 2.104}$$

where

$$C_{s1} = K_{u1} \quad \text{- 2.105}$$

$$C_{s2} = 4r^2K_{f1}^2K_{u1} + K_{u2} - 2rK_{f1}K_{u3} \quad \text{- 2.106}$$

$$C_{s3} = 4rK_{f1}K_{u1} - K_{u3} \quad \text{- 2.107}$$

$$\Omega_1 = \int_0^{L/2}x\,dx = \frac{L^2}{8}$$

$$\Omega_2 = \int_0^{L/2}xK_{qx}\,dx = \left[\frac{L^2C}{\pi^2}\left(1 - \frac{1}{\text{Cosh}\,\frac{\pi}{2\sqrt{C}}} - \frac{L^2}{8}\right)\right]$$

$$\Omega_3 = \int_0^{L/2} x\, K_{qx}^2\, dX = \frac{L^2 C}{\pi^2}\left[\int_0^{L/2} \frac{\text{Sinh}^2\left(\frac{\pi}{\sqrt{C}}\,\frac{x}{L}\right)}{x\,\text{Cosh}^2\,\frac{\pi}{2\sqrt{C}}}\,dx - \frac{2L\sqrt{C}}{\pi}\int_0^{L/2} \frac{\text{Sinh}\left(\frac{\pi}{\sqrt{C}}\,\frac{x}{L}\right)}{\text{Cosh}\,\frac{\pi}{2\sqrt{C}}}\,dx + \int_0^{L/2} x\,dx\right]$$

$$= \frac{L^2}{8}\left[\frac{1}{\text{Cosh}^2\,\frac{\pi}{2\sqrt{C}}}\left(1 + \frac{2\pi^2}{2C4!} + \frac{2\pi^4}{3C^2 6!} + \ldots\right) - \frac{16C}{\pi^2}\left(1 - \frac{1}{\text{Cosh}\,\frac{\pi}{2\sqrt{C}}}\right) + 1\right]$$

$$w_s = \frac{pL^2}{8}\left\{2C_{s1} + 2C_{s2}\left[\frac{1}{\text{Cosh}^2\,\frac{\pi}{2\sqrt{C}}}\left(1 + \frac{2\pi^2}{2C4!} + \frac{2\pi^4}{3C6!} + \ldots\right) - \frac{16C}{\pi^2}\left(1 - \frac{1}{\text{Cosh}\,\frac{2\pi}{2\sqrt{C}}}\right) + 1\right]\right.$$

$$\left. + 2C_{s3}\left[\frac{8C}{\pi^2}\left(1 - \frac{1}{\text{Cosh}\,\frac{\pi}{2\sqrt{C}}}\right) - 1\right]\right\} \qquad - 2.108$$

7.5 Shear stiffness factor using non-dimensional parameter α & β

Define: $\alpha = \frac{d_f}{d_2}$, $\beta = \frac{b_2}{b_f}$

assume $m = \frac{G_2}{G_f} = \frac{E_2}{E_f}$

substituing α, β and m in equations 2.105, 2.106 and 2.107, we get:

$$C_{s1} = \frac{6}{5}\,\frac{1}{b_f d_2 G_2 K_{ig}^2}\left\{\frac{K_{ig}^2}{K_{is}^2}\,\alpha^3(m + m^2\beta)\,(10-15\alpha+6\alpha^2) + \frac{\beta m^2}{2}\,(1-20\alpha^3+30\alpha^4-12\alpha^5)\right\}$$

$$- 2.105(a)$$

$$C_{s2} = \frac{6}{5} \frac{1}{b_f d_2 G_2 K_{ig}^2} \left\{ \frac{36\alpha^2(1-\alpha)^4}{K_{is}^2} \left[\alpha^3(m+m^2\beta)\ (10-15\alpha+6\alpha^2) + \frac{\beta m^2}{2}\ (1-20\alpha^3+30\alpha^4-12\alpha^5) \right] \right.$$

$$\left. + \frac{15\alpha^2(1-\alpha)^2(1-2\alpha)}{\beta} - \frac{30m\alpha^2(1-\alpha)^3(1-6\alpha^2+4\alpha^3)}{K_{is}} \right\} \qquad - 2.106(a)$$

$$C_{s3} = \frac{6}{5} \frac{1}{b_f d_2 G_2 K_{ig}^2} \left\{ \frac{K_{ig} 12\alpha(1-\alpha)^2}{K_{is}^2} \left[\alpha^3(m+m^2\beta)\ (10-15\alpha+6\alpha^2) + \frac{\beta m^2}{2}\ (1-20\alpha^3+30\alpha^4-12\alpha^5) \right] \right.$$

$$\left. - 5 \frac{K_{ig}}{K_{is}} \alpha\ (1-\alpha)\ (1-6\alpha^2+4\alpha^3) \right\} \qquad - 2.107(a)$$

where $K_{is} = \Sigma EI / \left(E_f \frac{b_f d_2^3}{12}\right) = 2\alpha^3 + m\beta$

$$K_{ig} = \overline{EI} / \left(E_f \frac{b_f d_2^3}{12}\right) = 2\alpha(3-6\alpha+4\alpha^2) + m\beta$$

we define the following quantities:

$$\acute{C}_{s1} = 2b_f d_2 G_2 K_{ig}^2 C_{s1}$$

$$\acute{C}_{s2} = 2b_f d_2 G_2 K_{ig}^2 C_{s2} \qquad - 2.109$$

$$\acute{C}_{s3} = 2b_f d_2 G_2 K_{ig}^2 C_{s3}$$

using eqns. 2.109 and 2.105(a), 2.106(a) and 2.107(a), eqn. 2.108 becomes

$$w_s = \frac{pL^2}{8b_f d_2 G_2 C_s} \qquad - 2.110$$

where

$$C_s = \frac{K_{ig}^2}{C_s^*} \qquad - 2.111(a)$$

$$C_s^* = C'_{s1}+C'_{s2}\left[\frac{1}{\text{Cosh}^2\frac{\pi}{2\sqrt{C}}}\left(1+\frac{2\pi^2}{2C4!}+\frac{2\pi^4}{2C^2 6!}+\ldots\right)-\frac{16C}{\pi^2}\left(1-\frac{1}{\text{Cosh}^2\frac{\pi}{2\sqrt{C}}}\right)+1\right]$$

$$+C'_{s3}\left[\frac{8C}{\pi^2}\left(1-\frac{1}{\text{Cosh}\frac{\pi}{2\sqrt{C}}}\right)-1\right] \qquad -2.111(b)$$

Shear stiffness factor for rigid case:

For rigid case, connector modulus tends to have an inifinite stiffness i.e. $k \to \infty$ and hence $C \to o$. Substituting $C = o$ in 2.111band values of C'_{s1}, C'_{s2}, C'_{s3}, we get:

$$C_s^* = \frac{6}{5}\left\{2\alpha^3(m+m^2\beta)(10-15\alpha+6\alpha^2)+\beta m^2(1-20\alpha^3+30\alpha^4-12\alpha^5)\right.$$

$$\left.+\frac{30\alpha^2}{\beta}(1-2\alpha)(1-\alpha)^2+10m\alpha(1-\alpha)(1-6\alpha^2+4\alpha^3)\right\} \qquad -2.112$$

and

$$C_s = \left[2\alpha(3-6\alpha+4\alpha^2)+m\beta\right]^2/C_s^* \qquad -2.113$$

Stieda (1967) derived a shear stiffness factor for rigid plywood web I-beams symmetrical about y and z axes. His equation is similar to that given by eqn. 2.113 except for the term $(m + m^2\beta)$ in eqn.2.112 which he gives as $(1+m\beta)^2$. This difference is because in his derivation he adopted the transformed section approach whereas in this thesis the sum of the shear energy of all components is obtained.

7.6 Other loading conditions

A procedure similar to that mentioned in section 6.4 is adopted to derive shear deflection for semi-rigid simply supported plywood web I-beam symmetrical about y and z axes and under four point loading, fig.2.13.

The derivation is also based on shear stress distributions similar to that given in fig.2.16, but appropriate formulae are used to give τ_{xzf}, τ_{xzw1} and τ_{xzw2} corresponding to this loading. These formulae for τ_{xzf}, τ_{xzw1} and τ_{xzw2} may be derived in a similar way to equation 2.90 given to describe web shear stress at neutral axis in section 6.7. Shear deflection may be given by eqn. 2.114 as follows :

$$w_s = \frac{Pb_f}{G_2}\left\{\left[mK_{f2}^2 + \frac{b_2}{b_f}K_w^2\,(K_{f2}+K_{w1})\right]\left[1 - 4r\Omega_4 + 4r^2\Omega_5\right]\right\} \qquad \text{—— 2.114}$$

where; $\Omega_4 = \int_0^1 K_{qxm}\,dx = \left[K'_{m1}\,\mathrm{Sinh}\lambda l + \frac{E_f A_f}{EI}\,rl\right]$

$$\Omega_5 = \int_0^1 (K_{qxm})^2\,dx = \left[\frac{\lambda K'_{m1}}{4}\,(\mathrm{Sinh}2\lambda l + 2\lambda l) + \frac{2E_f A_f r}{EI}\,K'_{m1}\,\mathrm{Sinh}\lambda l + \frac{E_f^2 A_f^2 r^2}{EI^2}\,l\right]$$

where; $K_{qxm} = K'_{m1}\,\lambda\,\mathrm{Cosh}\,\lambda x + \frac{E_f A_f r}{EI}$

and K'_{m1} is given by 2.59.

PART III

EXPERIMENTAL INVESTIGATION

PART III

Experimental Investigation

Chapter 8 Scope and objectives

The work described hereafter in part III of this thesis is of an experimental nature with the following objectives:

(a) to establish mechanical and physical properties of small clear specimens of timber and plywood used in the beam models described in chapter 12.

(b) to establish the elastic properties of timber in actual sizes used in the beam models described in chapter 12.

(c) to establish load-slip curves for timber to plywood joints.

(d) to verify the theoretical work given in part II of this thesis describing the behaviour of rigid and semi-rigid plywood web I-beams in bending by testing four beam models, details of which are described in chapter 12.

Chapter 9 Sampling and specimen cutting

9.1 Timber for flanges

The main requirements that governed the choice of timber used in the beam models described in chapter 12 were:

(a) it should have straight grains and free from defects and also it should be of uniform growth, i.e. no marked bands of spring and summer growth rings.

(b) It should be readily available in reasonable sizes such that there is enough material to make the beam models and to obtain satisfactory and representative number of small clear specimens.

It was found that it was difficult to meet both requirements as at the time of this experimental investigation clear timber was scarce in the market. The first requirement was considered to be more basic than the second one as failures due to local defects were to be avoided and also to obtain reliable strain gauges readings straight grain timber was required. Such timber to meet the first requirement and partly the second requirement was found stored in Princes Risborough Laboratory of the Building Research Establishment since the early 1940s. The timber was Canadian Sitka Spruce which was stored conditioned at 12% moisture content. The timber was available in four 4 x 6 x 96 inch joists.

The design of the models was then governed by the amount of timber available and hence the cutting schedule was prepared bearing in mind that after cutting the timber for flanges, enough material should be available for small clear specimens and joint specimens. To achieve this, each joist was considered as a separate unit and that it represents the material for one model and that the flanges size was chosen to be $1\frac{3}{4}$ x $1\frac{3}{4}$ x $95\frac{1}{2}$ inches. It should be noted that the length chosen for the flanges was based on the fact that the timber at the ends of one joist was damaged such that only $95\frac{1}{2}$ inch of its length was useful.

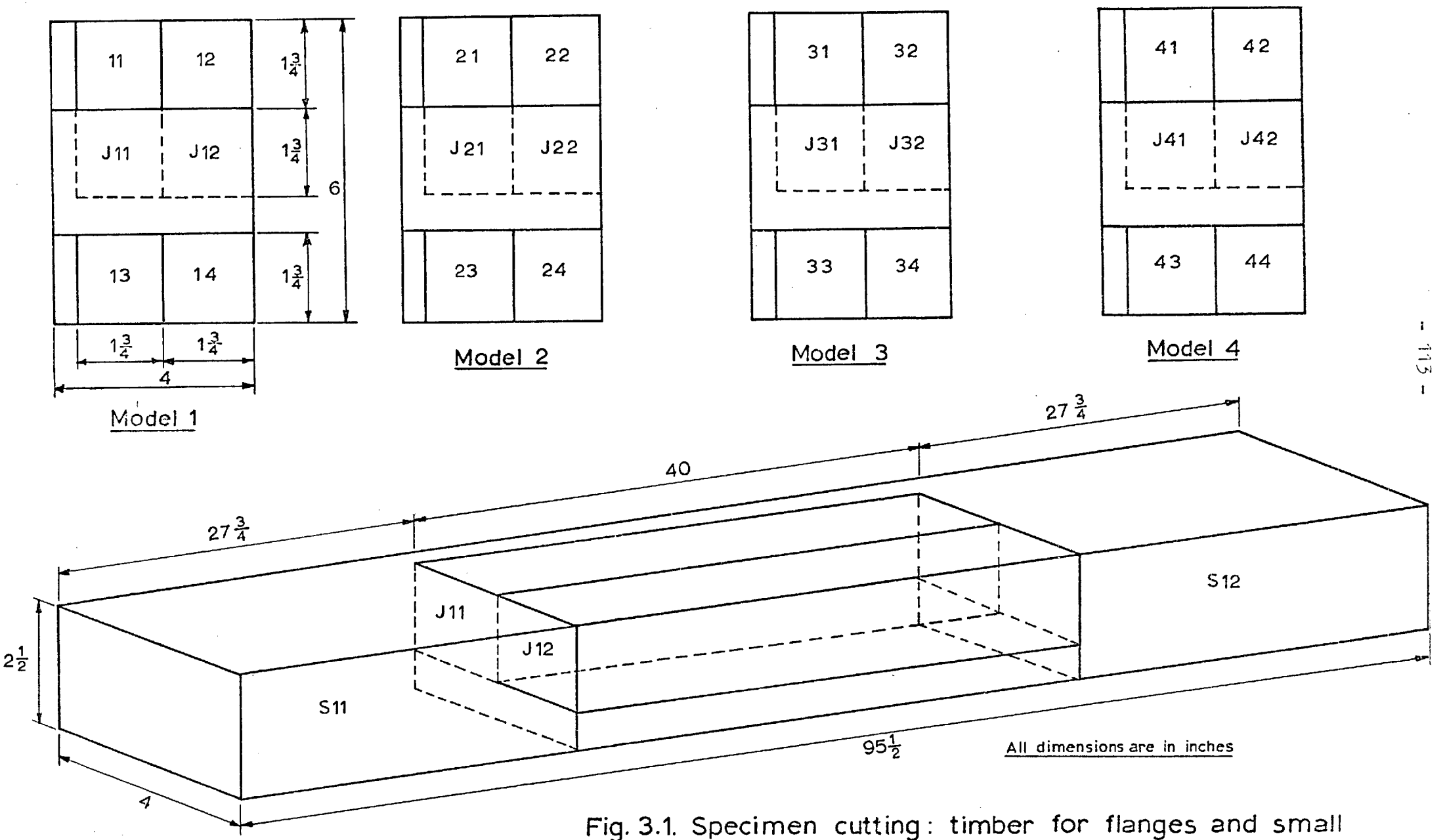
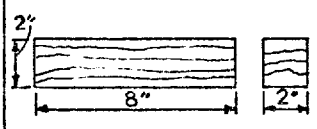
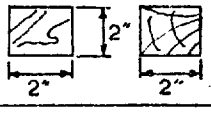
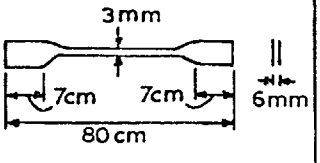
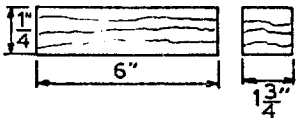
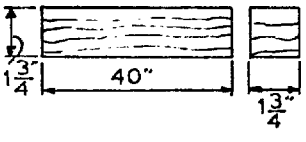
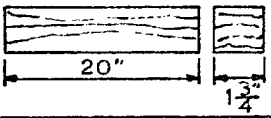


Fig. 3.1. Specimen cutting: timber for flanges and small clear specimens

MODEL N°		NUMBER OF SPECIMENS												
		1			2			3			4			
Test		S11	S12	Total	S21	S22	Total	S31	S32	Total	S41	S42	Total	Gross Total
Compression parallel to grain		3	3	6	3	3	6	3	3	6	3	3	6	24
Compn. ⊥ to grain and shear // grain		6	6	12	6	6	12	-	-	-	-	-	-	24
Tension // to grain		3	3	6	3	3	6	3	3	6	3	3	6	24
* Joint		-	-	-	-	-	-	3	3	6	3	3	6	12
		J11	J12		J21	J22		J31	J32		J41	J42		
Static Bending		1	"	2	1	1	2		1	2	1		2	8
* Static bending to determine modulus of rigidity G		3			3			3			3			12

* All dimensions are according to B.S. 373 (1957) except for:

(a) joint test where dimensions are based on beam models (3) and (4) joint dimensions

(b) static bending test to determine G where dimensions are based on $\frac{l}{d}$ ratio equal to that of the beam models, and on flange cross section since specimens were obtained from flange material after models were tested

Table 3·1(a). Cutting schedule for small clear specimens of timber

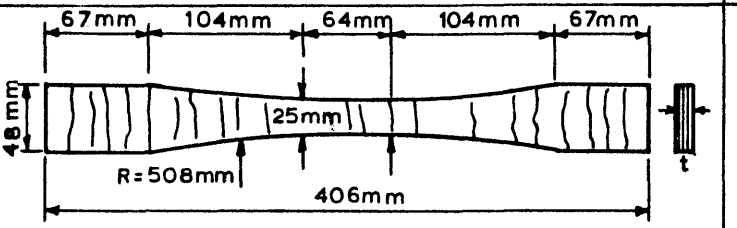
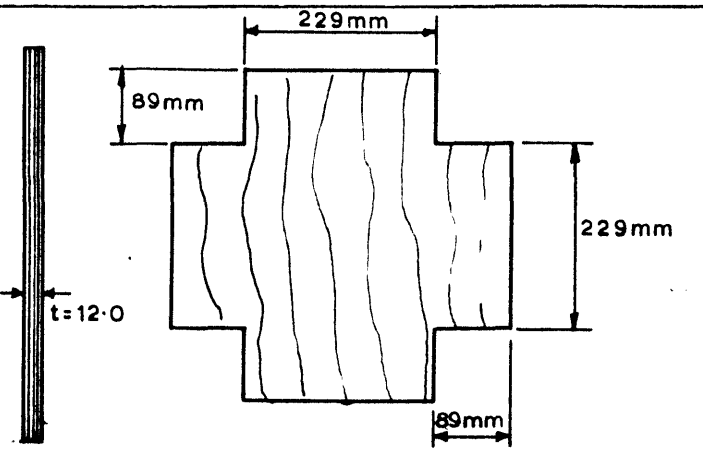
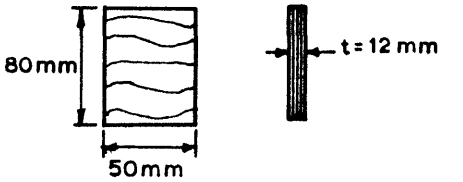
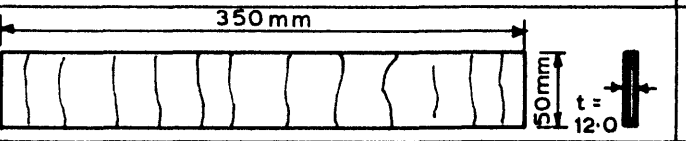
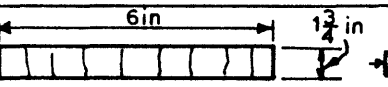
Fig.3.1 and table 3.1(a) illustrate the cutting schedule for the four joists to obtain the desired flange sizes and representative number of small clear specimens for that joist; e.g. flanges for model 1 are designated 11, 12, 13 & 14, bending specimens are designated J11 & J12 and small clear specimens are obtained from specimens designated S11 & S12. It should be noted that specimens for static bending tests are obtained from central region of joist span, as maximum bending moment will occur in that region.

All specimens to determine the physical properties of timber, i.e. density and moisture content were obtained from the small clear specimens after they had been tested.

It should be noted that no growth ring matching for small clear specimens was specified as this would have resulted in some material being wasted.

9.2 Plywood for web

The plywood used for the webs in the models and specimens to establish its mechanical and physical properties was Finnish birch plywood found stored in the stores of the Civil Engineering Department of Imperial College. The plywood was available in 4 x 8 feet sheets having $\frac{1}{4}$ inch thickness made of five plies. Two $\frac{1}{4}$ inch sheets were joined using Cascamite glue to make $\frac{1}{2}$ inch thick plywood, and also, so formed, $\frac{1}{2}$ inch sheets may be joined to make 1 inch thick sheets. It should be noted that the models webs were chosen to be of either $\frac{1}{2}$ inch or 1 inch thick and 8 x $95\frac{1}{2}$ inches for depth and length respectively.

Test	Specimen Dimensions	N°off
Tension		6
Panel Shear		6
Compression		6
Bending		6
Joints		6

All dimensions are according to B.S. 4512 (1969)
Similar schedule was also prepared for 1inch thick plywood for all the tests except for the panel shear test

Table 3·1(b)·Cutting schedule for plywood specimens

Three $\frac{1}{2}$ x 8 x 95$\frac{1}{2}$ inches and one 1 x 8 x 95$\frac{1}{2}$ inches sheets were cut for the models webs. Table 3.1(b) shows the cutting schedule for the specimens to determine mechanical properties of the plywood and load slip curves for timber to plywood joints. All the specimens to determine the physical properties of plywood were obtained from the small clear specimens after they had been tested.

The glue used was Cascamite "one shot"synthetic resin glue which was prepared and applied according to the manufacturers' instructions, The Borden Chemical Company (UK) Ltd. technical information No.32e.

Chapter 10 Small clear specimens and joints tests

10.1 Timber for flanges

The following tests were performed on small clear specimens, obtained for each beam model as indicated in section 9.1 to determine the mechanical properties of each beam model corresponding to these tests.

(1) Compression parallel to grain test

(2) Tension parallel to grain test

(3) Static bending tests to determine moduli of elasticity (E) and rigidity (G).

Also the following tests were performed on small clear specimens obtained from beam models (1) and (2) only to determine ultimate strength for compression perpendicular to grain and also ultimate strength for shear parallel to grain for the timber used for the flanges of those models. It is worth mentioning here that these tests were not carried out for beam

models (3) and (4) as the material available was not enough to make small clear specimens for those tests and specimens for joints tests, as these models are the models representing the semi-rigid cases.

(1) Compression perpendicular to grain test

(2) Shear parallel to grain test.

Tests to determine the moisture content and specific gravity were performed on specimens obtained from small clear specimens at the end of each of the previous tests.

All previous tests were carried out according to B.S.373 (1957). Extensometers were used for compression parallel to grain, tension parallel to grain and static bending tests to determine moduli of elasticity and also to find load-displacement curves of these properties. Fig.3.2 and fig.3.3 show the types of extensometers and the way they were attached to the tension and bending specimens. All extensometers were calibrated against a standard $\frac{1}{2}$ dial gauge in the same way for each test carried out and then magnification factors were found in compression, tension and bending.

Static bending test was also carried out to determine the modulus of rigidity of the timber of the models. A procedure similar to that described in B.S.373 (1957) for four point loading bending test was followed. Instead of using extensometers, three dial gauges were used at mid span and under the loads. Deflection relative to loading positions, i.e. in constant bending moment region, were found and pure bending stiffness was calculated from the following equation:

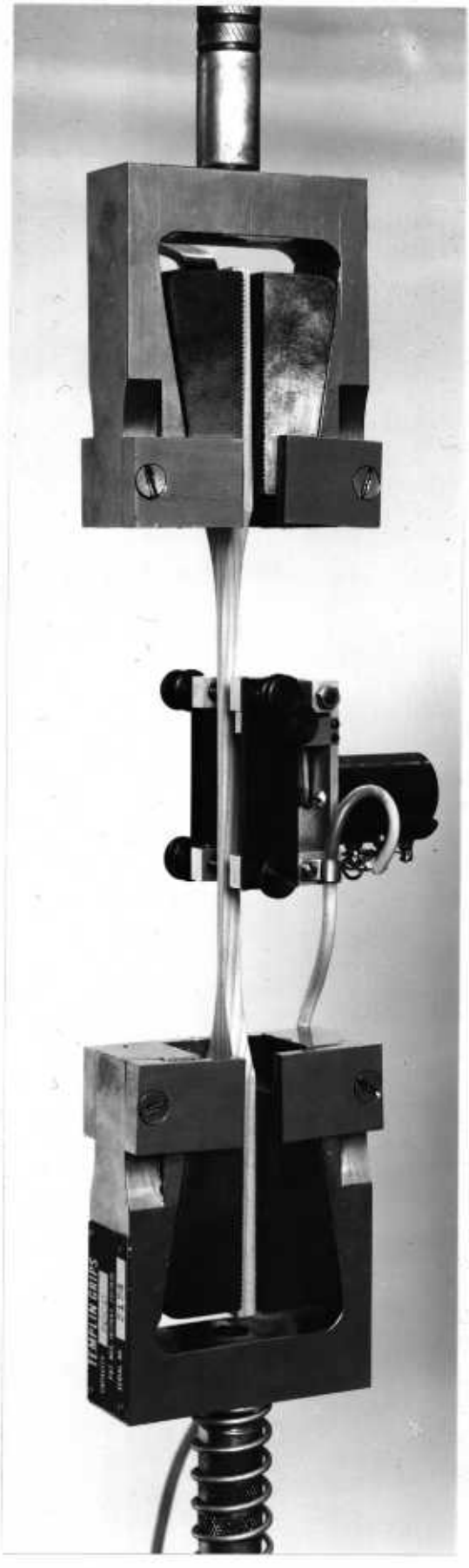


Fig.3.2 Tension parallel to grain test arrangement

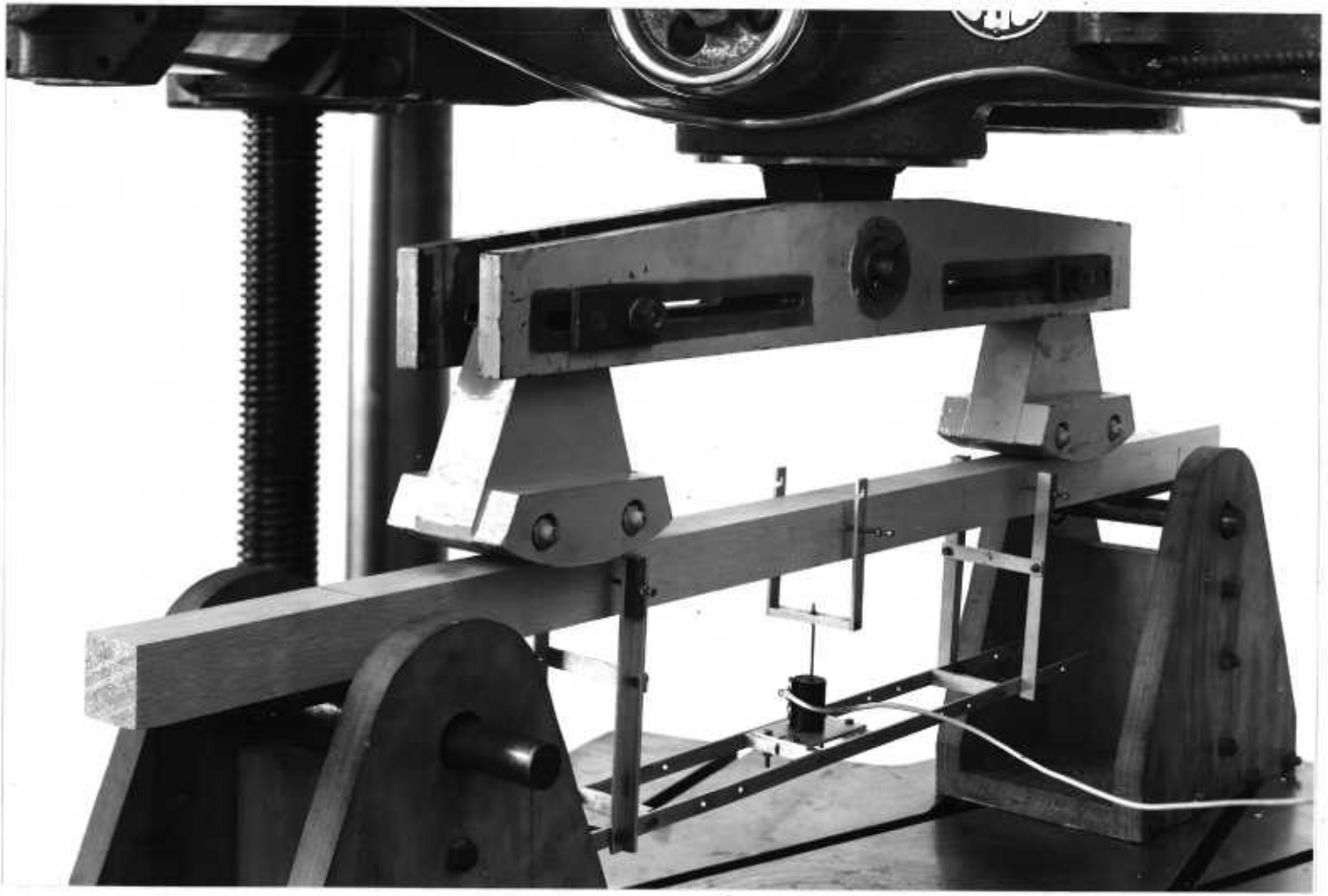


Fig. 3.3 Static bending test arrangement

$$\overline{EI} = \frac{Ml^2}{8w'}$$

where M = pure bending moment

l = length of pure bending section

w' = relative deflection at mid span

The pure bending deflection at mid span was calculated using pure bending stiffness for a load less or equal to the proportional limit load. Shear deflection was then calculated by subtracting the pure bending deflection at mid span from the total deflection at mid span for that load. The modulus of rigidity was then calculated from the following equation:

$$G = 0.4 \frac{PL}{Aw_s} \quad \text{(for four point loading at } \frac{1}{3} \text{ span)}$$

where P = load (lbs)

L = span (20 inch)

A = cross sectional area ($1\frac{3}{4}$ x $1\frac{3}{4}$ inch)

w_s = shear deflection found as shown before.

The mean values and coefficient of variations of all the mechanical and physical properties corresponding to the tests mentioned in this section are summarised in table 3.2 for each model. Also figs.3.4 and 3.5 show mean experimental and idealized $\sigma - \varepsilon$ curves in compression and tension parallel to grain for models 1, 2, 3 and 4.

		Compn. // grain					Tension // grain					Static Bending				Compn. ⊥ grain			Shear // grain			Static Bending
Mean Values	10^6 E lb/in^2	σ_{pL} lb/in^2	σ_u lb/in^2	ε_u 10^{-3}	Density lb/cu.ft	m.c. %	E lb/in^2	σ_u lb/in^2	ε_u 10^{-3}	Density lb/cu.ft	m.c. %	10^6 E lb/in^2	σ_u lb/in^2	Density lb/cu.ft	m.c. %	σ_u lb/in^2	Density lb/cu.ft	m.c. %	τ_u lb/in^2	Density lb/cu.ft	m.c. %	$''$ 10^5 G lb/in^2
Coefficient of Variation	Cv	Cv	Cv	Cv	Cv	Cv	Cv	Cv	Cv	Cv	Cv	Cv	Cv	Cv	Cv	Cv	Cv	Cv	Cv	Cv	Cv	Cv
MODEL 1	1·80	4780	5800	3·6	30·1	13·3	1·70	15340	9·1	30·0	13·2	1·35	13300	30·0	13·2	600	30·1	13·2	1570	29·7	13·1	1·09
	·024	·018	·026	·093	·03	·056	·135	·152	·134	·051	·042	·015	·12	·020	·066	·028	·043	·037	·048	·043	·012	·08
MODEL 2	1·29	3630	4970	4·4	25·0	13·7	0·96	12500	130	23·9	13·7	0·83	12510	24·0	13·5	560	23·4	13·4	1580	24·3	13·5	0·95
	·034	·078	·036	·11	·053	·012	·029	·04	·028	·010	·02	·027	·068	·014	·0015	·019	·040	·013	·057	·012	·015	·11
MODEL 3	1·73	4240	5300	3·7	25·6	13·4	1·70	12700	7·4	25·0	13·0	1·30	11960	25·3	13·2	—	—	—	—	—	—	1·14
	·057	·021	·036	·048	·061	·021	·062	·091	·13	·018	·017	·047	·021	·018	·011	—	—	—	—	—	—	·05
MODEL 4	1·70	4450	5240	3·7	26·4	13·3	1·53	14050	9·2	25·4	12·8	1·37	12460	25·9	13·1	—	—	—	—	—	—	1·06
	·025	·038	·019	·02	·054	·023	·099	·082	·054	·037	·025	·022	·033	·025	·0019	—	—	—	—	—	—	·13

Table 3·2. Summary of results of tests on clear specimen of timber of models 1, 2, 3 & 4

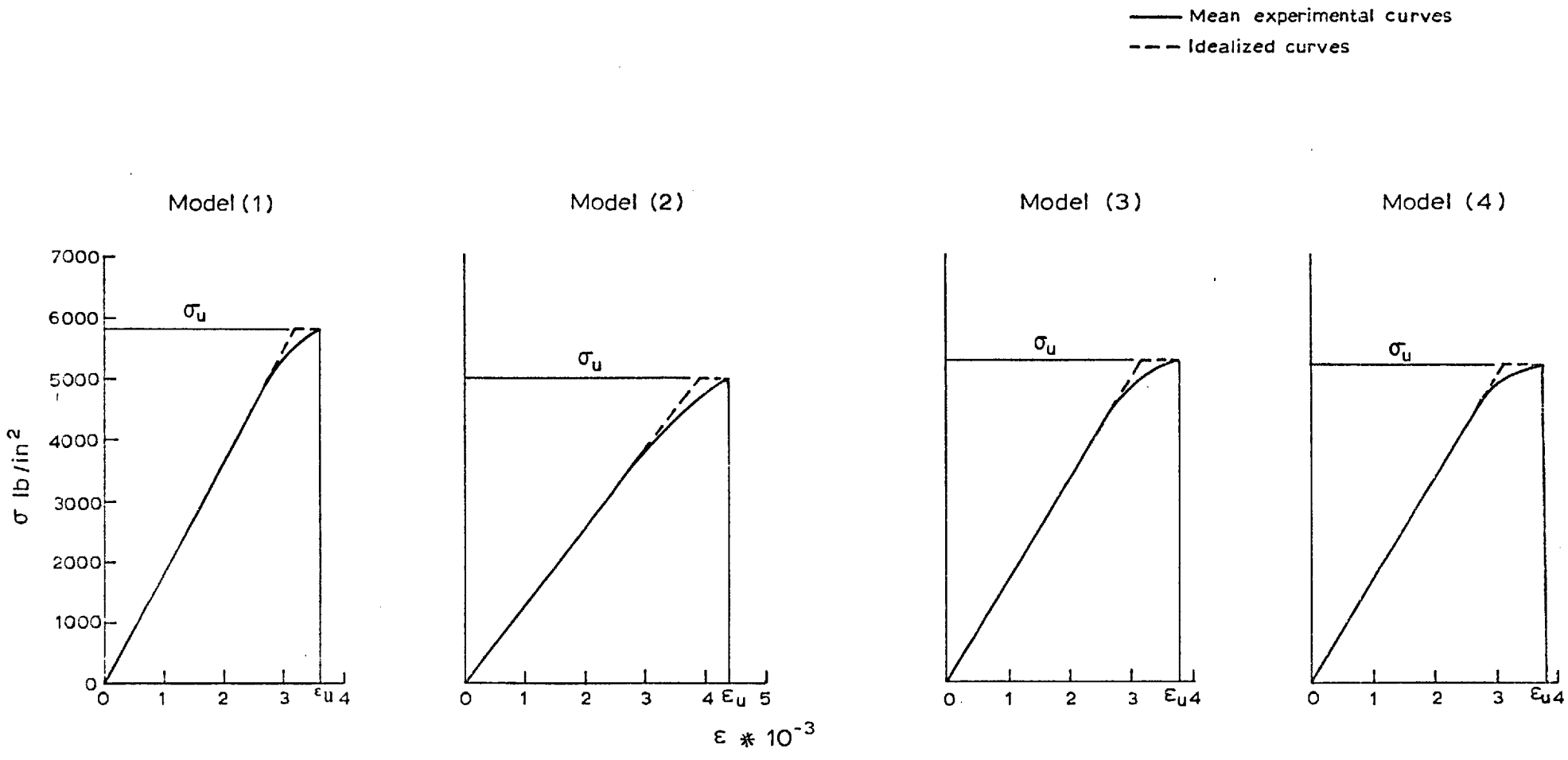


Fig. 3·4. Mean and idealized compressive σ- ε relationships for models 1, 2, 3 and 4

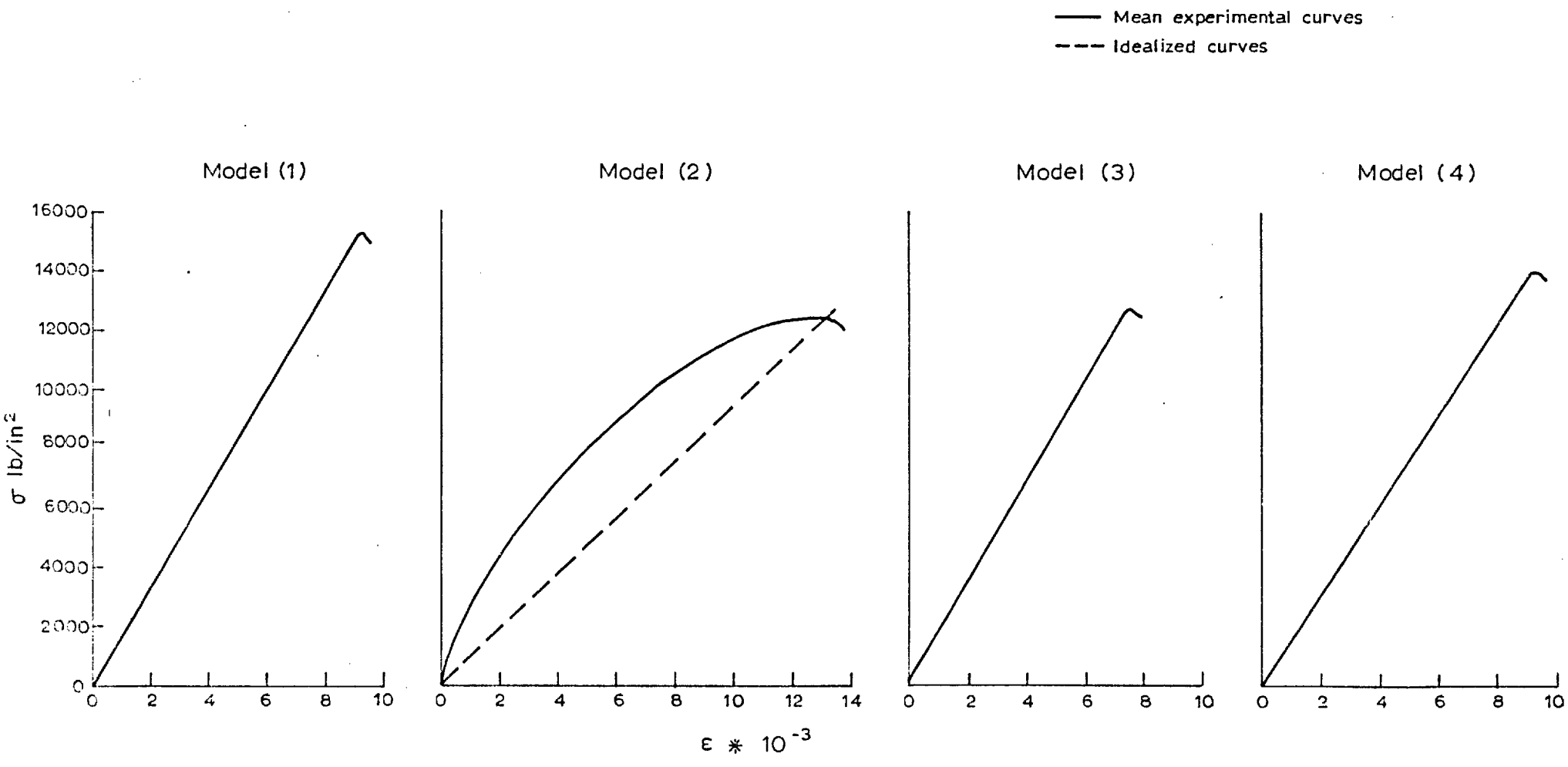


Fig. 3·5. Mean and idealized tensile σ - ε relationships for models 1, 2, 3 and 4

Low results of moduli of elasticity in tension and compression and also slight non-linearity of $\sigma - \epsilon$ curve in tension parallel to grain (fig.3.5) for model (2) are attributed to the presence of compression wood in model (2). It should be noted that all the models were Canadian Sitka Spruce and had more or less equal densities. It was found that specimens from timber of model (2) were free from biological detroiration and presence of compression wood was sighted from slides under the microscope. It was also thought that timber of model (2) was probably naturally of low density whose actual density had been increased by the presence of compression wood.

10.2 Plywood for web

The following tests were performed on clear specimens of plywood, obtained for both $\frac{1}{2}$ inch and 1 inch thick plywood as indicated in section 9.2, to determine the mechanical properties of $\frac{1}{2}$ inch and 1 inch thick plywood corresponding to these tests.

(1) Compression perpendicular to face grain

(2) Tension perpendicular to face grain

(3) Static bending test with face grain perpendicular to span

Also panel shear test was performed on specimens of plywood obtained for $\frac{1}{2}$ inch thick plywood only. Panel shear tests were not performed for 1 inch thick plywood as the apparatus available is only suitable for $\frac{1}{2}$ inch or less thick plywood and also because B.S.4512 (1969) does not recommend specimens dimensions for plywood thicker than $\frac{1}{2}$ inch.

Tests to determine the moisture content and specific gravity were performed on specimens obtained from plywood specimens at the end of each of the previous tests.

All tests were performed according to B.S.4512(1969). Extensometers similar to those used for timber tension and bending specimens given in figs.3.2 and 3.3 were used to determine load displacement curves in the tension perpendicular to face grain and bending tests for plywood.

In the compression test, it was impossible to fit an extensometer of the types available in the laboratory on the compression specimen because it was wide and short. Instead of an extensometer, a 2 inch demountable mechanical gauge (DEMEC) was fixed on one side of the specimen and an electric resistance gauge of type PL10 bonded with P2 glue was fixed on the same side of the compression specimen, both mounted in a direction parallel to that in which the load was applied, ie perpendicular to face grain. While with DEMEC gauge displacement results were recorded at chosen load increments, strain results were recorded from the PL10 electric gauge at the same increments.

In the panel shear test a 45^{o}PR10 rosette bonded with P2 glue was fixed on each side of the panel shear specimen. The gauges were placed on the specimens such that the mutually perpendicular gauge lines lie along the diagonals of the square panels. Loads and strains were recorded at chosen load increments up to failure. DEMEC gauges were used to measure displacements over 2 inch gauge length along the diagonals. The DEMEC gauges results were converted into strain and were used to find correction factors to rosette gauge factors. Also from panel shear results panel shear stresses (τ_{xz}) may be calculated at any load P as described in B.S. 4512(1969) and panel shear modulus may be calculated from equation 3.1.

$$G_{xz} = \frac{\tau_{xz}}{\gamma_{xz}} \qquad - 3.1$$

where $\gamma_{xz} = \left| \varepsilon_1 - \varepsilon_2 \right|$

and ε_1 & ε_2 are principal strains in any mutually perpendicular directions x and z and may be calculated for a 45^o rosette as given by equation 3.2.

$$\varepsilon_1, \quad \varepsilon_2 = \frac{1}{2} \left\{ \varepsilon_o + \varepsilon_{90} \pm \sqrt{\left[(\varepsilon_o - \varepsilon_{90})^2 + (2\varepsilon_{45} - \varepsilon_o - \varepsilon_{90}) \right]} \right\} \qquad - 3.2$$

ε_o, ε_{45} & ε_{90} are strain results obtained from rosette readings as shown by fig.3.6

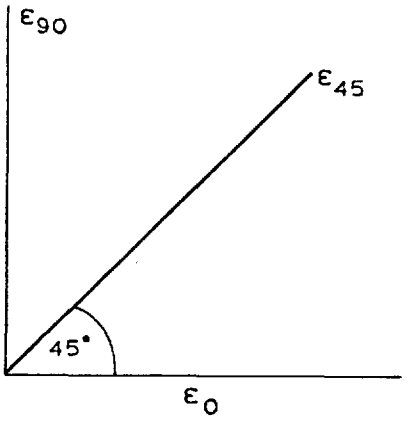


Fig. 3·6. Strains in a 45° rosette

Average results for all the mechanical properties calculated from the tests described in this section and also coefficients of variation of these properties are summarised in table 3.3 and fig.3.7.

It was found that the results for the mechenical properties of $\frac{1}{2}$ inch and 1 inch plywood when tested in tension perpendicular to face grain, compression perpendicular to face grain and bending do not vary considerably and that higher variations in the results of $\frac{1}{2}$ inch or 1 inch plywood when considered separately were encountered. For this reason results for $\frac{1}{2}$ inch and 1 inch thick plywood were considered together and mean values and coefficients of variation were accordingly found.

Table 3.4 gives average correction factors that should be applied to gauge factors of PL10 and PR10 electrical resistance strain gauges as determined by comparing strain results from these gauges with those obtained from DEMEC gauges. It is worth mentioning that the accuracy obtained from DEMEC gauges is up to 10^{-5} inches while that of electrical resistance gauges is up to 10^{-6}. DEMEC gauges were only used because extensometers to fit the specimens dimensions under investigation were not available in the laboratory at the time of test.

	Compn ⊥ face grain				Tension ⊥ face grain			Static Bending		Panel Shear		Density	Moisture Content
	E	σ_{pl}	σ_u	ε_u	E	σ_u	ε_u	E	σ_u	G	τ_u		m.c.
	lb/in^2 $x10^6$	lb/in^2	lb/in^2	$x10^{-3}$	lb/in^2 $x10^6$	lb/in^2	$x10^{-3}$	lb/in^2 $x10^6$	lb/in^2	lb/in^2 $x10^5$	lb/in^2	lb/ft^3	%
Mean	1.05	2480	4640	12.2	1.05	7600	7.25	.891	8690	1.16	2150	46.5	11.0
Coefficient of variation	.058	.054	.010	.067	.048	.146	.132	.066	.104	.112	.049	.024	.012

Table 3.3 Mean mechanical and physical properties for $\frac{1}{2}$ inch and 1 inch thick plywood

Gauge	Correction Factor	Original Gauge Factor	Corrected Gauge Factor
PL 10	0.883	2.08	1.837
PR 10	0.895	2.11	1.889

Table 3.4 Mean corrected gauge factor for electrical resistance gauges on plywood

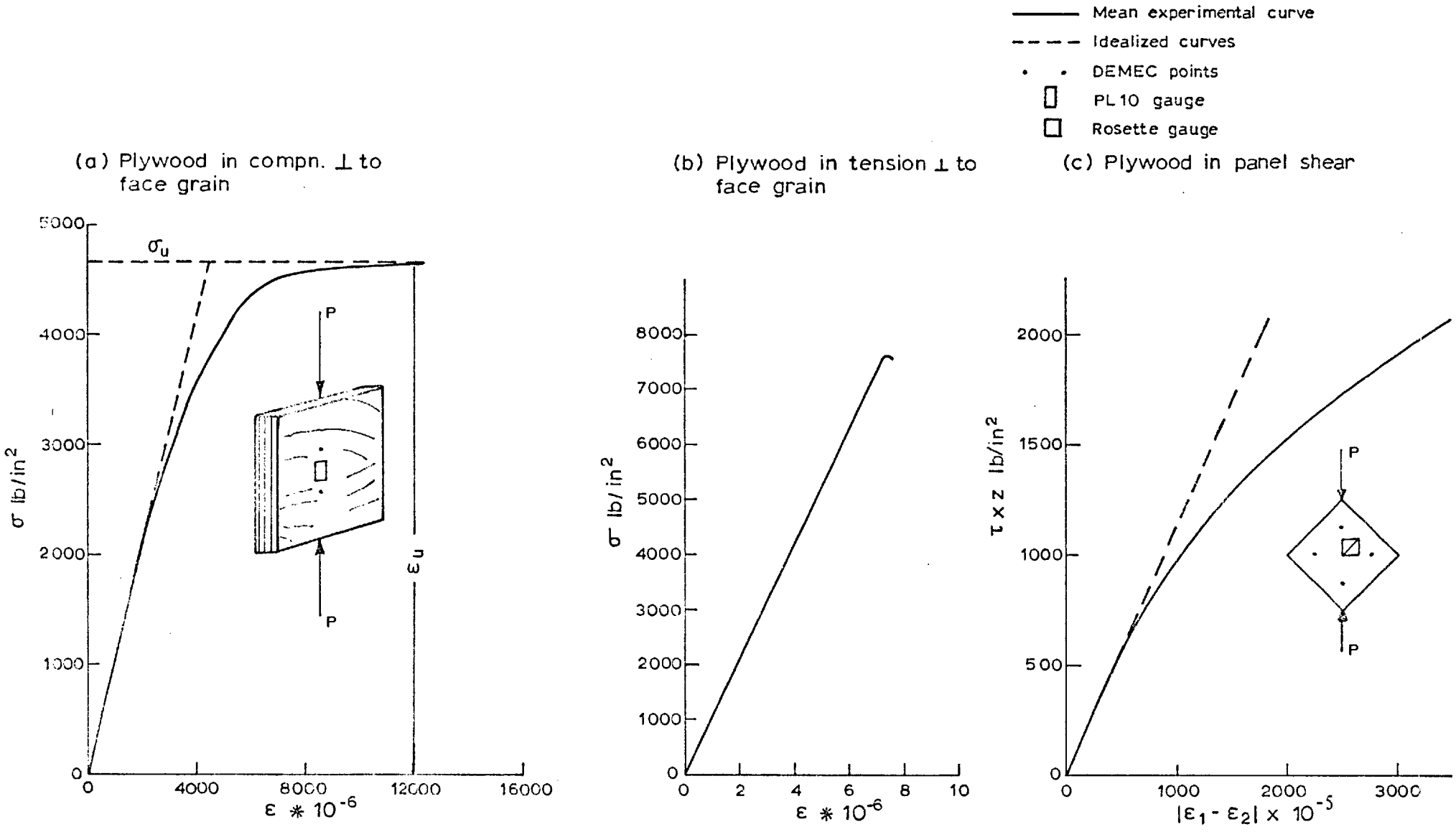


Fig. 3·7. Stress-strain relationships for plywood in compression ⊥ to face grain and tension ⊥ to face grain and panel shear

10.3 Timber to plywood nailed joints

Timber to plywood nailed joints were constructed to simulate joints for beam models (3) and (4). The dimensions of timber and plywood are given in tables 3.1(a & b) . It is noted that the timber cross-sections and plywood thicknesses are the same as those used in the beam models. Wire nails similar to those used in the beam models were used for the joints. The following nails were used

(a) Two SWG 8 wire nails which are of 0.16 inch diameter and of $3\frac{1}{2}$ inch length for each joint representing beam model (4).

(b) Two SWG7 wire nails which are of 0.176 inch diameter and of 4 inch length for each joint representing beam model (3).

The joints were fabricated in a similar way to that used in fabrication of beam models joints. 0.125 inch diameter holes were pre-drilled at the same nail spacing adopted for the beam models joints, i.e. at 2 inch spacing. The object of these pre-drilled holes are:

(a) to ensure that the nails were driven at right angles to both the timber and plywood.

(b) to comply with minimum edge and end distances and also minimum nail spacing as specified by CP112 (1967).

As shown in figs. 3.8 and 3.9, each nail was driven from one side of the joint through the timber and plywood components, i.e. each nail was acting in double shear.

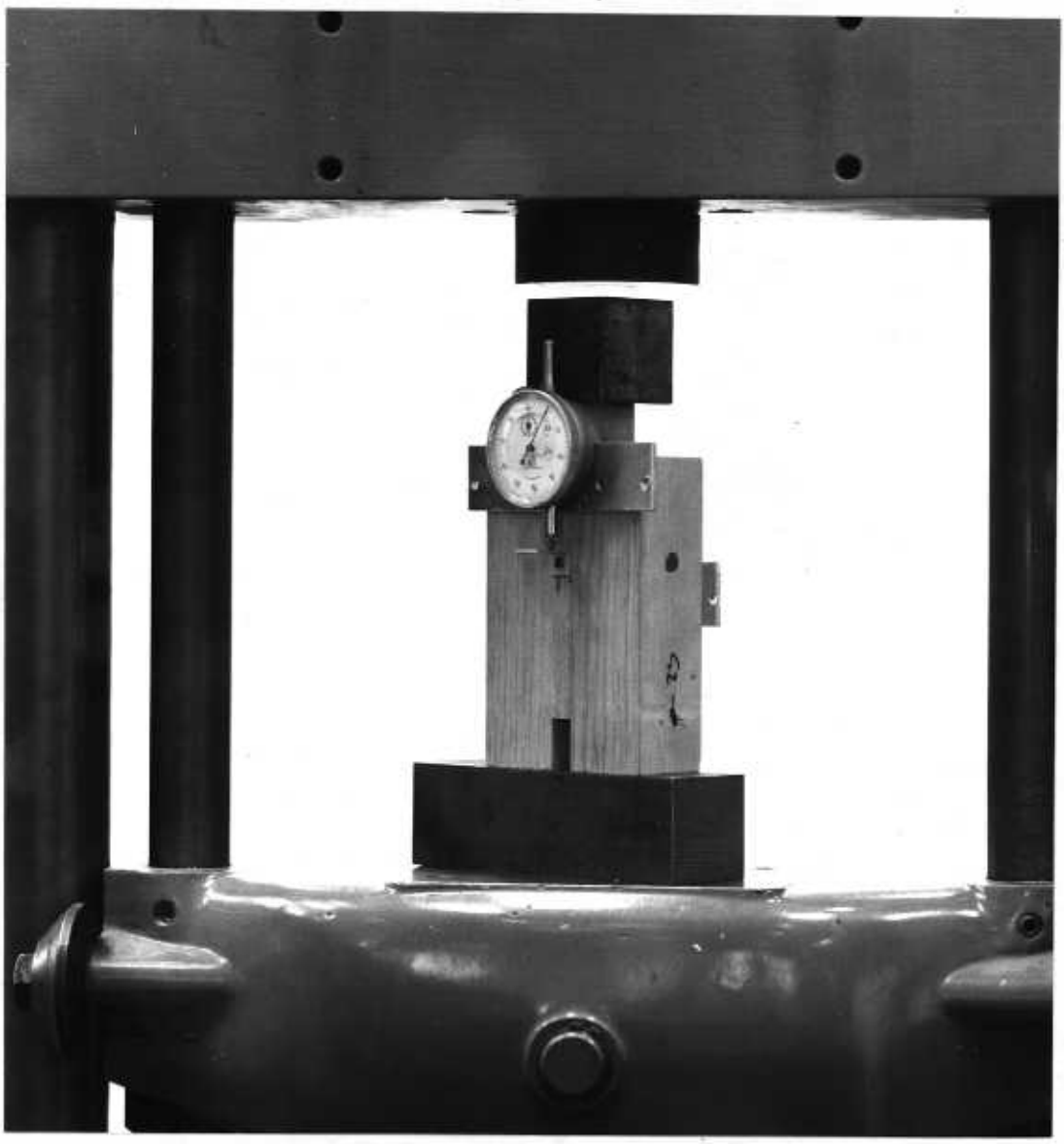


Fig. 3.8 Joint test arrangement

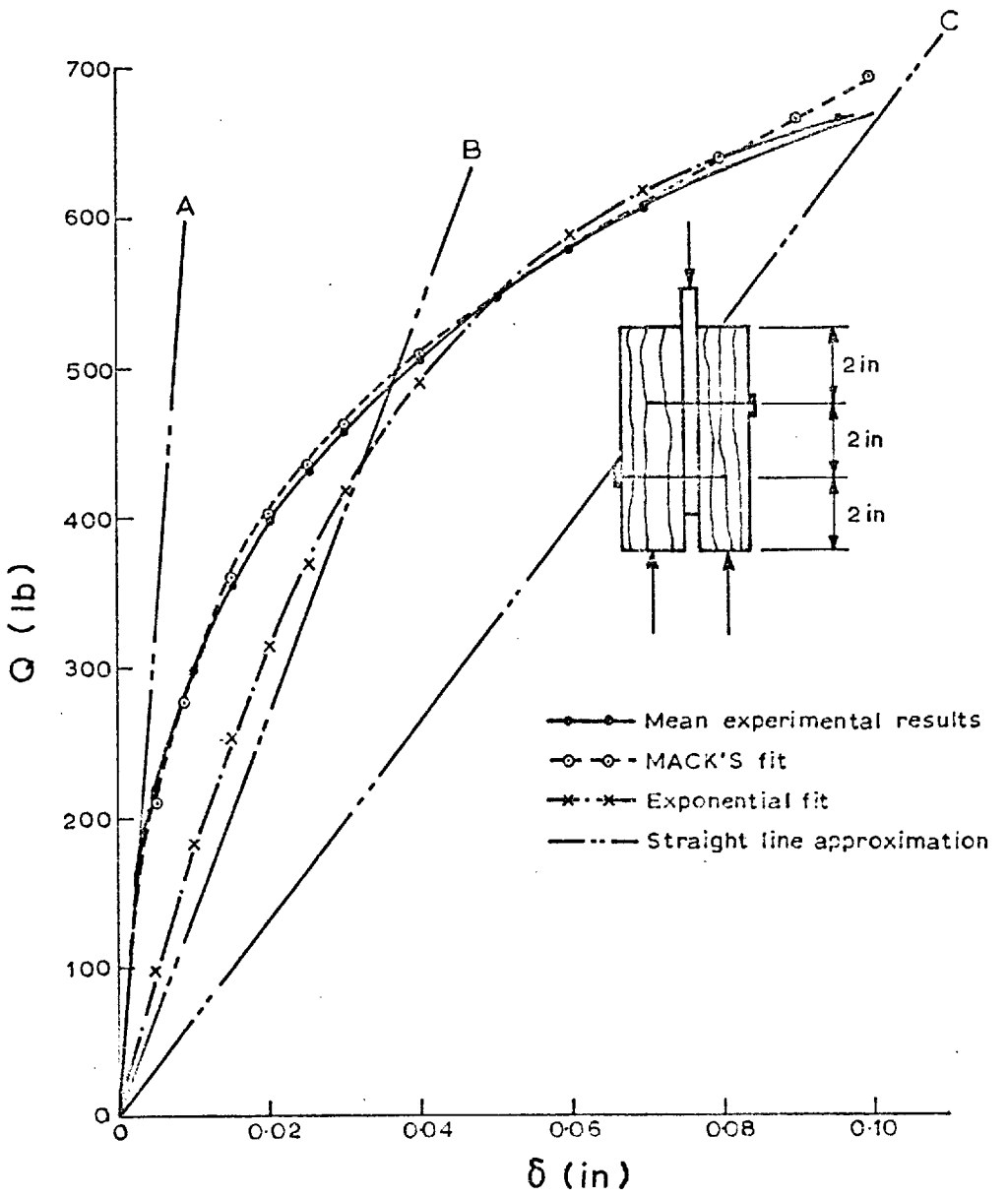


Fig. 3·9. Q - δ relationship for joint corresponding to model (4)

A 1 inch dial gauge was fixed on each face of the joint as shown in fig.3.8. The object of the dial gauges was to measure the relative slip between the plywood and timber as the load was applied.

The joints were tested in compression in a 10 ton Amsler machine. Load was applied at predetermined load increments and corresponding slips were recorded from both dial gauges. It was not possible to maintain a a constant rate of loading as the machine was slowed or kept at the same load until both dial gauges readings were taken. At high loads it was not possible to read both dial gauges because the slip tended to increase rapidly. For this reason only one dial gauge was read at high loads. Load was applied until the joint had failed.

The results from both dial gauges were averaged for each load increment. The variation was found to be negligible. Average results from joint specimens representing joints of beam models (3) and (4) were compiled and analysed separately. Load per nail in double shear and corresponding slip results from joint tests were analysed statistically to fit two equations:

(i) Mack's equation given by equation 2.20, such that the species factor k_{sf} is determined for each joint model.

(ii) Exponential equation of the form given by equation 3.3 such that the constants k_1 and k_2 are determined for each joint model.

$$Q = k_1 (1 - e^{-k_2 \delta}) \qquad - 3.3$$

A simple computer program was written to find the mean value for the species factor based on Mack's equation, noting that the nail diameter factor k_{ϕ} may be calculated from equation 2.20(a), for both joint models from test results of these joint models. Also the same program statistically fitted the results from both joint models based on linear regression and least square fitting, refer to Hald (1952), of $\log_e Q$ and $\log_e \delta$ so as to determine k_1 and k_2. The results of these are summarised in table 3.5 and fig.3.9. All analysis was based up to 0.1 inch slip only. Also moisture content and density were obtained at the end of each test.

Joint model	MACK Fit			Exponential Fit			Ultimate results		Density	
	k_{sf} (Mean)	c_v in k_{sf}	* M_v in Q %	k_1	k_2	M_v in Q %	Q_u lb	δ_u in.	lb/ft^3	m.c. of timber %
Model (3)	360	.035	8.2	740	29.9	65	1100	.85	25.2	13.15
Model (4)	345	.028	7.4	701	30.1	70	1057	.80	26.1	13.0

Table 3.5 Joint results

* M_v Maximum variation between predicted and actual loads

Fig.3.9 shows results for joint model (4) only. Results for joint model (3) were not plotted as these results were found to be similar to those given by joint model (4) shown in fig.3.9. It is also noticed that there is no significant difference in the ultimate load and corresponding slips between joints models (3) and (4).While the results of the test agree well with Mack's fit, their agreement with the exponential fit is poor at low and medium loads, refer to fig.3.9 and table 3.5.

Straight lines OA, OB & OC in fig.3.9, give straight line approximations for $Q - \delta$ relationship, for low loads, medium and high loads respectively. The connector moduli, i.e. $k = Q/\delta$ of these lines are summarised in table 3.6.

Load Level	Straight line	Connector Modulus k lb/in
Low	OA	70000
Medium	OB	13330
High	OC	7000

Fig. 3.6 Connector moduli for joint models (3) and (4)

Chapter 11 Tests on timber flanges prior to beam models fabrication.

11.1 Scope and objectives

The object of this test is to find the moduli of elasticity for timber in compression and tension in the actual sizes used in the beam models and to compare these results with those found in section 10.1 from small clear specimens. Specimens were obtained as shown in section 9.1. The specimens were tested in either tension or compression according to its position in the models as shown in table 3.7.

Test	Specimens			
	Model (1)	Model (2)	Model (3)	Model (4)
Tension	13,14	23,24	33,34	43,44
Compression	11,12	21,22	31,32	41,42

Table 3.7 Specimens for tests on timber flanges prior to beam models fabrication

Also from the same tests correction factors were found for the electrical resistance strain gauges when timber is tested in tension or compression.

11.2 Preparation of flanges

For the preparation of the specimens to carry tension or compression tests the following procedure was followed:

(a) All ends of the specimens were squared. Special attention was made to compression specimens where the load was applied, as the condition of the end surface was found to be of vital importance to the strain results across the depth of the compression specimens.

(b) Three electrical resistance strain gauges of type PL10 were glued with P2 glue across the depth of one vertical face of each specimen at the vertical centre line of each specimen, refer to figs.3.10 & 3.12.

(c) Two DEMEC points were fixed two inches apart along the line of the central PL10 gauge such that each point is one inch to one side of the vertical centre line.

In addition to the above the following procedure was followed in the preparation of the tension specimens:

(a) Four $1\frac{3}{4}$ x $1\frac{3}{4}$ x 3 inches timber blocks were carefully cut in length, to the nearest $\frac{1}{32}$ inch and squared at the ends for each tension specimen.

(b) Each block was carefully glued to each of the vertical faces at the ends of each specimen, refer to figs.3.10 and 3.11. The glue used was Cascamite "one shot" synthetic resin glue and was prepared and applied as shown in section 9.2. It should be noted that the alignment of the ends of the glued blcoks with the ends of the specimen and the squareness of their ends is of vital importance as this might influence the readings of each of the three strain gauges at the vertical centre line of each specimen. It should also be

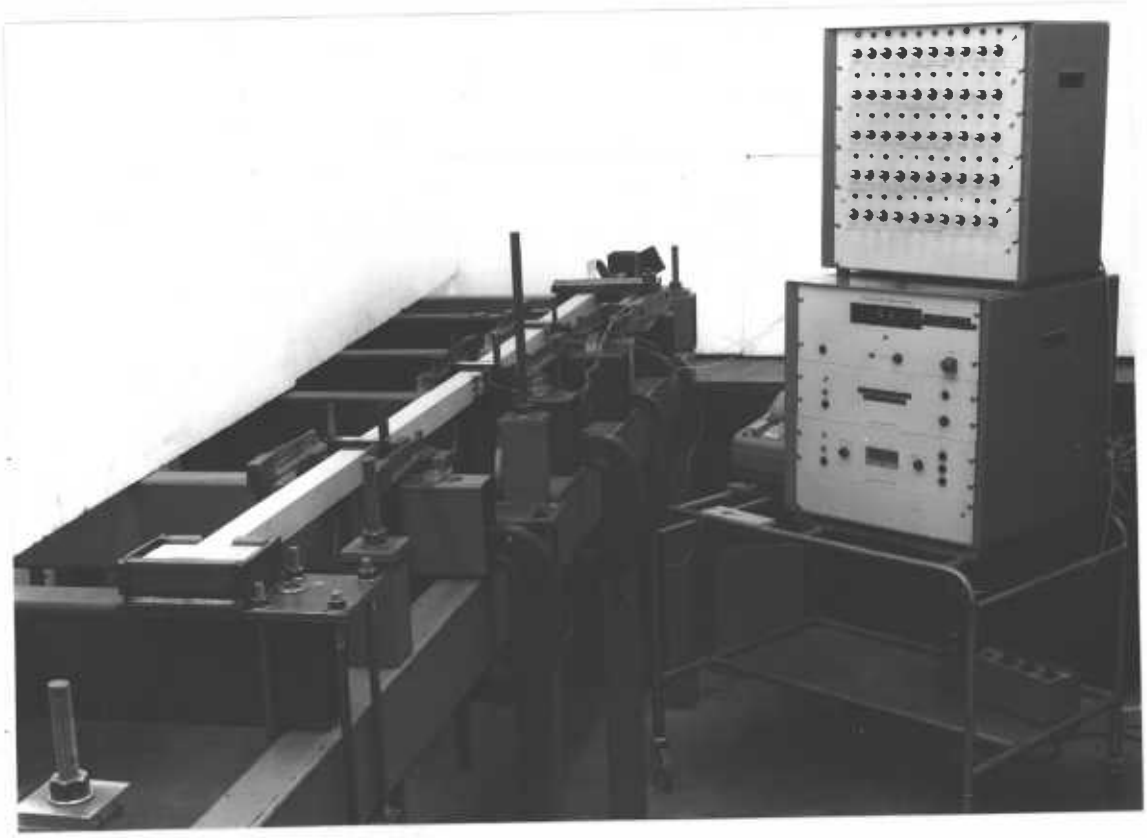


Fig.3.10 Arrangement of equipment and specimens for tests on timber flanges prior to models fabrication

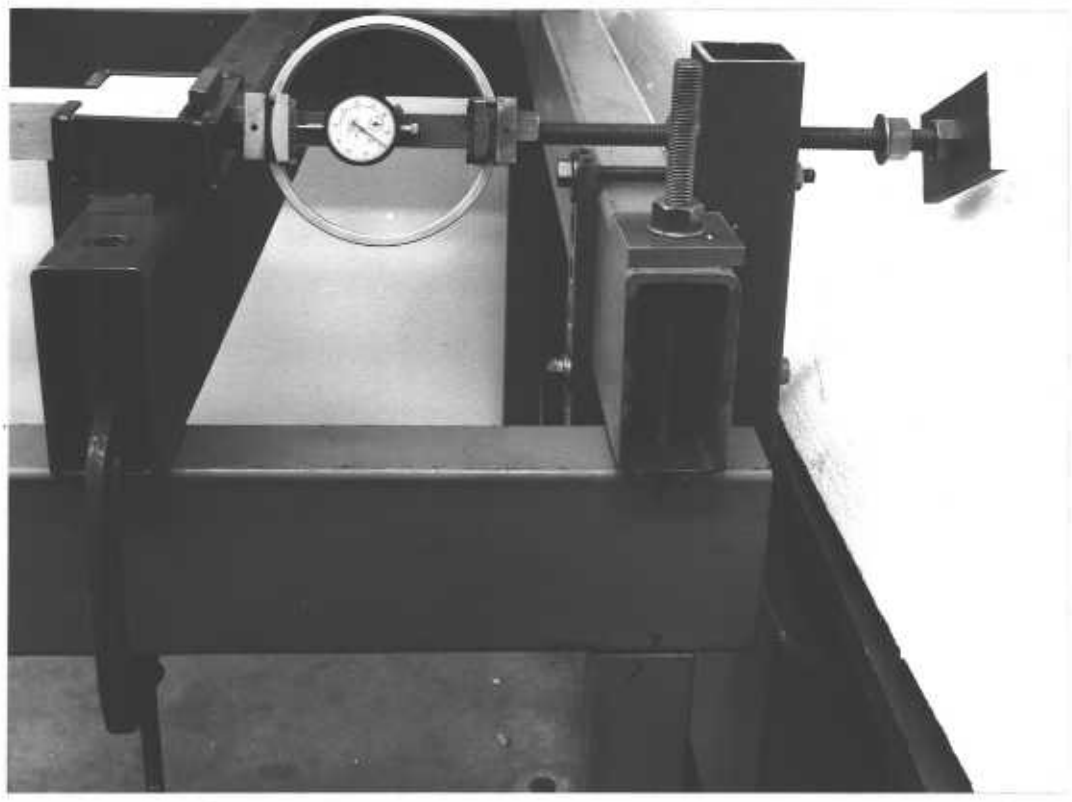


Fig. 3.11 Loading device for tests on timber flanges prior to models fabrication

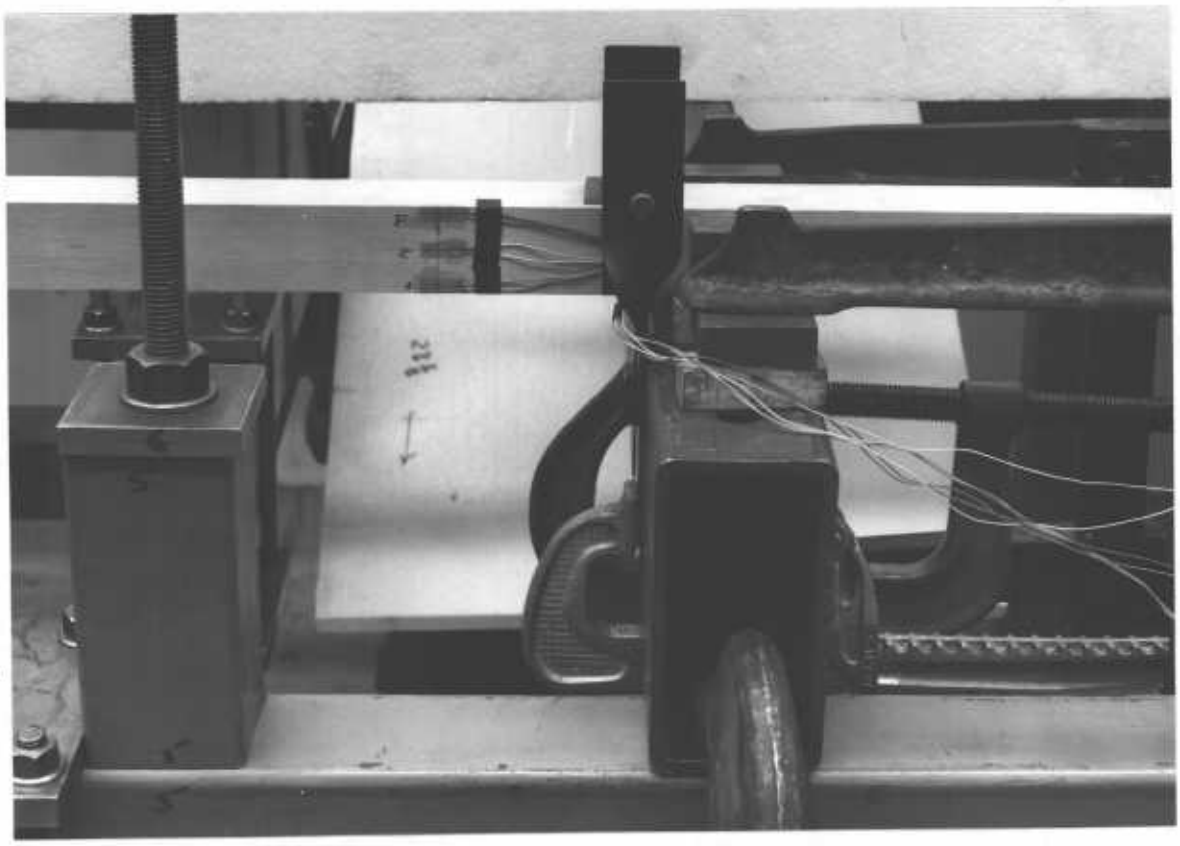


Fig. 3.12 Gauges and lateral restraint support for tension and compression tests on timber flanges prior to model fabrication

noted that the specimens were only tested up to a maximum load equal to about $\frac{1}{50}$ th of their ultimate load (1000 lbs), so that failure of glue line was avoided.

11.3 Description of test equipment

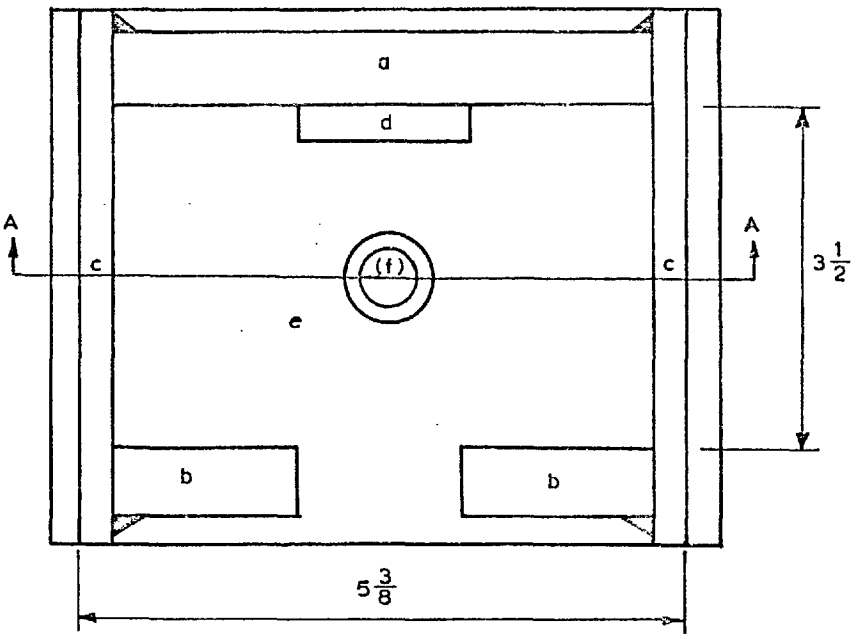
The same assembly of test equipment was used to test specimens in tension or compression. Fig.3.10 shows the equipment used in the tests and the description of which is given as follows:

11.3.1 End fixings

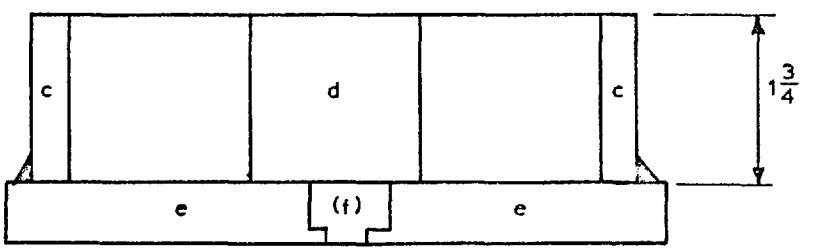
Two boxes were constructed by welding two $\frac{3}{4}$ inch plates at right angles to two $\frac{3}{8}$ inch plates at the sides and $\frac{5}{8}$ inch plate at the bottom. The top side was left open. Also on the front end plate $1\frac{3}{4}$ inch square opening was left, refer to figs. 3.10, 3.11 and 3.13. The object of these boxes is to hold the tension specimen from one end and to apply the load from the other end as follows:

(i) At the centre of the bottom of one box two holes were drilled ($\frac{3}{4}$ and $\frac{1}{2}$ inches diameters) so that a $\frac{1}{2}$ inch Allen headed bolt may be used to hold the box on the test frame such that this end was held firmly to the frame and was capable of rocking on a horizontal plane, refer to fig.3.13. The object of this rocking action is that, if there is a discrepancy in the lengths of the loading blocks then the whole assembly is capable of aligning itself such that the load is applied perpendicular to the loading blocks.

(ii) At the centre of the back side of the second box a 1 inch diameter hole was drilled such that the loading device may be screwed into it, refer to fig.3.11.



Top view of the holding box



Section A-A



$\frac{1}{2}$ in ϕ Allen Headed Bolt to fit in hole f

a : $\frac{3}{4}$ in back plate

b : $\frac{3}{4}$ in front plate

c : $\frac{3}{8}$ in side plates

d : $\frac{3}{8}$ in end plate to apply load on compression specimen

e : $\frac{5}{8}$ in bottom plate

f : $\frac{3}{4}$ in hole for Allen headed bolt

All dimensions are in inches

Fig. 3·13. Details of the holding box for tension and compression tests for timber flanges prior to models fabrication

11.3.2 Lateral restraints during compression tests

$\frac{1}{2}$ inch rollers were clamped as shown in fig.3.12 on top of $\frac{1}{8}$ inch plates at three equi-distant positions along the length of the specimen. Also $\frac{1}{2}$ inch rollers were sandwiched between two $\frac{1}{2}$ and $\frac{1}{4}$ inches plates and allowed to stand vertically at the sides of the specimens adjacent to the positions of the top rollers. In this case the outer $\frac{1}{2}$ inch plates were L shaped and clamped on the test frame. All plates and rollers were greased on the interfaces. The object of the whole arrangement is to prevent the specimen from buckling and to allow free movement of the specimen when it was loaded in compression.

11.3.3 Loading equipment

The loading device was a proving ring with a long screw and nuts as shown in fig.3.11. The proving ring and dial gauge were calibrated in a 10 ton Amsler machine in tension and compression up to a maximum load of 2000 lbs. Tension and compression may be applied using this arrangement, i.e. by turning the screw in a clockwise direction the specimen was loaded in tension and anti-clockwise direction produced compression. It should be noted that a $\frac{3}{8}$ inch plate was provided on the back of both the holding and loading boxes to transfer compressive forces to specimens from them, refer to fig.3.13.

11.3.4 Measuring equipment

The strains from PL10 gauges were recorded automatically using a Peckel electronic logger, where the results can be recorded and printed as fast as one gauge per second and a print of that recording may be obtained

instantly. Gauge drift was not recorded at this stage because the experiment took a short period of time. A 2 inch DEMEC gauge was used to obtain displacement results corresponding to central PL10 gauge strain results.

11.4 Loading Procedures:

The following loading procedure was followed for both tension and compression tests

(a) Load was first applied from zero up to 500 lbs in 100 lbs increments and released several times. Each time the load was applied strain was recorded from all gauges until the difference between two consecutive strain readings of each gauge at any load increment was about 5%. Each time the load was applied the gauge was allowed to settle for 2 minutes, then strains were recorded and the load was released to zero. Also gauges were allowed to settle for 2 minutes at zero load. The object of such procedure is that repetition of loading allows the removal of slackness from the apparatus and also removes the effect of loose fibres at the ends where the load was applied.

(b) Having established the starting condition from step (a), then initial strains from PL10 and displacements were recorded at zero load or any other load as determined by step (a), then the load was taken up to 1000 lbs in five increments and corresponding strains and displacements were recorded. Each time a strain measurement was made the gauges were allowed to settle for 2 minutes before taking the results.

(c) Having reached 1000 lbs, then the load was released in the same increments and strains and displacements were recorded likewise until the initial starting load was reached.

(d) Strain results obtained from steps (b) and (c) were compared and if they differed by more than 5% for any load increment for any of the three gauges, then the procedure given by step (b) and (c) was repeated until the desired accuracy was achieved.

11.5 Test results

The strain and displacement test results obtained for the specimens given in table 3.7 were analysed and mean values of moduli of elasticity for each model were obtained in both tension and compression. Also mean correction factors for PL10 gauges were obtained by comparing strain results from these gauges with those obtained from DEMEC gauges for timber in tension and compression. Both results are summarised in table 3.8.

The following conclusions are also made

(a) The test was found to be sensitive to the squareness of the timber at the ends where the load was applied. This was reflected by strain variations in the readings of the three gauges at any load level. Up to 15% variations were encountered in preliminary tests. This variation was reduced to as low as 5% by squaring the specimens properly.

Models	Mean moduli of elasticity lb/in^2 10^6					
	Compression // Grain			Tension // Grain		
	Actual Size Test	Small Clear Specimen test	% Variation of (a) on (b)	Actual Size Test	Small Clear Specimen test	% Variation of (d) on (e)
	(a)	(b)	(c)	(d)	(e)	(f)
Model (1)	1.75	1.80	- 2.8	1.61	1.70	- 5.3
Model (2)	1.17	1.29	- 9.0	0.81	0.96	- 16.0
Model (3)	1.68	1.73	- 2.9	1.58	1.70	- 7.0
Model (4)	1.65	1.70	- 3.0	1.43	1.53	- 6.5

Table 3.8 Results from actual size tests

Gauge	Correction factor	Original gauge factor	Corrected gauge factor
PL10	0.92	2.08	1.91

Table 3.9 Mean corrected gauge factors for PL 10 gauges on solid timber

(b) The rig was proved to be satisfactory for tension and compression tests at low loads. Obviously at high loads the problem of buckling in compression is more pronounced and a different arrangement is essential. Also a different method for applying the load is required if specimens are to be tested at high load levels.

(c) While the results obtained for moduli of elasticity in tension parallel to grain are considerably lower than those found from small clear specimens, refer to table 3.8, the moduli of elasticity in compression parallel to grain compare reasonably with those obtained from small clear specimens. Higher variations are noticed in values of moduli of elasticity in both tension and compression results of model(2). Reasons given earlier in section 10.1 for low values and variations in results of model (2) also apply here. It should be noted that the results given in table 3.8 were based on a short part of the stress-strain curve since the maximum stress achieved in this test was about 300 lb/in^2 compared with a value of the order of 15000lb/in^2 obtained from small clear specimens tests in tension parallel to grain.

Chapter 12 Tests on plywood web I-beams

12.1 Scope and objectives

The beam models described in table 3.10 were tested to verify the theoretical work derived in part II of this thesis to investigate the behaviour of rigid and semi-rigid plywood web I-beams. As shown in table 3.10 the tests were divided into three series.

Series I: A pilot test on one beam model to investigate:

(a) positions and adequacy of lateral restraint supports provided along the length of the beam model such that the effect of lateral instability on strain measurements was minimised.

(b) performance of electrical resistance strain gauges of type PL10 glued with P2 adhesive on timber and plywood of the pilot model when tested in bending compared with DEMEC gauges results and also with the results obtained from direct tension and compression tests on plywood and timber given in tables 3.4 and 3.9.

(c) loading procedure and loading increments.

Series II: Two beam models were tested in bending up to failure to investigate the behaviour of rigid plywood web I-beams.

Series III: Two beam models were tested in bending up to failure to investigate the behaviour of semi-rigid plywood web I-beams.

12.2 Fabrication of beams

The layout of the models of table 3.10 and locations of strain gauges, dial gauges, etc. is given by figs. 3.14(a) and (b).

12.2.1 Glued beams: series I and II

The models for these series of tests were prepared as follows:

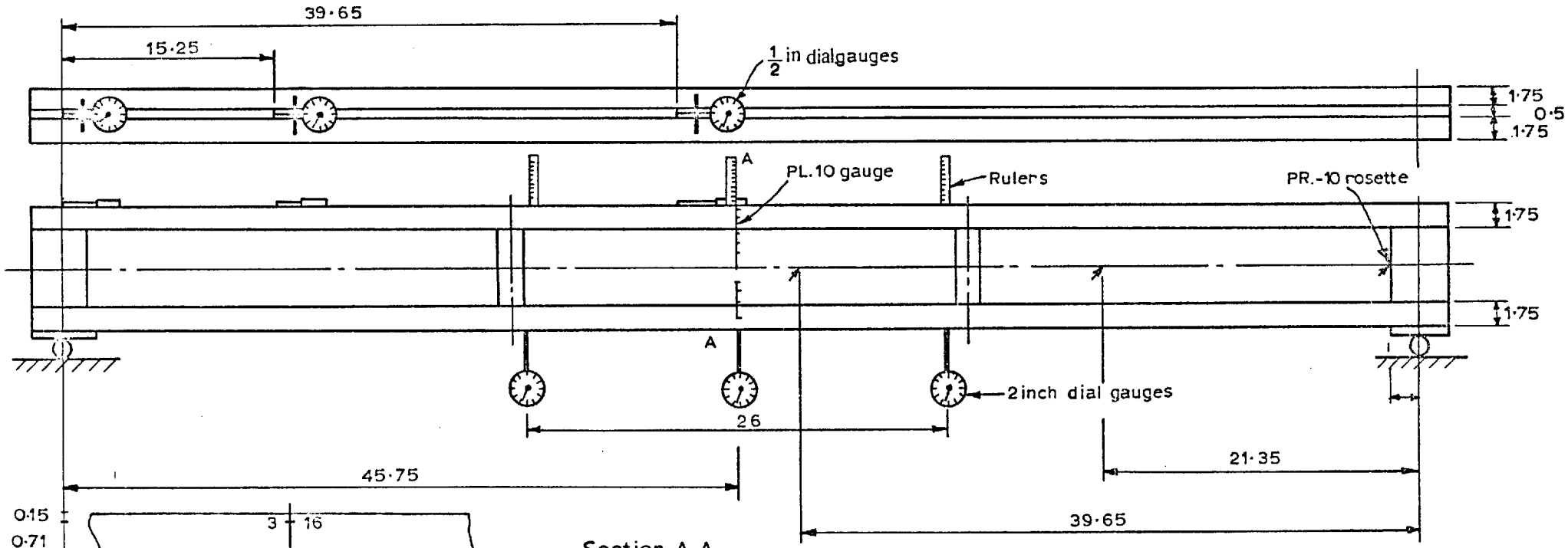
(1) Surfaces of flanges to be glued were planed before applying the glue.

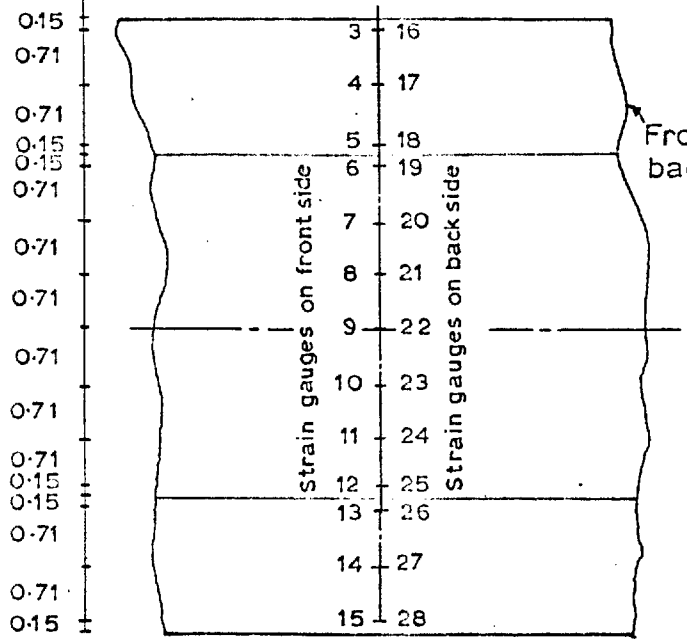
(2) Surfaces of plywood to be glued were sanded before applying the glue.

Table 3.10 Details of the Beam Models

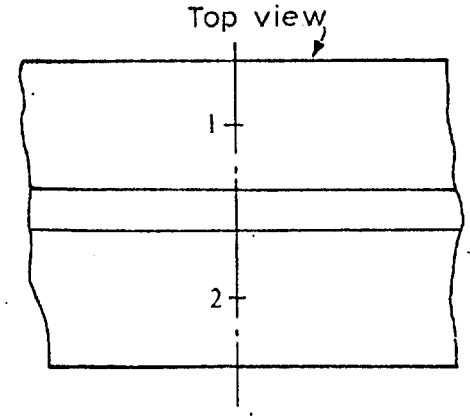
Test Series	Beam model no.	Details of beam models				
		Flange	Web	Joint	Stiffeners	
					End	Intermediate
Series I	Pilot	Unidentified species 4 planks $1\frac{3}{4}$x$1\frac{3}{4}$x96 ins	$\frac{1}{2}$in Finnish birch plywood face grain ⊥ span 8 x 96 in	Glued with casein glue	$1\frac{3}{4}$x$3\frac{1}{2}$x$4\frac{1}{2}$ in of flange material	$1\frac{3}{4}$x$1\frac{3}{4}$x$4\frac{1}{2}$ in of flange material
Series II	Model (1)	*Specimens 11,12,13&14	$\frac{1}{2}$in Finnish birch plywood face grain ⊥ to span	Glued with Cascamite glue	"	"
	Model (2)	*Specimens 21,22,23&24	$\frac{1}{2}$in Finnish birch plywood face grain ⊥ to span	Glued with Cascamite glue	"	"
Series III	Model (3)	*Specimens 31,32,33&34	1in Finnish birch plywood face grain ⊥ to span	Predrilled SWG7 wire nails 4 in length at 2in spacing	"	"
	Model (4)	*Specimens 41,41,43&44	$\frac{1}{2}$in Finnish birch plywood face grain ⊥ to span	Predrilled SWG8 wire nails $3\frac{1}{2}$in length at 2in spacing	"	"

* specimens were cut as shown in section 9.1





Section A-A



Beam Models (1) and (2)

NO slip $\frac{1}{2}$ inch - dial gauges

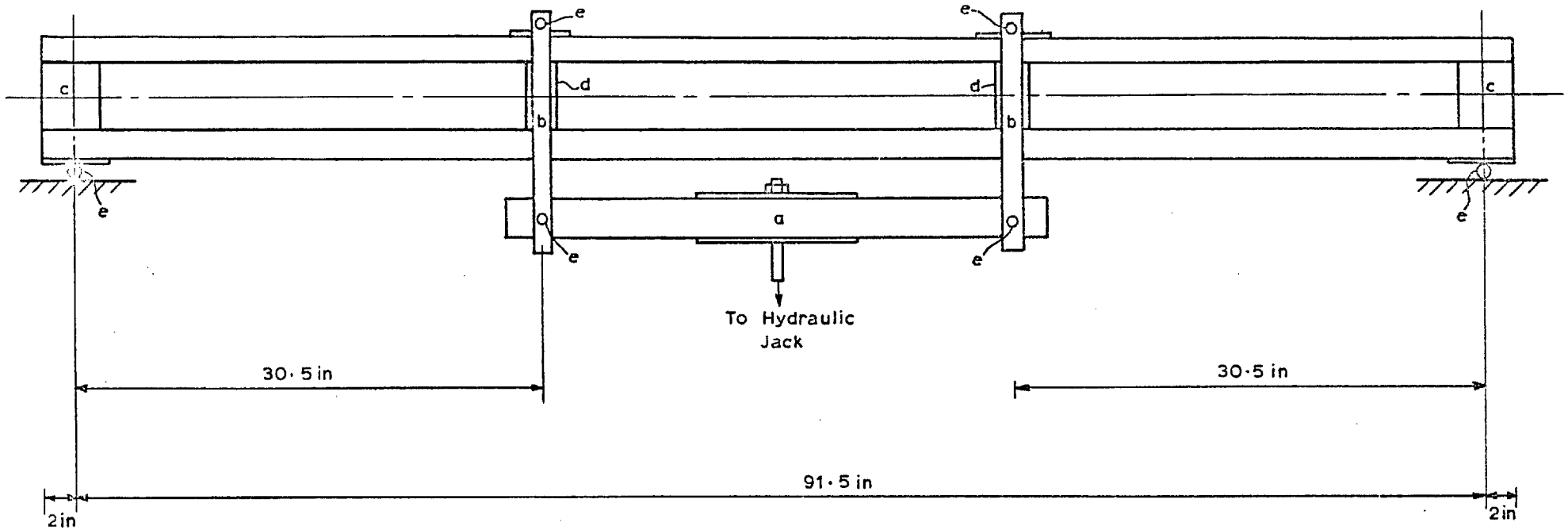
Beam Model (3)

Only one rosette 15·75 inches from support

Only two slip $\frac{1}{2}$ inch - dial gauges at 9·1 and 24·2 inches from the support

All dimensions are in inches

Fig. 3·14 (a) Typical layout for beam model (4)



a = Loading beam : $\frac{3}{16}$ inch box - section stiffened at the centre by welding $\frac{1}{8}$ inch steel plate

b = Loading strips : $\frac{1}{4}$ x 1 inch steel plates

c = End stiffeners

d = Intermediate stiffeners

e = Support and loading rollers : 1 inch diameter rollers and $\frac{1}{4}$ inch thick plates

Fig. 3.14(b) Loading and support arrangement for beam models 1, 2, 3 and 4

(3) Glue was mixed and prepared according to the manufacturers' instructions, refer to section 9.2.

(4) A thin layer of glue was then spread on the planed face of the timber using a brush and timber was then placed in position on each side of the sanded plywood web faces. A $\frac{1}{2}$ x 8 x $95\frac{1}{2}$ inch plywood sheet was then placed on each side of the beam. Then the timber flanges were clamped to the plywood web, through the plywood sheets on each side of the beam, at 6 inch distances using G-cramps. The object of the plywood sheets on the flanges is to distribute the spot pressures from the clamps on the glued timber to plywood interface. The glued joint was then allowed to cure as described by the manufacturers' instruction for 7 hours at a room temperature of 15°C with the clamps on.

(5) After the glue had cured, the clamps and the plywood sheets on the side of the beam were removed and stiffeners were glued in position.

12.2.2 Nailed beams: series III

The models for this series of tests were prepared as follows

(1) Holes were drilled on all timber flanges and plywood webs at 2 inch distances such that CP112 (1967) specifications were satisfied. Holes were drilled using $\frac{1}{8}$ inch drill.

(2) Flanges were placed in position on each side of the plywood web and nails were hammered alternately through the drilled holes of both flanges, from one side, then turned over to the other side and nails were driven through the remainder alternate holes of both flanges.

(3) Stiffeners were then placed in position and nailed.

12.3 Description of test equipment

The assembly of test equipment used in beam tests of table 3.10 is shown in figs. 3.14, 3.15 and 3.16. A description of this equipment is given as follows:

12.3.1 End supports

The models were treated as simply supported beams. This condition was provided by a single steel roller of 1 inch diameter at both ends of the beams. A $\frac{1}{4}$ inch thick steel plate between the roller and the beam prevented the roller from being pressed into the lower face of the beam and assured that movement along the beam axis could take place. At high load levels the roller may tend to slip past the plate and shoot. This was prevented by clamping a steel plate at the end of the frame where the roller was supported. It should be noted that this steel plate did not touch the roller or the steel plate on which the beam was supported on the roller and hence allowed for horizontal movement at all load levels except when the roller had slipped. It should be noted that the roller in the pilot test and all other tests did not slip at high loads.

12.3.2 Lateral restraint

Some recommendations were made by Council of the Forest Industries of British Columbia (1958) to stabilise plywood web I and box beams laterally at design loads based on the ratio I_{yy}/I_{zz}. On the other hand no recommendation had been made for lateral stability of plywood web I-beams at loads higher and up to ultimate loads. In this thesis the arrangement shown in figs. 3.14(c)- 3.16 for lateral stability supports was used. This arrangement essentially comprises of $\frac{1}{2}$ inch roller sandwiched between two $\frac{1}{8}$ inch plates. The plates and roller are then supported vertically against

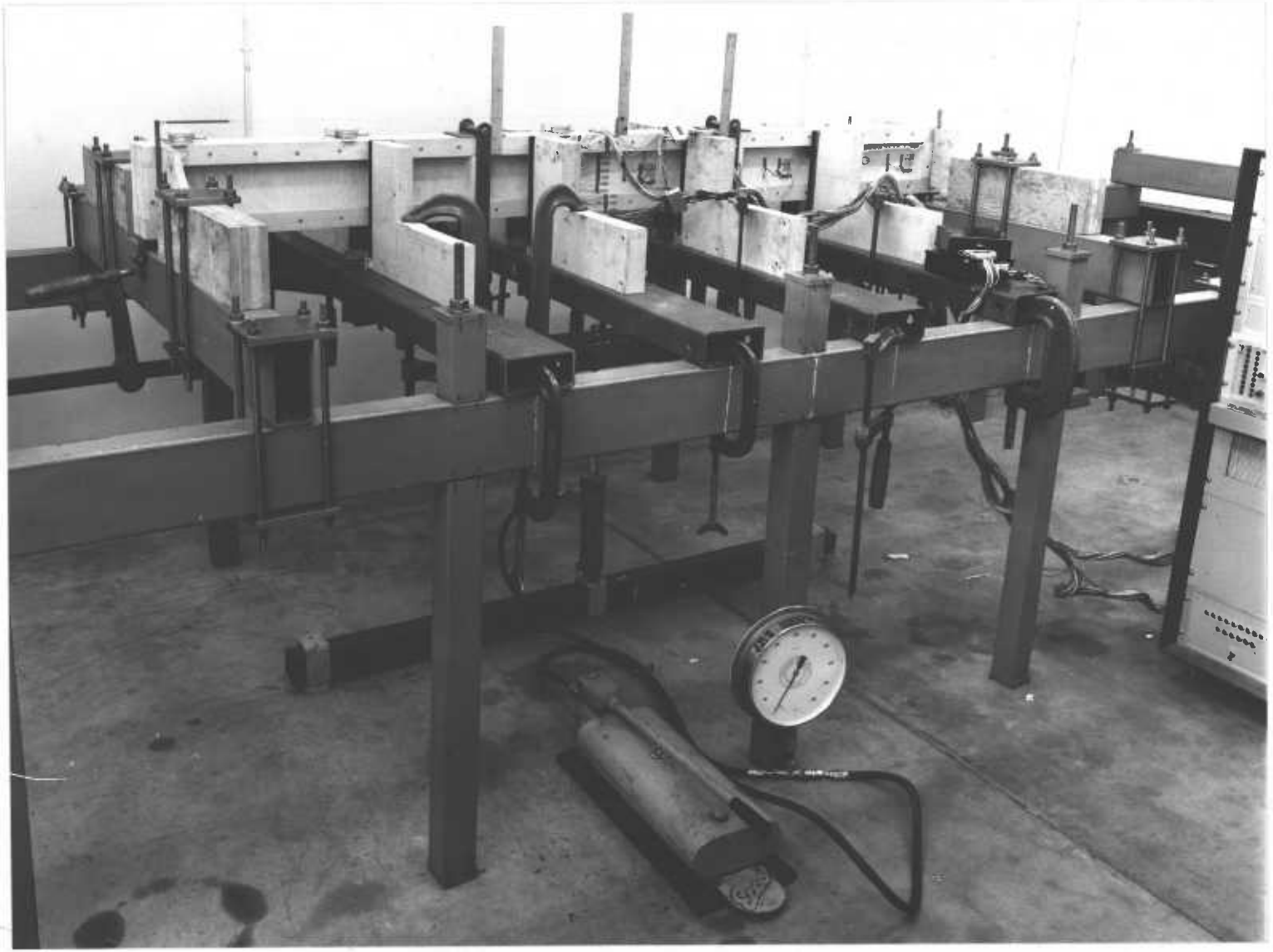


Fig. 3.14(c):General view for beam model (4) test arrangement



Fig. 3.15 Top view for beam model (4) test showing dial gauges to measure slip, lateral restraints supports and loading rollers and plates

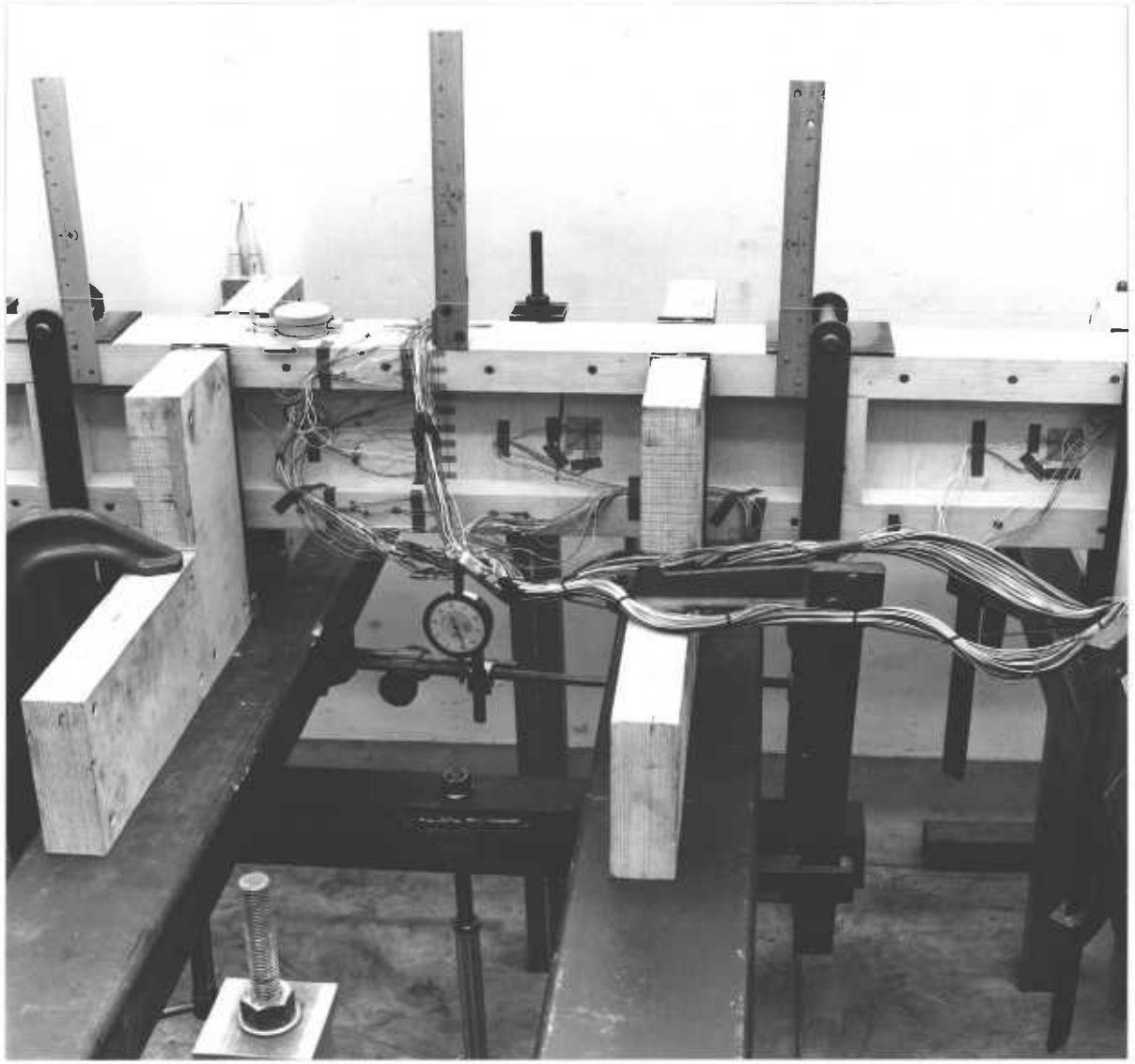


Fig. 3.16 A detailed front view for beam model (4) test arrangement showing strain gauges, rosettes, loading arrangement, dial gauges to measure slip and deflection and lateral restraints supports

the beam and a 2 inch plywood bracket which is clamped to the test frame. These supports are provided at four equidistant positions along the beam on both sides. All rollers should be greased. At the end supports the beam is slotted between two plywood wedges which are supported on the test frame. The object of these arrangements along the beam is to provide lateral stability to the beam and also to allow for horizontal and vertical movements of the beam. The pilot test proved the adequacy of this arrangement since strain measurements from similar strain gauges on front and back sides of the beam agreed within 5% difference, and movement along the beam was observed.

12.3.3 Loading equipment

Load was applied by a hydraulic jack and measurements were obtained from a pressure gauge. The hydraulic jack was calibrated for the pressure gauge in a 10 ton Buckton machine. The load was applied to the beam through a roller and plate arrangement at two points $\frac{1}{3}$ rd of span from each end, as shown in figs. 3.14(b) - 3.16.

12.3.4 Strain measuring equipment

For models of series II and III PL10 and PR10 electrical resistance gauges and rosettes were glued on positions shown in figs.3.14(a) and 3.16 with P2 glue. For PL10 and PR10 gauges a Modulog 50 channel data logger and a Franklin digital strip printer were used to read and print strain measurements. The Modulog is capable of scanning up to 15 channels per second. The rate that was used in these test series was 10 channels per second.

Before the test was started each gauge was calibrated to $\pm$ 5000 microstrains using a standard calibration box provided by the manufacturer. Also before the test, gauges drifts at no load condition were found by setting the automatic scan device to scan the gauges at 2 minute intervals for 3 hours, which is the approximate period to complete the test. All gauges in all the models were found to be stable over the 3 hours period to an accuracy of $\pm$ 2 microstrains in the no load condition.

In the pilot model 2 inch DEMEC gauges were used to measure strains at the locations of PL10 gauges 2, 4, 7, 11 & 14. The correction factors for PL10 gauges obtained by comparing the results of the PL10 gauges with the results obtained from the DEMEC gauges for gauges 2, 4, 7, 11 and 14 agreed with the correction factors obtained for plywood and timber in direct compression and tension, refer to tables 3.4 and 3.9.

12.3.5 Deflection measuring equipment for beam and flange web joint

(a) Beam

Deflections at three points shown in figs. 3.14 - 3.16 were measured using 2 inch standard dial gauges of 10^{-3} inch accuracy. The gauges were mounted on the test frame using magnetic bases. Rulers that measure up to $\frac{1}{32}$ inch accuracy were also provided to measure deflections at high loads after the dial gauges were dismantled.

(b) Flange web joint

For models of series III standard $\frac{1}{2}$ inch dial gauges were used to measure slip between plywood and timber at the three positions indicated in fig. 3.14(a). The accuracy of these gauges is 10^{-4} inches.

12.4 Loading procedure

The following loading procedure adopted for testing beam models (1),(2), (3)& (4) was established when the pilot model of series I was tested.

12.4.1 General

(1) All measurements of flange size, positions of strain gauges, dial gauges, rosettes, etc. were checked before loading was started.

(2) Gauges were allowed to settle for two minutes before strain recordings were made for loads equal to, or less than the calculated design loads. For higher loads strains were recorded instantly because strain tended to increase rapidly with small increases in load.

(3) Final loading was carried in 13 increments, five equal increments from zero to the calculated design load and eight equal increments from calculated design load to predicted ultimate load.

Ultimate load was predicted from theoretical solutions given in part II of this thesis, and the results of which are given in part IV of this thesis. It corresponds to the load when either the plywood or timber in compression or tension has started to fail.

(4) Three increments prior to ultimate load, the dial gauges to measure deflection were removed and deflection measurements were taken by rulers.

(5) After the beam had failed moisture content specimens were obtained from timber and plywood. Also specimens to determine the modulus of rigidity of the timber were obtained from the flanges.

12.4.2 Glued beams: series II

(1) The beam was loaded up to $\frac{1}{3}$ the calculated design load and released several times until any two consecutive readings of all strain gauges in the loaded position were within 5% variation. Obviously strain measurements were recorded each time the load was applied. The object of this procedure is to remove any slackness in the appratus.

(2) Having removed any slackness in the apparatus, initial readings were taken for strain gauges, deflection dial gauges and rulers. Load was incremented in predetermined increments up to design load and released to zero load in the same increments. At each load increment strains and deflections readings were recorded.

(3) Load was then applied in the predetermined increments up to failure. At each load increment strains and deflections readings were recorded. Also the type and position of failure were recorded.

12.4.3 Nailed beams: series III

(1) To remove slackness from the apparatus, load was not repeated in the same manner as for series II because this repetition of loading might introduce some deformations in the nails which could be irrecoverable when the load was released and this might influence the $Q - \delta$ relationship obtained by testing joints in direct compression without load repetition, refer to section 10.3.

To remove slackness from the apparatus an initial load of $\frac{1}{5}$ th of the calculated design load was applied and considered as the starting point. Initial readings were recorded for strain gauges, deflections and slip dial gauges at that load.

(2) Step (3) in the previous loading procedure for series II was followed. Also relative slip dial gauges readings were recorded at each load increment up to failure.

12.5 Analysis of test data

(1) Results from similar gauges at the back and front, viz. gauges 3 and 16, or gauges 1 and 2 on the top were averaged to remove any effect of lateral instability. Also percentage variations were obtained from the average result of each pair of gauges.

(2) For average results of strain gauges on either timber or plywood in compression corresponding residual strains were calculated from average results of $P - \varepsilon$ diagrams for small clear specimens of timber in compression parallel to grain and plywood perpendicular to grain summarised in figs.3.4 and 3.7 using equations 1.3 and 1.2. Corresponding stresses were calculated from equation 1.1.

A small computer program was written to calculate residual strains for timber and plywood of small clear specimens, average results of strains across depth of beam models at mid section, corresponding residual strains of those average strains which were based on interpolation from the small clear specimen residual strain results and also stresses corresponding to these average strains.

(3) Principal strains were calculated from eqn.3.2 and corresponding web shear stresses were calculated from equation 3.1. Web shear modulus of rigidity G was found as shown in section 10.2 and given in table 3.3. Web shear stress calculation was based on idealised τ_{xz} - γ_{xz} relationship of fig.3.7.

(4) Deflection plots were obtained at mid span and $\frac{1}{3}$ rd span positions.

(5) For test series III load slip plots were also obtained from slip dial gauges results at the positions shown in fig.3.14(a).

PART IV

THEORETICAL AND EXPERIMENTAL RESULTS

Part IV

Theoretical and Experimental Results

Chapter 13 Scope and objectives

In this chapter the following theoretical, experimental and comparative results are reported.

(a) Theoretical results of shear stiffness factors derived in chapter 7 for a symmetrical simply supported plywood web I-beam loaded with uniformly distributed load are reported. The effects of α, β, C and m (α, β, C & m are as defined in chapter 7) on shear stiffness factor are investigated and reported.

(b) Theoretical results as obtained from solutions described in part II for simply supported rigid and semi-rigid plywood web I-beams under uniformly distributed load and two point loading at $\frac{1}{3}$ rd span are reported. Theoretical results for stresses and strains across depths of beams, deflection, web shear stress, etc., are reported for beam models 1, 2, 3 and 4 at different points along their span under four point loading and also for beam models 1 and 3 under uniformly distributed load.

(c) Experimental results obtained for models 1, 2, 3 and 4 under four point loading at $\frac{1}{3}$ rd span as obtained from tests described in chapter 12 are reported and compared with theoretical results from similar models as obtained from solutions described in chapter 6.

Chapter 14 Theoretical results for shear stiffness factor at mid-span of a symmetrical simply supported semi-rigid plywood web I-beam under uniformly distributed load

14.1 General

A simple computer program was written to investigate the effects of varying α, β, m and C on the shear stiffness factor given by equation (2.110). The parameters α, β, C and m are as defined in Chapter 7 and figs.4.1, 4.2, 4.3 and 4.4.

It should be noted that the parameter C is defined by equation 2.47(b) and is dependent on:

(i) beam geometrical properties α, β, L and A_f

(ii) material properties m and E_f

(iii) Connector properties s and k. By varying s or k, the parameter C may take any value between zero and infinity,

e.g. The rigid case is defined by C = 0, or as k tends to take an infinitely large value, or s is small.

Also the effect of slip, i.e. C on shear deflection was compared with total deflection as derived from bending deflection of a semi-rigid beam and shear deflection of a rigid beam. The loads that a particular beam of defined geometry, material properties and connector properties, may carry and limited by total deflection in the two cases when the effect of slip on shear deflection is considered, and ignored, are reported.

14.2 Effect of varying α, β, C and m on shear stiffness factors:

Tables 4.1 and 4.2 and figs. 4.1, 4.2, 4.3 and 4.4 summarise some of the results that were computed for shear stiffness factors at mid span

	Values of shear stiffness factors														
β	0.5					0.2					0.05				
α \ C	1.0	0.50	.25	0.10	0.00	1.0	0.50	0.25	0.10	0.00	1.0	0.50	0.25	0.10	0.00
0.500	.376	.480	.595	.717	.833	.253	.356	.490	.654	.833	.169	.259	.394	.506	.833
0.480	.359	.450	.545	.640	.725	.232	.315	.412	.515	.607	.141	.196	.255	.287	.334
0.450	.338	.413	.486	.554	.609	.205	.269	.334	.392	.434	.111	.143	.167	.175	.178
0.425	.324	.388	.448	.500	.540	.188	.241	.290	.329	.354	.093	.116	.130	.133	.130
0.400	.312	.368	.417	.458	.488	.175	.219	.257	.285	.301	.080	.097	.107	.108	.104
0.350	.297	.338	.372	.398	.416	.156	.188	.214	.231	.239	.061	.073	.080	.081	.077
0.300	.288	.319	.343	.360	.372	.145	.170	.188	.200	.205	.049	.059	.065	.066	.063
0.250	.286	.308	.324	.336	.344	.142	.160	.173	.181	.185	.042	.051	.056	.057	.056
0.200	.286	.301	.313	.321	.327	.141	.155	.164	.170	.173	.040	.046	.050	.052	.052
0.100	.285	.297	.302	.306	.309	.141	.153	.157	.159	.161	.039	.044	.046	.047	.047

Table 4.1 Shear stiffness factor for plywood web I-beam for m = 1.0

	Shear stiffness factors					
C	0.5			0.0		
m / α	1.0	0.75	0.50	1.0	0.75	0.50
0.500	.356	.324	.283	.833	.826	.800
0.480	.315	.288	.253	.607	.603	.590
0.450	.269	.248	.218	.434	.432	.426
0.425	.241	.222	.195	.354	.353	.350
0.400	.219	.202	.178	.301	.301	.299
0.350	.188	.175	.153	.239	.239	.239
0.300	.170	.159	.139	.206	.205	.205
0.200	.155	.150	.135	.174	.174	.173
0.100	.153	.149	.149	.161	.161	.161

Table 4.2 Shear stiffness factor for plywood web I-beam for $\beta = 0.2$

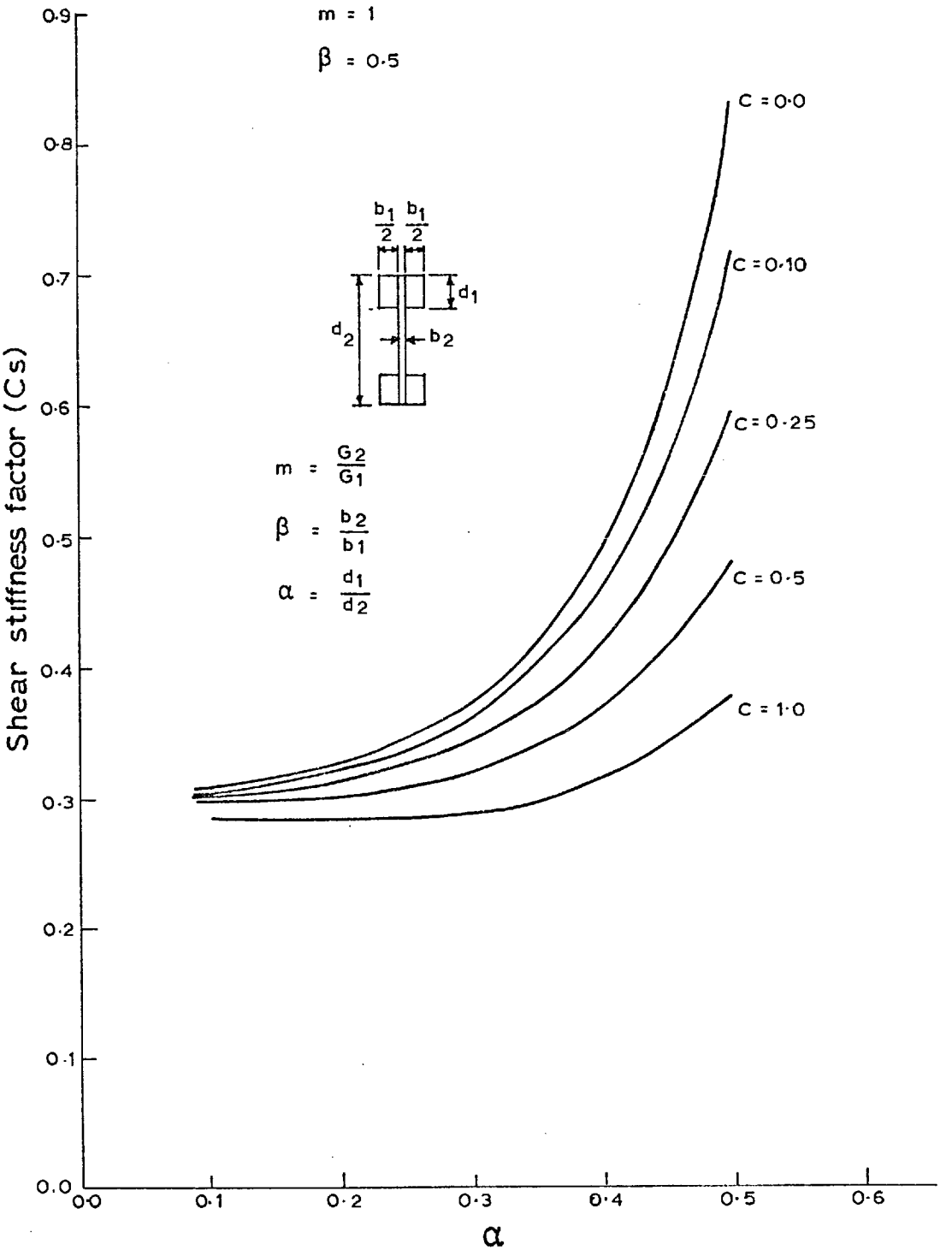


Fig. 4·1. Shear stiffness factors

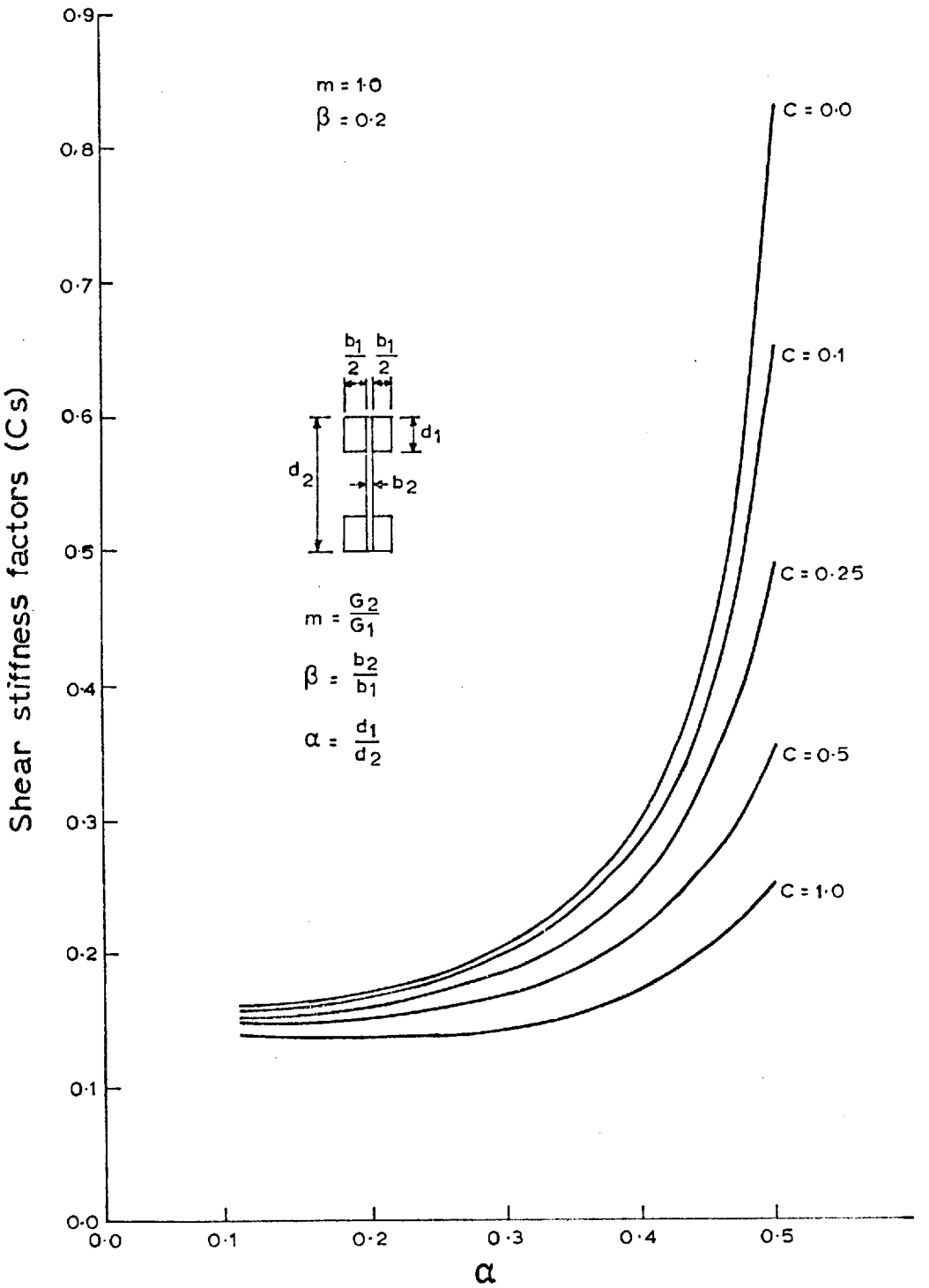


Fig. 4·2. Shear stiffness factors

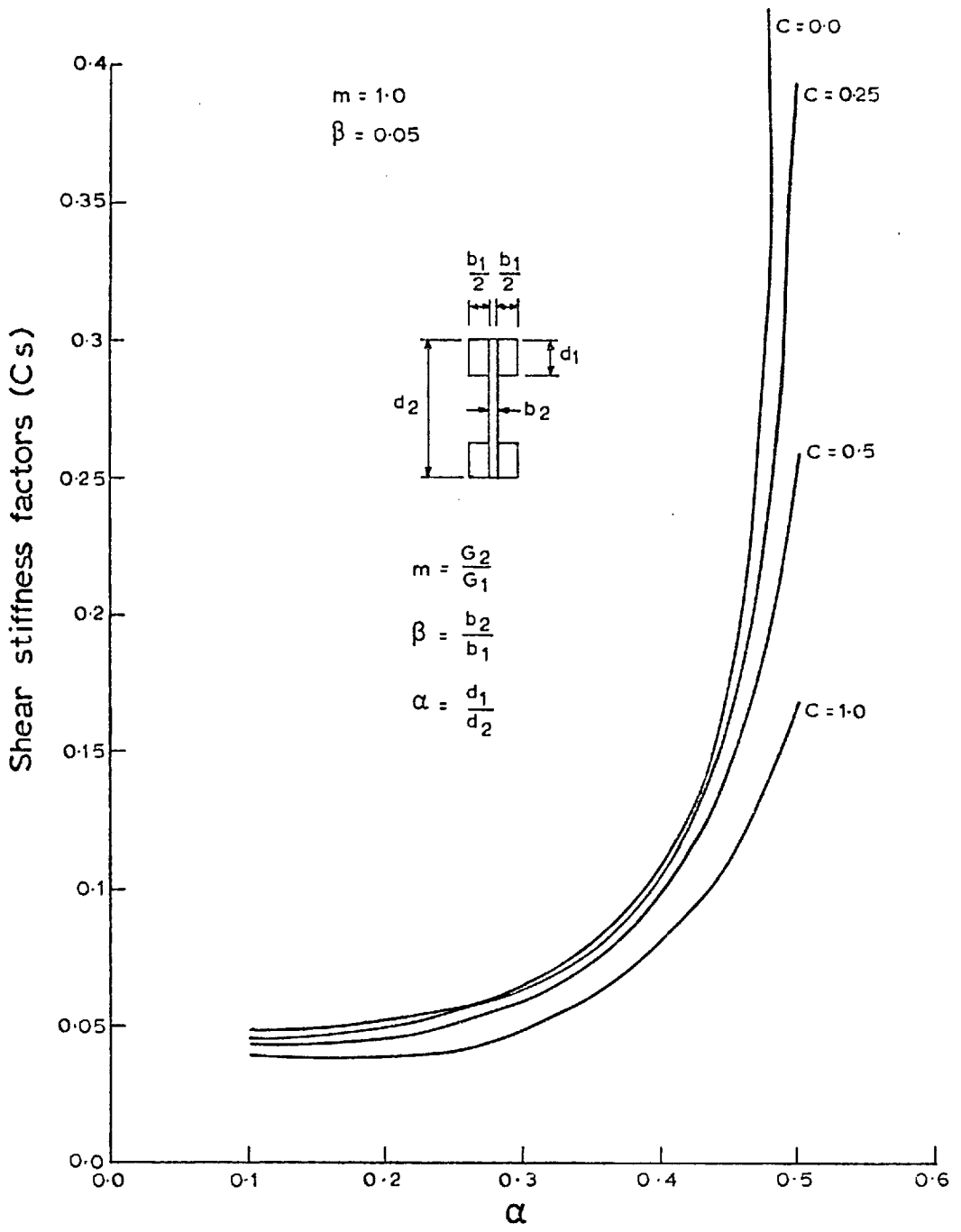


Fig. 4·3. Shear stiffness factors

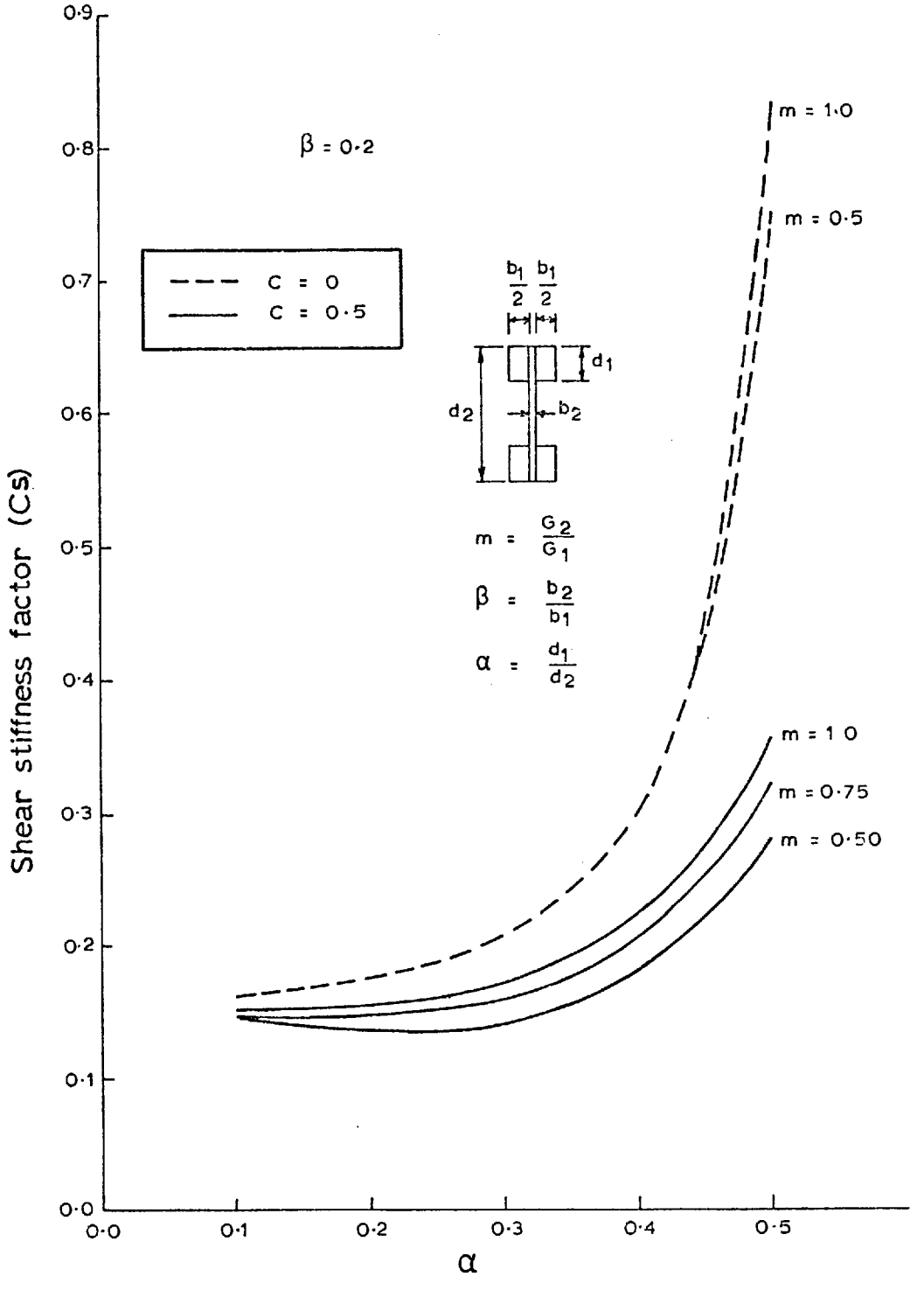


Fig. 4·4. Effect of m on shear stiffness factor

of plywood web I-beams for different values of α, β, C and m.

From figs. 4.1, 4.2, 4.3 and 4.4 it is evident that shear stiffness factor (C_s) decreases as α is decreased for constant values of C and β and hence high shear deflections at low values of α.

Also the effect of decreasing β, results in decreased values of C_s for constant values of α and C. The effect of varying C is evident from fig.4.1, 4.2 and 4.3. The general pattern is that the shear stiffness factor increases as C is decreased, ie as the beam connector stiffness is increased. It is noted that the shear stiffness factor given in table 4.1 for a beam with infinite connector stiffness (i.e. C = 0), α = 0.5 (i.e. rectangular section) and m equals unity (i.e. same flange and web materials), is given to be 0.833 for any value of β. This is the same as the shear stiffness factor that may be derived for a rectangular solid timber beam. It is also noted that the effect of beam connector stiffness factor (C) is more significant at high values of α and β, i.e. when the beam tends to be rectangular, than at low values of α and β where the differences between shear stiffness factors at different values of C tend to be insignificant. At moderate values of α (between .1 and .3) and also moderate values of β (between .1 and .3) i.e. at values of α and β that may be encountered in practical designs, the effect of C on shear stiffness factor is not substantial if its effect on the total deflection due to bending and shear is considered. An 18% difference in shear stiffness factors at β = 0.2 for C = 1.0 and C = 0.0 is noted. The contribution of shear deflection to total deflection for beams used in practice is in the range of 10% or less. Hence the effect of 18% variation

in shear stiffness factors mentioned above will produce about 2% variation in the total deflection. A 2% variation may be neglected.

It should also be noted that for certain values of C the shear stiffness factor may be higher than that for the rigid case, i.e. C = 0, for certain values of α and β, refer to fig.4.3. This agrees with findings of Booth (1969) where he noted that web shear stresses may be higher in some semi-rigid beams than in their equivalent rigid ones for a simply supported semi-rigid beam carrying uniformly distributed load.

From fig.4.4 it is noted that the effect of m is insignificant at low values of C, i.e. stiffer beam, than for high values of C. On the whole the effect of m on the shear stiffness factor is insignificant for beams used in practice as their m ratio in most cases vary between 0.75 and 1.1 and hence, as seen in table 4.2 and fig.4.4, an approximation of m equals to unity will not produce significant errors in the shear stiffness factor even for semi-rigid beams with low connector rigidity, say C = 0.5.

14.3 Effect of slip on shear deflection

The effect of slip on shear deflection may be reflected on the load limited by total deflection. Total deflection is based on bending deflection plus shear deflection. Bending deflection at mid-span of a symmetrical simply supported semi-rigid plywood web I-beam carrying uniformly distributed load over the whole span may be calculated from equation 4.1 as derived by Booth (1969) based on linear analysis.

$$w_b = \frac{5}{384}\frac{pL^4}{\overline{EI}} + pL^4\frac{C}{\pi^2}\left(\frac{1}{\Sigma EI} - \frac{1}{\overline{EI}}\right)\left[\frac{1}{8} - \frac{C}{\pi^2}\left(1 - \frac{1}{\text{Cosh}\frac{\pi}{2\sqrt{C}}}\right)\right] \qquad - 4.1$$

Shear deflection at mid span of a symmetrical simply supported semi rigid plywood web I-beam carrying uniformly distributed load may be calculated from equation 2.110 where C_s is the shear stiffness factor and may be found from equation 2.111(a). Shear stiffness factor will be considered for two cases:

(a) for an infinitely stiff connector, i.e. C = 0

(b) for the actual value of C corresponding to the connector modulus of rigidity used in a beam.

Maximum load limited by total deflection in both cases will then be calculated from equation 4.2, which may be derived for a simply supported symmetrical semi-rigid plywood web I-beam based on equation 4.1.

$$P = pL = 384\,\overline{EI}\,\nu \Big/ 5L^2\left\{1 + \frac{384}{5}\frac{C}{\pi^2}\left(\frac{\overline{EI}}{\Sigma EI} - 1\right)\left[\frac{1}{8} - \frac{C}{\pi^2}\left(1 - \frac{1}{\text{Cosh}\frac{\pi}{2\sqrt{C}}}\right)\right] + \frac{\overline{EI}}{GbdL^2C_s}\right\} \qquad - 4.2$$

where ν is permissible deflection factor given by Cp112 (1967) to take the value of .003.

Maximum loads limited by total deflection were calculated for the two cases mentioned earlier for a beam with the following geometrical material and connector properties at different spans and overall beam depths shown in table 4.3.

Over-all Beam Depths (inches)	Shear Stiffness Factor for Rigid Case	SPAN (Ft)														
		14			16			18			30			50		
		C_S for Semi rigid	Values of C	% Diff. in Loads	C_S for Semi rigid	Values of C	% Diff. in Loads	C_S for Semi rigid	Values of C	% Diff. in Loads	C_S for Semi rigid	Values of C	% Diff. in Loads	C_S for Semi rigid	Values of C	% Diff. in Loads
12	0·8324	·2616	·502	-5858	·3089	·384	-3·815	·3558	·304	-2·623	·5737	·109	- ·406	·7193	·039	- ·117
14	0·1652	·1458	·351	-1·931	·1534	·268	- ·984	·1584	·212	- ·480	·1658	·076	+ ·018	·1656	·027	0·0
16	0·1088	·1072	·268	- ·371	·1098	·205	+ ·183	·1110	·162	+ ·323	·1108	·058	+ ·186	·1096	·021	+ ·053
18	0·0892	·0896	·220	+ ·164	·0909	·169	+ ·533	·0914	·133	+ ·626	·0905	·048	+ ·217	·0897	·017	+ ·039
20	0·0796	·0801	·191	+ ·237	·0809	·146	+ ·567	·0812	·115	+ ·607	·0805	·042	+ ·206	·0799	·015	+ ·030
22	0·0740	·0742	·173	+ ·102	·0749	·132	+ ·440	·0751	·104	+ ·512	·0746	·038	+ ·175	·0743	·014	+ ·024
24	0·0705	·0704	·161	- ·089	·0710	·123	+ ·272	·0712	·097	+ ·353	·0709	·035	+ ·148	·0707	·013	+ ·019
26	0·0682	·0678	·154	- ·314	·0683	·118	+ ·080	·0685	·093	+ ·212	·0684	·033	+ ·089	·0683	·012	+ ·016
28	0·0665	·0658	·149	- ·528	·0663	·114	- ·114	·0666	·090	+ ·051	·0666	·032	+ ·052	·0665	·012	+ ·001
30	0·0652	·0644	·147	- ·721	·0649	·112	- ·269	·0651	·089	+ ·076	·0653	·032	+ ·019	·0652	·012	·00
32	0·0643	·0633	·146	- ·898	·0638	·112	- ·418	·0640	·088	- ·194	·0643	·032	- ·013	·0643	·011	·00
34	0·0635	·0625	·146	-1·045	·0629	·112	- ·553	·0632	·088	- ·302	·0635	·032	- ·045	·0635	·011	- ·009
36	0·0629	·0618	·147	-1·186	·0623	·113	- ·665	·0625	·089	- ·405	·0628	·032	- ·070	·0629	·012	- ·016
38	0·0625	·0613	·148	-1·306	·0617	·114	- ·770	·0620	·090	- ·480	·0623	·032	- ·096	·0624	·012	- ·022
40	0·0621	·0608	·150	-1·409	·0613	·115	- ·859	·0615	·091	- ·565	·0619	·033	- ·117	·0620	·012	- ·026
42	0·0617	·0604	·153	-1·505	·0609	·117	- ·944	·0611	·092	- ·628	·0616	·033	- ·137	·0617	·012	- ·030
44	0·0615	·0601	·155	-1·589	·0606	·119	-1·011	·0608	·094	- ·691	·0613	·034	- ·155	·0614	·012	- ·032
46	0·0612	·0599	·158	-1·657	·0603	·121	-1·077	·0606	·096	- ·739	·0610	·034	- ·173	·0612	·012	- ·035
48	0·0610	·0596	·161	-1·718	·0601	·124	-1·129	·0603	·098	- ·789	·0608	·035	- ·190	·0610	·013	- ·037

Table 4·3. Effect of slip on shear deflection as measured by load limited by total deflection for $\beta = 0625$

Geometry:

2 x 6 inches Douglas fir timber flanges

$\frac{1}{4}$ inch thick Finnish birch plywood

Material

$E_w = 1.03 \times 10^6$ lb/in^2

$E_f = 1.20 \times 10^6$ lb/in^2

$G_w = 1.16 \times 10^5$ lb/in^2

and $m = 0.86$

Connector

SWG 8 wire nail of $3\frac{1}{2}$ inch length, 0.16 inch diameter and 5030 lb/in connector modulus. Nails are drilled at 2.6 inch spacing.

Loads from both cases were compared and percentage differences between them were obtained as shown by equation 4.3.

$$\% \text{ difference in loads} = \frac{p_d - p_{ds}}{p_{ds}} \times 100 \qquad - 4.3$$

where p_d = load limited by total deflection when the effect of slip on shear deflection is not considered, i.e. C = 0

p_{ds} = load limited by total deflection when the effect of slip on shear deflection is considered.

Results are reported in table 4.3 and percentage differences are plotted against different values of overall beam depths for different spans as shown in fig.4.5. The following observations are evident:

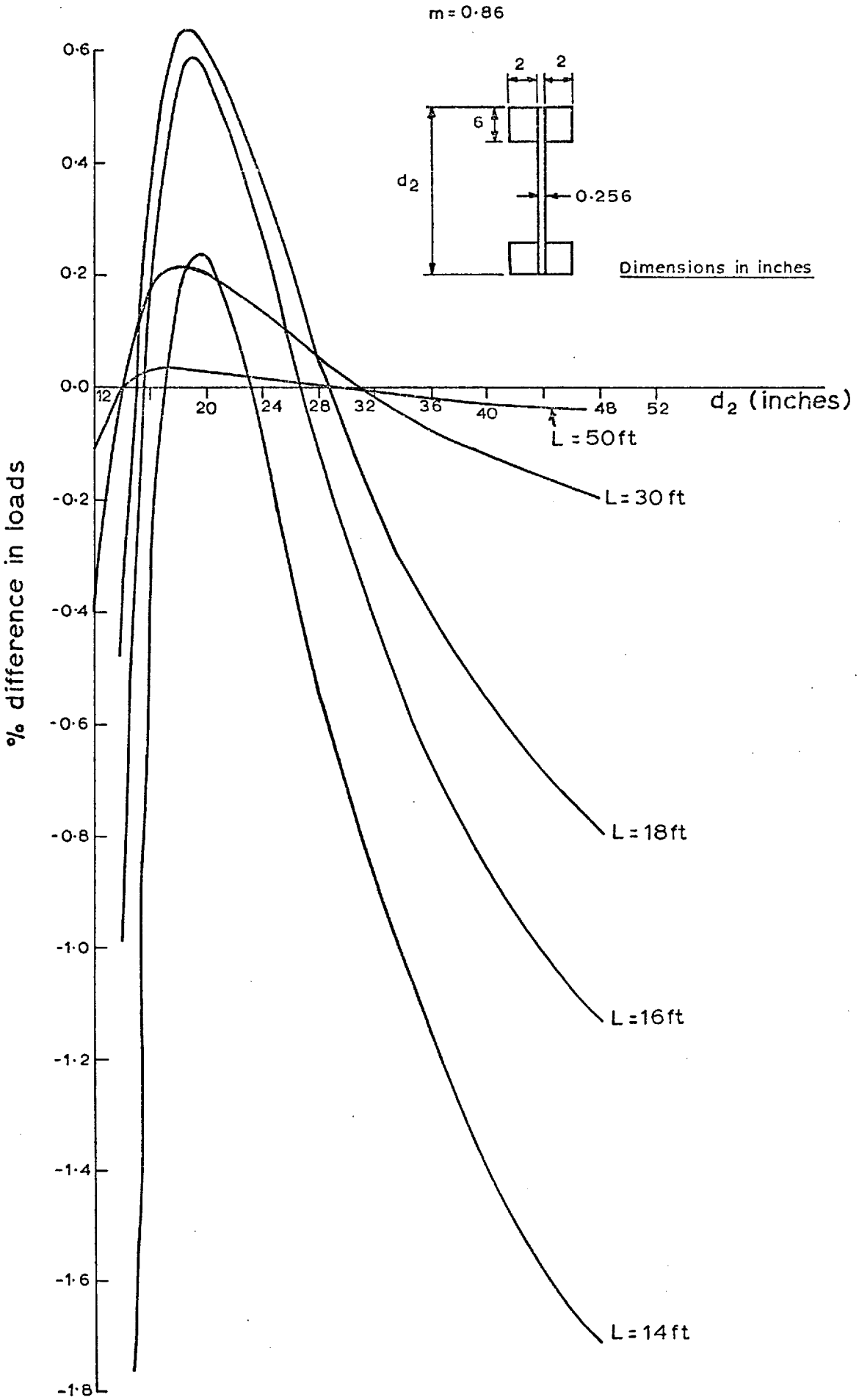


Fig. 4·5. Effect of slip on shear deflection as measured by load limited by total deflection

(a) The effect of slip on shear deflection as measured by percentage difference in loads limited by total deflection when slip is considered, and ignored for shear deflection calculation, is small and may be neglected. It varies from a maximum of about -6% for short span rectangular beams to about +0.63% for relatively short span (18 ft) and relatively shallow beams (18 inch).

(b) The percentage difference can be positive which means that the load calculated on the basis when effect of slip on shear deflection is considered on total deflection is higher than that when the effect of slip on shear deflection was not considered.

This agrees with previous finding in section 14.2 when shear stiffness factors of some semi-rigid beams were found to be higher than those of their equivalent rigid ones.

14.4 Shear stiffness factors for beam models 1, 2, 3 and 4

Models 1, 2, 3 and 4 (details of which are described in table 3.10) have symmetrical geometrical cross-sectional properties but have different moduli of elasticity for timber in tension and compression and also for plywood in tension and compression.

For calculation of shear stiffness factor at mid span of beam models 1, 2, 3 and 4 based on equation 2.114, the following two approximations should be made.

(a) Moduli of elasticity for timber and plywood in tension and compression are the same and that

$$m = \frac{G_w}{G_f} = \frac{E_w}{E_f}$$

(b) A linear $Q - \delta$ relationship is assumed to derive shear stiffness factors for models (3) and (4) for all solutions of the models even those based on non linear $Q - \delta$ relationship. Needless to say that for rigid models (1) and (2) the parameter $C = 0$.

Both approximations may be justified as seen from sections 14.2 and 14.3 that the effects of m and C on shear stiffness factors as measured by their effects on total deflection are not substantial for beams with moderate values of α and β. It should be noted that the values of α and β for models (3) are 0.219 and 0.286 respectively and those for model (4) are 0.219 and 0.143 and that all these values lie within the moderate range of α and β discussed in sections 14.2 and 14.3.

Chapter 15 Theoretical results for beam models 1, 2, 3 and 4.

15.1 General

Some of the theoretical results based on solutions described in part II are reported in this chapter. These results are based on the following solutions of beam models 1, 2, 3 and 4.

(1) Solution of beam models 1 and 2 based on rigid beam analysis described in chapter 5.

(2) Solution of beam models 3 and 4 based on the generalised governing differential equation described in chapter 6 where non-linear $Q - \delta$ relationship and linear or non-linear $\sigma - \varepsilon$ relationship - depending on position along span and load level, i.e. external moment - were adopted. The loading cases reported are:

   (a) four point loading at $\frac{1}{3}$ span for beam models (3) and (4)

   (b) Uniformly distributed load over the whole span for beam model (3) only.

(3) Solution of beam model (3) based on non-linear $Q - \delta$ relationship and linear $\sigma - \varepsilon$ relationship at all positions along span and load levels as described in section 5.6.1. Solution is given for four point loading at $\frac{1}{3}$ span.

(4) Solution of beam model (3) based on linear analysis, i.e. linear $Q - \delta$ and $\sigma - \varepsilon$ relationships at all positions along span and load levels as described in section 5.5.1. Solution is given for four point loading at $\frac{1}{3}$ span.

Solutions are given at different points along the span for direct strains and stresses for all four beam models. Stresses and strain distributions are also given across depths of beams at critical cross sections at theoretical ultimate load for all the beam models. Due to symmetry results will only be reported for half of the span. All solutions were found from computer programs reported in sections 4.6 and 6.8 for rigid and semi-rigid beams respectively.

15.2 Theoretical results based on solutions of the generalised governing differential equations

15.2.1 Direct stresses and strains along the spans of beam models 1, 2, 3 and 4 under four point loading at ultimate loads

Ultimate load results for direct stresses and strains at different points along the spans of beam models 1,2, 3 and 4 under four point loading at $\frac{1}{3}$ span are summarised in tables 4.4 and 4.5. Fig.4.6 shows the distribution of direct stresses along the spans of beam models 1, 2, 3 and 4. The rigid and semi-rigid cases will be considered separately.

(a) Rigid case Beam models (1) and (2)

From fig.4.6 it is evident that the variation of direct stresses follows the variation of bending moment along the span. Ultimate compressive stresses and strains in top timber flanges, as determined from small clear specimens (table 3.2) have been reached at extreme fibres (σ_{11} and ε_{11}) of beam models 1 and 2 (tables 4.4 and 4.5) in the middle third of their spans and hence compression failure of top timber flange is assumed. The distributions of the stresses and strains across the depths of beam models 1 and 2 at this critical zone is given in tables 4.10 and 4.11 and

Distance from one end (ins)	Direct stresses (lb/in^2)															
	Model (1)				Model (2)				Model (3)				Model (4)			
	σ_{11}	σ_{34}	σ_{21}	σ_{24}	σ_{11}	σ_{34}	σ_{21}	σ_{24}	σ_{11}	σ_{34}	σ_{21}	σ_{24}	σ_{11}	σ_{34}	σ_{21}	σ_{24}
0.00	0	0	0	0	0	0	0	0	0	0	0	0	0	0	0	0
9.15	-1943	1905	-1133	1177	-1708	1516	-1390	1658	-1404	1366	-1931	1971	-1266	1165	-1899	1995
18.30	-3886	3810	-2267	2353	-3415	3032	-2780	3316	-2812	2735	-3947	4028	-2556	2349	-3926	4123
27.45	-5800	5708	-3396	3526	-4967	4223	-4150	4947	-4430	4307	-4640	6486	-4093	3751	-4640	6523
30.50	-5800	6232	-3740	3849	-4967	4952	-4599	5417	-5113	4972	-4640	7559	-4777	4370	-4640	7650
36.60	-5800	6232	-3740	3849	-4967	4952	-4599	5417	-4814	4676	-4640	6201	-4248	3911	-4640	5910
45.75	-5800	6232	-3740	3849	-4967	4952	-4599	5417	-4637	4497	-4640	5301	-3853	3585	-4313	4649
Total ultimate load (lbs)	14250				12554				10847				7465			

Table 4.4 Theoretical direct stresses results at ultimate load for beam models 1, 2, 3 and 4 loaded with 4 point loading at $\frac{1}{3}$ span

Distance from one end X (in)	Model (1)				Model (2)				Model (3)						Model (4)					
	Strain (10^{-6})		Depth of yield from top edge (in)		Strain (10^{-6})		Depth of yield from top edge (in)		Strain (10^{-6})				Depth of yield from top edge (in)		Strain (10^{-6})				Depth of yield from top edge (in)	
	$\underline{\underline{\varepsilon}}_{11}$ $\underline{\underline{\varepsilon}}_{21}$	$\underline{\underline{\varepsilon}}_{14}$ $\underline{\underline{\varepsilon}}_{24}$	h_1	h_2	$\underline{\underline{\varepsilon}}_{11}$ $\underline{\underline{\varepsilon}}_{21}$	$\underline{\underline{\varepsilon}}_{14}$ $\underline{\underline{\varepsilon}}_{24}$	h_1	h_2	ε_{11}	ε_{14}	ε_{21}	ε_{24}	h_1	h_2	ε_{11}	ε_{14}	ε_{21}	ε_{24}	h_1	h_2
0·00	0·0	0·0	0·0	0·0	0·0	0·0	0·0	0·0	0·0	0·0	0·0	0·0	0·0	0·0	0·0	0·0	0·0	0·0	0·0	0·0
9·15	-1079	1121	0·0	0·0	-1324	1579	0·0	0·0	-811	803	-1839	1877	0·0	0·0	-744	762	-1808	1900	0·0	0·0
18·30	-2159	2241	0·0	0·0	-2648	3158	0·0	0·0	-1626	1609	-3759	3836	0·0	0·0	-1504	1535	-3739	-3927	0·0	0·0
27·45	-3235	3358	0·02	0·0	-3953	4711	0·09	0·0	-2561	2534	-6698	6177	0·0	1·42	-2407	2451	-6996	6212	0·0	1·56
30·50	-3562	3666	0·38	0·0	-4380	5159	0·44	0·0	-2955	2925	-8303	7199	0·0	2·00	-2810	2856	-8789	7286	0·0	2·17
36·60	-3562	3666	0·38	0·0	-4380	5159	0·44	0·0	-2783	2751	-6354	5905	0·0	1·26	-2499	2556	-6250	5629	0·0	1·23
45·75	-3562	3666	0·38	0·0	-4380	5159	0·44	0·0	-2680	2645	-4987	4797	0·0	0·46	-2266	2343	-4108	4428	0·0	0·0
Total ultimate load (lb)	14250				12554				10847						7465					

Table 4·5. Theoretical Direct Strain Results at ultimate load for beam models 1, 2, 3 and 4 loaded with 4 point loading at $\frac{1}{3}$ span

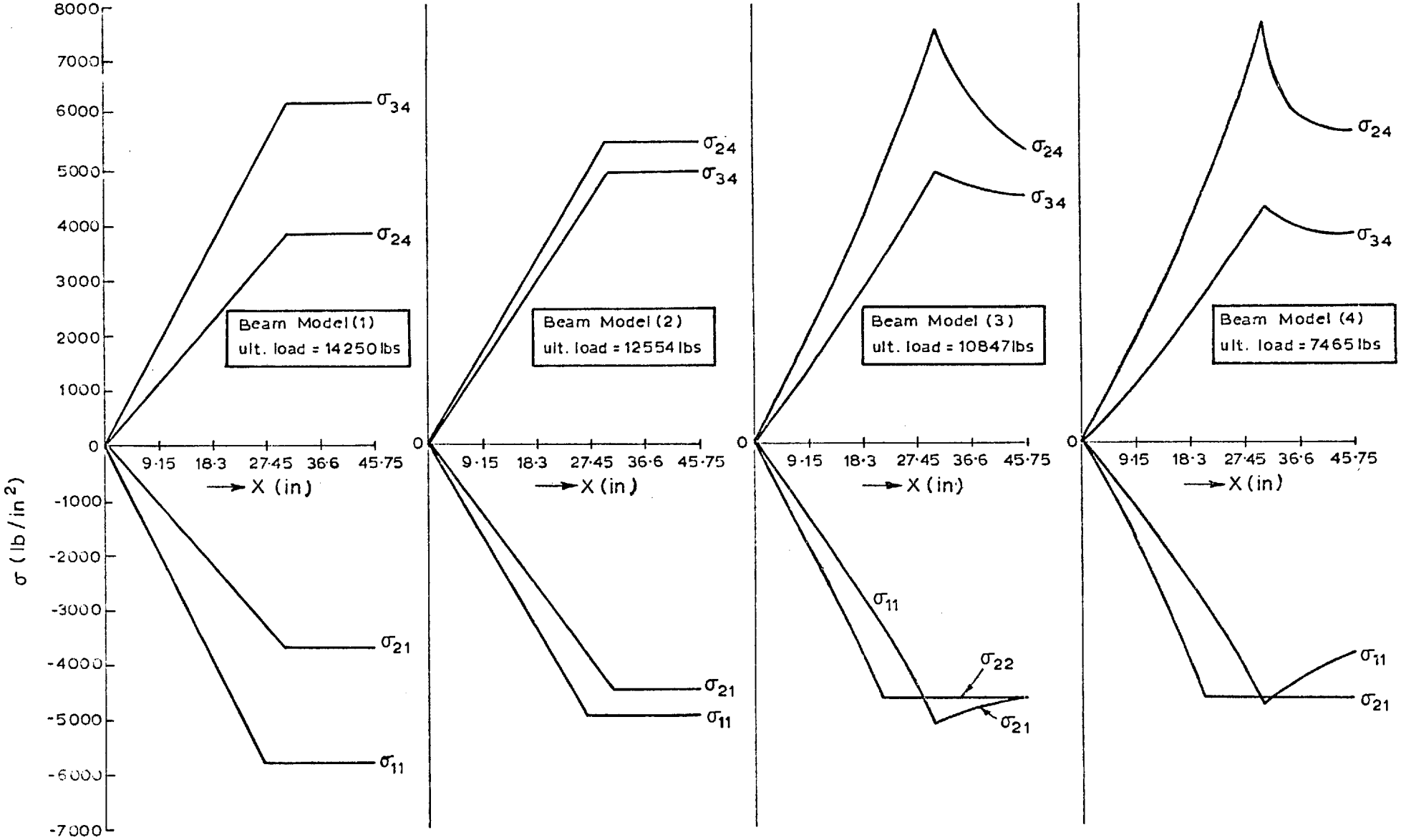


Fig. 4·6. Theoretical direct stresses at ultimate load along the spans of beam models 1, 2, 3 and 4 when loaded with four point loading

and figs. 4.9 and 4.12 and will be discussed in section 16.2 when they are compared with the experimental results.

Depending on the values of the moduli of elasticity of the timber and plywood in tension and compression and also on the ultimate compressive stresses and strains of the timber and plywood and noting that the strains at same levels of the timber and plywood are equal, i.e. no slips, it is noted that the values of direct stresses in the timber at a particular level across depth of beam may be greater or less than those in the plywood at the same level. This is shown in table 4.4 and fig.4.6 where $\sigma_{34} > \sigma_{24}$ for model (1) when $E_3 > E_2$, and $\sigma_{34} < \sigma_{24}$ for model (2) when $E_3 < E_2$: Similarly for σ_{11} and σ_{21}. Table 4.5 also shows the depth of penetration of yield from the top fibre of the beam for timber and plywood in compression, i.e. h_1 and h_2, at different points along the span. It is noted that the timber in compression has started to yield while the plywood has not started. Needless to say that the depth of the yield penetrations for the timber and plywood are dependent on the idealised compressive $\sigma - \varepsilon$ relationship of timber and plywood for models (1) and (2) found from small clear specimens, refer to figs.3.4 and 3.7.

(b) Semi-rigid case Beam models (3) and (4)

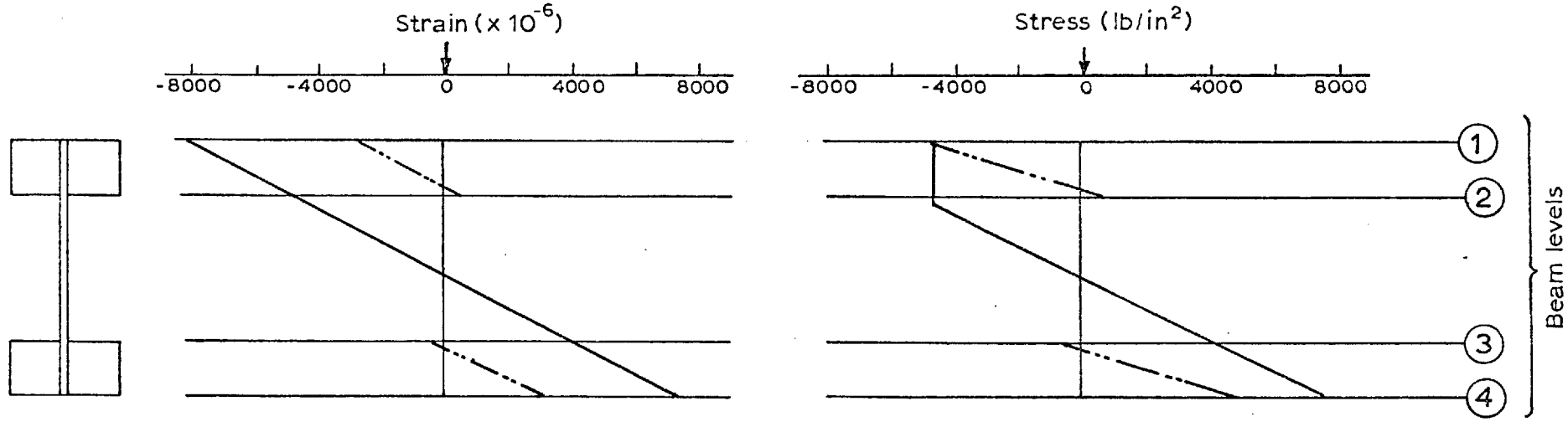
From fig.4.6 it is evident that the variation of direct stresses along the span does not follow the variation of the bending moment, as in the rigid case. The direct stresses σ_{11}, σ_{21}, σ_{24} and σ_{34} are maximum at $\frac{1}{3}$ of the span, i.e. at the point of application of the load. Ultimate tensile stresses and strains in the plywood, as determined from small clear specimens (table 3.3), have been reached at the extreme bottom fibres of the plywood (σ_{21} and ε_{21}) of beam models 3 and 4, refer to tables 4.4

and 4.5, at a distance equal to $\frac{1}{3}$ of the span from the supports and hence tension failure of bottom plywood is assumed.

From fig.4.7 the distribution of strains and stresses across the depth of the beam at critical section ($\frac{1}{3}$ span) are shown for both beam models (3) and (4). It is noted that the strains in the plywood at same levels across the depths of beam are much greater than those in the timber. Likewise the tensile direct stresses, in spite of the fact that the modulus of elasticity of the plywood in tension is less than that of the timber in tension. In the compression flange the ultimate compressive stress in plywood at the extreme fibre (σ_{21}) has been reached but the ultimate compressive strain (ε_{21}), as determined from small clear specimens (table 3.2), has not been reached and that the material has yielded considerably (h_2 = 2in,for beam model 4). It is also noted that the timber in the compression flange is still elastic and has not started to yield, i.e. $h_1 = 0$.

The difference in strain between the timber and plywood at the same levels across the depths of beam and the resulting stress distributions at different points along the beam (shown in fig.4.6) show the effect of slip on the behaviour of the semi-rigid beam models when compared with the rigid beam models.

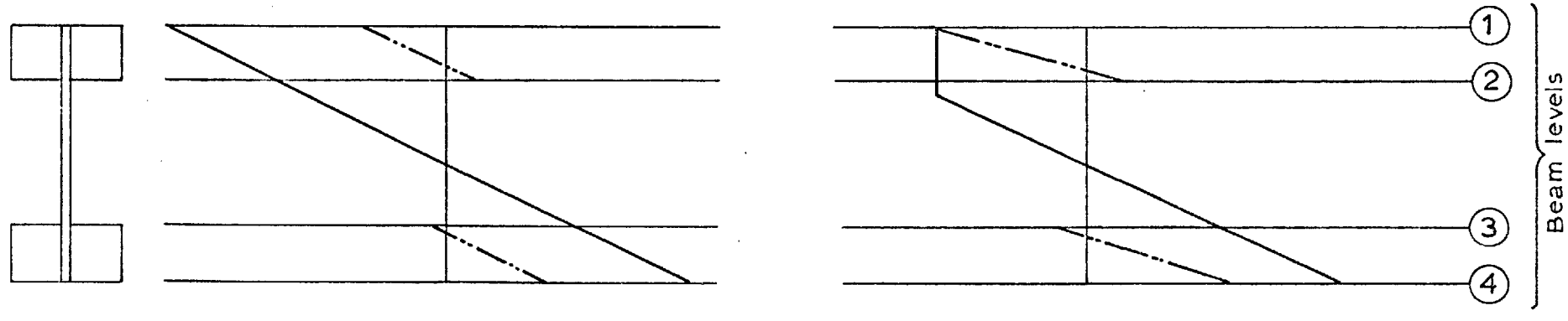
The effect of slip on the magnitude and distribution of direct stresses along the span of the semi-rigid beam models may be summarised as follows:



(a) Beam Model (3)

——— Distributions across web

—·—·— Distributions across flanges



(b) Beam Model (4)

Fig. 4·7. Theoretical ultimate strains and stresses across critical cross sections ($\frac{1}{3}$ span) of beam models (3) and (4)

Equation (2.56) may be generalised to give equation 4.4 as follows:

$$\sigma = f(M,N) \qquad - 4.4$$

While in the rigid cases N is dependent on M and $\sigma - \varepsilon$ relationship only, in the semi-rigid cases N is dependent on M, $\sigma - \varepsilon$ and $Q - \delta$ relationships. The curves chosen for $Q - \delta$ relationships, whether linear or non linear, will obviously affect the magnitude and distributions of the direct strains and stresses along the beam spans.

15.2.2 Results for beam models (1) and (3) under uniformly distributed load

Theoretical results for beam models (1) and (3) under uniformly distributed load over the whole span are summarised in tables 4.6 and 4.7.

It is noted in this case that compression failure of top flanges of beam model (1) and tensile failure of plywood of beam model (3) will occur at a higher total load over the whole spans than if the beams are loaded under four point loading at $\frac{1}{3}$ points. Also it is noted that under similar total loads when the beams are loaded under u.d.l. and four point loading, that the web shear stresses are higher in the former case than the latter case; and vice versa for deflections.

Web shear stresses are critical at a load lower than the ultimate load when compression failure of top flange of beam model (1) will occur.

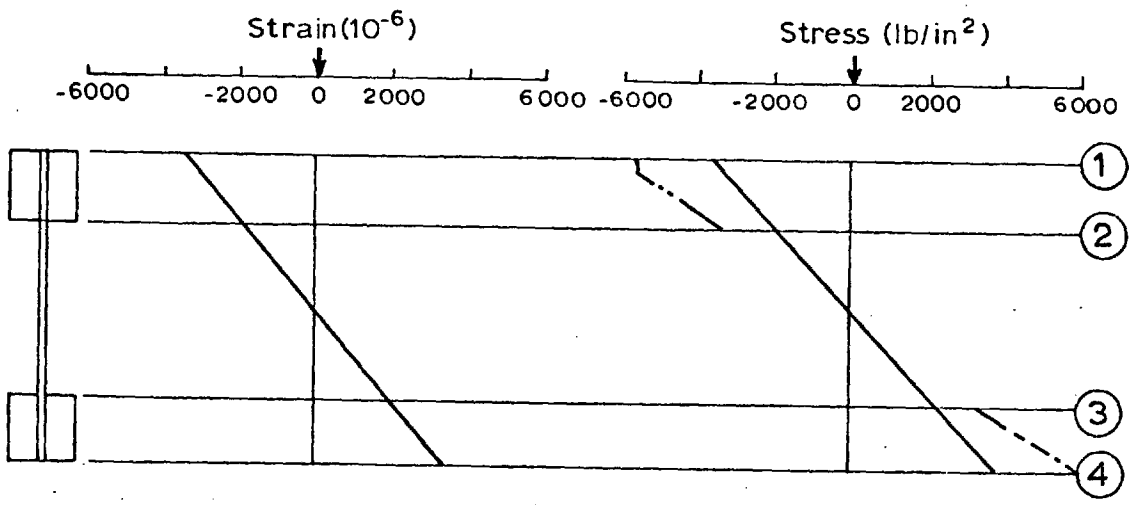
The distribution of stresses and strains across the depths of both beam models (1) and (3) are given in fig.4.8. Similar to the discussion given in section 15.2.1(a) for beam model (1), direct stresses at any fixed level across the timber flanges are greater than those at the same level across the plywood web. It is noted that plywood web shear failure of beam model (1) has started before either of the timber flanges or plywood web in compression has started to yield.

Load (lb/in)	Direct stress at mid span lb/in^2				Direct strain at mid span 10^{-6}		Depth of yield from top fibre (ins)		Shear stresses at support (lb/in^2)			Total deflection at mid span (ins)
									Flange web		Web at N.A.	
	σ_{11}	σ_{34}	σ_{21}	σ_{24}	ϵ_{11}	ϵ_{24}	h_1	h_2	τ_{yx1}	τ_{yx3}	τ_{xz}	
0	0	0	0	0	0	0	0.00	0.00	0.0	0.0	0	0.000
20	-624	612	-364	378	-347	360	0.00	0.00	37.1	36.7	291	0.119
80	-2495	2446	-1456	1511	-1386	1439	0.00	0.00	148.3	147.0	1136	0.477
150	-4678	4587	-2729	2833	-2599	2698	0.00	0.00	278.1	275.5	2181	0.895
200	-5800	6036	-3604	3728	-3433	3551	0.24	0.00	370.8	367.4	2908	1.189

Table 4.6 Theoretical results for beam model (1) under u.d.l.

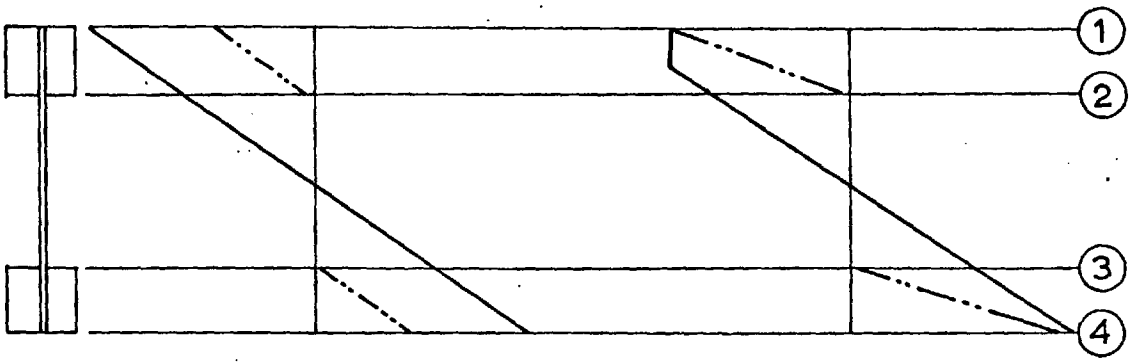
Load (lb/in)	Direct stress at mid span (lb/in^2)				Direct strain at mid span 10^6				Depth of yield from top fibre (ins)		Shear at support			Slip at Support (ins)		Total deflec. at mid span (ins)
											Flange web force lb/in		web at NA. lb/in^2			
	σ_{11}	σ_{34}	σ_{21}	σ_{24}	ε_{11}	ε_{34}	ε_{21}	ε_{24}	h_1	h_2	q_1	q_3	τ_{xz}	δ_1	δ_3	w
0	0	0	0	0	0	0	0	0	0.00	0.00	0	0	0	.0000	.0000	.000
20	-563	563	-376	376	-331	331	-358	358	0.00	0.00	94	94	149	.0026	.0026	0.095
80	-2269	2269	-1922	1922	-1335	1335	-1831	1831	0.00	0.00	296	296	599	.0294	.0294	0.523
140	-4016	4016	-4440	4440	-2362	2362	-4228	4228	0.00	0.00	423	423	1053	.0870	.0870	1.203
160	-4660	4613	-4640	5401	-2741	2714	-5285	5144	0.00	0.66	471	464	1208	.1126	.1089	1.481

Table 4.7 Theoretical results for beam model (3) under u.d.l. based on solutions of the generalised d.e.



Beam Model (1) at mid-span
at 200 lb/in

——— Distributions across depth of web
—·—·— Distributions across depth of flanges



Beam Model (3) at mid-span
at 160 lb/in

Fig. 4·8. Theoretical direct strains and stresses distributions for beam models(1)&(3) under U.d.L over the whole span

Similar to the discussion given in section 15.2.1(b) for beam model (3) under four point loading, it is evident that the magnitude of the direct strains in the plywood are greater than those in the timber flanges at the same level across the depth of the beam. Also the plywood in the compression flange has started to yield while the timber is still elastic. Also in spite of the fact that $E_2 < E_3$, yet $\sigma_{24} > \sigma_{34}$ and this is attributed to the fact that $\epsilon_{24} > \epsilon_{34}$ due to the effect of slip between the plywood and the timber.

15.2.3 Other theoretical results

The results for deflection, web shear, flange web shear (in case of rigid beam models) and slip (in case of semi-rigid beam models) were found at different points along the beam models spans. In this thesis some of these results are reported in chapter (16) when these results are compared with the experimental results found when beam models 1, 2, 3 and 4 were tested as described in part III of this thesis.

15.3 Comparison between theoretical results for beam model (3) obtained from solutions based on linear, semi-linear and totally non-linear governing differential equations

15.3.1 General

In this section theoretical results for beam model (3) under four point loading are reported at three load levels. These results are obtained from the following three solutions of the governing differential equations:

(a) Linear solution: This solution is based on linear relationship for $\sigma - \epsilon$ and $Q - \delta$. Analytical solutions described in section (5.7) have been used assuming symmetry of section of beam model (3), i.e. $E_1 = E_3$. Since $Q - \delta$ is assumed to be linear the connector moduli found from joint tests described in section (10.3) at low, medium and high load levels are used to give theoretical solutions for beam model (3) at low, medium and high load levels respectively.

(b) Semi-linear solution: This solution is based on linear $\sigma - \epsilon$ relationship and non-linear $Q - \delta$ relationship. In this case the solution described in section 5.6.1 is used to solve beam model (3) at low, medium and high load levels.

(c) Totally non-linear solution. This solution is based on non-linear $\sigma - \varepsilon$ and $Q - \delta$ relationships. In this case solutions described for the generalised differential equations in Chapter 6 are used to solve beam model (3) at low, medium and high load levels.

In table 4.8 the theoretical results are reported for the three load levels and the three cases mentioned above. These results describe the behaviour of the beam model such that the direct stresses at critical section ($\frac{1}{3}$ span), mid span bending deflection, neutral axis web shear stress at end support, shear force per unit length at end support and slip at end support are all reported.

15.3.2 Low load level: chosen load = 1650 lbs.

At this load level results are reported for the linear and semi-linear solutions only. As the timber and plywood in compression are well within the elastic limit then solutions are not reported for the totally non-linear case. It is noted from table 4.8 that the results given for both the linear and semi-linear cases are more or less equal. Such that the small variations of linear case (less than 1%) may be ignored and a linear approximation for $Q - \delta$ may be adopted. Needless to say that the results of the linear case are dependent on the choice of the connector modulus k.

15.3.3 Medium Load Level: chosen load = 5900 lbs

Similar to the case of the low load level, results are only reported for the linear and semi-linear cases, noting that the timber and plywood in compression are still within the elastic limit. It is noted from table 4.8 that some differences between the linear and semi-linear solutions occur. Web direct stress in tension or compression and deflection are most

Load Level lbs	Description of governing d.e.	Direct stresses at critical section ($\frac{1}{3}$ span) lb/in^2				Bending Deflection at mid span (ins)	N.A. web shear stress at end support lb/in^2	Shear force per unit length at end support (lb/in^2)		Slip at end support (ins)	
		σ_{11}	σ_{34}	σ_{21}	σ_{24}	w_b	τ_{xz}	q_1	q_3	δ_1	δ_3
1650 (low)	Linear $\{\sigma - \varepsilon$, $Q - \delta$ k = 70000 lb/in	-685	685	-634	634	.111	133	104	104	.00297	.00297
	Linear: $\sigma - \varepsilon$ Non linear: $Q - \delta$	-688	684	-627	633	.109	133	102	102	.00295	.00295
	Non linear $\{\sigma - \varepsilon$, $Q - \delta$	-	-	-	-	-	-	-	-	-	-
5900 (medium)	Linear $\{\sigma - \varepsilon$, $Q - \delta$ k = 13330 lb/in	-2496	2496	-3464	3464	.657	480	300	300	.04510	.04510
	Linear: $\sigma - \varepsilon$ Non linear: $Q - \delta$	-2494	2477	-3013	3039	.540	478	305	305	.03197	.03211
	Non linear $\{\sigma - \varepsilon$, $Q - \delta$	-	-	-	-	-	-	-	-	-	-
10375 (high)	Linear $\{\sigma - \varepsilon$, $Q - \delta$	-4452	4452	-7502	7502	1.479	849	428	428	.12200	.12200
	Linear: $\sigma - \varepsilon$ Non linear: $Q - \delta$	-4456	4419	-6691	6749	1.254	844	442	443	.09690	.09760
	Non linear $\{\sigma - \varepsilon$, $Q - \delta$	-4752	4653	-4640	7025	1.281	849	452	442	.10220	.09677

Table 4.8 Theoretical results at three load levels based on linear, semi-linear and non-linear governing differential equations for beam model (3) under four point loading

affected. The results of the semi-linear model are stiffer than the linear model, e.g. mid span deflection in the semi-linear case is less than in the linear case by about 3%.

The approximation of the semi-linear model by a linear model is then possible but it is dependent on the choice of the connector modulus k to correspond to the desired load level.

15.3.4 High load level: chosen load = 10375 lbs

At this load level results for the three cases are reported. It is noted from table 4.8 that the direct stresses of the timber and plywood are most affected if the totally non-linear solution is approximated by either linear or a semi-linear solution. Variations as high as 50% increase are noted for σ_{21} when a semi-linear solution is assumed. This may be understood since the plywood has started to yield, i.e. entered the non-linear zone, and that the analysis of the semi-linear case is based on linear $\sigma - \varepsilon$. Semi-linear solutions give low values for deflection, web shear stress, etc. than totally linear solution, i.e. stiffer beams. Deflection is decreased when the totally non-linear solution is approximated by the semi-linear one by about 2.1%. As solutions of the linear case are dependent on the choice of the connector modulus to correspond to the load level under consideration and also since it is based on linear $\sigma - \varepsilon$ and as we have seen above that linear approximations of $\sigma - \varepsilon$ may result in high variation in the predicted stresses and strains, then the linear approximation to represent the totally non-linear case may result in serious errors. Hence at high loads the non-linear case must be used if accurate beam behaviour is desired.

Chapter 16 Comparison of theoretical and experimental results

16.1 General

Experimental results from tests series II and III described in part III of this thesis are compared with the corresponding theoretical results. Comparisons are given for each test series separately, i.e. rigid and semi-rigid beams will be treated separately. The theoretical results are found from solutions based on the generalised governing differential equations. The following results are compared and reported.

Test series II and III

(a) Distribution of strains and stresses across mid span depth of beam models (1), (2), (3) and (4) at five load levels and up to the ultimate load

(b) N.A. Web shear stress at distances from support indicated in fig.3.14(a). Results are reported at different load levels up to the ultimate load.

(c) Also mid-span total deflection.

Test series III

Slip between top flange and web at distances from the support indicated in fig.3.14(a). Results are reported at different load levels and up to the ultimate load.

16.2 Results for test series II: Beam models (1) and (2)

16.2.1 Beam model (1)

Theoretical and experimental critical results for beam model (1) are briefly summarised in table 4.9. From table 4.9 it is predicted that compression failure of the top flange will occur at an ultimate load of 14250lbs. As mentioned in section 15.2(a) compression failure of the top flange has

Beam model no.	Total ultimate load (lbs)		Type of failure		Position of failure along span		σ_{11} at ultimate load lb/in^2		ε_{11} at ultimate load 10^{-6}		Average m.c.%			
											beam test		small clear specimen test	
	Theo.	Expt.	Theo.	Expt.	Theo.	Expt.	Theo.	Expt.	Theo.	Expt.	T	P	T	P
(1)	14250	12200	Compression failure of top flange	Premature flange web glue failure	Middle third of beam	At end support	-5800	-5528	-3562	-2966	13.7	11.7	13.1	11.0
(2)	12554	13900	Compression failure of top flange	Compression failure of top flange	Middle third of beam	Middle third of beam	-4970	-4963	-4380	-4150	14.4	11.8	13.6	11.0

Table 4.9 Summary of critical results at theoretical and experimental ultimate loads for test series II.

Symbols

m.c. moisture content

T Timber

P plywood

been assumed when the extreme fibre stresses and strains (σ_{11} and ε_{11}) have reached their ultimate values as determined from compression tests of small clear specimens (table 3.2). Also the position of failure has been predicted to occur in the middle third of the beam. The beam has actually prematurely failed at flange web interface near the end support due to glue failure. The beam failed at a load of 12200 lbs. Glue failure between the flange and web should not have occurred as the predicted flange web shear stress (247.5 lb/in^2) at that load is less than the ultimate rolling shear stress (375 lb/in^2) on the surface determined from CP112: (1967) or ultimate shear parallel to the grain stress (1570 lb/in^2) determined from small clear specimens (table 3.2). It is worth mentioning that the glue ultimate shear strength is assumed to be the lowest of the ultimate plywood rolling shear stress or ultimate shear parallel to the grain stress. Also flange web glue failure is uncommon for beams with similar geometry. It appears that the cause of failure is due to weakness of the glue near the support. The cause of that may be due to the fact that during the fabrication of the beam (section 12.2) pressure on the joint was applied using clamps on plywood sheets to give approximately continuous pressure. Using clamps in this manner may result in weak points because the intensity of pressure at each point along the beam where the clamps were applied may vary.

A detailed summary of the theoretical and experimental results at different load levels and up to the ultimate theoretical and experimental loads, are reported for the distribution of direct stresses and strains at mid span, mid span deflection and neutral axis web shear stress, at $x = 21.35$ ins, are summarised in table 4.10.

Load Level (lbs)	STRAIN (10^{-6}) at mid span						STRESS (lb/in^2) .15" from levels 1,2,3&4				mid span deflection (ins)		web shear stress lb/in^2	
	Theoretical				Av. Expt. .15" from 1,2,3 &4		Theoretical		Av. Expt.					
	at levels 1,2,3,&4		0.15" from levels 1,2,3 &4											
	ϵ_{11}	ϵ_{34}	ϵ'_{11}	ϵ'_{34}	ϵ'_{11}	ϵ'_{34}	σ'_{11}	σ'_{34}	σ'_{11}	σ'_{34}	Theo.	Expt.	Theo.	Expt.
0	0	0	0	0	0	0	0	0	0	0	0	0	0	0
679	-171	178	-165	172	-166	160	-296	292	-299	272	.060	.052	108	108
3393	-857	889	-824	856	-866	830	-1484	1456	-1559	1411	.299	.278	539	551
6786	-1713	1779	-1648	1714	-1764	1686	-2966	2913	-3176	2866	.597	.568	1078	1067
8144	-2056	2134	-1977	2055	-2118	2023	-3559	3494	-3812	3439	.717	.679	1294	1271
10858	-2742	2846	-2637	2741	-2834	2698	-4747	4660	-5035	4587	.96	.932	1725	1684
12200	-3084	3202	-2966	3084	-3218	3043	-5339	5243	-5528	5172	1.070	1.21	1941	1827
14250	-3562	3666	-3410	3520	-	-	-5800	5984	-	-	1.346	-	-	-

Table 4.10 Theoretical and experimental results for beam model (1) under four point loading

Load level (lbs)	Strain(10^{-6}) at mid span						Stress (lb/in^2) .15" from levels 1,2,3&4				Mid span deflection (ins)		Web shear stress (lb/in^2)	
	Theoretical				Av. Expt. .15" from 1,2 3 &4		Theo.		Av. Expt.					
	At levels 1,2,3 &4		0.15" from 1, 2,3 & 4											
	ϵ_{11}	ϵ_{34}	ϵ'_{11}	ϵ'_{34}	ϵ'_{11}	ϵ'_{34}	σ'_{11}	σ'_{34}	σ'_{11}	σ'_{34}	Theo.	Expt.	Theo.	Expt.
0	0	0	0	0	0	0	0	0	0	0	0	0	0	0
679	-239	284	-229	274	-205	199	-296	263	-264	191	.079	.070	108	85
3054	-1074	1280	-1030	1236	-976	939	-1329	1186	-1258	902	.356	.323	490	406
5768	-2028	2418	-1947	2335	-1879	1814	-2509	2241	-2424	1741	.673	.630	926	745
7465	-2624	3129	-2516	3021	-2540	2362	-3246	2900	-3161	2267	.871	.810	1198	957
9161	-3221	3841	-3089	3709	-3036	2907	-3984	3560	-3839	2791	1.069	1.020	1471	1168
10858	-3817	4552	-3660	4395	-3701	3488	-4722	4219	-4415	3348	1.270	1.221	1743	1391
12554	-4380	5159	-4150	4980	-4530	4166	-4970	4781	-4816	3952	1.454	1.442	2015	1635
13900	-	-	-	-	-5564	4716	-	-	-4963	4527	-	1.681	-	1720

Table 4.11 Theoretical and experimental results for beam model (2) under four point loading

Distribution of Strains and Stresses at mid span

Theoretical and experimental results for direct stresses and strains at mid span are plotted in fig.4.9 for five load levels including the ultimate experimental load. The following points are evident:

(a) Linear distribution of strain across depth of beam, assumed in theory (part II), is confirmed by experimental results at all load levels.

(b) At low load levels the strains and the stresses determined from theory agree reasonably well with the experimental results.

(c) At high load levels, say ultimate experimental load, a variation of the theoretical with respect to the experimental strain results as high as $\pm$ 20% is noted for strains measured on plywood in tension or compression sides: likewise with the stresses. Strains found from the experiment are lower in the tension side and higher in the compression side than the corresponding theoretical results. While experimental results indicate that the timber in compression has just started to yield, the theoretical results indicate that the timber is elastic. This may be understood if it is noted that the theoretical results are based on an idealised $\sigma - \epsilon$ distribution where the idealised yield strain is greater than the proportional limit strain (fig.2.1(b)) on which the analysis of the experimental results is based (refer to section 2.2, eqns.1.1 - 1.3).

(d) It is noted that the experimental result of the strain gauges on the plywood just below the timber flange (positions 6, 19, 12 and 25, refer to fig. 3.14a) are low and that they are off the straight line distribution across the depth of the beam. This may be attributed to the fact that when the flanges were glued to the web and clamps

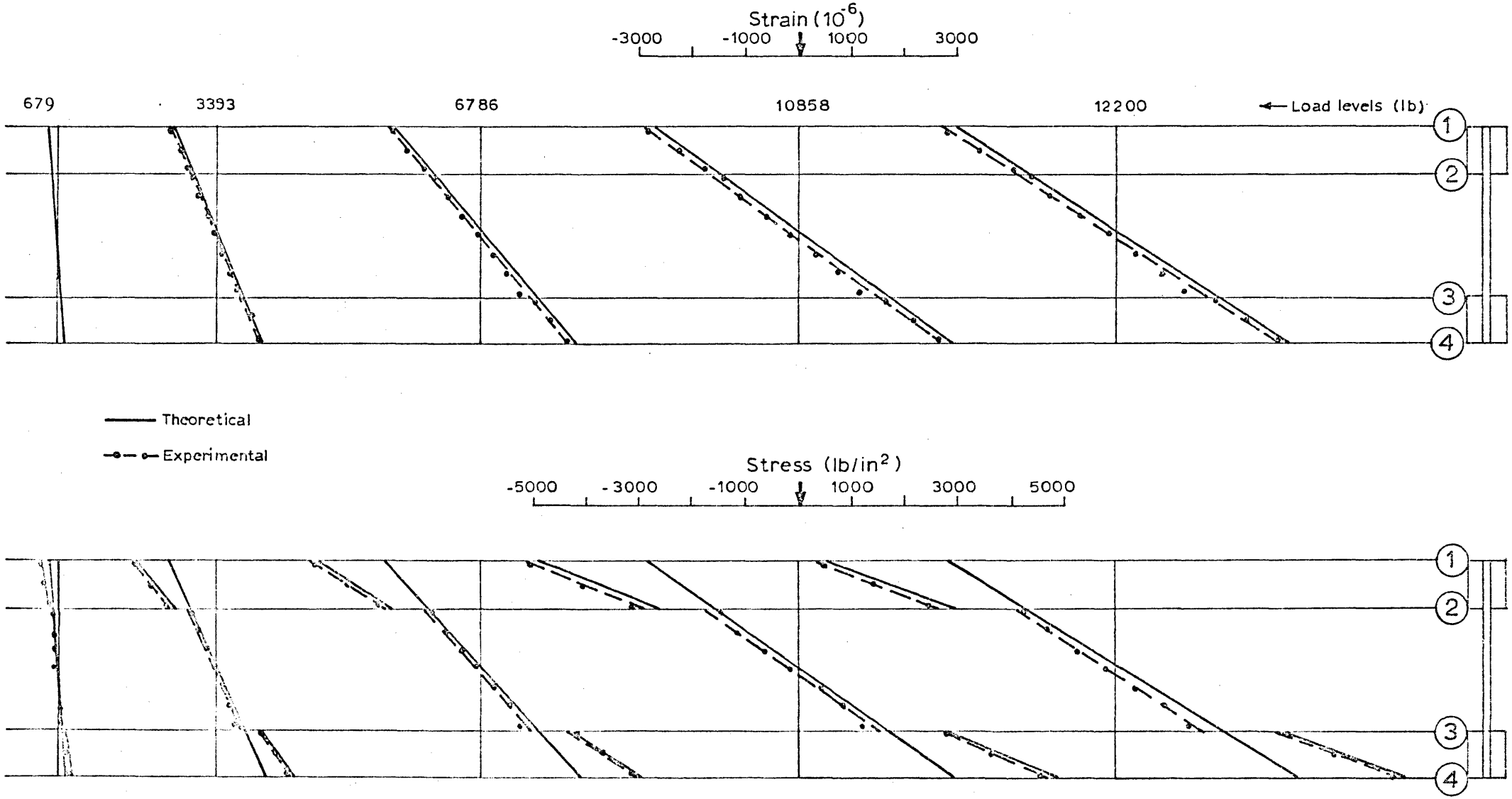


Fig. 4·9. Theoretical and experimental stress and strain distribution at mid span of beam model (1) under four point loading

were applied some glue was squeezed on the plywood under the flanges. Before the strain gauges were fixed in position, the squeezed glue was scraped using a razor. The glue might have stiffened the plywood under the gauge and caused these variations in the results.

(e) Analysis of strain results from experiment to find the stresses in a way similar to that suggested in section 12.5 resulted in the stress distributions shown in fig.4.9. It is noted that the total compressive force (C) in the beam is higher than the counter total tensile force (T) at ultimate expt. load by about 8%. This discrepancy may be understood if the variation in $\sigma - \varepsilon$ diagrams for timber and plywood are noted. Coefficient of variation as high as .13 are encountered e.g. modulus of elasticity of timber in tension for model (1), refer to table 3.2.

Mid span deflection

Experimental and theoretical results for mid span deflection reported in table 4.10 are plotted in fig.4.10. The experimental results are higher than the theoretical results by as much as 11.5% at the experimental ultimate load. All other experimental results at loads prior to ultimate load are lower than the corresponding theoretical ones, which indicates that the actual beam tested is stiffer than the theoretical model. This may be explained if it is noted that in the theoretical model the effect of the web stiffeners and the lateral stability supports were not considered. Lateral stability supports were designed in such a way that their effect on the behaviour of the beam is minimised but not completely eliminated, and this is indicated by the slight differences found between front and back strain gauges readings. The increase in the experimental deflection

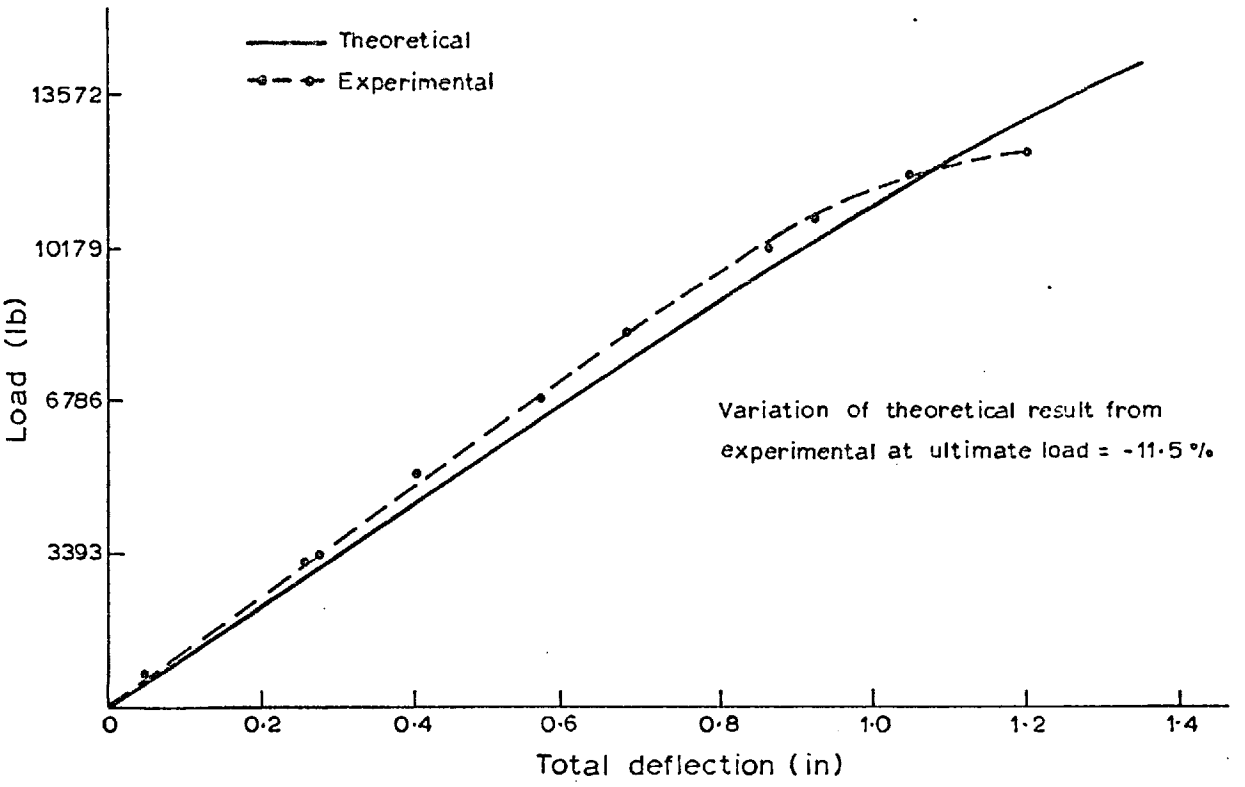


Fig. 4·10. Theoretical and experimental mid span deflection of beam model (1) under four point loading

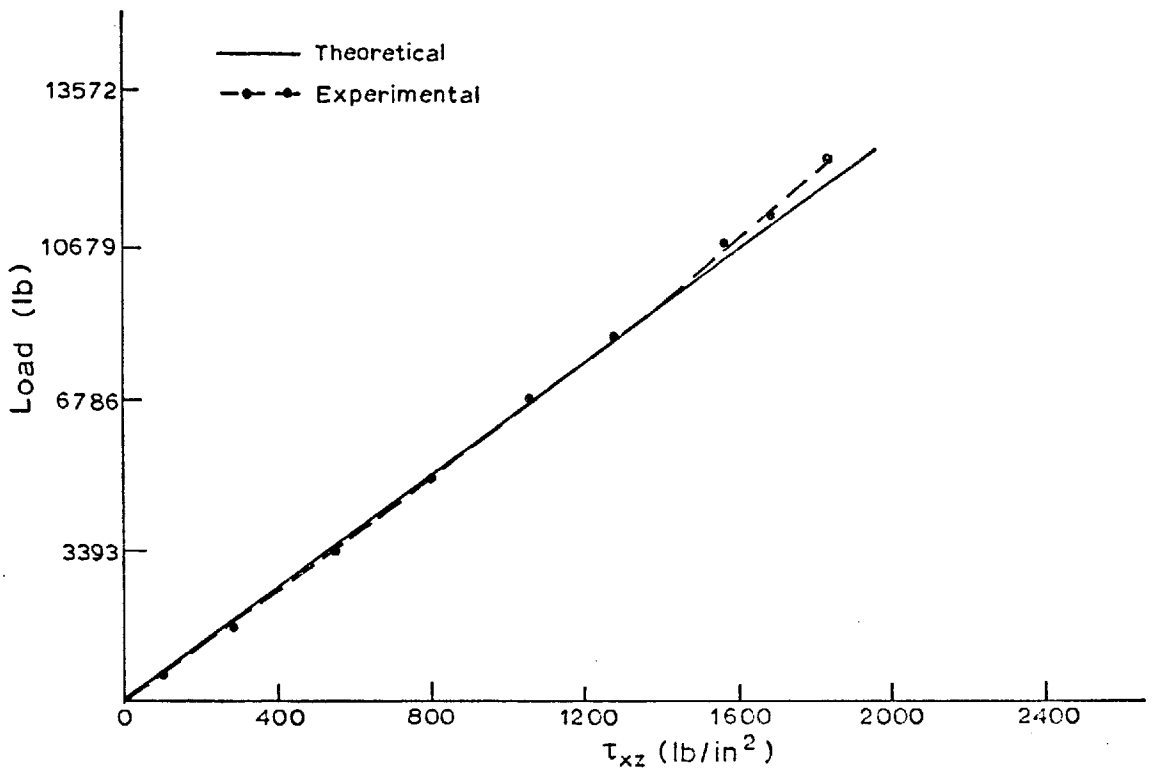


Fig. 4·11. Theoretical and experimental web shear stress at X = 21·35 in for beam model (1) under four point loading

at ultimate load may be explained by the fact that the experimental strain and stress results discussed before showed that the beam has started to yield while the theoretical results indicated that the beam is still elastic.

Neutral axis web shear stress

Theoretical and experimental results for web shear stress given in table 4.10 are plotted in fig.4.11. The theoretical results and experimental results agree reasonably well. It should be noted that the experimental results are based on linear $\tau_{xz} - \gamma_{xz}$ relationship and that the theoretical results are based on linear analysis. Ultimate predicted web shear stress at experimental ultimate load agree with the experimental within 6% and are both less than ultimate web shear stress determined from small clear specimens (2150 lb/in^2), refer to table 3.3.

16.2.2 Beam model (2)

Theoretical and experimental critical results for beam model (2) are briefly summarised in table 4.9. From table 4.9 it is evident that the predicted theoretical failure of the top compression flange at an ultimate load of 12554 lbs has occurred at an ultimated load of 13900lbs i.e. 10% higher, when beam model (2) was tested. Ultimate theoretical and experimental compression stresses and strains (σ_{11} and ε_{11}) agree within 6%. Experimental results are lower than the theoretical ones. Failure of the beam when the beam was tested occurred within the predicted region.

A detailed summary of the theoretical and experimental results at different loads levels and up to the ultimate theoretical and experimental loads are reported, for the distribution of the direct stresses and strains at mid span, mid span deflection and neutral axis web shear stress at x = 21.35 in are summarised in table 4.11.

Distribution of strains and stresses at mid span

Theoretical and experimental results for direct stresses and strains at mid span are plotted in fig.4.12 for five load levels including the ultimate experimental load. The following points are evident.

(a) Linear distribution of strain across depth of beam assumed in theory (part II) is confirmed by experimental results at all load levels.

(b) Strain and stress results from experiments in the compression side of the beam agree reasonably well with the predicted theoretical results, e.g. ε_{11} at ultimate theoretical load lies within 6.5% of the predicted theoretical results.

(c) Differences between theoretical and experimental strain results as high as 25% are experienced in the tension side of the beam, e.g. ε_{34} at ultimate theoretical load. Theoretical strain results are higher than experimental ones. This may be attributed to the fact that linear $\sigma - \varepsilon$ was assumed for timber of model (2) in tension while a non-linear relationship has been reported, refer to fig. 2.5.

Both experimental and theoretical ultimate strain and stress results indicate that the top compressive timber flange has yielded considerably while the plywood is still elastic.

(d) Point (d) discussed in section 16.2.1 for beam model (1) also applies for beam model (2).

(e) Similar to beam model (1), section 16.2.1e, it is noted that the total compressive force (C) in beam model (2) is higher than its counter tensile force (T) by about 17%, determined from the experimental stress distribution at ultimate load. This high variation may be partly due to variations in the $\sigma - \varepsilon$ diagrams for timber and plywood, tables 3.2 and 3.3, and partly due to the linear idealisation of tensile $\sigma - \varepsilon$ relationship for timber; non-linear behaviour has been reported in fig. 3.5.

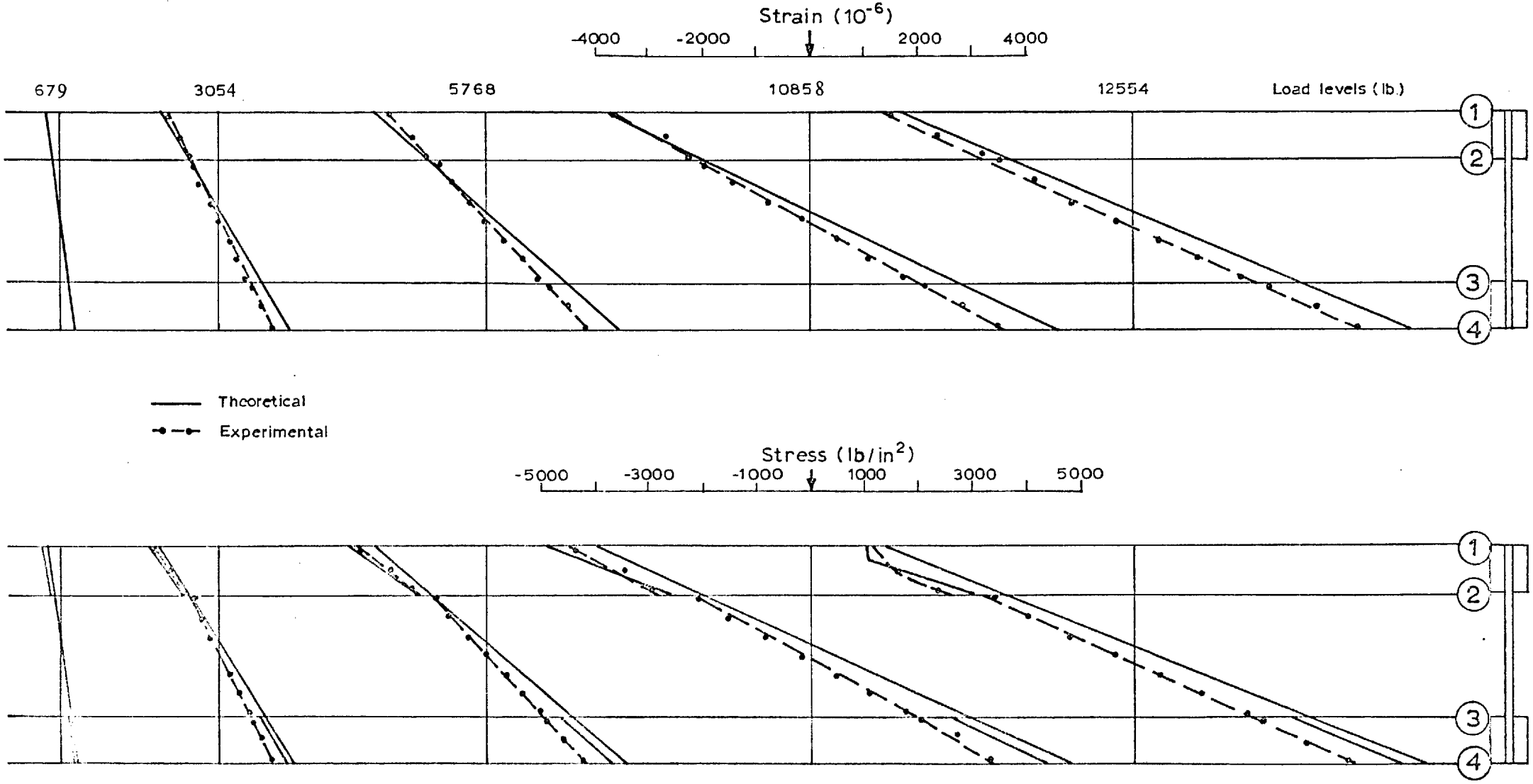


Fig. 4·12. Theoretical and experimental stress and strain distribution at mid span of beam model (2) under four point loading

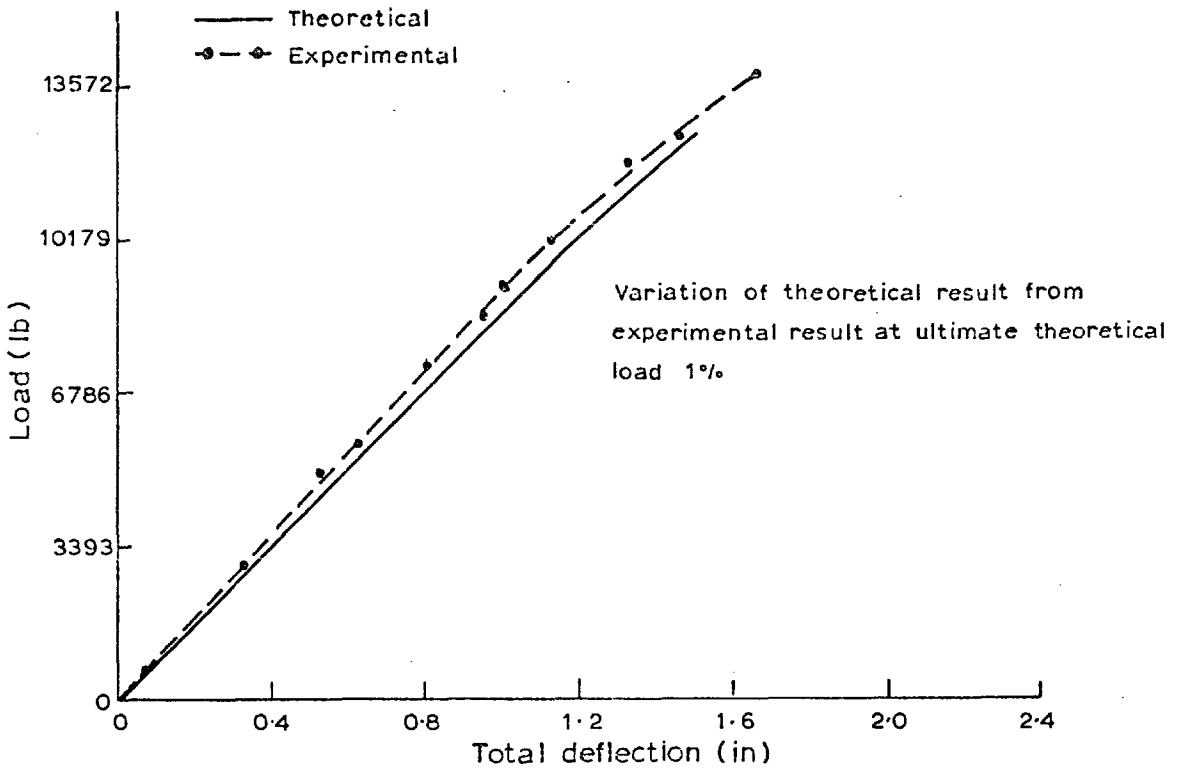


Fig. 4·13. Theoretical and experimental mid span deflection of beam model (2) under four point loading

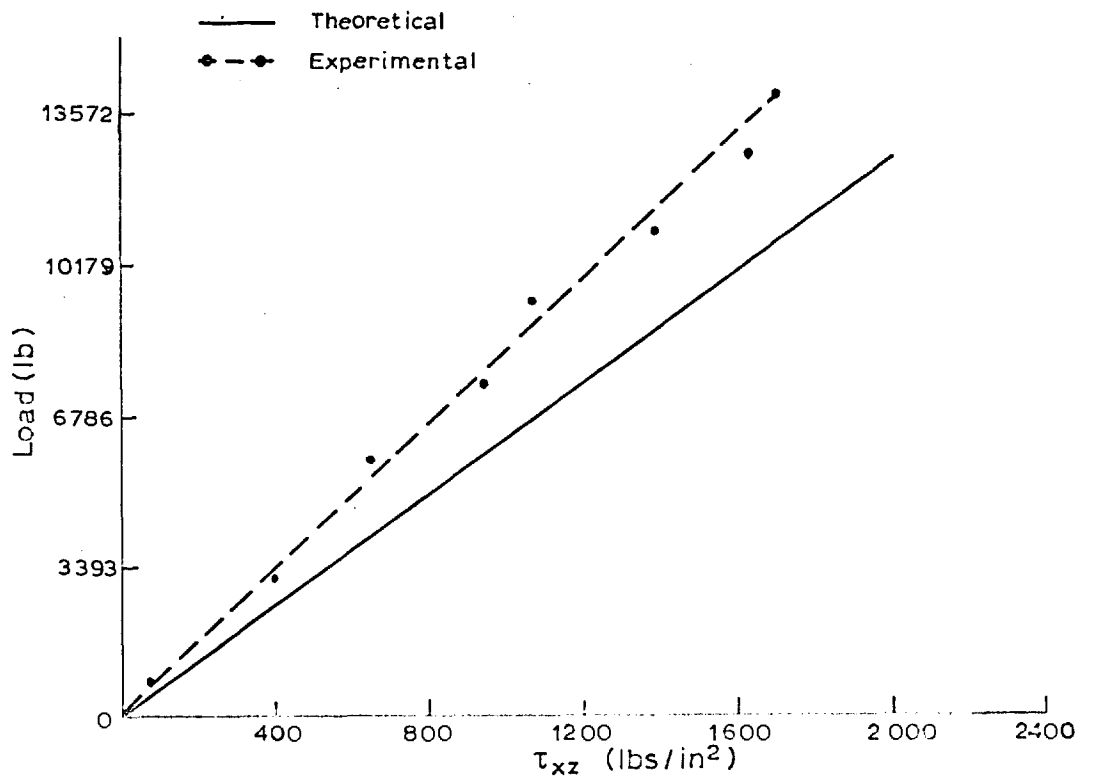


Fig. 4·14. Theoretical and experimental web shear stress at X = 21·35 in for beam model (2) under four point loading

Mid span deflection

Theoretical and experimental results for mid span deflection reported in table 4.11 are plotted in fig.4.13. All experimental results, at reported loads, are lower than the corresponding theoretical ones. A 1% variation is reported between experimental and theoretical at ultimate load. All experimental and theoretical results agree reasonably well. Similar discussion to that of section 16.2.1 to explain stiffer beam experimental results of beam model (1), also apply for beam model (2).

Neutral axis web shear stress:

Theoretical and experimental results for web shear stress given in table 4.11 are plotted in fig.4.14. Considerable variations between theoretical and experimental results are noted. Experimental results at reported loads are lower than the theoretical results. Variation of theoretical results with respect to experimental result as high as 20% is noted at ultimate experimental load. Both ultimate theoretical and experimental results are lower than ultimate web shear stress determined from small clear specimens (2150 lb/in^2), refer to table 3.3. Theoretical web shear stresses are based on linear τ_{xz} - γ_{xz} relationship.

16.3 Results for test series III: Beam models (3) and (4)

16.3.1 General

Theoretical and experimental results for beam models (3) and (4) are summarised in tables 4.13, 4.14, 4.15 and 4.16 at different load levels. These results includethe following:

Beam model no.	Ultimate load (lbs)		Type of failure		Position of failure along span		σ_{24} at ultimate load lb/in^2		ϵ_{24} at ultimate load 10^{-6}		Average m.c.			
											Beam test		small clear specimen test	
	Theo.	Expt.	Theó.	Expt.	Theo	Expt.	Theo.	Expt.	Theo.	Expt.	T	P	T	P
(3)	10847	10800	Tensile failure of bottom plywood web	Tensile failure of bottom plywood web	At $\frac{1}{3}$ span	At $\frac{1}{3}$ span	7559	-	7199	-	13.9	11.5	13.1	11.0
(4)	7465	7800	"	"	"	"	7650	-	7286	-	13.5	11.3	13.05	11.0

Table 4.12 Summary of critical results at theoretical and experimental ultimate loads for tests series III.

(a) Distribution of stresses across the depths of beam models (3) and (4) at mid span. It is worth mentioning here that strains were not measured at critical section of the beam models ($\frac{1}{3}$ span) because of the presence of the web stiffeners at these points and also the load applied there may produce stress concentrations that may influence the readings.

(b) Mid span deflections.

(c) Neutral axis web shear stresses at distances indicated in tables 4.14 and 4.16.

(d) Slip between top timber flange and plywood web at distances indicated in tables 4.14 and 4.16.

From table 4.12 both beam models' predicted ultimate loads agreed with the experimental ones and also tensile failure of extreme bottom plywood fibre at $\frac{1}{3}$ span, i.e. under the load, has been predicted theoretically and confirmed experimentally at the ultimate loads reported in table 14.12. In both beam models theoretical ultimate σ_{24} and ϵ_{24}, as determined from small clear specimens (table 3.3), has been reached. Discussion of that has been given in section 15.2.1(b).

16.3.2 Distribution of stresses at mid span

Theoretical and experimental results for direct stresses and strains of table 4.13 and 4.15 for beam models (3) and (4) are plotted in figs. 4.15 and 4.19 for five load levels including the ultimate loads. The following points are evident:

Load Level (lb)	STRAIN (10^{-6})																		STRESS (lb/in^2) 0·15" from Levels 1, 2, 3 & 4											
	* THEORETICAL												Av. EXPERIMENTAL 0·15" from Levels 1,2,3 & 4						* THEORETICAL						Av. EXPERIMENTAL					
	A.L. Levels 1, 2, 3 & 4						0·15" from Levels 1,2,3 & 4																							
	ε_{11}	ε_{12}	ε_{33}	ε_{34}	ε_{21}	ε_{24}	ε'_{11}	ε'_{12}	ε'_{33}	ε'_{34}	ε'_{21}	ε'_{24}	ε'_{11}	ε'_{12}	ε'_{33}	ε'_{34}	ε'_{21} •	ε'_{24} •	σ'_{11}	σ'_{12}	σ'_{33}	σ'_{34}	σ'_{21}	σ'_{24}	σ'_{11}	σ'_{12}	σ'_{33}	σ'_{34}	σ'_{21} •	σ'_{24} •
0	0	0	0	0	0	0	0	0	0	0	0	0	0	0	0	0	0	0	0	0	0	0	0	0	0	0	0	0	0	0
1651	-392	-214	219	397	-405	409	-377	-229	234	382	-390	394	-354	-201	204	333	-379	388	-652	-397	398	649	-409	413	-613	-348	346	566	-398	408
3537	-842	-413	426	855	-987	984	-805	-450	463	818	-941	947	-820	-436	447	772	-914	933	-1393	-778	787	1391	-988	995	-1418	-754	760	1311	-960	980
4716	-1127	-509	525	1142	-1406	1418	-1074	-562	578	1089	-1353	1365	-1111	-567	588	1050	-1310	1330	-1858	-972	-982	1852	-1421	1433	-1921	-981	1000	1785	-1375	1400
7074	-1704	-589	609	1724	-2536	2562	-1608	-685	705	1628	-2440	2466	-1667	-773	832	1605	-2100	2200	-2783	-1184	1198	2768	-2562	2590	-2901	-1337	1415	2732	-2205	2310
9432	-2293	-551	568	2310	-3971	3992	2144	-700	717	2161	-3822	3843	-2269	-887	989	2202	-3380	3371	-3704	-1212	1219	3673	-4013	4035	-3925	-1534	1681	3743	-3550	3540
10375	-2542	-540	530	2532	-4025	4527	-2370	-712	702	2390	-4453	4355	-2501	-899	1007	2429	-3900	3750	-4101	-1231	1193	4013	-4640	4573	-4325	-1555	1712	4129	-4095	3970
10800 (ult)	-2900	-537	505	2645	-4087	4797	-2497	-723	688	2462	-4804	4614	-2632	-903	1011	2554	-4450	4300	4319	-1252	1170	4185	-4640	4844	-4476	-1561	1718	4342	-4610	4515

• Extrapolated from experimental results

* Theoretical results are based on solutions of the generalized d.e.

Levels 1, 2, 3 & 4 are defined as in fig. 2·9

Table 4·13. Theoretical and experimental strain and stress results at mid-span of beam model (3) under four point loading

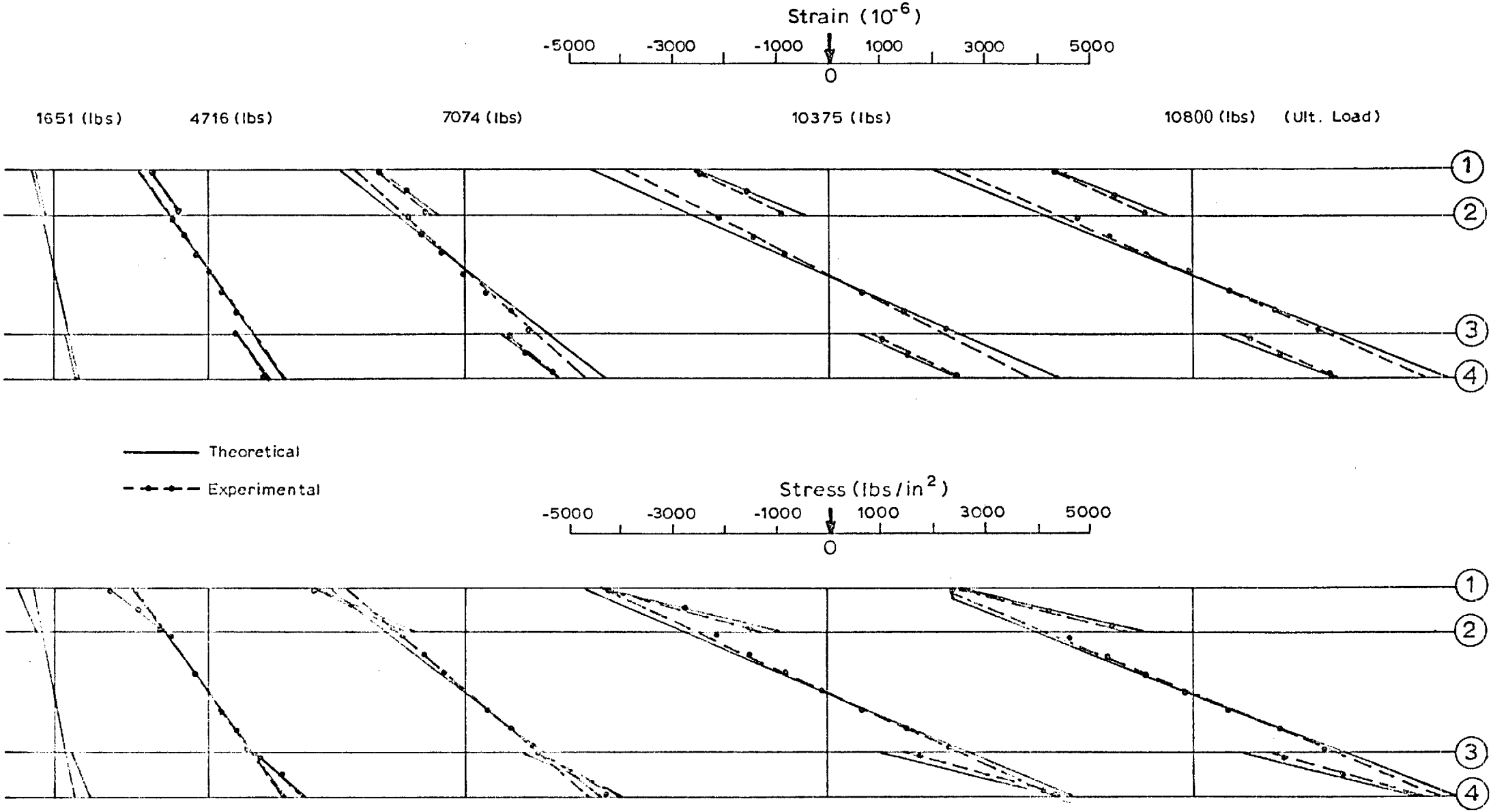


Fig. 4·15. Theoretical and experimental stress and strain distributions at mid-span of beam model (3) under four point loadin-

(a) Linear distributions of strain across depth of beam, assumed in theory (part II of this thesis), is confirmed by experimental results at all load levels.

(b) At high and low load levels the strains and stresses determined theoretically and experimentally agree reasonably well with each other. e.g. at ultimate loads of both beam models the highest variation encountered between theoretical and experimental results is 15% for ϵ_{11} for beam model (4). Stresses follow the same pattern. It is worth mentioning that at low load levels, about 3393 lbs, the theoretical strains and the stresses across depths of plywood and timber of both models agree within 7% variation with the experimental results.

In beam model (3) the ultimate theoretical result, refer to fig.4.15, indicate that yield has started in the plywood in compression while the ultimate experimental results indicate that the plywood is still elastic. In both cases the timber in compression is still elastic, and also the timber and plywood in compression of beam model (4).

(c) It is noted that the total compressive force (C) in either of beam models (3) or (4) agree within 5% with their respective counter total tensile forces determined from the experimental stress distributions.

16.3.3 Mid span deflection

Experimental and theoretical results for mid span deflections of beam models (3) and (4) reported in tables 4.14 and 4.16 are plotted in figs. 4.16 and 4.20. For each beam, the experimental results at reported load levels, are lower than the corresponding theoretical ones. Highest variation encountered is at ultimate load of beam model (4) when the variation is about 11%.

Also in fig.4.16 the theoretical solutions for mid span deflection based on the analytical solution of section 5.7 for beam model (3) are plotted for three load levels; low, medium and high corresponding to the connector moduli chosen for these load levels in section 10.3.

16.3.4 Neutral axis web shear stress

Experimental and theoretical results for web shear stresses at neutral axis given in tables 4.14 and 4.16 are plotted in figs.4.17 and 4.21 for beam models (3) and (4). Theoretical and experimental results agree reasonably well. Variations within 7.5% are encountered in both beam models. For each beam, the experimental results, at reported load levels, are lower than the corresponding theoretical ones at any distance from end support. It is noted that for beam model (4) the experimental results at a distance equal to 3.05 inches from the end support are very low and even lower than those at a distance equal to 15.25 ins. These results might have been influenced by the presence of the end stiffener since these results were obtained from a rosette on plywood adjacent to the end stiffener. These results were not plotted.

Load level (lbs)	Total mid-span deflection (ins)		Web shear stress at x=15.25 ins lb/in^2		Top flange slip (ins)			
					*Theoretical		Experimental	
	*Theoretical	Experimental	*Theo.	Expt.	At x=9.1	At x=24.4	At x=9.1	At x=24.4
0.0	0.0	0.0	0.0	0.0	0.0	0.0	0.0	0.0
1651	.135	.133	133	98	.0029	.0021	.0018	.0014
3537	.325	.323	286	250	.0110	.0076	.0091	.0055
4716	.467	.449	382	335	.0193	.0130	.0165	.0110
7074	.819	.742	574	522	.0446	.0300	.0382	.0258
9432	1.245	1.142	769	718	.0795	.0546	.0717	.0495
10375	1.442	1.330	850	791	.0977	.0692	.0935	.0630
10800	1.552	1.442	893	832	.1086	.0781	.1030	.0700

* Theoretical results based on generalised d.e. solution

Table 4.14 Deflection, web shear and slip results of beam model (3) under four point loading

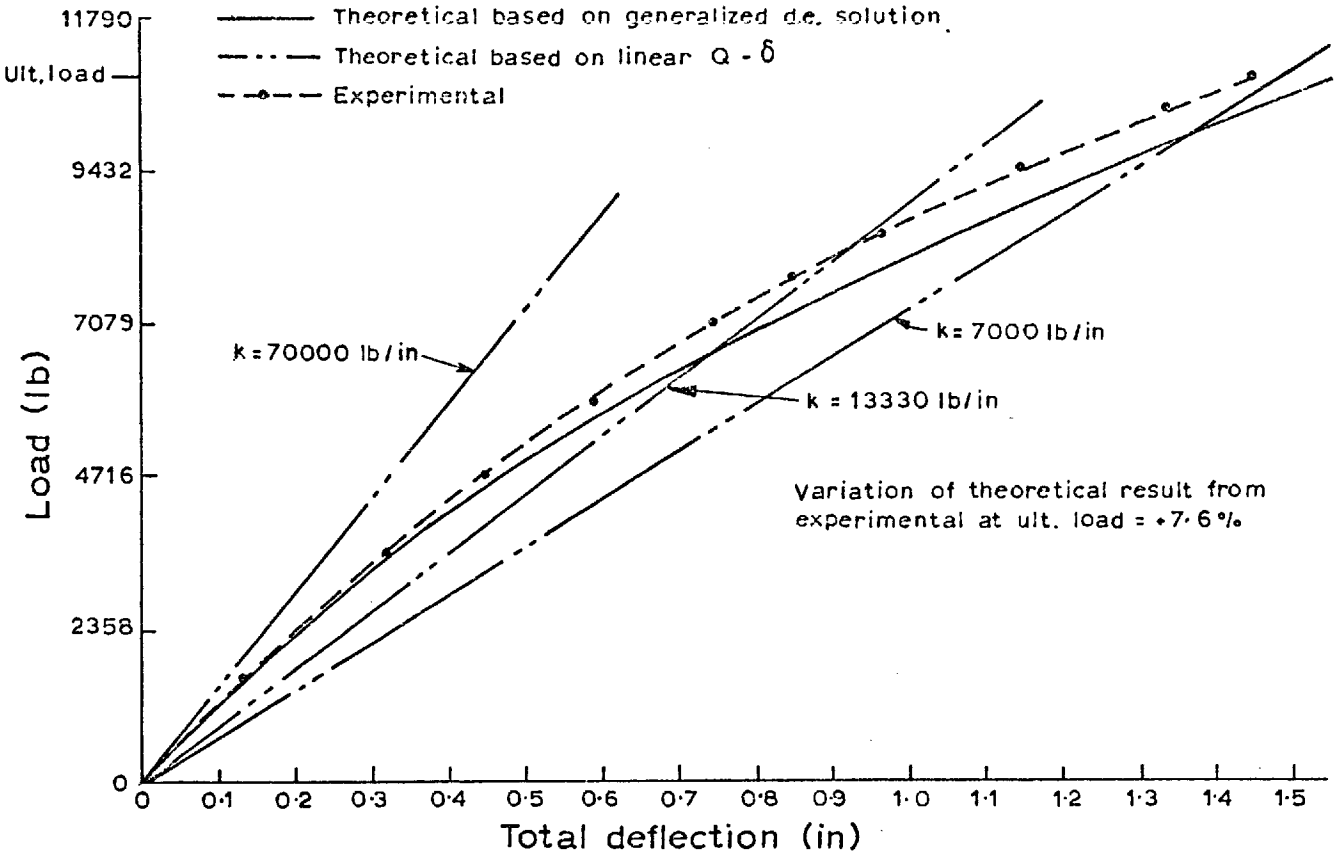


Fig. 4·16. Theoretical and experimental mid span deflection of beam model (3) under four point loading

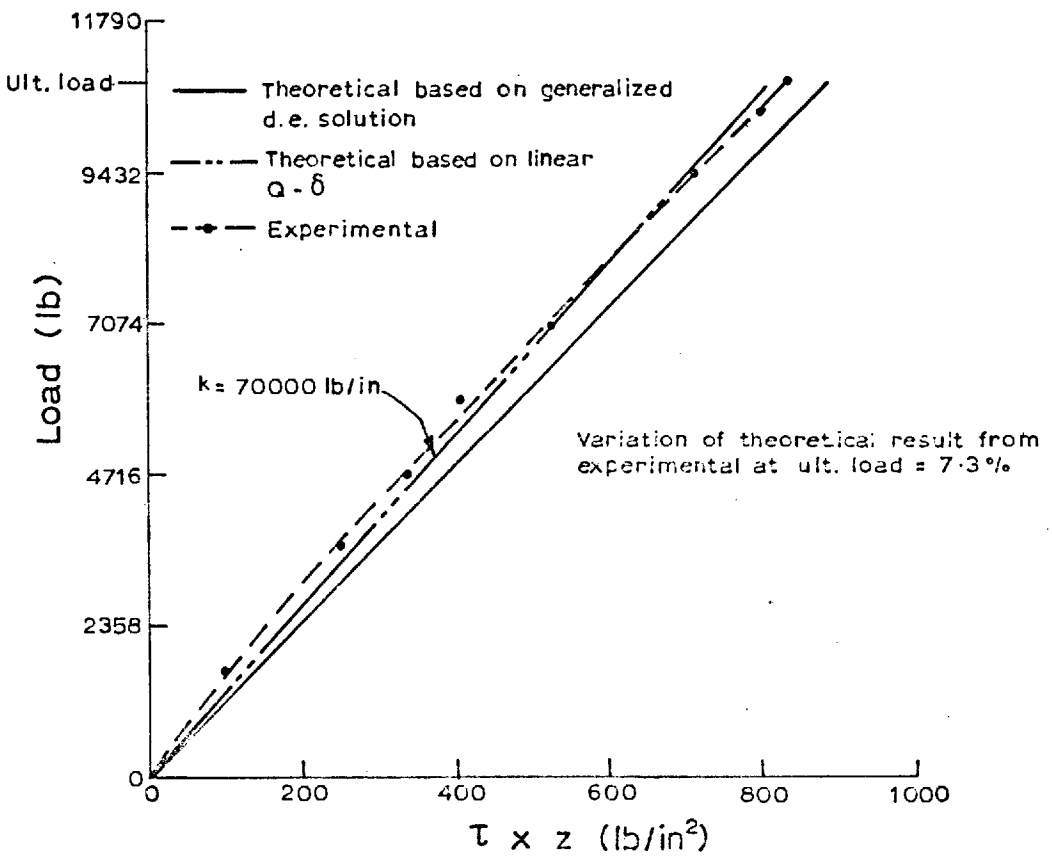


Fig. 4·17. Theoretical and experimental web shear stress at X = 15·25 in for beam model (3) under four point loading

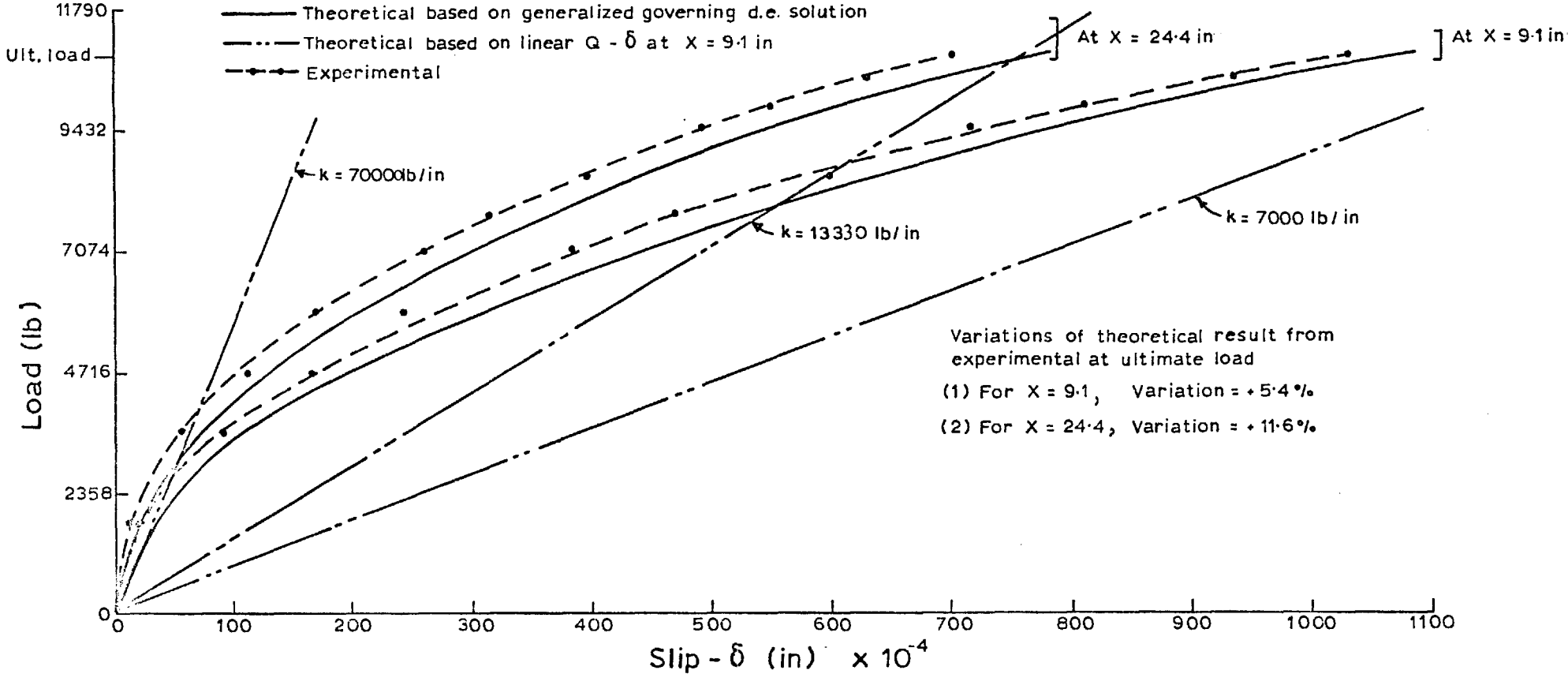


Fig. 4·18. Theoretical and experimental slip results for beam model (3) under four point loading

16.3.5 Top flange web slip

Experimental and theoretical results for top flange web slip given in tables 4.14 and 4.16 are plotted in figs.4.18 and 4.22 for beam models (3) and (4). Theoretical and experimental results agree reasonably well. Variations within 12% have been encountered in results from both models at distances of 9.1 and 24.4 inches for beam models (3) and 15.25 and 39.65 inches for beam model (4) from the end support. Low experimental results have been encountered in results near the end support of beam model (4), at x = 3.05 ins. This is attributed to the effect of the end stiffener which was ignored in the theoretical solutions. For each beam, the experimental results, at reported load levels, are lower than the corresponding theoretical ones at any distance from the end support.

Also in fig.4.18 the theoretical solutions of flange web slips at x = 9.1 inches based on the analytical solution of section 5.7 for beam model (3) are plotted for three load levels; low, medium and high corresponding to the chosen connector moduli for these load levels given in section 10.3.

16.3.6 Corollary

It should be noted that in all the theoretical and experimental results, reported above for deflection, web shear stress and slip of beam models (3) and (4), all the experimental results are lower than their corresponding theoretical results. This indicates that the actual beams tested are stiffer than the theoretical models. This may be explained in the same way as discussed in section 16.2.1.

Load Level (lb)	STRAIN (10^{-6})																		STRESS (lb/in^2)											
	*THEORETICAL												Av. EXPERIMENTAL						*THEORETICAL						Av. EXPERIMENTAL					
	At levels 1, 2, 3 & 4						0·15 in from levels 1,2,3&4						0·15 in from levels 1,2,3&4						0·15 in from levels 1,2,3&4						0·15 in from levels 1,2,3&4					
	ε_{11}	ε_{12}	ε_{13}	ε_{14}	ε_{21}	ε_{24}	ε'_{11}	ε'_{12}	ε'_{13}	ε'_{14}	ε'_{21}	ε'_{24}	ε'_{11}	ε'_{12}	ε'_{13}	ε'_{14}	$\dot{\varepsilon}'_{21}$	$\dot{\varepsilon}'_{24}$	σ'_{11}	σ'_{12}	σ'_{13}	σ'_{14}	σ'_{21}	σ'_{24}	σ'_{11}	σ'_{12}	σ'_{13}	σ'_{14}	$\dot{\sigma}'_{21}$	$\dot{\sigma}'_{24}$
0	0	0	0	0	0	0	0	0	0	0	0	0	0	0	0	0	0	0	0	0	0	0	0	0	0	0	0	0	0	0
1697	-453	-239	278	492	-474	505	-435	-257	296	474	-456	487	-386	-237	252	389	-370	375	-739	-438	453	725	-478	511	-656	-402	385	596	-389	394
3393	-927	-410	488	1005	-1150	1214	-883	-454	532	961	-1106	1170	-820	-491	512	823	-990	1050	-1501	-772	814	1470	-1161	1228	-1395	-834	783	1260	-1040	1103
5090	-1445	-447	565	1563	-2232	2330	-1360	-533	651	1478	-2147	2245	-1268	-721	733	1269	-1410	-1420	-2311	-905	995	2261	-2254	2357	-2155	-1225	1121	1942	2397	2414
6786	-2027	-392	498	2133	-3675	3301	-1867	-532	638	1993	-3535	3661	-1742	-881	860	1746	-3105	3210	-3208	-905	976	3049	-3712	3844	-2961	-1499	1316	2671	-3260	3371
7465	-2266	-399	476	2343	-4108	4423	-2106	-553	636	2183	-3949	4268	-1971	-899	836	1970	-3450	3800	-3580	-950	973	3340	-4145	4481	-3351	-1529	1279	3015	-3623	3990
7800	-	-	-	-	-	-	-	-	-	-	-	-	-2080	-992	805	2083	-3700	4050	-	-	-	-	-	-	-3552	-1517	1231	3187	-3885	4253

• Extrapolated from experimental results

* Theoretical results are based on solutions of the generalized d. e.

Levels 1, 2, 3 & 4 are as defined in fig. 2·9

Table 4·15. Theoretical and experimental strain and stress results at mid-span of beam model (4) under four point loading

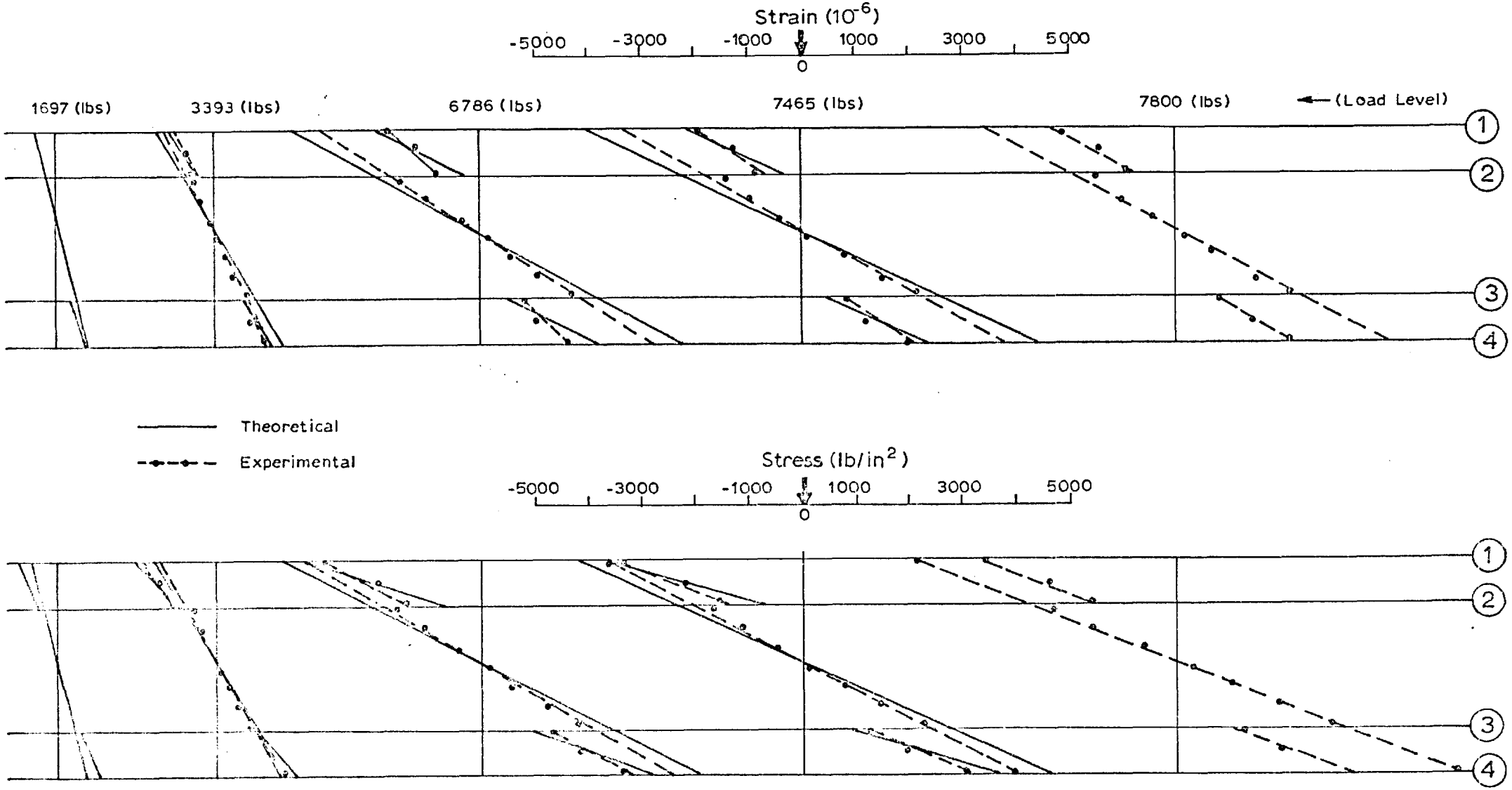


Fig. 4·19. Theoretical and experimental stress and strain distribution at mid span of beam model (4) under four point loading

Load level (lbs)	Total mid span deflection (ins)		Web shear stress (lb/in^2)				Top flange slip (ins)					
			*Theoretical		Experimental		*Theoretical			Experimental		
	*Theo.	Expt.	x=3.05	x=21.35	x=3.05	x=21.65	At x=3.05	x=15.25	x=39.65	x=3.05	x=15.25	x=39.65
0.0	0	0	0	0	0	0	0	0	0	0	0	0
1697	.199	.179	266	263	172	211	.0054	.0053	.0004	.0032	.0043	.0007
3393	.474	.452	528	523	358	452	.0208	.0200	.0019	.0160	.0180	.0017
5090	.864	.831	784	779	599	715	.0503	.0481	.0054	.0350	.0420	.0050
6786	1.357	1.262	1052	1045	843	1011	.0957	.0919	.0113	.0700	.0790	.0100
7465	1.581	1.482	1169	1163	942	1123	.1201	.1158	.0149	.0805	.1010	.0134
7800	-	1.550	-	-	1008	1218	-	-	-	.0920	.1150	.0154

* Theoretical results are based on generalised d.e. solution

Table 4.16 Deflection web shear and slip results of beam model (4) under four point loading

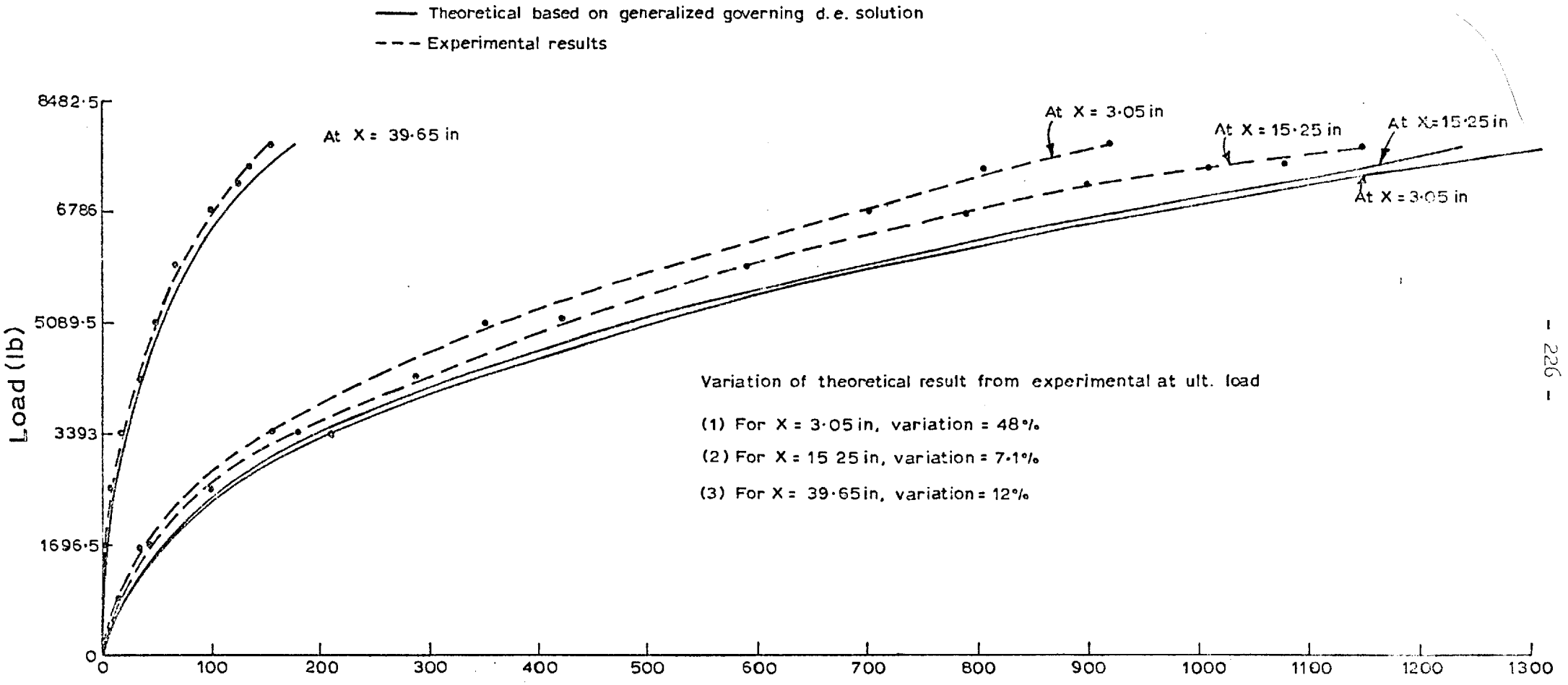


Fig. 4·22. Theoretical and experimental slip results for beam model (4) under four point loading

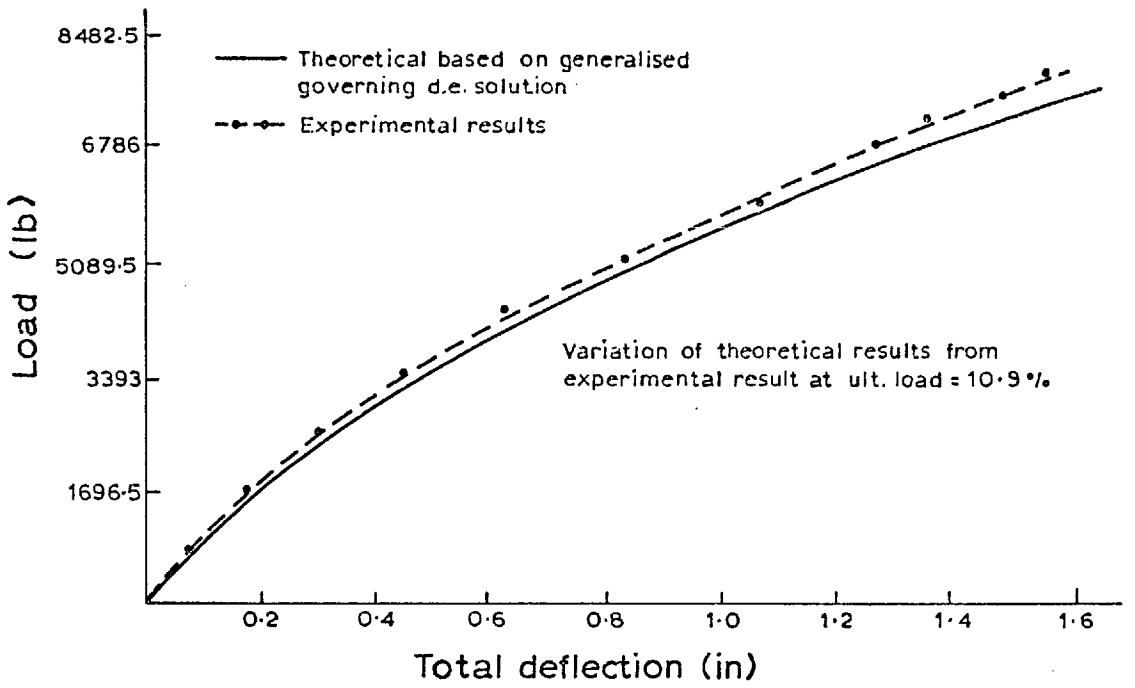


Fig. 4·20. Theoretical and experimental mid span deflection of beam model (4) under four point loading

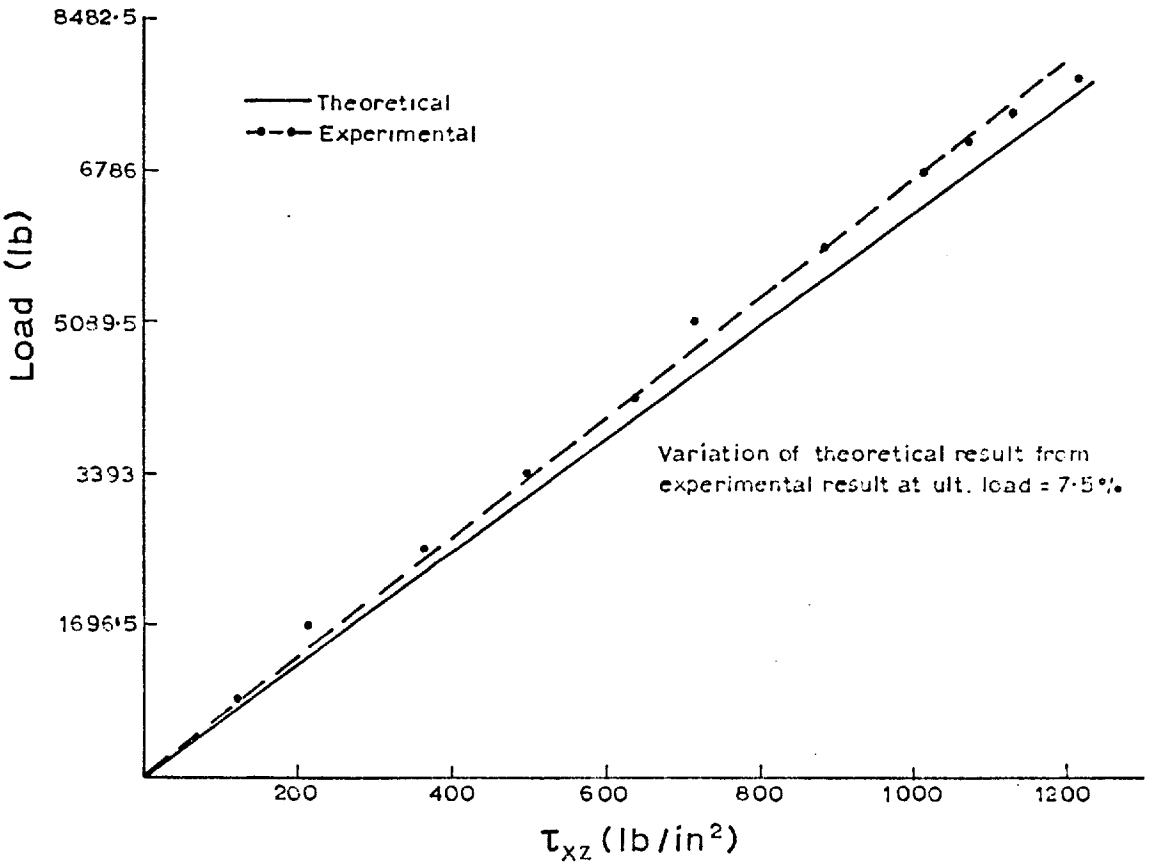


Fig. 4·21. Theoretical and experimental web shear stress results at X = 21·35 in for beam model (4) under four point loading

PART V

SUMMARY, CONCLUSIONS AND FUTURE WORK

Part V

Summary, Conclusions and Future Work

Chapter 17 Summary

17.1 Scope

The ultimate load behaviour of rigid and semi-rigid plywood web I-beams has been investigated theoretically and experimentally.

The theoretical investigation presents the cases of rigid and semi-rigid plywood web I-beams seprately.

17.2 Theoretical

17.2.1 Rigid plywood web I-beams

The theoretical solutions presented to describe the behaviour of a rigid plywood web I-beam are based on the engineer simple bending theory and also on the assumption that complete interaction between the flanges and web occur, i.e. no strain difference. Solutions have been given to find the stress distributions across the depth of a rigid plywood-web I-beam at different points along its span. To find the stress distributions, the stress-strain relationship ($\sigma - \varepsilon$) for timber and plywood in tnesion and compression are defined. A linear $\sigma - \varepsilon$ relationship has been adopted for timber and plywood in tension. Also two $\sigma - \varepsilon$ relationships have been considered for timber and plywood in compression: a linear one and an idealised non-linear one. A numerical procedure based on linear Newton-Raphson method has been employed to find the stress distributions across the depth of the beam at any point along its span when the generalised idealised non-linear $\sigma - \varepsilon$ relationships are adopted for timber and plywood in compression. Bending deflections have also been found using two methods depending on the cases when a linear or a non-linear $\sigma - \varepsilon$ relationship has been adopted for timber and plywood in compression. While for analysis based on linear $\sigma - \varepsilon$ relationships analytical solutions are given for bending deflection, a numerical procedure based on finite

differences has been employed to find bending deflection at any point along the span of the beam when the analysis is based on idealised non-linear $\sigma - \varepsilon$ relationships. Webs have been assumed to be thick enough to prevent them from buckling and analytical solutions have been given for web shear stress at the neutral axis based on linear $\sigma - \varepsilon$ relationship for timber and plywood in compression. Also analytical solutions, based on linear $\sigma - \varepsilon$ relationships for timber and plywood in compression, have been given for flange web shear stresses at the interfaces of the top flange and bottom flanges. Based on the concepts mentioned above, a computer program has been written to find the bending stress distributions at different points along the beam span, bending and shear deflections, web shear stresses at the neutral axis and flange web shear stresses at the interfaces of the top and bottom flanges.

17.2.2 Semi-rigid plywood web I-beams

The theoretical solutions presented to describe the behaviour of semi-rigid plywood web I-beams, are based onthe engineer's simple bending theory and also on the assumption that incomplete interaction between flanges and web will occur. Hence strain differences between flanges and web will take place and it is assumed that these occur at the centre of gravity of the joints. Hence the joints $Q - \delta$ relationships are defined. A linear and a non-linear $Q - \delta$ relationships are considered separately. The non-linear relationship is based on Mack's equation (1966). As in the case of the rigid beam analysis, $\sigma - \varepsilon$ relationships for timber and plywood in tension and compression are defined to find the stress distributions

across the depth of the beam at any point along its span. Whereas a linear $\sigma - \varepsilon$ relationship is defined for timber and plywood in tension, linear and also idealised non-linear $\sigma - \varepsilon$ relationships are defined for timber and plywood in compression for each of the linear and non-linear $Q - \delta$ relationships. Hence four cases are considered:

(a) Linear $Q - \delta$: (i) Linear $\sigma - \varepsilon$ timber and plywood

(ii) Non-linear $\sigma - \varepsilon$ timber and plywood in compression; linear in tension

(b) Non-linear $Q - \delta$: (i) Linear $\sigma - \varepsilon$ timber and plywood

(ii) Non-linear $\sigma - \varepsilon$ timber and plywood in compression; linear in tension.

Generalised governing differential equations have been derived in terms of flange direct forces (N) and joint slip (δ) of the top and bottom flanges. Analytical solutions of these differential equations are found when the analysis is based on linear $Q - \delta$ and $\sigma - \varepsilon$ relationships. In all the other cases numerical procedures are adopted to solve the governing differential equations. The adopted numerical procedure is based on the predictor corrector method due to Hamming (1959, 1962). In the numerical procedure, values of the unknowns are guessed at one end of the beam (first boundary point) and integration then proceeds from one node to the next along the beam span using predictor corrector method until the other end (second boundary point) is reached, where the results of unknowns obtained from integration are compared with the desired given values at that boundary point. If the calculated values of the unknowns from integration at the second boundary point are different from the desired given values, then convergence towards the desired given values is obtained by finding new guesses for the unknown values at the first boundary point.

These new guesses are obtained by applying a combination of two methods. These methods are based on a direct search method and a directional search method based on the Newton Raphson method to solve simultaneous algebraic equations. After finding the correct stress distributions across the depths of the beam at various points along the span and hence curvatures, then bending deflection, flange web shear force per unit length, etc., are also found. Similar procedures are employed to find bending deflection as those mentioned above for the rigid beam.

Analytical solutions are given for web shear stress and shear deflections of a simply supported semi-rigid plywood I-beam. The solutions are based on linear $Q-\delta$ and $\sigma-\varepsilon$ relationships. The effect of slip on shear deflection has been investigated for a simply supported beam loaded with uniformly distributed load over the whole span.

Based on the above, a generalised computer program has been written to solve the generalised governing differential equations in terms of flange direct forces (N) and flange-web slips (δ) of top and bottom flanges. Also solutions for total deflections, flange web shear force per unit length and web shear stress may be found using the computer program.

17.3 Experimental

The experimental work includes the testing of four simply supported plywood-web I-beams under four point load at $\frac{1}{3}$ points of the span. Two of the beams were rigid and the other two were semi-rigid. The beams were tested up to failure and strain measurements were made across the depths of the beams at mid spans. Also deflections at mid span and at $\frac{1}{3}$ points, and shear strains at various points along the beam were made.

In the case of the semi-rigid beams also slip measurements at various points along the top flange were made. Prior to testing the beams, tests on small clear specimens of timber and plywood and also on timber to plywood joints were made to determine material properties of timber and plywood used in the beam and also the timber to plywood joint $Q - \delta$ relationships. Strain measurements using electrical resistance gauges and mechanical gauges were made on some of the tension and compression small clear specimens to determine $\sigma - \varepsilon$ relationships of timber and plywood and also to find the true gauge factors of electrical resistance gauges. Tension and compression tests were made on timber flanges prior to beam fabrication to compare their results with the results obtained from tests on small clear specimens.

Chapter 18 Conclusions and applications to design

18.1 Conclusions

Several conclusions arise from the theoretical, experimental and comparative studies made on plywood web I-beams and described in parts II, III and IV of this thesis.

It has been shown that corrections factors should be applied to electrical resistance gauges factors when they are used to measure strains in timber and plywood. Strains measured by electrical resistance gauges of the type used in this thesis are up to 12% lower than those measured by mechanical gauges. This agrees with Solvey (1952) and Youngquist (1957) who found up to 10% decrease in strain when electrical resistance gauges are used to measure strains in timber and plywood.

$\sigma - \epsilon$ results obtained from compression and tension tests on small clear specimens of timber and plywood have been satisfactorily represented by a linear idealisation for tension and a non-linear elastoplastic idealisation for compression. It has been found that it is possible to predict satisfactorily the behaviour of both a rigid and a semi-rigid plywood web I-beam by adopting these idealisations for the $\sigma - \epsilon$ relationships of timber and plywood in tension and compression when these beams are analysed theoretically.

$Q - \delta$ results obtained from compression tests on timber to plywood joints have been satisfactorily represented by Mack's equation (1966). It has been found that it is possible to predict the behaviour of a semi-rigid plywood web I-beam by adopting Mack's equation to describe the $Q - \delta$ relationship of a timber to plywood joint of a semi-rigid plywood web I-beam when this beam is analysed theoretically.

It has been shown that the results obtained for the moduli of elasticity of the timber flanges in actual sizes, when tested at low loads in tension and compression parallel to the grain prior to beams fabrication, are slightly lower than those obtained from small clear specimens.

Strain measurements across the depths of the beam models at mid-span show that the strain distribution across the depth of the beam is linear and hence validated the basic assumption that plane sections before bending remain plane after bending.

From the theoretical study on plywood I-beams the effect of joint slip between the timber flanges and the plywood web is evident and is reflected in the bending stresses and strains and deflection, etc. distributions along the beam span. In the case of rigid beams the bending stress distribution along the beam span follows the bending moment distribution, whereas in the case of the semi-rigid beams the effect of joint slip, i.e. strain difference between flanges and web, plays an important role and may force the distribution of bending stresses along the span to depart from the distribution of bending moment, and is dependent on the choice of the joint $Q - \delta$ relationship.

It has been confirmed theoretically and experimentally that the magnitudes of the bending strains and stresses at the same levels of plywood and timber are dependent on the materials $\sigma - \varepsilon$ relationships and the relative magnitude of ultimate and yield strains and stresses of timber and plywood, also on the degree of stiffness of the timber to plywood joint, i.e. $Q - \delta$ relationship, and also on the load level for a beam with fixed geometry. This has been confirmed theoretically and

experimentally from results obtained for beam models (1), (2), (3) & (4). In the case of the rigid beams it is found that the strains are the same in timber and plywood at any level across the beam depth and also at all load levels and that the timber in compression has started to yield before the plywood in compression and that compression failure of the top timber flanges has been predicted and confirmed for beam model (2). In the cases of the semi-rigid beams it is found that the magnitude of the strains and hence the stresses at any particular level across the depth of the beam varies with the load level and strength of the joint. It is found that as the load is increased the strains in plywood tend to be higher than at the same level in the timber flange and this may be understood from the shapes of the timber and plywood $\sigma - \epsilon$ relationships in compression. In the semi-rigid beams it is found that the plywood in compression has started to yield before the timber in compression and that a tension failure of the bottom plywood at $\frac{1}{3}$ span has been theoretically predicted and experimentally confirmed for both beam models (3) and (4).

While it has been shown that the effect of slip is to increase the bending deflection, it is established theoretically that the effect of slip may increase or decrease the shear deflection. Also it has been established theoretically that the effect of slip on shear deflection is small if this effect is compared with the total deflection, i.e. bending plus shear deflection, for beams with moderate flanges sizes, web thicknesses and overall depths.

While it has been shown theoretically that a totally linear analysis based on linear $Q - \delta$ and $\sigma - \varepsilon$ relationships is possible for semi-rigid beams at low and moderate load levels, it has been established that a totally non-linear analysis based on non-linear $Q - \delta$ and $\sigma - \varepsilon$ relationships is essential for semi-rigid beams at high loads near their ultimate.

Close agreement between theoretical and experimental results for strain and stress distributions, deflection, slip and shear stresses indicate that the basic assumptions on which the theoretical analysis is based and the method by which experimental strain results are converted into stresses are valid. Also it indicates the adequacy of the experimental rig.

18.2 Applications to the analysis and design of semi-rigid plywood web I-beams

In this thesis theoretical and experimental studies of semi-rigid plywood web I-beams at ultimate load proved that deflections are excessive and that they are much greater than the permissible given by CP 112 (1967). For beams of similar spans to those considered in this thesis (91.5 in), the permissible deflection is about 0.27 in. Deflections as high as 1.6 in have been recorded at ultimate load for beam model (4). In most cases the maximum permissible deflection may limit the design load of a semi-rigid plywood web I-beam and may be considered as the limit state of that beam. Other limit states, e.g. bending stresses and web shear stresses, are checked for.

In cases where permissible deflection is the limit state of the beam design, then a linear analysis based on linear $Q - \delta$ and $\sigma - \varepsilon$ relationship

for timber and plywood in tension and compression may produce solutions accurate enough for design purposes, since the beam may be considered at low or moderate load level. For a more refined analysis, a non-linear $Q - \delta$ with linear $\sigma - \varepsilon$ relationships should be considered.

In other cases where high deflections may be tolerated, or beams precambered, then the analysis may be based on the ultimate load concept when the analysis should be based on non-linear $Q - \delta$ and $\sigma - \varepsilon$ relationships for timber and plywood in compression and also a linear $\sigma - \varepsilon$ for timber and plywood in tension.

Chapter 19 Suggestions for future work

The following suggestions, have not been considered in this thesis and their investigation in the future will complete the picture of ultimate load behaviour of rigid and semi-rigid plywood web I-beams.

(1) Distribution of shear stresses across the depth of plywood in a plywood web I-beam at ultimate load.

(2) Buckling of plywood webs in plywood I-beams and the lateral stability of the whole section at ultimate load.

(3) Shear deflection of semi-rigid plywood web I-beams at ultimate load based on non-linear $\sigma - \varepsilon$ relationships for timber and plywood in compression and also on non-linear $Q - \delta$ relationship for a timber to plywood nailed joint.

BIBLIOGRAPHY

Amana, E.J. (1967). Applications of orthotropic plate theory to stiffened plywood plates. Ph.D. thesis. London.

Baumann, R. (1922). Die bisherigen Ergebnisse der Holzprüfungen in der Materialprüfungsanstalt an der Tech. Hochschule Stuttgart, Forsch. Gebiete Ingenieurw H231. Berlin.

Becket, R. and Hurt, J. (1967). Numerical calculations and algorithms. McGraw Hill. New York.

Beghtel, S.C. and Norris, C.B. (1959). The strength of wood beams of rectangular cross section as affected by span-depth ratio. FPL rep. no. 1910.

Booth, L.G. (1969). On the analysis of plywood I-beams. Unpublished work.

Booth, L.G. (1969). Some problems in the use of force-displacement equations of mechanical timber fasteners. Paper presented at meeting of structural utilization group, IUFRO Section 41. London.

Booth, L.G. (1974). The effect of flange-web joint displacement on the design of plywood-web I-beams. JRL Institute of Wood Science. (In press).

B S I (1957). BS 373. Methods of testing small clear specimens of timber. London.

B S I (1969). BS4512. Methods of testing clear specimens of plywood. London.

B S I (1967). CP112. The structural use of timber. London.

Comben, A.J. (1957). The effect of depth on the strength properties of timber beams. FPR spe. rep. no.12. HMSO. London.

Council of Forest Industries of British Columbia (1958). Fir plywood-web beam design. Vancouver.

Hald, A. (1952). Statistical theory with engineering applications. John Wiley & Sons, Inc. New York. Chapman and Hall, Ltd., London.

Hamming, R.W. (1959). Stable predictor corrector methods for ordinary differential equations. JRL of Assoc. for computing machinery, Vol.6.

Hamming, R.W. (1962). Numerical methods for scientists and engineers. McGraw Hill. New York.

Kollman, F.F.P. and Cote, W.A. (1968). Principles of wood science and technology. Vol.I. Springer-Verlag. Berlin. Heidelberg.

Lewis, W.C. and Dawley, E.R. (1943). Supplement to design of plywood webs in box beams. FPL rep. no. 1318A. Madison.

Lewis, W.C., Heebink, T.B., Cottingham, W.S. and Dawley, E.R. (1960). Supplement to design of plywood webs in box beams. FPL rep. no. 1318B. Madison.

Lewis, W.C., Heebink, T.B., Cottingham, W.S. and Dawley, E.R. (1960). Supplement to design of plywood webs in box beams. FPL rep.no. 1318C. Madison.

Lewis, W.C., Heebink, T.B. and Cottingham, W.S. (1959). Supplement to design of plywood webs in box beams. FPL rep. no. 1318D. Madison.

Lewis, W.C., Heebink, T.B. and Cottingham, W.S. (1959). Supplement to design of plywood webs in box beams. FPL rep.no.1318E. Madison.

Mack, J.J. (1966). The strength and stiffness of nailed joints under short duration loading. Div. of FP Tech. paper no.40. CSIRO. Australia.

Milne, W.E. (1953). Numerical solutions of differential equations. John Wiley and sons, Inc. New York.

Morris, E.N. (1968). The rotational rigidity of nailed joints with plywood gussets subjected to short term loading. TRADA res. rep. E/RR/32. High Wycombe, Bucks.

Nadai, A. (1950). Theory of flow and fracture of solids. Vol.I. McGraw Hill. New York.

Newmark, N.M., Siess, C.P. and Viest, I.M. (1951). Tests and analysis of composite beams with incomplete interaction. Proc. of the Soc. of stress analysis, Vol.9, No.1.

Ramos, A.N. (1961). Stress-strain distribution in Douglas. Fir beams within the plastic range. FPL rep. no.2231. Madison.

Smith, J.O. and Sidebottom, O.M. (1965). Inelastic behaviour of load carrying members. John Wiley and Sons, Inc. New York.

Solvey, J. and Blecher, G.L. (1952). Application of electrical resistance strain gauges on strain measurements in plywood faces of sandwich panels. Struc. and Materials, note 198. Aero. Res. Lab. Melbourne, Australia.

Stieda, C.K.A. (1967). A shear stiffness factor for plywood box beams. FPL information rep. VP-X-31. Vancouver.

Suenson, E. (1941). Die Lage der Nullinie in gebogenen Holzbalken. Holz als Roh und Werkstoff 4.

Vermeyden, P. (1968). Test results of three nailed timber box beams with plywood webs - span 7 and 9 metres. Stevin-Laboratorium, rep. no. 4-68-1. Delft, Holland.

Withey, O.M. (1943). Design of plywood webs in box beams. FPL rep. no. 1318. Madison.

Yam, L.C.P. and Chapman, J.C. (1968). The inelastic behaviour of simply supported composite beams of steel and concrete. Proc. of Institute of Civ. Engrs., Vol.41.

Youngquist, W.G. (1957). Performance of bonded wire strain gauges on wood. FPL rep. 2087. Madison.

APPENDIX

Flow Charts for Computer Programs'

Symbols

NSET	Number of data sets
IW	Number of loads to be considered
ISP	Number of spans to be considered
ISOL	Type of $\sigma - \varepsilon$ relationship to be considered
ISOL = 1,	analysis is based on linear $\sigma - \varepsilon$
ISOL = 2,	analysis is based on non linear $\sigma - \varepsilon$
ICASE	Type of $Q - \delta$ relationship to be considered
ICASE = 1,	analysis is based on linear $Q - \delta$
ICASE = 2,	analysis is based on Mack's equation for $Q-\delta$ relationship
ξ	Desired accuaracies to which solutions are iterated
η	A parameter to obtain an initial guess for first derivatives such that the Newton Raphson method may be applied.

Subroutines

IGUESS — Is a subroutine based on analytical solutions of generalised governing differential equations to find initial guesses of slips at first boundary point, e.g. using equations 2.65 and 2.66 for a symmetrical simply supported beam under four point loading at $\frac{1}{3}$ span and noting that $\delta = \frac{q\ s}{k}$, upper bound slips at low loads may be guessed by choosing k slightly stiffer than the actual and vice versa for lower bound slips

BENDID — Is a subroutine based on finite difference method given in section 4.3.3 to find bending deflection

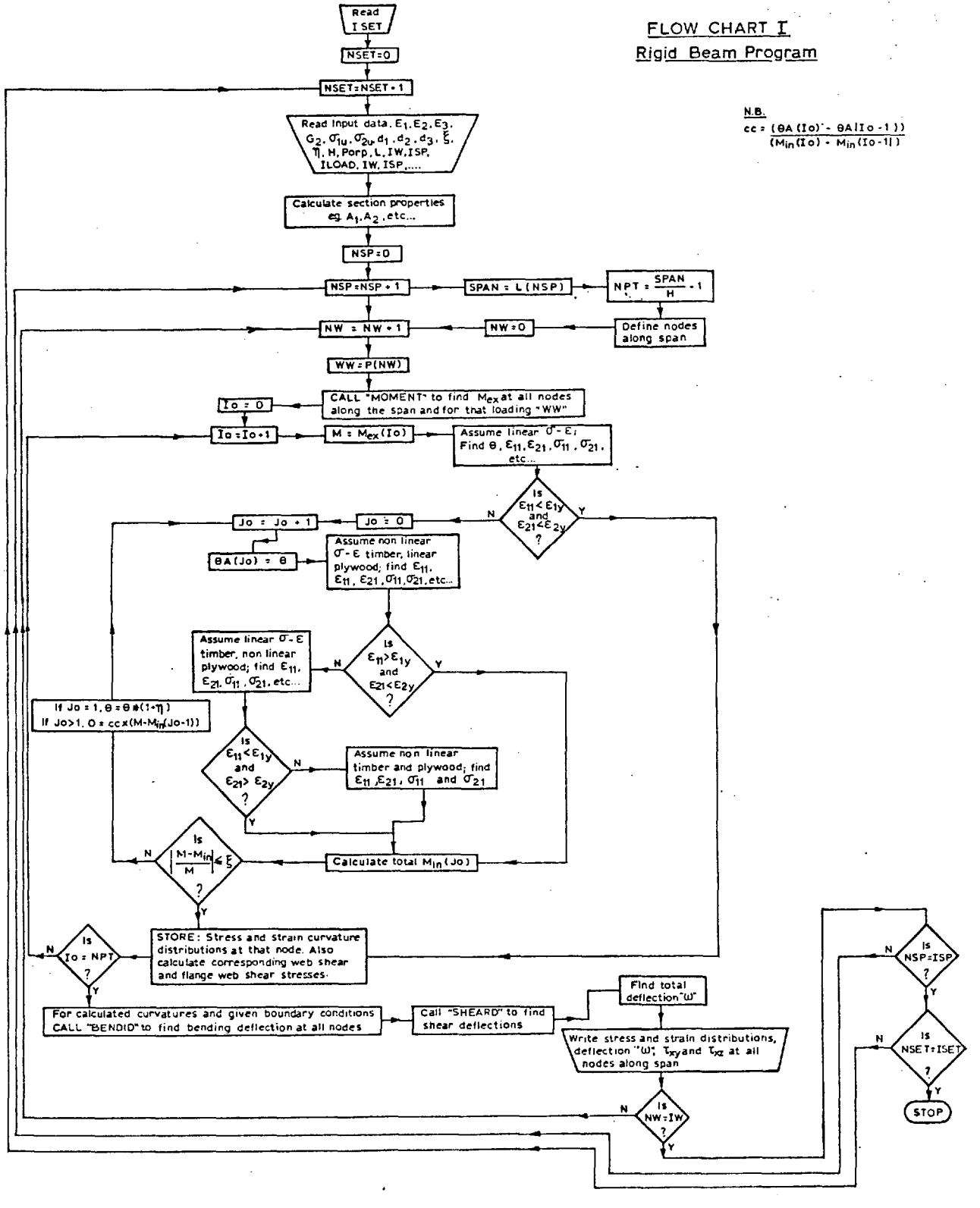
SHEARD — Is a subroutine based on equations 2.108 and 2.114 to find shear deflection of a simply supported beam at mid span of a plywood web I-beam under uniformly distributed load and four point loading

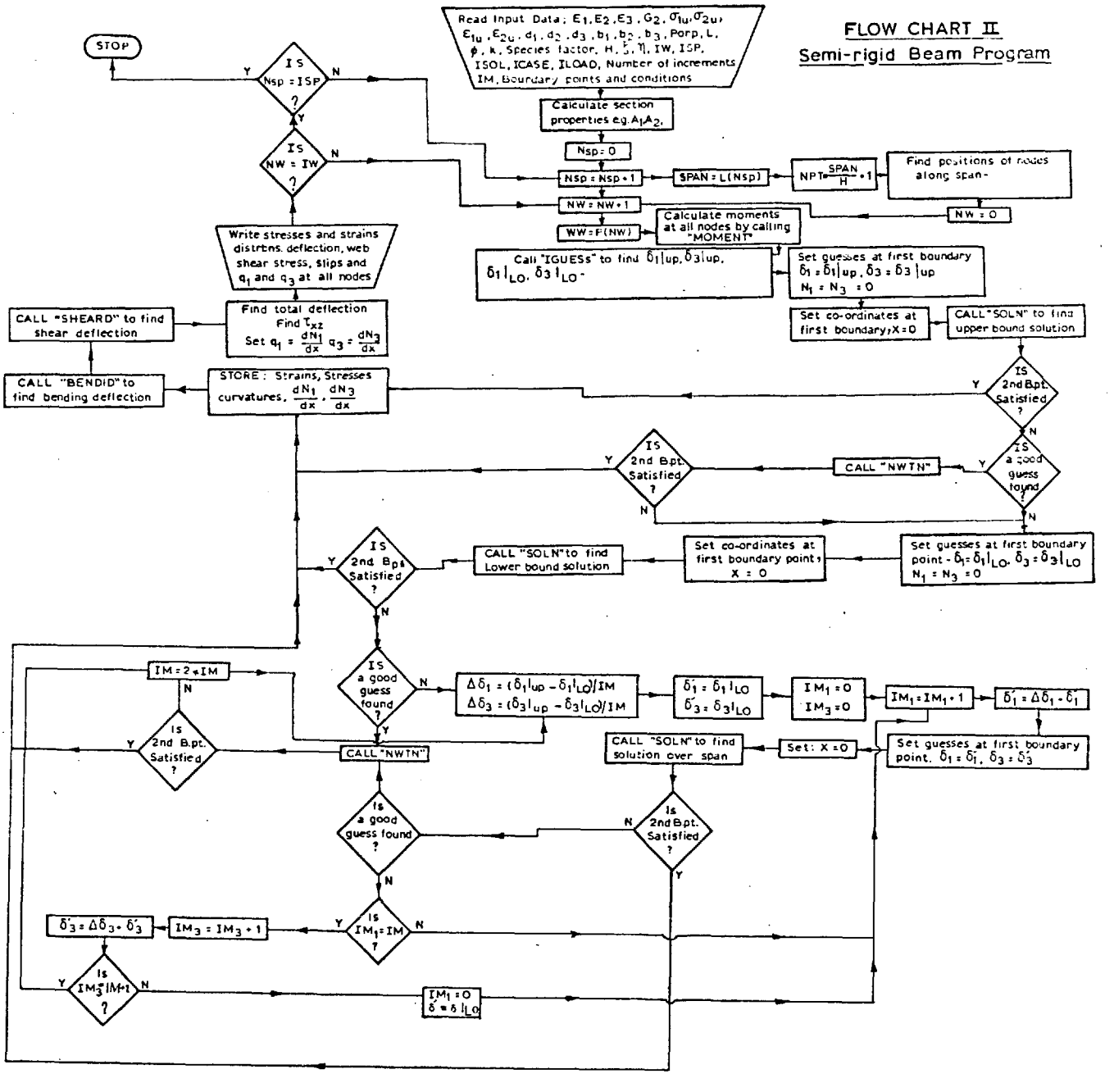
DFEQS — Is a subroutine based on predictor corrector method described in section 6.2 to integrate from one node to the next along the beam span. It is worth mentioning that DFEQS is called at each node to predict the solution at the next node and then correcting that solution as outlined in section 6.2.2

MOMENT — Is a subroutine to calculate the bending moment and shear force at each node along the beam span for two loading cases, mainly: a four point loading and also a uniformly distributed load over the whole span

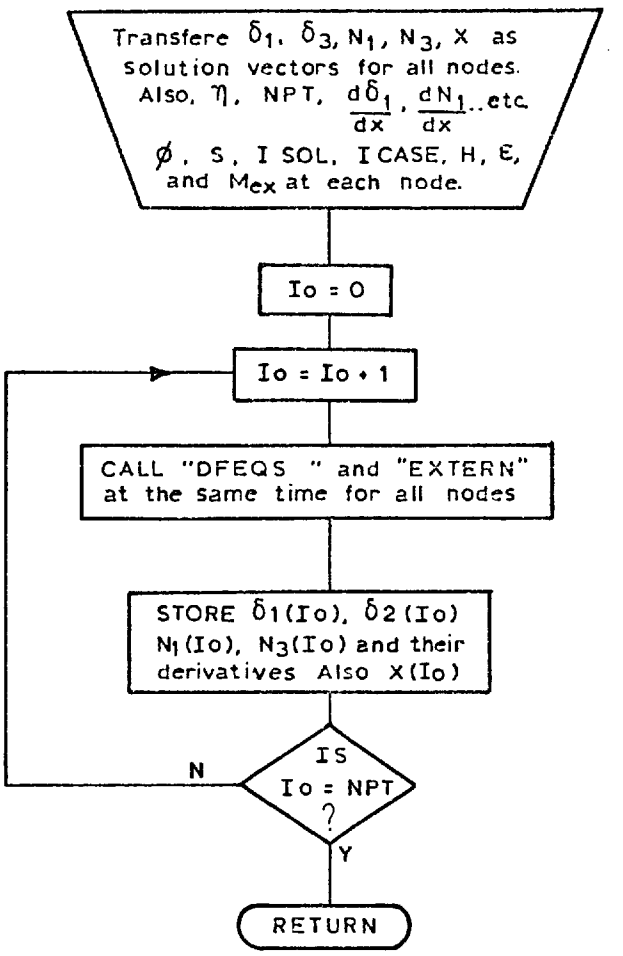
Other subroutines are described in flow charts given later in this appendix.

The same notation adopted earlier in the thesis is also adopted in the flow charts described later in this appendix.

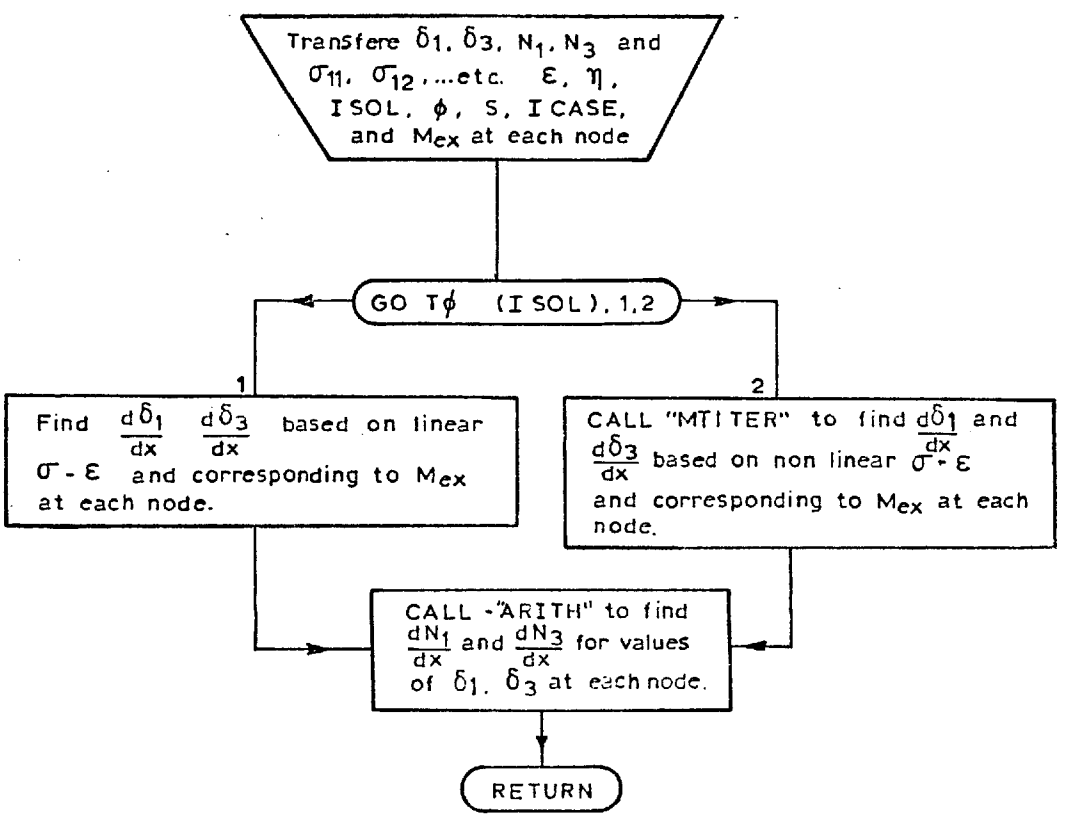

FLOW CHART I
Rigid Beam Program
N.B.
cc = (θA(Io) - θA(Io-1)) / (Min(Io) - Min(Io-1))
Read ISET
NSET=0
NSET=NSET+1
Read Input data. E1, E2, E3, G2, σ1u, σ2u, d1, d2, d3, ξ, η, H, Porp, L, IW, ISP, ILOAD, IW, ISP,.....
Calculate section properties eg. A1, A2, etc...
NSP=0
NSP=NSP+1
SPAN = L(NSP)
NPT = SPAN/H + 1
NW = NW + 1
NW=0
Define nodes along span
WW=P(NW)
CALL "MOMENT" to find Mex at all nodes along the span and for that loading "WW"
Io = 0
Io=Io+1
M = Mex(Io)
Assume linear σ-ε; Find θ, ε11, ε21, σ11, σ21, etc...
Is ε11<ε1y and ε21<ε2y ?
N
Y
Jo = Jo + 1
Jo = 0
θA(Jo) = θ
Assume non linear σ-ε timber, linear plywood; find ε11, ε21, σ11, σ21, etc...
Assume linear σ-ε timber, non linear plywood; find ε11, ε21, σ11, σ21, etc...
Is ε11>ε1y and ε21<ε2y ?
If Jo = 1, θ = θ*(1+η)
If Jo>1, θ = cc*(M-Min(Jo-1))
Is ε11<ε1y and ε21>ε2y ?
Assume non linear timber and plywood; find ε11, ε21, σ11 and σ21
Is |(M-Min)/M| ≤ ξ ?
Calculate total Min(Jo)
Is Io = NPT ?
STORE: Stress and strain curvature distributions at that node. Also calculate corresponding web shear and flange web shear stresses.
For calculated curvatures and given boundary conditions CALL "BENDID" to find bending deflection at all nodes
Call "SHEARD" to find shear deflections
Find total deflection "ω"
Write stress and strain distributions, deflection "ω", τxy and τxz at all nodes along span
Is NW=IW ?
Is NSP=ISP ?
Is NSET=ISET ?
STOP


FLOW CHART II
Semi-rigid Beam Program
STOP
Read Input Data; E1, E2, E3, G2, σ1u, σ2u, ε1u, ε2u, d1, d2, d3, b1, b2, b3, Porp, L, φ, k, Species factor, H, ξ, η, IW, ISP, ISOL, ICASE, ILOAD, Number of increments IM, Boundary points and conditions
Calculate section properties eg. A1, A2,
Nsp = 0
Nsp = Nsp + 1
SPAN = L(Nsp)
NPT = SPAN/H + 1
Find positions of nodes along span
NW = 0
NW = NW + 1
WW = F(NW)
Calculate moments at all nodes by calling "MOMENT"
Call "IGUESS" to find δ1|up, δ3|up, δ1|LO, δ3|LO
Set guesses at first boundary δ1 = δ1|up, δ3 = δ3|up N1 = N3 = 0
Set co-ordinates at first boundary, X = 0
CALL "SOLN" to find upper bound solution
IS 2nd Bpt. Satisfied ?
IS a good guess found ?
CALL "NWTN"
IS 2nd Bpt. Satisfied ?
Set guesses at first boundary point - δ1 = δ1|LO, δ3 = δ3|LO N1 = N3 = 0
Set co-ordinates at first boundary point X = 0
CALL "SOLN" to find Lower bound solution
IS 2nd Bpt Satisfied ?
IS a good guess found ?
Δδ1 = (δ1|up − δ1|LO)/IM
Δδ3 = (δ3|up − δ3|LO)/IM
δ'1 = δ1|LO
δ'3 = δ3|LO
IM1 = 0
IM3 = 0
IM1 = IM1 + 1
δ'1 = Δδ1 - δ'1
Set guesses at first boundary point. δ1 = δ'1, δ3 = δ'3
Set: X = 0
CALL "SOLN" to find solution over span
Is 2nd Bpt. Satisfied ?
Is a good guess found ?
IM = 2 * IM
Is 2nd Bpt. Satisfied ?
CALL "NWTN"
IS IM1 = IM ?
δ'3 = Δδ3 - δ'3
IM3 = IM3 + 1
Is IM3 = IM+1 ?
IM1 = 0
δ = δ1|LO
Write stresses and strains distrtns. deflection, web shear stress, slips and q1 and q3 at all nodes
Find total deflection
Find τxz
Set q1 = dN1/dx q3 = dN3/dx
CALL "SHEARD" to find shear deflection
CALL "BENDID" to find bending deflection
STORE : Strains, Stresses curvatures, dN1/dx, dN3/dx
IS Nsp = ISP ?
IS NW = IW ?

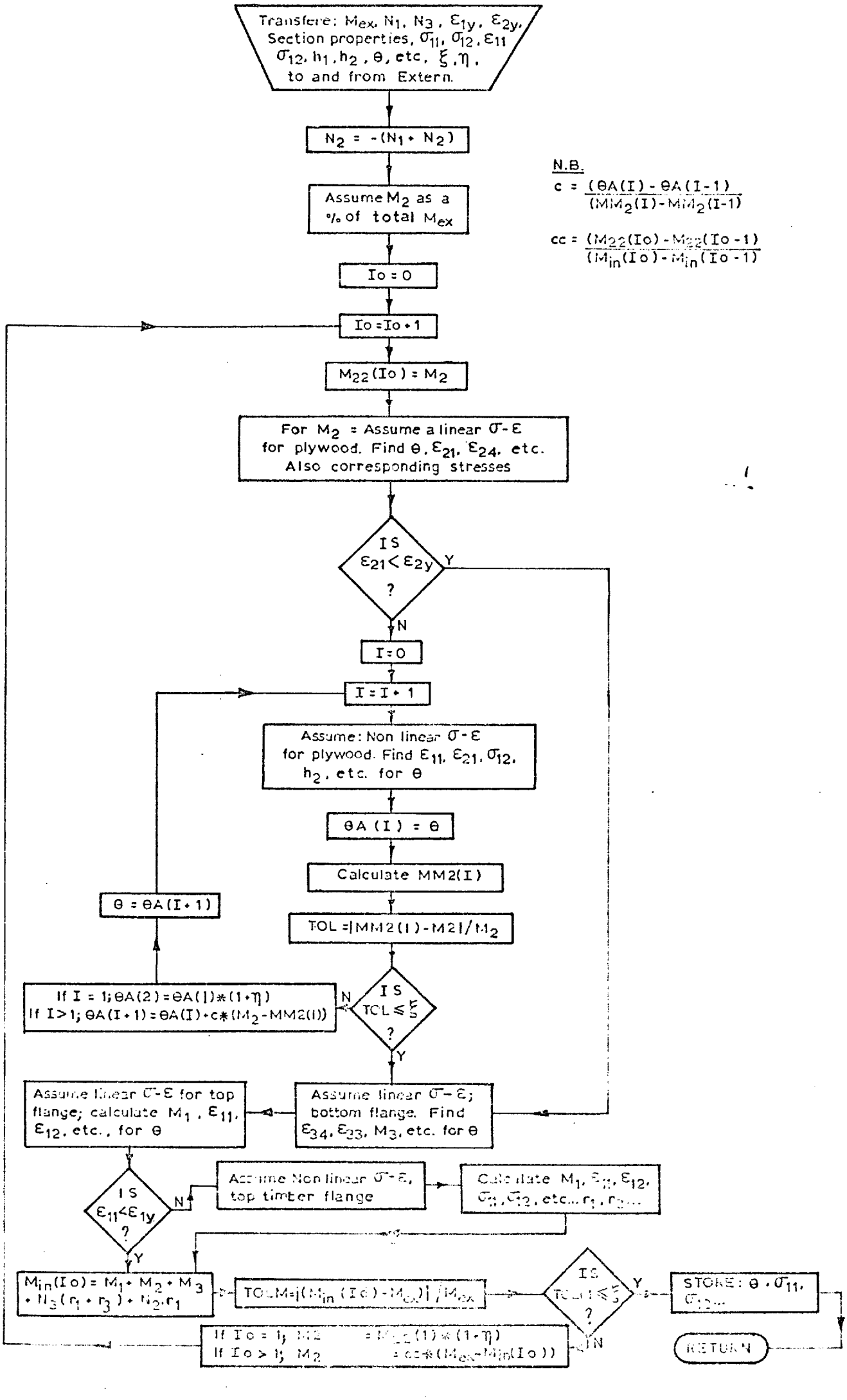
Subroutine "SOLN"



Subroutine "EXTERN"



Subroutine "MTITER"

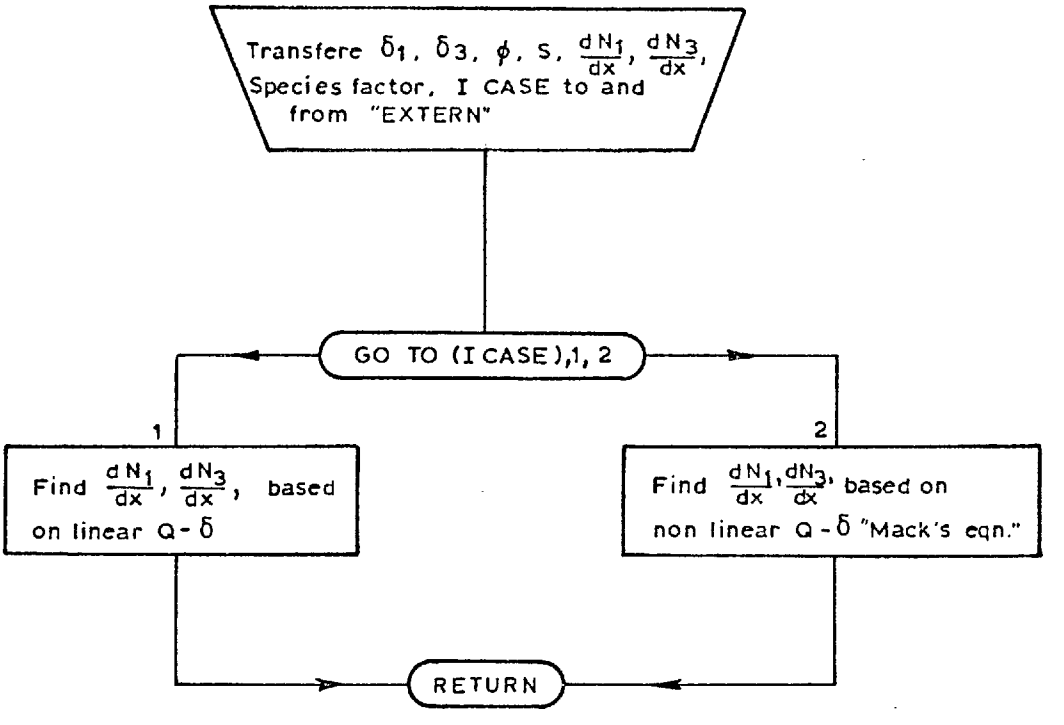


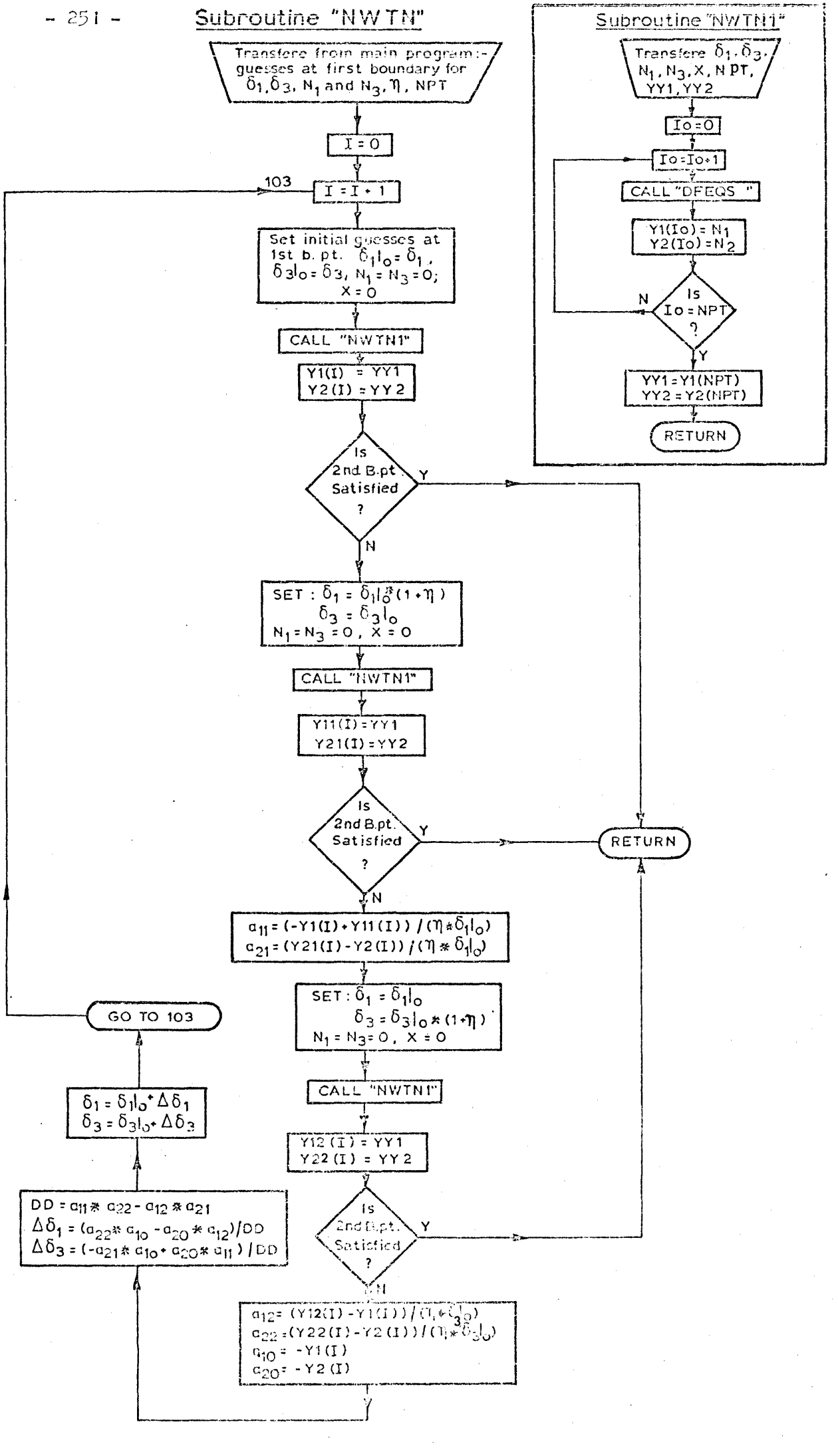
N.B.

$$c = \frac{(\theta A(I) - \theta A(I-1)}{(MM_2(I) - MM_2(I-1)}$$

$$cc = \frac{(M_{22}(Io) - M_{22}(Io-1)}{(M_{in}(Io) - M_{in}(Io-1)}$$

Subroutine "ARITH"




Subroutine "NWTN"
Transfere from main program:- guesses at first boundary for δ_1, δ_3, N_1 and N_3, η, NPT
I = 0
103
I = I + 1
Set initial guesses at 1st b. pt. $\delta_1|_o = \delta_1$, $\delta_3|_o = \delta_3$, $N_1 = N_3 = 0$; X = 0
CALL "NWTN1"
Y1(I) = YY1
Y2(I) = YY2
Is 2nd B.pt. Satisfied ?
Y
N
SET : $\delta_1 = \delta_1|_o^*(1+\eta)$
$\delta_3 = \delta_3|_o$
$N_1 = N_3 = 0$, X = 0
CALL "NWTN1"
Y11(I) = YY1
Y21(I) = YY2
Is 2nd B.pt. Satisfied ?
Y
RETURN
N
$a_{11} = (-Y1(I) + Y11(I)) / (\eta * \delta_1|_o)$
$a_{21} = (Y21(I) - Y2(I)) / (\eta * \delta_1|_o)$
SET : $\delta_1 = \delta_1|_o$
$\delta_3 = \delta_3|_o * (1+\eta)$
$N_1 = N_3 = 0$, X = 0
CALL "NWTN1"
Y12(I) = YY1
Y22(I) = YY2
Is 2nd B.pt. Satisfied ?
Y
N
$a_{12} = (Y12(I) - Y1(I)) / (\eta * \delta_3|_o)$
$a_{22} = (Y22(I) - Y2(I)) / (\eta * \delta_3|_o)$
$a_{10} = -Y1(I)$
$a_{20} = -Y2(I)$
$DD = a_{11} * a_{22} - a_{12} * a_{21}$
$\Delta\delta_1 = (a_{22} * a_{10} - a_{20} * a_{12}) / DD$
$\Delta\delta_3 = (-a_{21} * a_{10} + a_{20} * a_{11}) / DD$
$\delta_1 = \delta_1|_o + \Delta\delta_1$
$\delta_3 = \delta_3|_o + \Delta\delta_3$
GO TO 103
Subroutine "NWTN1"
Transfere $\delta_1, \delta_3, N_1, N_3, X$, NPT, YY1, YY2
Io = 0
Io = Io + 1
CALL "DFEQS "
Y1(Io) = N_1
Y2(Io) = N_2
N
Is Io = NPT ?
Y
YY1 = Y1(NPT)
YY2 = Y2(NPT)
RETURN